UNIVERSIDAD DE GRANADA

TESIS DOCTORAL

PROGRAMA DE DOCTORADO EN BIOQUÍMICA Y BIOLOGÍA MOLECULAR

Engineering *Pseudomonas putida* for sustainable production of styrene

Ana Ángeles García Franco

Director

Juan Luis Ramos Martín

Estación Experimental del Zaidín

Consejo Superior de Investigaciones Científicas

Granada, 2024

Editor: Universidad de Granada. Tesis Doctorales
Autor: Ana Ángeles García Franco
ISBN: 978-84-1195-762-5
URI: https://hdl.handle.net/10481/103229

La doctoranda / *The doctoral candidate* Ana Ángeles García Franco y el director de la tesis / *and the tesis supervisor* Juan Luis Ramos Martín, Profesor de Investigación del Departamento de Biotecnología y Protección Ambiental de la Estación Experimental del Zaidín:

Garantizamos, al firmar esta tesis doctoral, que el trabajo ha sido realizado por la doctoranda bajo la dirección del director de la tesis y hasta donde nuestro conocimiento alcanza, en la realización del trabajo, se han respetado los derechos de otros autores a ser citados, cuando se han utilizado sus resultados o publicaciones.

Guarantee, by signing this doctoral thesis, that the work has been done by the doctoral candidate under the direction of the thesis supervisor and, as far as our knowledge reaches, in the performance of the work, the rights of other authors to be cited (when their results or publications have been used) have been respected.

Granada, 18 de noviembre de 2024

Doctorando / *Doctoral candidate*

Fdo. Ana Ángeles García Franco

Director de la Tesis / *Thesis supervisor*

Fdo. Juan Luis Ramos Martín

Financiación

La investigación que ha conducido a la realización de esta tesis doctoral se ha llevado a cabo en el grupo de Microbiología Ambiental y Biotecnología del Departamento de Biotecnología y Protección Ambiental de la Estación Experimental del Zaidín (Consejo Superior de Investigaciones Científicas), Granada, gracias a los proyectos RTI-2018-094370-B-100 y TED-2021-129632B-I00 y al contrato contrato de Formación de Personal Investigador PRE2019-087808, financiados por La Agencia Estatal de Investigación (AEI), Ministerio de Ciencia e Innovación (MCIN), y FEDER "Una manera de hacer Europa".

A mis padres,
A mis hermanos,
A Pablo.

Agradecimientos

Antes de finalizar esta tesis, me gustaría agradecer a todas aquellas personas que me han acompañado y han sido parte fundamental de esta enriquecedora etapa, haciendo mucho más fácil el camino.

A mi director de tesis, Juan Luis Ramos, por darme la oportunidad de realizar esta tesis doctoral en su grupo. Gracias por tu profesionalidad, tu disposición, el trato cercano y por hacerlo todo tan sencillo. Tu guía ha sido esencial para aprender a dar mis primeros pasos en el mundo de la ciencia.

A Estrella, por compartir tu inmensa experiencia, por tu apoyo constante y por estar siempre dispuesta a ayudar. Gracias por tu amabilidad, tu alegría y tu cercanía.

A Patricia Godoy, Patri, por ser el corazón del laboratorio y mi mayor apoyo desde aquel primer día en que llegué para empezar el TFM. Gracias por tu cercanía, por estar siempre disponible, por ayudar en todo lo posible y por tu confianza.

A Jesús, por compartir toda tu experiencia, por tu paciencia al enseñar y tus valiosos consejos.

A Rocío Palacios, por llenar de vitalidad el laboratorio desde que llegaste. Gracias por tu energía positiva, tu confianza, tus sabios consejos y por amenizar los momentos de escritura: con un simple "¿Vamos a la cafetería?" se arreglaba la mañana.

A Maribel, por tu inigualable sentido del humor gaditano, siempre capaz de llenar cualquier momento de alegría y risas. Gracias por tu apoyo, tu cercanía y tu disposición para ayudar siempre.

A Ana Sánchez, por ser la primera incorporación joven post-COVID, marcando el inicio de lo que sería "Juventudes EEZ". Gracias por amenizar aquellos días de almuerzos en la cafetería, por tu cercanía, confianza y todos los buenos momentos que hemos compartido.

A Rocío Fernández, Inés y Mario, por las risas y las charlas durante las comidas, unas más motivadoras que otras, pero siempre reconfortantes. A Cristina, Paul, Roberta, Marina e Irene, por vuestra cercanía y los buenos momentos compartidos.

Al laboratorio 316: Pacheco, Sophie y Patri Marín. Gracias por vuestra disposición para ayudar y por ser el laboratorio más charlatán.

Al resto de integrantes del grupo de Microbiología Ambiental y Biotecnología, gracias por vuestra amabilidad, ayuda y consejos.

I would also like to thank the Groningen team, especially Marco Fraaije. Thank you for accepting me into your group, where I had the chance to explore the fascinating world of proteins and cofactors. To all my colleagues—Sara, Saniye, Ariel, Alessio, Anna, Kerlen, Lars, Ogi, Ben, Darren and Chiara—thank you for making my experience enriching. Especially to Saniye and Sara, I truly enjoyed our chats in the coffee corner. You made me feel instantly welcome in your office and in the group.

A mis amigos Biotec, por esos viajecitos de verano y esas comidas navideñas que recargaban las pilas para todo el año. A Cristina, Carmen y Emsi, por estar siempre ahí desde que nos conocimos, hace ya diez años. A Java, por tu apoyo y los buenos momentos cada vez que venías de Pamplona. A Juan y Abel, por compensar el grupo, siendo los menos viejóvenes.

A mis amigas de siempre, Irati y María, por seguir estando presentes, viéndonos crecer a lo largo de los años.

A mi familia. A mis padres, gracias por vuestro amor, cariño y comprensión. En especial a mi madre, mamita, por ser el pilar de la familia. Gracias por tu apoyo y tus consejos, que me han ayudado a enfrentar los nuevos retos. Cuando me agobio por algo, siempre me escuchas, y tu "agobiarse no sirve pa' ná" me calma un poquito. A mis hermanos. A David, por ser el hermano mayor que siempre está ahí. A Sergio, por la alegría que transmites y tu forma de ver las cosas. A Jose, por estar cerca, incluso en la distancia, por escucharme siempre y por ser un gran apoyo. A mis sobrinas, Laura y Noa, por compartir tantos momentos de juego.

Y finalmente, a Pablo. Gracias por confiar siempre en mí, por tu cariño, tu apoyo incondicional y tu comprensión. Gracias por haberme acompañado en cada paso de este camino, por hacer que todo sea más sencillo y lograr que incluso en los días grises brille el sol. Gracias por ser hogar.

Contents

List of Abbreviations 15
Abstract 17
Resumen 21

I Introduction **25**

I.1 Biorefineries based on lignocellulosic materials 27
I.1.1 First-generation (1G) biofuels and bioproducts 28
I.1.2 Second-generation (2G) biofuels and bioproducts 30
I.2 Styrene: an overview 34
I.2.1 Styrene production by industrial methods 34
I.2.2 Uses and applications of styrene 35
I.2.3 Styrene toxicity 36
I.2.4 Styrene recycling 38
I.2.5 Styrene biosynthesis 39
I.3 Choosing the chassis for the biosynthesis of chemical compounds . . 44
I.4 *Pseudomonas putida* 48
I.4.1 *Pseudomonas putida* DOT-T1E 50
I.4.2 Mechanisms of solvent tolerance 51
I.4.2.1 Membrane modifications 51
I.4.2.2 Chaperones 54
I.4.2.3 Metabolism of the toxic compounds 54
I.4.2.4 Efflux pumps 54
I.5 New trends in synthetic biology 60

II Justification and Objectives **63**

III Results **67**

Chapter 1. Insights into the susceptibility of *Pseudomonas putida* to industrially relevant aromatic hydrocarbons that it can synthesize from sugars **69**

1.1 Introduction 73
1.2 Experimental procedures 74
1.2.1 Bacterial strains and growth conditions 74
1.2.2 Growth parameters 75
1.2.3 *Pseudomonas putida* DOT-T1E tolerance to *trans*-cinnamic acid and styrene over the long term 75
1.2.4 Survival in response to *trans*-cinnamic acid or styrene sudden shock 75
1.2.5 Analysis of phospholipids 76
1.2.6 Transcriptomics 76
1.2.7 Proteomics 77
1.2.8 DNA techniques 78
1.2.9 Electroporation 78
1.2.10 Construction of stress response-deficient mutants 78
1.2.11 Glucose concentration in culture supernatants 79
1.3 Results 79
1.3.1 Growth of DOT-T1E in the presence of different concentrations of *t*CA in liquid medium containing or not styrene in the gas phase 79
1.3.2 Survival of DOT-T1E in response to *trans*-cinnamic acid or styrene shock 82
1.3.3 Transcriptional and proteomic responses to *trans*-cinnamic acid and styrene 85
1.3.4 Mutational analyses to identify genes functionally relevant to stress responses induced by *trans*-cinnamic acid or styrene . . 92
1.4 Discussion 94
1.5 Supplementary Information 98

Chapter 2. Engineering styrene biosynthesis: Designing a functional *trans*-cinnamic acid decarboxylase in *Pseudomonas* 103

2.1 Introduction . . . 107
2.2 Materials and methods . . . 110
2.2.1 Chemicals . . . 110
2.2.2 Bacterial strains, plasmids and growth conditions . . . 110
2.2.3 DNA techniques . . . 111
2.2.4 Electroporation . . . 111
2.2.5 *In silico* identification of sequences with high similarity to the *Saccharomyces cerevisiae* enzyme *trans*-cinnamic acid decarboxylase 1 (FDC1). Design and *in vitro* synthesis of FDC1-like enzymes . . . 112
2.2.6 PAL activity assay in *P. putida* whole cells . . . 112
2.2.7 *Trans*-cinnamic acid decarboxylase activity assay in *P. putida* whole cells . . . 113
2.2.8 Styrene production from glucose by *P. putida* . . . 113
2.2.8.1 Metabolite analysis . . . 113
2.2.8.2 Styrene analysis . . . 114
2.2.9 Phylogenetic tree . . . 115
2.2.10 Statistical analysis . . . 115
2.3 Results . . . 115
2.3.1 Design and synthesis of a functional *trans*-cinnamic acid decarboxylase in *P. putida* . . . 115
2.3.2 *In vivo* assay of a synthetic *trans*-cinnamic acid decarboxylase in *P. putida* . . . 116
2.3.3 Conversion of L-phenylalanine into *trans*-cinnamic acid . . . 119
2.3.4 Styrene biosynthesis from glucose . . . 120
2.4 Discussion . . . 121
2.5 Supplementary Information . . . 125

Chapter 3. Sustainable biosynthesis of styrene: Exploiting a consensus-designed decarboxylase, its purification and crystal structure 139

3.1 Introduction . . . 143
3.2 Materials and methods . . . 146

3.2.1 Bacterial strains, plasmids and culture media 146
3.2.2 Protein purification 147
3.2.3 Analytical ultracentrifugation 147
3.2.4 Dynamic light scattering (DLS) 148
3.2.5 Differential scanning fluorimetry (DSF) 148
3.2.6 Plasmid DNA extraction and generation of the mutant proteins of PSC1 148
3.2.7 Substrate profile of PSC1 149
3.2.8 Crystallization of PSC1 150
3.3 Results 151
3.3.1 Purification of PSC1 protein, molecular mass and oligomeric state 151
3.3.2 Thermal stability 153
3.3.3 The PSC1 enzyme exhibits narrow substrate specificity 154
3.3.4 PSC1 crystal structure determination and identification of critical catalytic residues 155
3.4 Discussion 160
3.5 Supplementary Information 163

IV Discussion **169**

V Conclusions **179**

VI References **185**

List of Abbreviations

1G	First-generation	MFS	Major facilitator superfamily
2G	Second-generation	MSA	Multiple sequence alignment
ABC	ATP binding cassette	MSW	Municipal solid waste
ABE	Acetone–butanol–ethanol	OD	Optical density
ABS	Acrylonitrile butadiene styrene	PAL	Phenylalanine ammonia lyase
Ap^R	Ampicillin resistance	PDB	Protein Data Bank
CFA	Cyclopropane fatty acid	PE	Phosphatidylethanolamine
CFU	Colony-forming unit	PET	Polyester polyethylene terephthalate
DDG	Dried distillers grains	PG	Phosphatidylglycerol
DEGs	Differentially expressed genes	P_{OW}	Octanol-water partition coefficient
DLS	Dynamic light scattering	prFMN	Prenylated FMN
DMAP	Dimethylallyl monophosphate	PS	Polystyrene
DMAPP	Dimethylallyl pyrophosphate	Rif^R	Rifampicin resistance
DPG	Diphosphatidylglycerol	RMSD	Root mean square deviation
DSF	Differential scanning fluorimetry	RND	Resistance-nodulation-cell division
EPS	Expanded polystyrene	ROS	Reactive oxygen species
FMN_{ox}	Oxidized flavin mononucleotide	SAN	Styrene acrylonitrile
FMN_{red}	Reduced flavin mononucleotide	SBL	Styrene-butadiene latex
Gm^R	Gentamicin resistance	SBR	Styrene-butadiene rubber
GO	Gene Ontology	SMR	Small multidrug resistance
GRAS	Generally recognized as safe	SPME	Solid-phase microextraction
HAL	Histidine ammonia lyase	TAL	Tyrosine ammonia lyase
HS	Head-space	*t*CA	*Trans*-cinnamic acid
Km^R	Kanamycin resistance	tg	Generation time
LB	Luria-Bertani	T_m	Midpoint temperature
L-Phe	L-phenylalanine	TOD	Toluene dioxygenase
MATE	Multidrug and toxic compound extrusion	Tol	Toluene
MB	Methylbenzoate	Tol^R	Toluene resistance
MDR	Multi-drug resistance	UPR	Unsaturated polyester resins based on styrene

Abstract

The depletion of fossil fuels and increased environmental awareness have driven interest in sustainable alternatives for producing valuable chemicals, such as styrene, via microbial biosynthesis. Styrene is a key monomer in the production of polystyrene, its copolymers, and synthetic rubber, with applications in packaging, disposable products, electronics, and tires, amongst others. Conventional styrene production relies on non-renewable petrochemical processes that contribute to environmental pollution and carbon emissions. Consequently, microbial styrene biosynthesis has emerged as a promising sustainable alternative.

While styrene can be naturally synthesized by certain plants, the yields are extremely low, making the process economically unfeasible. To improve yields, a biosynthesis pathway has been developed using L-phenylalanine (L-Phe) derived from glucose through two enzymatic reactions. The pathway starts with the deamination of L-Phe into *trans*-cinnamic acid (*t*CA) via phenylalanine ammonia-lyase (PAL) enzymes, followed by decarboxylation of *t*CA to styrene, a step catalysed by ferulic acid decarboxylases (FDC). Although styrene production from glucose has been achieved in organisms such as *Escherichia coli* and *Saccharomyces cerevisiae*, yields remain limited due to the toxicity of styrene and *t*CA. These aromatic compounds disrupt cell membranes, compromising their structure and proton gradients, leading to energy depletion and cell death.

Addressing this bottleneck requires using more tolerant microorganisms, such as certain *Pseudomonas* species. Among these, *Pseudomonas putida* DOT-T1E, a solvent-tolerant strain isolated from a wastewater treatment plant in Granada, is particularly promising. This strain can thrive in the presence of highly toxic compounds such as toluene, propylbenzene, *m*-xylene, and ethylbenzene, amongst others. Its solvent tolerance is multifactorial, involving adjustments in membrane lipid fluidity, activation of general stress-response systems, increased energy generation, and the induction of specific efflux pumps that extrude solvents.

Due to the remarkable ability of *P. putida* DOT-T1E to tolerate a wide range of aromatic compounds, it was thought that this strain would be an excellent platform for synthesizing aromatic chemicals from sugars. In this way, this thesis explores the engineering of *P. putida* DOT-T1E as a chassis for sustainable styrene biosynthesis.

First, we investigated the physiological and genetic responses of *P. putida* DOT-T1E to *t*CA and styrene, the intermediate and final product of the biosynthetic pathway. Upon exposure to these compounds, the strain strengthens membrane impermeability through a *cis-trans* isomerase that converts *cis* unsaturated fatty acids to their corresponding *trans* isomers. It also activates stress responses, including chaperone production and the upregulation of reactive oxygen species (ROS)-detoxifying enzymes such as peroxidases and superoxide dismutases. Metabolic adaptations were also observed, with increased activity in the glucose phosphorylative pathway, Entner-Doudoroff enzymes, Krebs cycle enzymes, and the Nuo complex. Furthermore, the strain employs efflux pumps to expel toxic chemicals, with TtgGHI, regulated by TtgV, identified as the most critical pump.

Building on this understanding, we focused on the biosynthetic pathway of styrene using *P. putida* DOT-T1E as a chassis. This involves the conversion of L-Phe to *t*CA via PAL and the subsequent decarboxylation of *t*CA to styrene. Since effective decarboxylases for this transformation are typically of fungal origin, we developed a consensus *trans*-cinnamic acid decarboxylase (PSC1) based on homologous yeast FDC sequences, using the "wholesale" approach. The *Pseudomonas*-optimized *psc1* gene demonstrated effective decarboxylation of *t*CA to styrene and the optimal pH and temperature conditions for the PSC1 enzyme were established. Then, for styrene production we used *P. putida* CM12-5, a derivative of DOT-T1E that overproduces L-Phe. Co-expression of *pal* and *psc1* genes in this strain enabled efficient conversion of L-Phe to styrene, achieving a maximum styrene production of over 220 mg L^{-1}.

The characterization of PSC1 enzyme revealed that it is a globular dimer with a molecular mass of 104.7 kDa, high thermal stability (T_m 63°C) and it is stable across a range of conditions, operating effectively at 50°C. The crystal structure of PSC1, resolved at 2.1 Å, reveals a homodimer with each monomer comprising three distinct domains. Domain 2 contains a hydrophobic pocket critical for binding both the cofactor (prFMN) and substrate. Mutagenesis experiments identified Arg175, Glu280, and Glu285 as essential for catalytic activity, as substituting these residues with alanine completely inhibited the decarboxylation process.

In summary, this thesis highlights the potential of *P. putida* as a biofactory for sustainable toxic aromatic compound production, providing an eco-friendly alternative to traditional petrochemical processes. Through enzyme engineering, genetic modification and metabolic optimization, this work is a viable approach for bio-based styrene production that aligns with the goals of reducing carbon emissions, decreasing dependence on fossil resources and advancing bio-based chemical production to contribute meaningfully to a circular bioeconomy.

Resumen

El agotamiento de los combustibles fósiles y el creciente interés por la sostenibilidad ambiental han impulsado la búsqueda de alternativas para la producción de compuestos químicos de valor añadido, como el estireno, a través de procesos de biosíntesis microbiana. El estireno es un monómero esencial en la fabricación de poliestireno, sus copolímeros y caucho sintético, con aplicaciones en sectores como embalaje, productos desechables, electrónica y neumáticos. La producción tradicional de estireno depende de procesos petroquímicos no renovables que generan importantes emisiones de carbono y contribuyen a la contaminación ambiental. En este contexto, la biosíntesis microbiana de estireno ha emergido como una alternativa sostenible y prometedora.

Aunque algunas plantas pueden sintetizar estireno de manera natural, los rendimientos son extremadamente bajos, lo que hace que este proceso sea económicamente inviable. Para superar esta limitación, se ha desarrollado una ruta biosintética que utiliza L-fenilalanina (L-Phe, *L-phenylalanine*), derivada de la glucosa, mediante dos reacciones enzimáticas sucesivas. La primera reacción consiste en la desaminación de L-Phe a ácido *trans*-cinámico (*t*CA, *trans-cinnamic acid*) por acción de la fenilalanina amonio-liasa (PAL, *phenylalanine ammonia-lyase*). En una segunda reacción, el *t*CA se descarboxila a estireno mediante la acción de la ferulato descarboxilasa (FDC, *ferulic acid decarboxylase*). Aunque se ha logrado producir estireno a partir de glucosa en organismos como *Escherichia coli* y *Saccharomyces cerevisiae*, los rendimientos siguen siendo limitados debido a la toxicidad tanto del estireno como del *t*CA. Estos compuestos aromáticos afectan las membranas celulares, alterando su estructura y afectando al gradiente de protones en las cadenas respiratorias, lo que resulta en la pérdida de la capacidad de generar energía y, finalmente, en la muerte celular.

Para abordar este desafío, se hace necesario recurrir a microorganismos tolerantes a estos compuestos tóxicos, como ciertas cepas de la especie *Pseudomonas putida*. En

particular, *Pseudomonas putida* DOT-T1E, una cepa altamente resistente a disolventes tóxicos y aislada por nuestro grupo de investigación de una planta de tratamiento de aguas residuales en Granada, ha demostrado un notable potencial para estos procesos. DOT-T1E es capaz de sobrevivir en presencia de compuestos altamente tóxicos como tolueno, propilbenceno, *m*-xileno y etilbenceno. Su tolerancia a los disolventes es multifactorial e involucra varios mecanismos, como ajustes en la fluidez de los lípidos de la membrana, activación de sistemas de respuesta general a estrés y la inducción de un conjunto de bombas de extrusión que exportan los disolventes orgánicos desde el citoplasma, la membrana celular o el periplasma al medio externo.

Debido a su gran capacidad para tolerar una amplia gama de compuestos aromáticos, se consideró que *P. putida* DOT-T1E era una plataforma potencial para la biosíntesis de compuestos aromáticos a partir de azúcares. Esta tesis explora la ingeniería de *P. putida* DOT-T1E como un chasis para la biosíntesis sostenible de estireno. En primer lugar, investigamos las respuestas fisiológicas y genéticas de *P. putida* DOT-T1E frente a la exposición a *t*CA y estireno, intermediario y producto final de la ruta biosintética propuesta. En respuesta a estos compuestos, la cepa refuerza la impermeabilidad de su membrana mediante la isomerización *cis-trans* de ácidos grasos insaturados, además de activar respuestas al estrés que incluyen la producción de chaperonas y la inducción de enzimas frente a especies reactivas de oxígeno (ROS, *reactive oxygen species*), como peroxidasas y superóxido dismutasas. También se observaron adaptaciones metabólicas, como un aumento en la actividad de las rutas fosforilativas de la glucosa, la ruta de Entner-Doudoroff, el ciclo de Krebs y el complejo Nuo. Además, la cepa emplea de manera cooperativa bombas tipo RND para la expulsión de los compuestos tóxicos al medio. Entre las distintas bombas RND destaca el papel de TtgGHI, cuya expresión está regulada por TtgV en respuesta a estireno y *t*CA.

Esta ruta requiere la conversión de L-Phe a *t*CA mediante una fenilalanina amonio-liasa (PAL), seguida de la descarboxilación de *t*CA a estireno. Dado que los genes *pal* que codifican enzimas eficientes en la conversión de L-Phe en *t*CA habían sido descritos previamente, nosotros nos centramos en el diseño de descarboxilasas de ácido *trans*-cinámico. Debido a que las descarboxilasas eficaces para este segundo paso suelen ser de origen fúngico, se diseñó una descarboxilasa para ácido *trans*-cinámico por consenso (denominada PSC1) a partir de secuencias homólogas de FDC de levaduras y otros hongos, utilizando la aproximación *wholesale*, previamente

descrita para el diseño de proteínas consenso de otras familias. El uso de codones del gen *psc1* se optimizó para *Pseudomonas*. PSC1 mostró actividad descarboxilasa frente a *t*CA y se determinaron las condiciones óptimas de pH y temperatura para la síntesis de estireno a partir de *t*CA. Posteriormente, para la producción de estireno, se utilizó *P. putida* CM12-5, un mutante múltiple de DOT-T1E que sobreproduce L-Phe. La co-expresión de los genes *pal* y *psc1* en esta cepa permitió la conversión eficiente de glucosa a L-Phe, a *t*CA y a estireno, alcanzando una producción máxima de estireno del orden de 220 mg L^{-1} con bajos niveles de los intermediarios en el medio de cultivo.

La caracterización de la enzima PSC1 reveló que se trata de un dímero globular con una masa molecular de 104.7 kDa, alta estabilidad térmica (T_m 63°C) y capacidad de operación en un amplio rango de condiciones, siendo eficaz a 50°C. La estructura tridimensional de PSC1 se resolvió a 2.1 Å, y mostró que era un homodímero. Cada monómero está compuesto de tres dominios distintos, con un bolsillo hidrofóbico en el dominio 2, crítico para la unión del cofactor (prFMN) y el sustrato. Mediante mutagénesis, se identificaron los residuos Arg175, Glu280 y Glu285 como esenciales para la actividad catalítica, ya que la sustitución de éstos por alanina inhibió completamente la descarboxilación.

En resumen, esta tesis resalta el potencial de *P. putida* como chasis para la producción sostenible de compuestos aromáticos tóxicos, proporcionando una alternativa ecológica a los procesos petroquímicos tradicionales. A través de la ingeniería de enzimas, la modificación genética y la optimización metabólica, este trabajo representa un enfoque viable para la producción de estireno de origen biológico que se alinea con los objetivos de reducir las emisiones de carbono, disminuir la dependencia de recursos fósiles y avanzar en la producción química de base biológica para contribuir significativamente a una bioeconomía circular.

I

Introduction

I.1 Biorefineries based on lignocellulosic materials

Currently, the chemical industry continues to focus on the production of petroleum-derived products. However, the fact that petroleum is a non-renewable natural resource and the growing awareness that the traditional chemical industry contributes to climate change, have increased interest in the production of bio-based chemicals, in addition to biofuels. This alternative approach to the chemical synthesis of chemical products is based on biorefineries, which can produce value-added products from sugars using mild bioprocess conditions, such as low temperature and ambient pressure, thereby contributing to reduce greenhouse gas emissions, a major goal of sustainability (Bertacchi et al., 2022; Branduardi, 2021; Valdivia et al., 2016). However, while these biorefineries offer significant environmental benefits, the main challenge lies in the sustainable production of biomass and the associated land use. The bioeconomy leverages biotechnology to produce chemicals and pharmaceuticals, which use significantly fewer raw materials than bioenergy due to lower production volumes of plastics and chemicals than those of fuels and higher land area efficiency, particularly when bioplastics are involved. Thus, biobased chemicals have less impact on land use compared to bioenergy. The list of biologically derived compounds currently synthesized is quite extensive, including amino acids, vitamins, polymers such as alginate or xanthan and enzymes, amongst others. In recent years, the biobased chemicals sector has grown much faster than the petrochemical sector and is expected to continue increasing in the coming years (Becker & Wittmann, 2019; Bertacchi et al., 2022; Branduardi, 2021; Mycroft et al., 2015; Philp et al., 2013; Sainsbury et al., 2013; Spence et al., 2021).

Energy crops are cultivated specifically for biofuel production and differ according to the region. In the United States, common energy crops include corn, soybeans, willows and switchgrass. Northern Europe primarily grows rapeseed, wheat, sugar beet and willows. Brazil focuses on sugarcane, whilst southeast Asia cultivates palm oil and *Miscanthus giganteus*. In China, sorghum and cassava are prevalent. Globally, corn grain and sugarcane are the most common biofuel crops, with *Miscanthus* considered the most efficient. Besides plant materials, algae and the organic fraction of municipal solid waste are also used as biofuel feedstock (Ramos et al., 2022).

I.1.1 First-generation (1G) biofuels and bioproducts

Depending on the source of the feedstock, biofuels (and bioproducts) are categorized as first, second, third or fourth generation. First-generation (1G) biofuels, also known as conventional biofuels, are produced from food crops such as cereals (wheat, barley, corn and sorghum) and sugarcane grown on arable land (Mohr & Raman, 2013). These crops yield sugar, starch and vegetable oil, which can be converted into biodiesel or ethanol through processes such as transesterification (for biodiesel) or fermentation mediated by yeast or bacteria. Other bioproducts are butanol and isobutanol, but ethanol is the most significant biofuel globally, producing nearly 30 million gallons per year (Renewable Fuels Association, 2024). The ethanol production process involves grinding corn grain, mixing it with hot water to create a mash, and treating it with amylases and glucoamylases to convert the starch into glucose, which is then fermented by yeasts into ethanol with over 90% efficiency. However, producing just ethanol from corn grain is not economically viable, unless a wide range of byproducts are also collected and sold. For instance, the CO_2 generated during fermentation can be harvested, liquefied, and used for carbonated drinks and medical gases. Additionally, the dried distillers grains (DDG), the major co-product from the production of ethanol from grain, which consists of the solids remaining after fermentation and contains undigested corn components and yeast, is sold as protein-rich animal feed. Ethanol production plants are highly efficient, but the economic viability is influenced by the price of grain and the natural gas price (Ramos & Duque, 2019).

Butanol is considered a better blending component than ethanol for gasoline due to its higher fuel density and compatibility with the existing petroleum infrastructure (Green, 2011). Produced mainly through acetone–butanol–ethanol (ABE) fermentation by *Clostridium* strains, butanol production has been optimized, with solvent yields close to 90% of the theoretical yield (Jiménez-Bonilla & Wang, 2018; Qureshi et al., 2007). Efforts to increase the butanol ratio include engineering traditional ABE pathways (Jang et al., 2012) and retrofitting 1G ethanol plants for butanol production (Jiménez-Bonilla & Wang, 2018), which is economically attractive, due to the use of some technologies such as fed-batch fermentation and continuous solvent extraction, which improve efficiency.

The initial push to bring 1G biofuels to market was motivated by the desire to reduce greenhouse gas emissions, stabilize oil prices and enhance energy security. Following United Nations (2016) recommendations, significant efforts have focused on producing new non-contaminant fuels to replace gasoline, diesel and jet fuel with biofuels. To be viable, a biofuel must provide a net energy gain, have environmental benefits, be economically competitive and be produced in large amounts without reducing food supplies (Hill et al., 2006). These criteria also apply to biochemicals intended to replace chemically synthesized compounds. Biofuels and biochemicals that meet these requirements can reduce CO_2 emissions, improving air quality and life expectancy (Fargione et al., 2008; Kim et al., 2015).

Many companies are exploring the production of biochemicals from sugars, either by retrofitting existing ethanol plants or constructing new facilities. The starch-based ethanol industry is well-established, with well-documented production costs that enable straightforward economic feasibility calculations for bioproducts from starch (Ramos & Duque, 2019).

To determine the feasibility of bioproducts, it is necessary to establish the theoretical maximum yield of biotransformation, set the expected industrial yield and estimate the costs for product recovery. Key metabolites such as pyruvate, citric acid, tyrosine, aspartate and acetyl-CoA are critical for biosynthesis. Ramos and Duque (2019) identified itaconic acid, succinic acid, isoprene, acrylic acid, lactic acid and mid-chain alcohols as being economically viable products, which could serve as the building blocks for the polymers currently derived from petroleum.

Microbial production of succinic acid, using recombinant *Escherichia coli* strains, offers advantages over the traditional petrochemical process, including fewer impurities, production at ambient conditions and better carbon efficiency, so it is turning out to be a mature technology (Isikgor & Becer, 2015). Bio-succinic acid can also be used to make renewable polymers such as polyester and polyamides (Adkins et al., 2012).

Bacterial routes to lactic acid production, primarily using *Lactobacillus acidophilus* and *Streptococcus thermophilus*, achieve high yields from starch. The production of enantiopure L-lactic and D-lactic acid depends on the bacterial strain used (Isikgor & Becer, 2015).

Isoprene, used in synthetic rubber production, can be biosynthesized in *E. coli* through metabolic engineering, achieving titres around 200 mg/L (Liu et al., 2013)

and up to 532 mg/L under fed-batch fermentation conditions (Yang et al., 2012). Although biologically produced isoprene is slightly more expensive than its petrochemical counterpart, it offers economic and environmental benefits.

Ongoing efforts aim to enhance *E. coli* (Liu et al., 2013), *Pseudomonas* (Calero & Nikel, 2019) and various yeasts to produce new value-added chemicals, reinforcing the potential of bioproducts from starch as a sustainable alternative to traditional petrochemical processes.

Despite these advantages, 1G biofuels and bioproducts quickly became controversial because they competed with food production for arable land, representing a threat to food security. To address these issues, the industry has shifted its focus towards developing second-generation biofuels, which use alternative feedstock and innovative technologies (Ramos et al., 2022).

I.1.2 Second-generation (2G) biofuels and bioproducts

Second-generation (2G) biofuels are produced from cellulose and hemicellulose from lignocellulosic biomass, found in woody crops, agricultural waste and the organic fraction of municipal solid waste (MSW). Utilizing municipal and household waste for biofuel production is a novel approach, leveraging the currently unused lignocellulose. A critical factor in biofuel sustainability is choosing land that minimizes competition with food production. Thus, 2G processes offer the advantage of using agricultural residues that would have no value and the possibility of using marginal lands for growing biomass to be used as raw material for biofuel (Ramos et al., 2016; Valdivia et al., 2020). Initially, the use of 2G sugars focused on biofuel production, but recently, the synthesis of biochemical products has become an area of interest in biotechnology.

Generally, lignocellulosic biomass consists of 35–50% cellulose, 20–35% hemicellulose and 10–25% lignin, with the remaining fraction made up of proteins, oils and ash. Cellulose, unlike other glucan polymers, has a repeating unit of the disaccharide cellobiose. Hemicellulose has a random and amorphous structure composed of various heteropolymers, including xylan and xyloglucan, amongst others, formed by different 5- and 6-carbon monosaccharides, such as xylose, arabinose and glucose. Hemicellulose integrates with plant cell walls, linking cellulose fibres into microfibrils and cross-linking with lignin to provide structural strength. Finally, lignin is a

three-dimensional polymer of phenylpropanoid units, which acts as the cellular glue, offering compressive strength and stiffness to the cell wall and resistance against insects and pathogens (Isikgor & Becer, 2015).

Despite lignocellulosic biomass is the most abundant raw material on Earth for the production of biofuels, some challenges remain for the industrial production of biofuels and biochemicals: i) the inherent difficulty of breaking down cellulose and hemicellulose into their sugar components (known as 2G sugars); ii) the limited number of studies on the direct use of raw materials enriched in 2G sugars to synthesize new chemical products; iii) the assurance of long-term feedstock supplies, which is a cost and location problem; and iv) to have 2G facilities able to work with heterogeneous lignocellulosic materials (Valdivia et al., 2016).

The process of converting lignocellulosic biomass into biofuels or other products consists of several stages (Figure I.1): firstly, a physicochemical pre-treatment to improve the digestibility of the lignocellulosic biomass; secondly, a saccharification process that consists of the application of specialized enzymatic cocktails that break down the cellulose and hemicellulose polymers into their constituent monosaccharides; thirdly, a fermentation of the sugars to produce the target biofuels or bioproducts; and fourthly, distillation to produce a purified liquid biofuel or bioproduct (Baral et al., 2019; Isikgor & Becer, 2015; Valdivia et al., 2016).

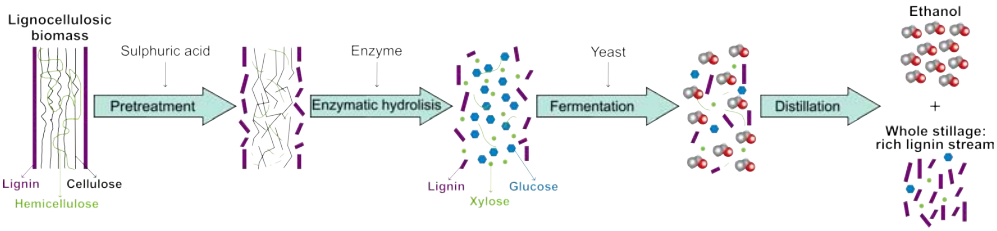

Figure I.1: Lignocellulosic process for converting biomass into biofuels and coproducts, specifically detailing the steps involved in the conversion of agricultural residues into ethanol. Modified from Valdivia et al. (2016).

The first step aims to release cellulose and hemicellulose from lignin in the lignocellulosic biomass. Various types of pre-treatments exist, including chemical, physical and biological processes, each one having a different effect on the cellulose, hemicellulose and lignin. Some of them have shown high potential, such as steam explosion, lime, hot water and acid (e.g. sulphuric acid) or base (e.g. ammonia) pre-treatments. For example, steam explosion involves heating biomass in water

under pressure, followed by the abrupt decompression of the reaction vessel. This rapid decompression disrupts the lignocellulose structure, effectively opening up the fibres and enhancing the accessibility of sugar polymers for subsequent enzymatic hydrolysis (Klinke et al., 2004). Despite its advantages, steam explosion has notable drawbacks. For instance, the water and energy demands are excessively high, making this configuration difficult to implement on a commercial scale (Yang & Wyman, 2008). Combining steam explosion with dilute aqueous solutions of inorganic acids (HCl, H_2SO_4) or bases (ammonia) effectively depolymerizes and releases hemicellulose and cellulose. However, this pre-treatment needs high capital investment due to the corrosive nature of acids and bases, requiring specialized reactor metallurgy. Additionally, lignin removal remains a crucial step in biofuel production, and in both pre-treatments mentioned, lignin is retained until the distillation phase (Ramos & Duque, 2019). The pre-treatment step also leads to the formation of degradation products (e.g. phenols, furans and carboxylic acids), which can be inhibitors, affecting the productivity and end-product formation (Klinke et al., 2004).

The second step consists of an enzymatic hydrolysis to release the monosaccharides, mainly glucose, xylose and arabinose (Álvarez et al., 2016), from the cellulose and hemicellulose through the addition of cellulases and hemicellulases (Hendriks & Zeeman, 2009; Valdivia et al., 2016). Efficient breakdown of cellulose requires the action of endoglucanases, cellobiohydrolases, β-glucosidases and exoglucanases (de Vries & Visser, 2001). The degradation of hemicellulose is more complex, due to its more heterogeneous composition compared to cellulose. It needs the coordinated activity of backbone depolymerizing enzymes such as endoxylanases and β-xylosidases, along with accessory enzymes that hydrolyse side chains on the xylan backbone, including α-L-arabinofuranosidases, acetyl xylan esterases, feruloyl esterases and α-glucuronidases (Álvarez et al., 2016).

Several fungi are used to produce enzymatic cocktails that contain a broad spectrum of enzymes secreted into the growth broth (Álvarez et al., 2016; Ramos & Duque, 2019), but the high cost of these hemicellulolytic enzymes remains a significant bottleneck in the production of 2G bioproducts. To improve them, several strategies can be implemented: reducing enzyme loading by improving enzyme activity through genetic engineering; lowering protein production costs through optimized production methodologies; and increasing overall hydrolysis yield by tailoring the enzyme cocktail performance to the specific process conditions (Valdivia et al., 2016).

The third step in converting the lignocellulosic biomass into bioproducts is fermentation, where ethanol or other types of alcohols or bioproducts are produced from the C5 and C6 monomers. Whilst current fermentation technology efficiently converts glucose and xylose to ethanol with yields exceeding 95%, alternative bioproducts such as alkanes, long-chain alcohols and butanol are also viable (Valdivia et al., 2016). Ethanol fermentation typically uses *Saccharomyces cerevisiae*, although other microorganisms such as *Clostridium* (Green, 2011; Ni & Sun, 2009) or *Pseudomonas* (Molina-Santiago et al., 2016) are used in other production processes. To improve yields, highly optimized yeasts capable of co-fermenting glucose and xylose have been developed, although fermentation efficiency diminishes when inhibitors from woody biomass pre-treatments are present (Heer & Sauer, 2008; Tomás-Pejó & Olsson, 2015). Utilizing the C5 sugars, shortening the fermentation time and optimizing the conditions, such as pH and temperature, could further reduce production costs (Valdivia et al., 2016).

The final stage involves distillation to produce a purified liquid fuel or a product separation step from the culture broth (Valdivia et al., 2016). A critical aspect of this step is the valorisation of the stillage produced during distillation. This stillage contains a high concentration of lignin (20-30%) and is currently used in cogeneration plants to produce power vapour for the 2G process. In configurations lacking cogeneration facilities, the lignin stream is sometimes used for irrigation or sent to wastewater treatment plants, both of which incur significant costs (Ramos et al., 2016). Although several reviews on lignin valorisation exist (Becker & Wittmann, 2019; Isikgor & Becer, 2015; Ragauskas et al., 2014; Weiland et al., 2022; Zakzeski et al., 2010), successful implementations are rare. Current efforts focus on extracting lignin from stillage to synthesize new resins that could replace petrochemical-based compounds (Miao et al., 2023; Zhang et al., 2023).

Despite these challenges, some compounds are already produced from 2G sugars. For example, various species of *Brevibacterium* and *Corynebacterium* are able to produce glutamic acid from a range of carbon sources, including glucose, ethanol and glycerol (Isikgor & Becer, 2015); succinic acid, widely used in the chemical, food, pharmaceutical and textile industries, has been successfully produced from bio-oil using *E. coli* strains (Wang et al., 2013) and various yeasts (Akhtar et al., 2014; Yuzbashev et al., 2010). In addition, L-phenylalanine (L-Phe) (Godoy et al., 2021) and 2-phenylethanol (Godoy et al., 2024) can be synthesized by *Pseudomonas putida*

achieving yields of 250 mg/L and 100 mg/L, respectively, when grown in 2G pre-treated corn stover or sugarcane straw.

Apart from 1G and 2G biofuels, new technologies have emerged, but they are still under development and not yet ready for industrial-scale production. These technologies are third-generation biofuels (derived from algae), and fourth-generation biofuels (that encompass electro-fuels and photobiological solar fuels) (Hannon et al., 2010; Mathuriya & Yakhmi, 2016). Building on the success of these bioprocesses, there is significant interest in expanding the range of biotechnologically produced chemicals, including key industrial monomers such as styrene, which is the focus of this thesis.

I.2 Styrene: an overview

Styrene has a molar mass of 104.15 g/mol and is one of the most important monomers for the production of polystyrene, polystyrene copolymers and rubber, amongst many others (de Meester et al., 1977; IARC, 2019; McKenna & Nielsen, 2011). It is a colourless, oily liquid with a water solubility of 0.31 g/L. Styrene oxidizes upon exposure to light and air, and it easily polymerizes at room temperature in the presence of oxygen. For this reason, styrene is stabilized with a small amount of a polymerization inhibitor (e.g. 4-tert-butylcatechol). If the inhibitor is not present at an adequate concentration, styrene could polymerize and the reaction, which is extremely exothermic, could lead to an explosion. Polymerization is also accelerated if the temperature exceeds 66°C, so storage is recommended at a temperature of 25°C or lower (Bond, 1989; Leibman, 1975).

I.2.1 Styrene production by industrial methods

Commercially, there are two ways to produce styrene. One important method consists of the catalytic dehydrogenation of petroleum-derived ethylbenzene at 600°C, which yields 64% styrene, 2% toluene, 1% benzene and 1% other substances, with 32% of the ethylbenzene being recycled. The separation of the different components must be carried out quickly, with a short time at high temperatures to minimize the polymerization of styrene. The most complicated step is the separation of ethylbenzene, which has a boiling point very similar to that of styrene (Tossavainen, 1978).

The second method also uses ethylbenzene as the starting material, but it involves the co-production of propylene oxide. First, ethylbenzene is oxidized to ethylbenzene hydroperoxide. In the subsequent step, this hydroperoxide oxidizes propylene to propylene oxide in the presence of a metallic catalyst. The ethylbenzene hydroperoxide is then reduced to α-methylbenzyl alcohol, which is finally dehydrated to styrene at 250°C and low pressure using a suitable metal oxide catalyst. The process operates at moderate temperatures and pressure, so it offers advantages over traditional high-temperature dehydrogenation by reducing capital and operating costs whilst still achieving high selectivity and yield (Tossavainen, 1978).

A third method, which proposes the oxidative dehydrogenation of ethylbenzene to styrene using carbon dioxide, has been suggested (van den Berg & van der Ham, 2010). In all three methods, the single most energy-consuming step in the petrochemical industry is the steam cracking of hydrocarbon feedstock (Worrell et al., 2000).

I.2.2 Uses and applications of styrene

Current demand for styrene is estimated to be about 37 million metric tons per year (ChemAnalyst, 2023), due to its numerous applications as a monomer. There are six main families of styrene, in decreasing order of demand: polystyrene (PS), styrene-butadiene rubber (SBR), styrene-butadiene latex (SBL), acrylonitrile butadiene styrene (ABS), unsaturated polyester resins based on styrene (UPR), and styrene acrylonitrile (SAN). The uses of styrene vary by family; for example, PS is mainly used in packaging, disposable products and low-cost consumer goods, although some types of enhanced PS are used in home electronics and appliances. It is also used as an insulator in its expanded polystyrene (EPS) form. SBR is a thermoplastic synthetic elastomer used in the production of tyres. SBL is another thermoplastic synthetic elastomer used, for example, in carpet backing. ABS and SAN have numerous applications in the world of toys, electronics and musical instruments such as recorders, amongst others. UPRs are used in gel-coating and laminating processes to manufacture fibreglass-reinforced plastic products, including boats, bathtubs, shower stalls, tanks and drums. These products are designed to offer extended durability for both indoor and outdoor use (IARC, 2019).

I.2.3 Styrene toxicity

Aromatic hydrocarbons such as benzene, toluene, ethylbenzene, xylene and styrene are among the top 50 most produced chemicals globally, used in numerous applications including the production of polymers, rubbers, and plastics. They are often found together as soil and groundwater contaminants, especially in areas near oil production plants, as they occur naturally in oil and its derivatives. Some strains of *P. putida* can thrive in the presence of high concentrations of these compounds, making them ideal for bioremediation systems that remove contaminants from soil and water, and for serving as a chassis to synthesize value-added chemicals that can be toxic to microorganisms (Ramos et al., 1995, 2015; Udaondo et al., 2013).

The toxicity of these organic solvents to bacteria lies in their disruption of membrane structure, due to hydrophobic interactions between the lipid bilayer and the solvents, owing to their lipophilicity. There is a correlation between the toxicity of organic solvents and the partition coefficient of these compounds in an octanol-water biphasic system (log P_{OW}) (Sikkema et al., 1994). Organic solvents with log P_{OW} values between 1.5 and 4 accumulate in the cytoplasmic membrane of microorganisms, altering their structure and leading to cell lysis, making them highly toxic. Conversely, compounds with log P_{OW} values below 1.5 or above 4 are generally non-toxic and well-tolerated by microorganisms (de Smet et al., 1978; Inoue & Horikoshi, 1991; Vermuë et al., 1993). However, the toxicity of a solvent also depends on the intrinsic tolerance of bacterial strains (Ramos et al., 2002). Segura et al. (2003) reported that various *P. putida* strains showed different levels of sensitivity to toluene and xylenes. For example, the strains *P. putida* KT2440, *P. putida* OUS82, *P. mendocina* KR1, *P. aeruginosa* SSS1, *P. aeruginosa* 7NSK2, *P. fluorescens* EEZ23, *P. stutzeri* and *P. syringae* pv. *syringae* were classified as toluene-sensitive. In contrast, *P. putida* DOT-T1E and *P. putida* MTB6 were considered highly tolerant, whilst *P. putida* S12 was categorized as medium- to highly tolerant.

The effect of lipophilic compounds on membrane integrity depends on their position within the membrane, which also depends on the molecular structure of the compound, its aromatic nature and its substituents (Weber & de Bont, 1996). Alkanes with log P_{OW} values above 3 tend to embed in the bilayer and align with the acyl chains of the fatty acids of phospholipids (Lohner, 1991). More hydrophilic compounds such as alcohols (with log P_{OW} values below 3) also align their non-polar

chain with the acyl chains of fatty acids, whilst the polar hydroxyl group interacts with the polar head group of the phospholipids, anchoring at the liquid/water interface (Pope & Dubro, 1986; Pringle & Miller, 1979). Toluene similarly aligns between the acyl chains of fatty acids near the polar head group of the phospholipid (de Smet et al., 1978).

Regardless of their position in the cell membranes, solvent molecules affect van der Waals interactions between the acyl chains of fatty acids in phospholipids, disrupting the lipid bilayer structure locally (Pringle & Miller, 1979). The resulting membrane disorder alters its permeability, causing both the massive entry of compounds into the cytoplasm and the release of essential ions and metabolites into the external environment. This increased membrane permeability leads to a collapse of membrane potential, resulting in the loss of energy generation capacity and inhibiting energy-dependent membrane functions, which leads to metabolic collapse (Sikkema et al., 1994). These effects are particularly relevant when considering compounds such as styrene, which, despite its industrial significance and natural presence in certain foodstuffs, shares similar toxicological properties with other aromatic hydrocarbons.

Styrene is naturally present in foodstuff such as strawberries, beef and spices, and is produced during the processing of wine and cheese. The Food & Drug Act permits styrene as a direct food additive in small amounts and as an indirect food additive from packaging materials. Due to its rapid biodegradation and volatility, styrene concentrations in surface and groundwater are typically very low (less than 1 µg/L) or non-detectable (Miller et al., 1994).

de Meester et al. (1977) investigated the mutagenic effects of styrene and its primary potential carcinogenic metabolite, styrene 7,8-oxide, using various strains of *Salmonella typhimurium*. Mutagenicity tests show that styrene and its metabolite can induce mutations in bacteria such as *Salmonella*, *Bacillus subtilis* or *Photobacterium phosphoreum*, yeast and plants (Gibbs & Mulligan, 1997). Studies have shown that 300 mg/L of styrene affects the viability of *E. coli* (McKenna & Nielsen, 2011), whilst 200 mg/L inhibits the growth of *S. cerevisiae* (McKenna et al., 2014).

Studies on the toxicity of styrene to aquatic organisms have primarily focused on acute conditions, showing variable results due to the poor solubility and high volatility of styrene. Styrene is metabolized by microorganisms through various pathways, similar to mammalian liver metabolism. Hartmans et al. (1990) demonstrated that

certain bacteria and fungi can utilize styrene. Additionally, styrene levels ranging from 67 to 256 mg/L negatively impacted algae, bacteria and protozoan species. Toxicity values for fish and aquatic invertebrates vary, with significant adverse effects observed at specific concentrations (e.g. 2.5 mg/L for rainbow trout) (Gibbs & Mulligan, 1997).

Acute exposure to styrene causes skin and respiratory tract irritation and central nervous system effects in both humans and laboratory animals. Skin contact causes erythema and, with prolonged exposure, can lead to blistering and the development of dermatitis. Chronic exposure is associated with potential carcinogenic effects, although data are inconclusive. Pharmacokinetic studies reveal the absorption, distribution and metabolism of styrene in humans and animals, with metabolites mainly excreted in urine (Bond, 1989). In humans, exposure to workers can result in memory loss, difficulties in concentration and learning, brain and liver damage and cancer. Therefore, it is crucial to develop accurate methods to monitor its exposure (Gibbs & Mulligan, 1997).

Long-term bioassays in mice and rats have analysed the carcinogenic potential of styrene and styrene oxide. These studies have shown an increase in mammary tumours in rats exposed to styrene, though the results were inconclusive for risk assessment. Styrene oxide increased stomach cancer incidence in rats and mice via gavage, but not with dermal exposure (Conti et al., 1988; Lijinsky, 1986; Ponomarkov et al., 1984).

I.2.4 Styrene recycling

Currently, approximately 10% of the total global plastic is recycled, while the remaining 90% is incinerated, discarded in landfills, or littered into the environment. Therefore, it is crucial to develop recycling strategies (Jiménez-Arroyo et al., 2022; Pereyra-Camacho & Pardo, 2024).

The most commonly used technology for treating styrene-derived plastic waste is mechanical recycling. This process consists of washing to remove solid residues, shredding, melting and reshaping the polymer. The recycled material is usually mixed with virgin plastic of the same type to produce a material with suitable properties for manufacturing. However, this technology has limitations, as each type of plastic responds differently to the process based on its chemical composition, mechanical behaviour and thermal properties (Garcia & Robertson, 2017; Uekert et al., 2023).

Other recycling methods include chemical recycling, which involves pyrolysis to produce gases, fuels, or waxes using catalysts (Aguado et al., 2002); or incineration of the materials to collect energy in the form of heat, which has the disadvantage of not being able to recover and reuse the original components (Rahimi & García, 2017).

The shortcomings in current plastic recycling methods have motivated numerous efforts to develop alternative technologies. One promising approach is chemical or tertiary recycling using hydrolytic enzymes. This method presents a significant opportunity for microbial biotechnology due to its lower energy requirements and reduced production of undesired side products compared to other chemical recycling processes such as pyrolysis and solvolysis. Enzymatic recycling has primarily focused on the polyester polyethylene terephthalate (PET), enabling the recovery of the constituent monomers of the PET, terephthalic acid and ethylene glycol, which can be repolymerized to create recycled PET with properties similar to virgin PET (Kim et al., 2022). Additionally, recent advancements in oxidative thermochemical depolymerization of mixed PET, polyethylene and polystyrene have generated a mixture of organic acids that can be converted by engineered bacterial strains into single products, utilizing a "biological funnelling" approach (Sullivan et al., 2022). This strategy leverages the metabolic versatility of microbes to transform complex substrate mixtures into desired products. This method also offers an attractive solution to manage the presence of additives added during mechanical recycling of plastic (Pereyra-Camacho & Pardo, 2024).

Improving plastic recycling methods offers numerous advantages, such as reducing greenhouse gas emissions, decreasing waste accumulation in the environment and reducing dependence on finite petroleum resources by recovering the economic value of solid plastic waste (Garcia & Robertson, 2017). In addition to recycling plastics, a potential solution to dependence on finite resources such as petroleum could be the biological production of styrene, from which various types of plastics can be derived.

I.2.5 Styrene biosynthesis

Some plants and microorganisms can naturally produce low concentrations of styrene from L-Phe. For example, it has been reported that *Penicillium camemberti* makes styrene, which was found as a trace metabolite in cheese, where it negatively affects the aroma (Pagot et al., 2007). It is also known that styrene can be synthesized by

some plant species of the *Liquidambar* genus, such as *L. styraciflua* and *L. orientalis Mill.*, although it accumulates in very small amounts, not exceeding 0.55% of the dry weight (Fernandez et al., 2005). This styrene can be purified through distillation or liquid-liquid extraction. However, considering its low productivity, large-scale biological production of styrene is not a sustainable process. A more sustainable alternative would be to carry out industrial microbiological processes using microorganisms capable of synthesizing styrene from renewable sources (McKenna & Nielsen, 2011).

In recent years, several pathways in different microorganisms have been described for the production of various aromatic compounds, similar in structure to styrene, from renewable substrates such as glucose. For instance, a biosynthetic pathway has been constructed in *E. coli* (Qi et al., 2007) and *P. putida* (Verhoef et al., 2009) to produce *p*-hydroxystyrene, a monomer used in the synthesis of polymers applied in resins, inks, elastomers and coatings.

Styrene can be biosynthesized from L-Phe via a two-step enzymatic process (Figure I.2). Initially, phenylalanine ammonia lyase (PAL) catalyses the conversion of L-Phe to *trans*-cinnamic acid (*t*CA) through non-oxidative deamination (Nijkamp et al., 2005; Noda et al., 2011). PALs are common in plants and fungi, catalysing the initial step in phenylpropanoid biosynthesis. Few prokaryotic PALs are known, involved in secondary metabolite biosynthesis in *Streptomyces* and *Photorhabdus* species. PALs belong to an ammonia lyase superfamily, including HAL (histidine ammonia lyase) and TAL (tyrosine ammonia lyase). HALs, found in eukaryotes and prokaryotes, share a core structure with PALs and catalyse L-Histidine deamination in the degradation of histidine. Few TALs deaminate L-Tyrosine to *p*-coumarate, used as a chromophore in the photoactive yellow protein of purple phototropic bacteria such as *Rhodobacter capsulatus* and in saccharomicin biosynthesis by *Saccharothrix*. Several studies have reported the identification of cyanobacterial PALs in the genomes of *Nostoc punctiforme* PCC73102 and *Anabaena variabilis* ATCC29413 (Berner et al., 2006; Moffitt et al., 2007; Vannelli et al., 2007; Xiang & Moore, 2005).

After the deamination of L-Phe, *t*CA is decarboxylated to produce styrene, a reaction catalysed by ferulic acid decarboxylases, as previously described in *S. cerevisiae* by Mukai et al. (2010). Clausen et al. (1994) reported that phenylacrylic acid decarboxylase PAD1 from *S. cerevisiae* contributes to cinnamic acid decarboxylation. Subsequently, Mukai et al. (2010) demonstrated that, in addition to PAD1, FDC1 is essential for the decarboxylation of phenylacrylic acids in *S. cerevisiae*.

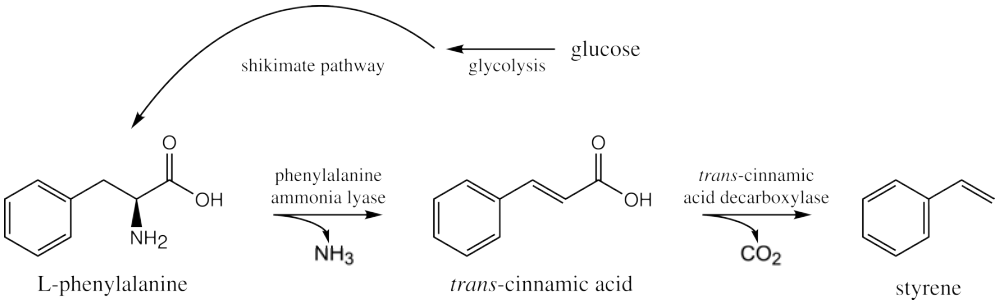

Figure I.2: Enzymatic pathway to produce styrene from the precursor L-phenylalanine via the intermediate *trans*-cinnamate. This two-step conversion is achieved by the co-expression of one or more genes encoding phenylalanine ammonia lyase (PAL) activity, and one or more genes which encode *trans*-cinnamic acid decarboxylase activity. Modified from McKenna and Nielsen (2011).

Protein crystallography studies have identified several non-oxidative decarboxylases, classifying them into three different groups. The first X-ray structure of phenylacrylic acid decarboxylase (Pad1 from *E. coli*) (Rangarajan et al., 2004) revealed that it is a dodecameric flavoprotein with monomers of approximately 23-25 kDa, with a Rossman fold motif and a noncovalently bound flavin mononucleotide (Kopec et al., 2011). Genetic studies indicate that Pad1 is involved in ubiquinone biosynthesis, catalysing the decarboxylation of 4-hydroxy-3-octaprenyl-benzoate (Clarke, 2000; Gulmezian et al., 2007).

The second class contains dimeric proteins with monomers of 19-22 kDa that exhibit a flattened β-barrel structure similar to the lipocalin fold. Phenolic acid decarboxylases from *Lactobacillus plantarum* (Rodríguez et al., 2010), *Bacillus pumilus* (Matte et al., 2010) and *Enterobacter sp.* Px6-4 (Gu et al., 2011) belong to this group.

A third type, identified in *Pseudomonas aeruginosa*, includes UbiD-related decarboxylases involved in ubiquinone biosynthesis, which function as dimeric or hexameric proteins with 50-kDa monomers (Jacewicz et al., 2013).

Bhuiya et al. (2015) reported the three-domain crystal structure of FDC1 from *S. cerevisiae* (Figure I.3). The N-terminal portion consists of domains 1 and 2, connected to the C-terminal domain 3 by α-helix 8. A central four-stranded β-sheet flanked by two α-helices, shape domain 1. Two α-helices link domain 1 to domain 2, the largest domain, which contains multiple β-structural elements, including a six-stranded anti-parallel β-sheet. Domain 3 has a core β-sheet capped by several α-helices and is connected to the C-terminal helix and terminus by an extended flexible

loop. Dimerization of yeast FDC1 occurs through domain 3 of each monomer, giving the dimer a "U" shape, with domains 1 and 2 extending from the dimerization region of domain 3. There is high structural similarity between FDC1 from *S. cerevisiae* and PA0254 from *P. aeruginosa*, as well as UbiD from *E. coli*, so this protein could be classified in the third group of decarboxylases previously described.

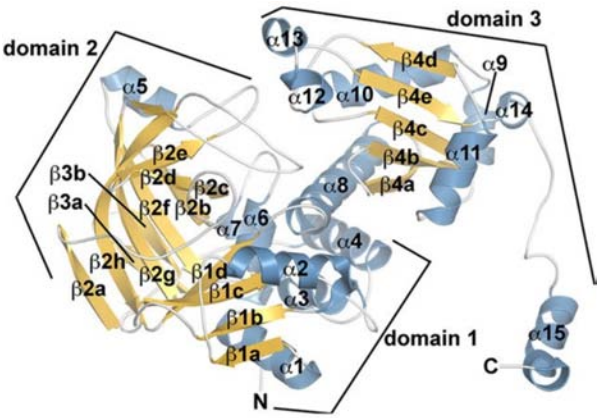

Figure I.3: Monomeric structure and domain architecture of yeast FDC1, represented as a ribbon diagram. The α-helices (blue) and β-strands (yellow) are labelled, with domains 1 to 3 identified, and the N and C termini also indicated (Bhuiya et al., 2015).

Bhuiya et al. (2015) highlighted important features of the FDC1 active site. Arg175 and Glu285 interact with 4-vinylphenol, the product of *p*-coumaric acid decarboxylation. The ligand binding site consists of several apolar residues, including Met228, Met286, Thr326, Ile330, Phe397, Ile398, Phe440, Pro441 and Leu442. Additionally, Val188, Ile189 and Lys190 help enclose the bound ligand on one side of the hydrophobic pocket. The β2e-α5 loop caps the active site, indicating that its movement is necessary for substrate entry into the catalytic site.

Biochemical analysis revealed that yeast FDC1 catalyses the decarboxylation of ferulic acid and *p*-coumaric acid (Bhuiya et al., 2015; Mukai et al., 2010), leading to further investigations into the active site of the enzyme. Studies on FDC1 mutants in *Aspergillus niger* revealed that the R173A, E277Q and E282Q variants were all inactive (Payne et al., 2015). Bailey et al. (2018) further reported that while R173A retained low activity, E277Q exhibited very low decarboxylase activity, and E282Q was completely inactive. Additionally, they constructed three new mutants: R173K, E277D and E282D. No activity was detected for R173K, E282D retained considerable decarboxylase activity, and E277D was active. The corresponding variants were

constructed in *S. cerevisiae* FDC1, showing similar trends: decarboxylase activity was present in E285D, E280D and E280Q (*S. cerevisiae* numbering), but not in R175A, R175K or E285Q.

Biochemical and crystallographic studies on *A. niger* Fdc1 and the *E. coli* homologue UbiD, have detected a highly modified form of flavin, prenylated FMN (prFMN), in their active sites (Marshall et al., 2019; Payne et al., 2015). prFMN consists of an FMN molecule modified by the addition of a fourth non-aromatic ring joined via N5–C1' and C6–C3' linkages between the flavin and prenyl moieties (Bailey et al., 2018). The enzyme responsible for the biosynthesis of prFMN is UbiX in bacteria and PAD1 in yeast (Lin et al., 2015; White et al., 2015), which adds an isoprene moiety from dimethylallyl-monophosphate (DMAP) to $FMNH_2$. It has been proposed that prFMN is released from UbiX and bound by apo-UbiD enzymes in a reduced form ($prFMN_{reduced}$), forming holo-UbiD. The prFMN then oxidizes to the catalytically active oxidized prFMN species. Atomic resolution crystal structures of *A. niger* Fdc1 revealed two forms of the oxidized cofactor: an isoalloxazine N5-iminium form ($prFMN_{iminium}$) and the isomeric N5-secondary ketimine form ($prFMN_{ketimine}$). Although both forms have been proposed as playing roles in decarboxylation (Ferguson et al., 2016; Lan & Chen, 2016; Payne et al., 2015), Bailey et al. (2018) reported that the light-dependent isomerization of $prFMN_{iminium}$ to $prFMN_{ketimine}$ inactivates the enzyme, indicating that $prFMN_{iminium}$ is the active form of the cofactor, which acts catalysing substrate (de)carboxylation via 1,3-dipolar cycloaddition, through the formation of a covalent prFMN-substrate cycloadduct. The isomerization of $prFMN_{iminium}$ to $prFMN_{ketimine}$ is likely to occur after C1' deprotonation, possibly involving prFMN O4 or Glu282 acting as the base. Similar to the isomerization process, the maturation of $prFMN_{reduced}$ to $prFMN_{iminium}$ involves C1' proton abstraction and oxidation, influenced by residue Arg173.

Prior to the detailed understanding of the role of prFMN in decarboxylation, McKenna and Nielsen (2011) developed a styrene production pathway from endogenous L-Phe (synthesized from glucose) through two enzymatic reactions. First, they tested different PAL enzymes from bacterial, yeast and plant genetic sources for the deamination of endogenous L-Phe to convert it into *t*CA. They also tested different phenylacrylate decarboxylase isoenzymes from *Lactobacillus plantarum*, *B. subtilis*, and *S. cerevisiae* to decarboxylate *t*CA into styrene. Finally, the co-expression of PAL2 (from *Arabidopsis thaliana*) and FDC1 (from *S. cerevisiae*) in an L-Phe super-

producing *E. coli* strain allowed styrene titres of 260 mg/L.

McKenna et al. (2014) demonstrated for the first time the bioproduction of styrene from glucose in *S. cerevisiae*, reaching styrene titres of 29 mg/L. Low levels of styrene were reached, in part due to the sensitivity of the yeast to the toxic products (styrene and *t*CA), which results from their tendency to integrate into cell membranes, altering their structure and proton gradients, which leads to an energy collapse and ultimately cell death (Horinouchi et al., 2010; Weber & de Bont, 1996). This sensitivity has also been observed in synthetic pathways to produce aromatic hydrocarbons and medium-chain alcohols, such as butanol production by *Clostridium* (Green, 2011). Therefore, to meet the current demand for "green" alternatives to traditional chemical synthesis methods, a key challenge that must be addressed is to overcome the chemical toxicity to the host microorganism. A possible solution to this bottleneck could be the use of microorganisms with greater tolerance to these toxic compounds, such as some species of the *Pseudomonas* genus.

I.3 Choosing the chassis for the biosynthesis of chemical compounds

A biological chassis can be defined as the physical, metabolic and regulatory framework that facilitates the integration and removal of specific genetic circuits and regulatory elements (Calero & Nikel, 2019). The choice of a metabolic chassis involves several issues: (i) sufficient basic knowledge of the microorganism; (ii) simple nutritional requirements; (iii) "built-in" high resistance to physicochemical stress; (iv) rapid and efficient growth; (v) possession of as many of the necessary functionalities as possible (generally, it is preferable to select a chassis with complex native traits required for the application); (vi) availability of tools for targeted genome manipulations; (vii) efficient secretion systems to aid downstream purification; and (viii) well-suited to the intended environment (Bird et al., 2023; Calero & Nikel, 2019). Some examples of widely used bacterial chassis are *E. coli*, *B. subtilis* and *P. putida*.

Escherichia coli, one of the best-studied prokaryotes, is a Gram-negative, rod-shaped, facultative aerobe bacterium that can be found in mammalian intestines, various natural environments, and sometimes in contaminated foods. Some characteristics

make it a suitable host for bioproduction: (i) rapid growth rates, (ii) low nutrient requirements, (iii) the ability to establish high-cell-density cultures through fed-batch fermentation, (iv) a versatile metabolism, and (v) a wide range of tools for genetic manipulation and strain development (Calero & Nikel, 2019).

Some *E. coli* strains have been engineered for specific purposes. For instance: *E. coli* BL21 Rosetta was engineered for the production of heterologous proteins by utilizing tRNAs that can recognize rare codons in mRNA; *E. coli* BL21(DE3) contains an integrated gene encoding the RNA polymerase from phage T7 in its chromosome (Jeong et al., 2009); and *E. coli* C41(DE3) and C43(DE3) are notable for their high tolerance to membrane protein expression (Miroux and Walker, 1996). Various *E. coli* strains have been developed to enhance the production of key metabolites in central carbon metabolism, such as pyruvate or acetyl-coenzyme A, which can then be used as key precursors for target compounds, such as butanol (Shen et al., 2011) or fatty acids (Sarria et al., 2017).

Another appropriate bacterial chassis is *Bacillus subtilis*, an aerobic, rod-shaped, Gram-positive bacterium that thrives in soil and the plant rhizosphere and is certified as "generally recognized as safe" (GRAS) (Calero & Nikel, 2019). It is highly valued in biotechnology for its ability to produce recombinant proteins, natural enzymes and proteases, primarily due to its efficient secretory machinery (Kim et al., 2010). This capability allows proteins to be secreted into the culture medium at concentrations reaching grams per litre, significantly reducing purification and recovery costs (van Dijl & Hecker, 2013). These enzymes have different applications in detergents, textiles, food additives, cosmetics and waste degradation (Singh et al., 2016). Beyond enzyme production, *B. subtilis* plays a crucial role in synthesizing nucleotides, vitamins, surfactants and antibiotics (Chen et al., 2005; Stein, 2005; Sumi et al., 2015). The production of *p*-aminobenzoic acid (Averesch & Rothschild, 2019) and mosquitocidal toxins using *B. subtilis* has also been reported (Ursino et al., 2020).

Bioprocess yields are influenced by the metabolic pathways and their stoichiometry, as well as the intrinsic properties of the chemicals involved. Additionally, microbial tolerance to high concentrations of both substrates and products is crucial for the efficient industrial production of commodities (Bator et al., 2020), because they can inhibit bacterial growth or even cause cell death, thereby negatively affecting the yields and titres of the bioprocess (Keasling, 2010). Thus, the development and adoption of bacterial chassis with enhanced tolerance to chemical stresses is essential

(Kusumawardhani et al., 2018; Nicolaou et al., 2010).

Pseudomonas putida, a ubiquitous saprophytic soil-colonizer, is increasingly being utilized as a chassis for applications under harsh operating conditions (Calero & Nikel, 2019). The most studied strain within this genus, *P. putida* KT2440, is recognized as a safe host for cloning and expressing heterologous genes (Poblete-Castro et al., 2017). It possesses desirable traits for an ideal bacterial chassis, such as rapid growth, low nutritional requirements and a comprehensive suite of tools for genome and genetic manipulation (Nikel & de Lorenzo, 2018). Some compounds produced by *P. putida* strains are polyhydroxyalkanoates (PHAs) (Prieto et al., 2016), 3-methylcatechol (Hüsken et al., 2001), *o*-cresol (Faizal et al., 2005), terpenoids (Beuttler et al., 2011; Mi et al., 2014), cinnamic acid (Molina-Santiago et al., 2016; Nijkamp et al., 2005), 2-phenylethanol (Godoy et al., 2024; Molina-Santiago et al., 2016), phenol (Wierckx et al., 2005; Wynands et al., 2018), *p*-hydroxystyrene (Verhoef et al., 2009), *p*-hydroxybenzoate (Yu et al., 2016b), vanillate (Graf & Altenbuchner, 2014) and *p*-coumarate (Calero et al., 2016; Nijkamp et al., 2007).

P. putida DOT-T1E is an interesting host for producing aromatic chemicals from sugars, due to its high resistance to a wide range of aromatic compounds, including aromatic hydrocarbons such as toluene, xylenes and styrene (Ramos et al., 2015; Rojas et al., 2003). This resistance offers a significant advantage over other *P. putida* strains, such as KT2440, which are only moderately tolerant to solvents (Segura et al., 2003; Segura et al., 2012).

The pangenome analysis revealed that *P. putida* is characterized by a limited ability to consume sugars, the most common being glucose, gluconate and fructose, which are primarily metabolized through the Entner–Doudoroff pathway (Calero & Nikel, 2019; Daddaoua et al., 2009; Daniels et al., 2010; del Castillo et al., 2007; Nelson et al., 2002). *P. putida* DOT-T1E aligns with this observation, and it also has a limited capacity to metabolize xylose and arabinose, some of the sugars released after the hydrolysis of cellulose and hemicellulose from lignocellulosic biomass (Daniels et al., 2010; Molina-Santiago et al., 2016). Genomic analysis of this strain also revealed a versatile metabolic landscape, which can be engineered to synthesize a wide range of chemicals (Udaondo et al., 2016). Bator et al. (2020) demonstrated that up to three peripheral xylose pathways can be implemented in *P. putida* KT2440 to enable growth on xylose. These pathways include the isomerase pathway and the

oxidative Dahms and Weimberg pathways (Bañares et al., 2021; Bator et al., 2020). Their analyses revealed that the isomerase pathway achieved the maximum yields of xylose metabolites (Bator et al., 2020). In this pathway, xylulose-5-phosphate enters the pentose phosphate cycle and is eventually transformed into erythrose-4-phosphate, a precursor for the synthesis of aromatic amino acids via the shikimate pathway.

The isomerase pathway involves the presence of a xylose isomerase (XylA), which converts xylose into xylulose, and a xylulokinase (XylB), which subsequently phosphorylates xylulose to xylulose-5-phosphate, entering the Pentose Phosphate cycle (Amore et al., 1989; Wilhelm & Hollenberg, 1985). The *xylA* and *xylB* genes from the *E. coli* isomerase pathway have been engineered into *P. putida* S12 (Meijnen et al., 2008), *P. putida* KT2440 (Le Meur et al., 2012) and EM42 (Dvořák & de Lorenzo, 2018) strains to enable xylose utilization. Meijnen et al. (2008) reported that *P. putida* S12 was able to grow on xylose upon the incorporation of *xylAB*. However, *P. putida* KT2440 additionally requires the *xylE* gene, encoding a proton-coupled symporter, to facilitate xylose entry into the cell (Dvořák & de Lorenzo, 2018; Elmore et al., 2020). In all these strains, efficient xylose utilization as a carbon source requires the inactivation of the broad substrate range quinone-dependent glucose dehydrogenase (Gcd) to prevent the misrouting of xylose to the dead-end product xylonate.

P. putida DOT-T1E and CM12-5, a mutant derivative of DOT-T1E that overproduces L-Phe (Molina-Santiago et al., 2016), were engineered to metabolize xylose (Godoy et al., 2021). To this end, mutants lacking the *gcd* gene and harbouring the *xylA*, *xylB* and *xylE* genes from *E. coli* were constructed. These strains were able to metabolize glucose and xylose simultaneously, reaching high cell density. In addition, *P. putida* CM12-5 Δ*gcd* (*xylABE*) produced up to 250 mg/L of L-Phe from 2G lignocellulosic biomass (corn stover and sugarcane straw), becoming an interesting chassis for the synthesis of value-added aromatic products, such as 2-phenylethanol (Godoy et al., 2024), *t*CA or styrene.

Apart from bacterial chassis, *S. cerevisiae* is the best-studied eukaryote microorganism and has numerous biotechnological applications (Becker & Wittmann, 2015). It is certified as a GRAS microorganism, and it is able to grow aerobically and anaerobically on different carbon substrates and in a wide pH range. Due to these characteristics and exceptionally well-developed genetics, *S. cerevisiae* has been engineered for the production of organic acids (Otero et al., 2013), biofuels (Buijs et al., 2013), materials and pharmaceutically relevant products (Krivoruchko &

Nielsen, 2015; Leavell et al., 2016).

In addition to the well-studied chassis mentioned above, several emerging bacterial chassis present exceptionally promising features for development as bioproduction hosts. For example, *Vibrio natriegens*, notable for its remarkably fast growth rate; cyanobacteria, valued for their photosynthetic capabilities (Ellis et al., 2019); and marine bacterial species such as *Roseobacter* and *Halomonas*, which exhibit unique tolerance to saline stress, are among these up-and-coming candidates (Calero & Nikel, 2019).

I.4 *Pseudomonas putida*

Pseudomonas putida, as previously mentioned, is a widely used bacterial chassis. Bacteria of the genus *Pseudomonas* are Gram-negative, straight or slightly curved rods (0.5–1.0 x 1.5–5.0 μm) and motile due to the presence of one or several polar flagella (Moore et al., 2006). They are aerobic, although some species can switch to anaerobic growth using nitrate as an alternative electron acceptor (Moore et al., 2006), and are widely distributed in nature, with some species being pathogenic for humans, animals, or plants (Palleroni, 2015). For instance, some strains of *P. aeruginosa* are opportunistic pathogens that colonize the human lungs of cystic fibrosis patients, where they can form biofilms (Horcajada et al., 2019). Similarly, several strains of *Pseudomonas monteilii* are able to cause opportunistic infections (Moore et al., 2006). Additionally, soil-dwelling strains of *P. syringae* are globally distributed phytopathogens, causing diseases in a wide range of crop plants (O'Brien et al., 2011). In contrast with these pathogenic species, the majority of *Pseudomonas* species are saprophytic and non-pathogenic. Some of them, such as *P. putida* and *P. fluorescens*, stimulate plant growth through solubilization of nutrients or the production of plant hormones and act as biocontrol agents against plant pathogens through iron chelation, niche occupation, and production of antimicrobial compounds (Costa-Gutierrez et al., 2022; Mavrodi et al., 2007; Molina et al., 2016).

Our laboratory in Granada has studied different strains of the species *P. putida* for years, which are characterized by their ability to thrive in different niches. This is the result of its genetic arsenal (genome size around 6 Mb), which contains highly sophisticated genes and pathways that mediate adaptation to changes in the local

environment (Udaondo et al., 2016). Different strains of *P. putida* share a wide repertoire of gene expression regulators, including canonical alternative σ70 kind factors, one and two-component transcriptional regulators, as well as an array of small RNAs and enzymes involved in metabolic responses and defenses against reactive oxygen species (ROS) and other environmental stresses (Moreno et al., 2012; Ramos et al., 2015; Sonnleitner et al., 2009; Udaondo et al., 2012). This genetic diversity gives rise to an intricate network that allows them to adapt and survive in different ecological niches (Udaondo et al., 2018). To further explore the genetic diversity of *P. putida*, the genomes of nine strains of *P. putida* were analyzed using pangenomic approaches. This analysis revealed that the core genome, consisting of genes present in all the strains, comprises approximately 3,386 genes, with those encoding nutrient transporters being the most abundant (Udaondo et al., 2016). *Pseudomonas* species exhibit a core genome with conserved genes involved in central carbon metabolism, such as those for the Entner-Doudoroff pathway, arginine and proline metabolism, and the degradation of aromatic compounds. Additionally, all sequenced genomes contain genes for the pentose phosphate pathway, citric acid cycle and glyoxylate shunt, with the citric acid cycle playing a crucial role in regulating cellular catabolism and biosynthesis (Molina et al., 2019; Moore et al., 2006). The core genome also includes genes for amino-acid metabolism (both synthesis and degradation), various electron transporters for aerobic metabolism, 30 genes for flagella biosynthesis, and at least 12 key genes for biofilm formation (Udaondo et al., 2016). The accessory genome includes genes related to habitat colonization and the metabolism of certain chemicals that are not degraded by all *P. putida* strains, such as toluene. This aromatic compound can be metabolized either by the chromosomally encoded toluene dioxygenase (TOD) pathway (e.g. strains F1 and DOT-T1E) or by the pathway encoded within the TOL plasmid (Phoenix et al., 2003; Udaondo et al., 2016).

Owing to their robust metabolism and high tolerance to toxic solvents such as *p*-xylene, styrene, octanol and toluene (Huertas et al., 1998; Isken & de Bont, 1996; Ramos et al., 1995; Segura et al., 2012), coupled with the ease of genetic manipulation, *Pseudomonas* have increasingly become an important workhorse in the laboratory with a growing number of biotechnological and environmental applications (Abram & Udaondo, 2020; Batianis et al., 2020; Duque et al., 2022; Molina-Santiago et al., 2016; Weimer et al., 2020).

Recent studies have proposed reclassifying the well-known *P. putida* strains, including *P. putida* KT2440 (GenBank accession number AE015451) (Nelson et al., 2002), BIRD-1 (Roca et al., 2013), F1 (Zylstra et al., 1988) and DOT-T1E (Ramos et al., 1995), as *Pseudomonas alloputida* (Keshavarz-Tohid et al., 2019). This reclassification was based on the observation that these strains show significant genetic divergence from the type strain of the species, *P. putida* NBRC 14164 (Ohji et al., 2014). Despite this new taxonomic classification, in this PhD thesis I will refer to the strain DOT-T1E and its derivatives as *P. putida*.

I.4.1 *Pseudomonas putida* DOT-T1E

P. putida DOT-T1E is a solvent-tolerant strain capable of growing in the presence of toxic aromatic hydrocarbons. This strain was isolated from a wastewater treatment plant in Granada and has the ability to grow in the presence of high concentrations (90% [v/v]) of toluene (Ramos et al., 1995). In addition to toluene, the strain is capable of growing in the presence of several organic solvents with a log P_{OW} value between 3.6 and 2.9, such as propylbenzene, *m*-xylene and ethylbenzene (Rojas et al., 2001), which are extremely toxic for bacteria. The capacity for using toluene as a carbon and energy source by this strain is mediated by the TOD pathway (Gibson et al., 1970; Mosqueda et al., 1999). In this pathway, toluene is oxygenated to yield 3-methylcatechol, which subsequently undergoes meta-cleavage fission to form 2-hydroxy-6-oxo-2,4-heptadienoate. This compound is further metabolized to 2-hydroxypenta-2,4-dienoate and acetate, which are channelled into the tricarboxylic acid cycle (Parales et al., 2008; Zylstra et al., 1988).

The genes in this pathway are arranged in two adjacent transcriptional units: *todXFC1C2BADEGIH* and *todST*. The *todST* genes encode the TodS/TodT two-component system, which mediates the activation of the TOD pathway in response to toluene, benzene and ethylbenzene. The catabolic genes of the TOD pathway are transcribed from the P_{todX} promoter when the response regulator TodT is activated through phosphorylation by the TodS sensor kinase in response to pathway substrates (Busch et al., 2007; Krell et al., 2012; Lacal et al., 2008).

The sequencing of *P. putida* DOT-T1E genome helped to identify potential solvent tolerance clusters responsible for its enhanced solvent tolerance (Udaondo et al., 2012). Using 454 technology, it was revealed that the genome consists of a single

chromosome of 6,260,702 bp with a GC content of 63%, and a 133,451 bp self-transmissible plasmid, pGRT1, with a 58% GC content and a copy number of one plasmid per chromosome. The plasmid encodes 126 proteins, representing less than 2% of the total bacterial proteins. The genome of DOT-T1E contains 5,756 open reading frames, of which 84% are shared with other *P. putida* strains. In addition, the strain possesses 170 unique coding sequences not found in other sequenced *Pseudomonas* genomes, suggesting a possible origin from other microorganisms.

The solvent tolerance of this strain is multi-factorial, involving adjustments in membrane lipid fluidity, activation of general stress-response systems, increased energy generation and induction of specific efflux pumps to extrude solvents. It also involves the upregulation of proteins related to energy metabolism, highlighting the importance of enhanced energy generation for operating efflux pumps and maintaining solvent tolerance. Proteomic studies have confirmed that exposure to solvents leads to the induction of proteins involved in the citric acid cycle and energy production pathways (Ramos et al., 2015; Rojas et al., 2001; Segura et al., 1999, 2005, 2012).

I.4.2 Mechanisms of solvent tolerance

To mitigate the harmful effects of solvents, Gram-negative bacteria use different defensive strategies that partly prevent the entry of solvents into the bacteria. They make adaptive changes in their cell membranes to increase rigidity, use chaperones to refold denatured proteins and activate degradation pathways and efflux pumps. The latter two strategies specifically aim to reduce the intracellular solvent load (Figure I.4) (Segura et al., 2012).

I.4.2.1 Membrane modifications

Phospholipids in the cytoplasmic membrane are generally arranged in a bilayer, embedding membrane proteins within their structure. The main phospholipids in Gram-negative bacteria are phosphatidylethanolamine (PE), phosphatidylglycerol (PG) and diphosphatidylglycerol (DPG) or cardiolipin (Cronan & Rock, 2008; Silhavy et al., 2010). The physical state of membrane lipids affects the enzymatic activities of proteins. Under physiological conditions, the cytoplasmic membrane is primarily in a

fluid state. However, in the presence of organic solvents with a log $P_{OW} > 2.7$, there is an increase in the protein-to-lipid ratio in the membrane, leading to increased rigidity, as proteins restrict lipid movement (Keweloh et al., 1990; Weber & de Bont, 1996).

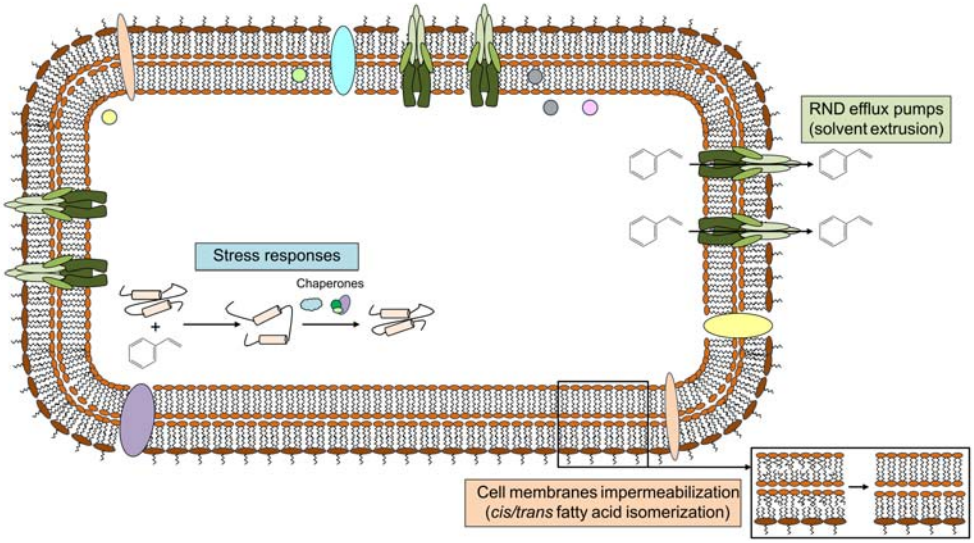

Figure I.4: Schematic representation of the main mechanisms involved in the multi-factorial solvent tolerance process in Gram-negative bacteria, including solvent extrusion by efflux pumps, chaperones induction and membrane compaction.

There are two main mechanisms to regulate membrane fluidity, short-term and long-term responses. The first involves *cis/trans* isomerization of unsaturated fatty acids, whilst the second refers to the alteration of the saturated/unsaturated fatty-acid ratio. In some cases, there is also a change in the long-chain/short-chain fatty-acid ratio (Segura et al., 1999).

The *cis/trans* isomerization phenomenon is catalysed by a *cis/trans* isomerase (Cti) (Heipieper et al., 2007; Junker & Ramos, 1999). This process alters the configuration of the double bond in unsaturated fatty acids, affecting the melting temperature of the membrane, which is higher in the *trans* isomers. Therefore, the increase in the *trans/cis* ratio in response to organic solvents leads to increased membrane rigidity (Segura et al., 1999).

The steric behaviour of *trans* fatty acids and saturated fatty acids is very similar, both having an extended conformation that allows a denser membrane packing. In contrast, *cis* isomers have a 30° non-movable bend in the acyl chain, leading to

increased steric hindrance and membrane fluidity (Figure I.5) (Keweloh & Heipieper, 1996; Segura et al., 1999).

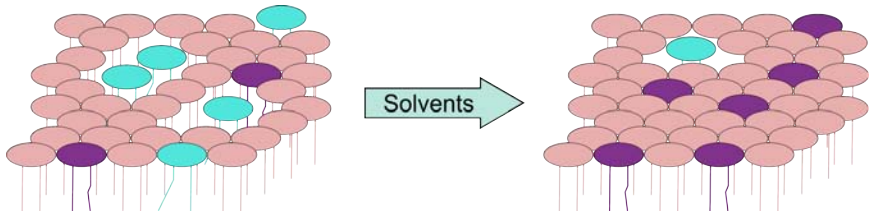

Figure I.5: Impact of *cis/trans* isomerization on membrane structure. The exposure to solvents induces the conversion of *cis*-unsaturated fatty acids (blue) to *trans*-unsaturated fatty acids (purple), which leads to a denser molecular packing of the phospholipids. The saturated fatty acids are depicted in pink. Adapted from Segura et al. (1999).

Alternatively, altering the saturated/unsaturated fatty-acid ratio is considered a long-term membrane fluidity regulation mechanism, as it requires the *de novo* synthesis of fatty acids, which has been detected 15 minutes after solvent exposure (reaching maximum saturation 2 hours later) (Pinkart & White, 1997).

Another strategy to counteract the increased membrane fluidity caused by organic solvents is altering the composition of the polar head groups of phospholipids. Some strains of *P. putida* decrease the amount of PE (which has a low transition temperature), whilst the amounts of PG and DPG (with higher transition temperatures) increase, leading to increased rigidity of the cell membrane (Ramos et al., 1997, 2002, 2015; Weber & de Bont, 1996).

The formation of cyclopropane fatty acids (CFAs) has also been suggested to occur in response to environmental stresses (Bernal et al., 2007a; Ramos et al., 1997). During the late-exponential and early-stationary phases, cyclopropane synthases convert *cis* unsaturated fatty acids into CFAs by adding a methylene group across the double bond of the unsaturated fatty acids (Grogan & Cronan, 1997; Muñoz-Rojas et al., 2006). This process helps to counteract the increased membrane fluidity caused by solvent exposure and enhances membrane packing density. Evidence of this process was demonstrated by a cyclopropane synthase mutant (*cfaB*) of *P. putida* DOT-T1E, which exhibited greater sensitivity to a sudden toluene shock compared to the parental strain (Pini et al., 2009).

I.4.2.2 Chaperones

Although solvent contact induces modifications in membranes that decrease their permeability, the resulting impermeabilization is not complete. Solvents still enter the cell, denaturing proteins and triggering a general stress response, which includes the induction of several chaperones to refold the denatured proteins. Segura et al. (2005) reported that proteins such as the heat shock protein GroES, the cold shock protein CspA, the xenobiotic reductase XenA and the translational elongation factor EF-Tu-1, were significantly induced, suggesting their roles in stress tolerance. Mutants deficient in these proteins showed reduced growth and survival under toluene stress, highlighting their importance.

I.4.2.3 Metabolism of the toxic compounds

Another strategy to prevent the accumulation of toxic solvents within bacteria involves modifying the compound to decrease its lipophilicity or metabolizing it into non-toxic forms, which, in the case of aromatic hydrocarbons, is achieved through oxidation. Although this pathway might be involved in microbial tolerance to toxic compounds, it should be noted that some microorganisms are tolerant to certain organic solvents but incapable of metabolizing them (Aono et al., 1991; Inoue & Horikoshi, 1989; Isken & de Bont, 1996). Therefore, there does not seem to be a direct relationship between tolerance to an organic solvent and its metabolism. This hypothesis was confirmed through experiments with the toluene-tolerant strain *P. putida* DOT-T1E, which can also degrade toluene via the TOD pathway. Mutants generated in the toluene degradation pathway were unable to metabolize it but were as tolerant to toluene as the wild-type strain. Additionally, while the TOD pathway did not enable the strain to metabolize *m*-xylene, ethylbenzene or benzene, it still exhibited high tolerance to these chemicals (Mosqueda et al., 1999).

I.4.2.4 Efflux pumps

The active extrusion of toxic compounds to the external environment is another protective mechanism employed by bacteria when exposed to these toxics. This mechanism of solvent tolerance is particularly efficient in Gram-negative bacteria, enabling them to survive in the presence of toxic solvents (Segura et al., 2012).

It is carried out by multi-drug resistance (MDR) pumps, which are unidirectional flow systems that actively expel a large number of compounds, such as antibiotics, xenobiotics and solvents, from the bacterial cytoplasm, periplasm or inner membrane to the external medium, allowing the bacteria to maintain a low concentration of the toxic compound within the cell (Nikaido & Takatsuka, 2009; Piddock, 2006). The first studies that showed evidence of an energy-dependent export system that could explain the resistance against organic solvents in bacteria were carried out in *P. putida* S12 (Isken & de Bont, 1996) and DOT-T1E (Ramos et al., 1997; Rojas et al., 2001). After that, various efflux pumps were identified in different bacteria; for example, White et al. (1997) highlighted the critical role of the *acrAB* locus in facilitating active efflux and solvent tolerance in *E. coli* K12. AcrB determines substrate specificity and operates using the proton motive force. It is capable of handling a variety of structurally different substances, including cephalosporins, fluoroquinolones, penicillins and chloramphenicol, amongst others (Vargiu & Nikaido, 2012). The MexAB-OprM system was identified as a key contributor to organic solvent tolerance in *P. aeruginosa*, with MexCD-OprJ and MexEF-OprN also playing roles (Li et al., 1998). *P. fluorescens* cLP6a utilizes the EmhABC efflux system to actively transport polycyclic aromatic hydrocarbons (PAHs) such as phenanthrene, anthracene and fluoranthene out of the cell, contributing to antibiotic resistance and survival in contaminated environments (Bugg et al., 2000; Hearn et al., 2003).

Several families of MDR transporters have been identified in bacteria, which are classified according to their mode of action and the substrates they export: ABC (ATP binding cassette), MFS (major facilitator superfamily), MATE (multidrug and toxic compounds extrusion), SMR (small multidrug resistance) and the RND superfamily (resistance-nodulation-cell division). In the case of *P. putida* and other Gram-negative bacteria, the most efficient efflux pumps expelling solvents belong to the RND family, although ABC transporters have also been defined as relevant in solvent extrusion. The main characteristic of RND efflux pumps is their ability to extrude different chemicals, thereby conferring multi-drug resistance (Segura et al., 1999). Efflux pumps of the RND family (Figure I.6) consist of three components: an energy-dependent inner membrane transporter, an outer membrane channel and a periplasmic fusion protein that connects both structures to facilitate the expulsion of toxic compounds outside the cell (Eda et al., 2003; Nikaido, 1996; Segura et al., 1999). These efflux pumps use the proton motive force to expulse compounds from the periplasm or the cytoplasm to the external medium (Ramos et al., 2015).

The best studied RND efflux pumps are from *E. coli* and *P. aeruginosa*. In *E. coli*, AcrAB-TolC is responsible for extruding several antimicrobial agents, including antibiotics and biocides, among others (Nikaido & Pagès, 2012). Several studies have shown that AcrB features a distal and a proximal binding pocket. These pockets contribute to broad-spectrum antibiotic resistance by accommodating substrates of different sizes and characteristics (Blair et al., 2015; Vargiu & Nikaido, 2012). Fluoroquinolone resistance in *E. coli* is mediated by the AcrAB-TolC system (Nikaido & Pagès, 2012) but also by QepA, a plasmid-mediated efflux pump (Yamane et al., 2007).

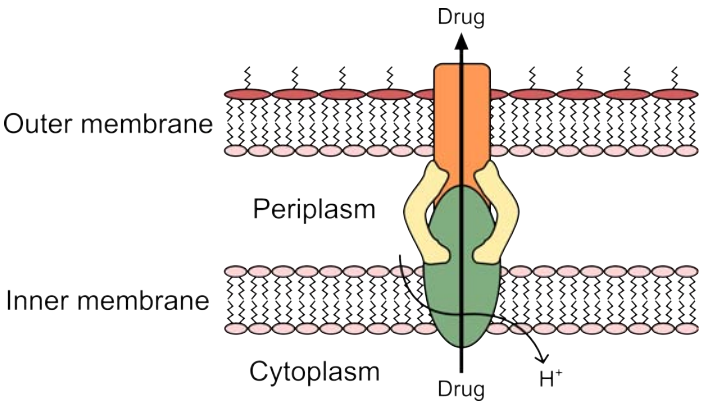

Figure I.6: Model reconstruction of an RND efflux pump, illustrating the structural organization of its components.

In *Pseudomonas aeruginosa*, a major opportunistic pathogen responsible for severe infections, RND efflux pumps such as MexAB–OprM, MexCD–OprJ, MexEF–OprN and MexXY–OprM, contribute significantly to reducing antibiotic susceptibility (Aeschlimann, 2003; Lomovskaya et al., 2001; Mine et al., 1999; Nikaido & Pagès, 2012; Poole & Srikumar, 2001). *P. aeruginosa* has 12 RND family transporters that operate independently and share antibiotic substrates (Fernando & Kumar, 2013; Poole, 2008). The MexAB–OprM system, highly conserved in clinical isolates, expels various antimicrobials such as chloramphenicol, tetracycline and ciprofloxacin (Wu et al., 2024). Unlike MexAB–OprM, MexCD–OprJ does not expel conventional cephalosporins but targets cephalosporins with a quaternary-nitrogen group at the 3-position. MexCD–OprJ handles drugs such as quinolones and macrolides, as well as detergents, dyes and organic solvents, amongst others (Wu et al., 2024). MexEF–OprN increases resistance to chloramphenicol and quinolones

but remains sensitive to other antibiotics. MexXY–OprM provides resistance to acriflavine, ethidium bromide, fluoroquinolones and erythromycin, while also offering partial resistance to tetracycline, kanamycin and chloramphenicol (Abavisani et al., 2021).

In *P. putida* DOT-T1E, three extrusion pumps encoded by the *ttg* (toluene tolerance gene) genes have been described: TtgABC (Ramos et al., 1998), TtgDEF (Mosqueda & Ramos, 2000) and TtgGHI (Rojas et al., 2001), although the genome encodes up to 20 RND efflux pumps (Udaondo et al., 2012), which could be relevant in the tolerance against toxic compounds.

Ramos et al. (1995) demonstrated that the toluene tolerance of *P. putida* DOT-T1E is influenced by cultivation conditions. When pre-exposed to low concentrations of toluene, survival after a toluene shock was nearly 100%, whereas without pre-exposure, only 0.1% of the cells survived. Toluene tolerance assays on a mutant strain with a disrupted gene encoding the TtgABC pump showed no survival without pre-exposure, leading to the conclusion that the TtgABC pump is constitutively expressed, contributing to innate solvent tolerance (Ramos et al., 1998). Ramos et al. (1998) also proposed the existence of inducible efflux pumps for toluene extrusion, identifying two other RND-type pumps, TtgDEF and TtgGHI. TtgDEF is linked to the *tod* genes of the TOD pathway, allowing growth on toluene as the sole carbon source (Mosqueda & Ramos, 2000; Mosqueda et al., 1999). Toluene tolerance assays with a double mutant strain (with inactive TtgABC and TtgDEF pumps) showed survival rates between 0.01% and 0.1% with pre-exposure, but no viability without induction. These results led to a series of assays (Rojas et al., 2001) that identified the TtgGHI pump, encoded by the pGRT1 plasmid (Udaondo et al., 2012). Rojas et al. (2001) tested single mutants in each efflux pump, double mutants and a triple mutant. That work confirmed the additive effect of TtgABC with TtgDEF and TtgDEF with TtgGHI, as double mutants were less tolerant to toluene than the corresponding single mutants. Regarding the toluene extrusion rate, the TtgGHI pump was the most relevant for toluene tolerance, because the mutants lacking this pump were extremely sensitive to the solvent. The coordinated expression of these efflux pumps provides *P. putida* DOT-T1E with high resistance levels, with each pump contributing to the extrusion of different toxic compounds (Mosqueda & Ramos, 2000; Segura et al., 2003; Terán et al., 2003).

RND efflux pump regulation

Multi-drug efflux pumps are typically expressed at a low basal level. However, due to the high energy costs associated with the production of these proteins, a regulatory system is necessary to control their expression levels. Overexpression of these pumps can negatively impact bacteria by physically disrupting membrane integrity or causing the unintended export of essential metabolites. Additionally, the increased presence of transporter substrates or certain physiological or environmental conditions can trigger a higher expression of these regulatory systems. Their regulation occurs through various mechanisms and at multiple levels (Alonso et al., 2004; Grkovic et al., 2002).

RND pumps are regulated by both local and global regulators. Overexpression of these pumps often occurs after interactions between specific molecules and local repressors, leading to operon derepression. Additionally, mutations in these repressors, which prevent their action, have also been reported as a cause of pump overexpression (Webber & Piddock, 2003). For example, mutations in the repressor genes *acrR* and *mexR* lead to the overexpression of the AcrAB pump in *E. coli* and the MexAB-OprM pump in *P. aeruginosa*, respectively (Fernando & Kumar, 2013; Nikaido, 1996). MexR regulates its own expression by binding to its own promoter as well as the *mexA* promoter (Evans et al., 2001). The *nalB* mutation leads to MexAB–OprM overexpression (Lomovskaya et al., 1999; Nikaido, 1996), whilst MexCD–OprJ overexpression is controlled by the local repressor gene *nfxB* (Nikaido, 1998). In *E. coli*, AcrAB pump overexpression can be induced by bile salts and fatty acids, as well as by the global regulator Rob (Fernando & Kumar, 2013). AcrAB is also regulated by MarA and its homologs SoxS (Webber & Piddock, 2003) and RobA, which enhance efflux by increasing *acrAB* transcription and downregulating OmpF porin synthesis through increased MicF antisense RNA production (Fernando & Kumar, 2013; Nikaido, 1996, 1998; Okusu et al., 1996).

Regulation of TtgABC, TtgDEF and TtgGHI efflux pumps in *P. putida*

Several studies have examined the regulation of the *ttgABC*, *ttgDEF* and *ttgGHI* operons in *P. putida* KT2440 and DOT-T1E. The TtgABC efflux pump is expressed at a relatively high basal level, and its expression increases in the presence of specific antibiotics and flavonoids in the culture medium. Although TtgGHI is also expressed at a basal level, its expression is increased in the presence of solvents, as well

as TtgDEF. The genes for these efflux pumps are organized into operons, each accompanied by a gene encoding the regulatory protein for the respective system (Duque et al., 2001; Mosqueda & Ramos, 2000; Terán et al., 2003, 2006).

TtgR, the regulator of the TtgABC efflux pump, is encoded in a divergent orientation to the *ttgABC* operon. This transcriptional regulator controls the transcription of the pump genes and belongs to the TetR family, whose members exhibit a high degree of sequence similarity at the DNA binding domain (Ramos et al., 2005; Terán et al., 2003, 2006). TtgR binds to a pseudo-palindromic site that overlaps the *ttgR* and *ttgA* promoters. In solution, TtgR forms stable dimers, and two of these dimers bind to the operator. Several assays have revealed that optimizing the palindrome does not significantly affect the binding of the first TtgR dimer, but it enhances the cooperativity of binding, thereby increasing the overall affinity. The smallest fragment required for TtgR binding is a 30-mer DNA duplex, and sequence analysis of this fragment showed two partially overlapping inverted repeats within the large pseudo-palindromic operator (Krell et al., 2007). The TtgR crystal structure identified two distinct ligand-binding sites: a broader, mainly hydrophobic site, and a deeper, more polar site, with Arg176 playing a key role in binding (Alguel et al., 2007).

The *ttgDEF* and *ttgGHI* operons are regulated by TtgT and TtgV, respectively, both belonging to the IclR family of transcriptional regulators (Rojas et al., 2003; Terán et al., 2007). Typically, IclR regulator genes are located upstream of their target gene clusters and are transcribed in the opposite direction (Tropel & Van Der Meer, 2004). The regulation of *ttgDEF* and *ttgGHI* is more complex since TtgT and TtgV bind to the same promoter regions, and TtgV is a more efficient repressor. Additionally, TtgR and TtgV regulate their own expression, enabling cells to quickly respond to solvent stress.

TtgV is a protein of 259 amino acids that binds to DNA, preventing RNA polymerase from accessing the promoter region by physical competition and by provoking a distortion that prevents RNA polymerase contact (Guazzaroni et al., 2004), because it induces a 57° convex bend in its operator DNA (Guazzaroni et al., 2007). TtgV is a tetramer in solution, and it does not change this oligomeric state in the presence of effectors. The recognition specificity of TtgV is limited to a 34-nucleotide segment within the operator. In this short segment, TtgV can interact with intercalated inverted repeats that do not have significant DNA sequence similarities. Different compounds, such as aromatic hydrocarbons or aliphatic alcohols, bind to

TtgV and cause a conformational change that releases it from its operator (Guazzaroni et al., 2004). This release allows RNA polymerase to bind to the *ttgG-ttgV* promoter region and initiate the transcription of *ttgG* and *ttgV* (Fillet et al., 2012).

The previously described mechanisms can confer microorganisms with a certain level of resistance to toxic compounds (Hancock, 1997; Nakae et al., 1999; Nikaido, 1996; Ramos et al., 1997), making these tolerant microorganisms extremely useful in biotechnological applications. However, all these responses consume energy, making the elimination of toxic products and the survival of microorganisms a costly process (Ramos et al., 2015). Therefore, it is necessary to find more efficient and customizable solutions. This is particularly relevant in the context of biorefineries and the biosynthesis of complex chemical compounds, where the traditional approaches may not be sufficient to meet industrial and environmental demands. In this regard, synthetic biology offers promising new strategies to overcome these challenges by enabling the rational design and engineering of biological systems, thereby advancing the capabilities of biotechnological applications.

I.5 New trends in synthetic biology

Synthetic biology, an interdisciplinary field that merges the principles of biology and engineering, has emerged in recent years. It applies engineering approaches to the genetic components of natural systems, aiming to generate novel designed biological networks. Devoted to the rational design and engineering of organisms and their components, synthetic biology is revolutionizing our understanding and manipulation of biological systems (Adams, 2016; Bird et al., 2021).

Different tools have been developed to rationally design, synthesize and construct genetic networks to achieve customized biological functions. Synthetic biology initially relied on a small set of laboratory organisms, primarily *E. coli* and *S. cerevisiae*. They were widely used in molecular biology and genetic engineering due to their rapid growth rates and abundant protein production, making them the foundational chassis for synthetic biology as the field evolved from its molecular biology and genetic engineering roots. However, it is increasingly evident that these organisms are not the ideal chassis and require the development of new chassis to advance synthetic biology capabilities (Adams, 2016).

Synthetic biology integrates, amongst others, protein design strategies to build complex biological systems and organisms with specific, engineered functions (Sternke et al., 2019). Physics-based, structure-based (Chen et al., 2009) and directed evolution-based (Jäckel et al., 2008; Lane & Seelig, 2014) approaches are different strategies applied to engineer proteins. Although these strategies have produced proteins with high stability, their implementation is often complex, with low success rates. *De novo* design strategies typically emphasize protein structure, making the introduction of specific activity into these newly designed proteins a significant challenge (Kries et al., 2013).

Consensus sequence design is another strategy that has shown success in enhancing the thermodynamic stability of natural proteins (Sternke et al., 2019). This approach identifies "consensus" residues as those with the highest frequency at specific positions in a multiple sequence alignment (MSA) of existing sequences from a given protein group. About 50% of conserved residues are associated with improved stability, whilst approximately 10% are stability-neutral and around 40% are destabilising, leading to some challenges during implementation (Porebski & Buckle, 2016). A consensus residue at any given position should optimize stability, activity and other essential properties. Related to this, different studies have reported an increase in the melting temperature of several consensus proteins (Dai et al., 2007; Lehmann et al., 2002; Paatero et al., 2016; Wirtz & Steipe, 1999).

Two experimental approaches have been used to evaluate the effectiveness of consensus information in protein design: point-substitution and “wholesale” substitution. In the point-substitution approach, individual residues in a well-characterized protein that differ from the consensus are replaced with the consensus residue (Polizzi et al., 2006; Steipe et al., 1994). In these studies, about 50% of the single point mutants showed some degree of stabilization, with most of them being fully additive. The frequency of stabilizing mutations is higher than that of random mutations (approximately 1 in 1000) (Giver et al., 1998; Zhao & Arnold, 1999). However, the net increase in stability is still likely to be low because the stabilizing substitutions are offset by the destabilizing substitutions (Sternke et al., 2019).

The “wholesale” approach involves combining all substitutions toward the consensus into a single consensus polypeptide, composed of the most frequent amino acid at each position in the sequence. This method can collectively harness the incremental effects of individual substitutions, as well as the non-additive effects that

arise from incorporating each residue into the new context of the consensus protein (Sternke et al., 2019). The application of this approach has successfully increased the stability of different proteins (Blatt et al., 1996; Lehmann et al., 2002; Sullivan et al., 2011), but the effects on biological activity are variable. Tripp et al. (2017) created a consensus-designed homeodomain sequence that showed increase in thermostability and in DNA-binding affinity, and Sternke et al. (2019) characterized six consensus proteins from different families and found that all of them adopted cooperatively folded structures in solution and four proteins showed increased thermostability.

II

Justification and Objectives

Justification and Objectives

The involvement of the chemical industry in climate change and its high demand for non-renewable resources, have led to increasing interest in more sustainable alternatives, such as the biological synthesis of chemicals, where microorganisms produce value-added compounds using sugars as feedstocks.

Given the high global demand for styrene, this research focuses on its biosynthesis. Although styrene has been synthesized from glucose, the process has been limited by low yields, primarily due to the high toxicity of the products and the low activity of the enzymes involved.

Taking into account this background, this PhD thesis explores the synthesis of value-added chemical compounds from sugars derived from agricultural waste, which are among the most abundant second-generation (2G) feedstocks. Specifically, this study explores the biosynthesis of styrene using glucose and xylose, key sugars present in lignocellulosic residues such as corn stover and sugarcane straw. By leveraging *Pseudomonas putida* strains as the biological chassis, this study aims to address the toxicity challenges reported in previous work, paving the way for more efficient and sustainable bioproduction processes. To achieve this general objective, three specific objectives were established:

1. Characterization of the response of *P. putida* DOT-T1E and its derivatives to *trans*-cinnamic acid and styrene, the intermediate and final products, respectively, of the styrene synthesis pathway.

2. The *in silico* design of enzymes responsible for catalysing the transformation of *trans*-cinnamic acid into styrene, and the *in vitro* synthesis of the genes encoding these enzymes: characterization of PSC1, the consensus enzyme that converts *trans*-cinnamic acid into styrene.

3. Construction of a *P. putida* host platform that performs optimally and remains viable whilst achieving high yields of toxic *trans*-cinnamic acid and styrene.

III

Results

Chapter 1

Insights into the susceptibility of *Pseudomonas putida* to industrially relevant aromatic hydrocarbons that it can synthesize from sugars

Published as:

Ana García-Franco, Patricia Godoy, Estrella Duque and Juan L. Ramos. Insights into the susceptibility of *Pseudomonas putida* to industrially relevant aromatic hydrocarbons that it can synthesize from sugars. *Microbial Cell Factories*. **2023**, 22(22).

Abstract

Pseudomonas putida DOT-T1E is a highly solvent tolerant strain for which many genetic tools have been developed. The strain represents a promising candidate host for the synthesis of aromatic compounds —opening a path towards a green alternative to petrol-derived chemicals. We have engineered this strain to produce phenylalanine, which can then be used as a raw material for the synthesis of styrene via *trans*-cinnamic acid. To understand the response of this strain to the bioproducts of interest, we have analyzed the in-depth physiological and genetic response of the strain to these compounds. We found that in response to the exposure to the toxic compounds that the strain can produce, the cell launches a multifactorial response to enhance membrane impermeabilization. This process occurs via the activation of a *cis* to *trans* isomerase that converts *cis* unsaturated fatty acids to their corresponding *trans* isomers. In addition, the bacterial cells initiate a stress response program that involves the synthesis of a number of chaperones and ROS removing enzymes, such as peroxidases and superoxide dismutases. The strain also responds by enhancing the metabolism of glucose through the specific induction of the glucose phosphorylative pathway, Entner-Doudoroff enzymes, Krebs cycle enzymes and Nuo. In step with these changes, the cells induce two efflux pumps to extrude the toxic chemicals. Through analyzing a wide collection of efflux pump mutants, we found that the most relevant pump is TtgGHI, which is controlled by the TtgV regulator.

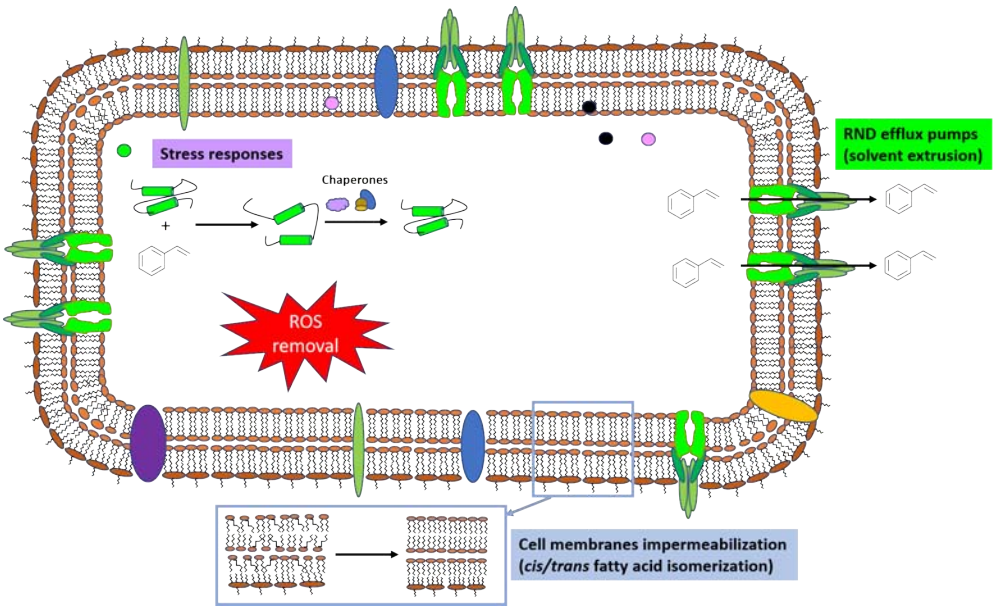

1.1 Introduction

Currently, an immense volume of petrol-derived chemicals are used for synthesis of polymers, detergents, textiles, fuels, pharma, and more (Cao et al., 2020; Jain et al., 2022; Linger et al., 2014; Schwanemann et al., 2020). With demand for these chemicals increasing, and limitations for fossil fuel resources mounting—combined with a global awareness of the climate crisis—there is a drive toward the sustainable, bio-based production of chemicals from renewable feedstocks (Cywar et al., 2022; Ramos & Duque, 2019; Ramos et al., 2022). Efforts to produce added-value chemicals through microbial fermentation are gaining momentum because the process offers a series of advantages over chemical synthesis; namely, the process (i) uses sustainable feedstocks, (ii) it can be operated at room temperature and ambient pressure, (iii) it can be easily scaled to an industrial level, and (iv) in most cases it can be used to produce highly pure compounds (Sravan & Mohan, 2022). In order to fulfill cost-effectiveness prerequisites, the process requires a microbial cell platform that can efficiently and robustly generate a diverse range of chemicals with high yields in large-scale industrial processes (Cywar et al., 2022; Hatti-Kaul et al., 2007; Molina-Santiago et al., 2016; Straathof et al., 2019; Valdivia et al., 2020). To achieve this requirement and to advance fermentation technology, researchers are using *in silico* metabolic flux predictions along with metabolic engineering as part of the so-called design-build-test-learn (DBTL) cycle (Opgenorth et al., 2019). We have used the DBTL cycle to develop a platform for the biosynthesis of aromatic compounds, including a range of industrial chemicals. Synthesis of aromatic compounds via chemical synthesis is highly energy intensive and requires toxic catalysts. Conversely, the synthesis of aromatic chemicals from bio sources requires the generation of aromatic amino acids (e.g., phenylalanine, tyrosine or tryptophan) as starting materials (Godoy et al., 2021; Huccetogullari et al., 2019; Lee & Wendisch, 2017; Loeschcke & Thies, 2015; Nijkamp et al., 2007; Otto et al., 2019; Schwanemann et al., 2020; Wang et al., 2018a; Wierckx et al., 2005, 2009).

In previous studies, it was shown that *Escherichia coli* and *Saccharomyces cerevisiae* bearing genes encoding a phenylalanine ammonia lyase and a *trans*-cinnamic decarboxylase enable them to produce styrene from phenylalanine via *trans*-cinnamic acid (*t*CA). However, production capability of this process is limited by the internal level of phenylalanine and the intrinsic styrene tolerance of the producer strains

(Machas et al., 2021; McKenna & Nielsen, 2011; McKenna et al., 2014, 2015). These studies revealed that, in addition to requiring genes to enable the metabolic steps, the chassis must be able to grow and thrive in the presence of the intermediates and final products being synthesized.

Pseudomonads are a promising chassis for the bioproduction of chemicals. They display unique characteristics needed for the production of aromatic compounds, including tolerance to toxic chemicals (Calero & Nikel, 2019; Nikel et al., 2014; Ramos et al., 1995; Udaondo et al., 2013; Wierckx et al., 2005). *Pseudomonas putida* DOT-T1E was described by our group as a microorganism with extremely high tolerance to organic solvents (Bitzenhofer et al., 2021; Ramos et al., 1995, 2015; Schwanemann et al., 2020). Genomic analysis of this strain revealed a versatile metabolic landscape that can be engineered to synthesize various chemicals (Udaondo et al., 2016).

We have previously shown that CM12-5, a derivative of DOT-T1E, is able to produce 0.5–1 g L^{-1} phenylalanine when glucose is supplied as a single carbon source or as part of a mixture of chemicals that originate from the hydrolysis of lignocellulosic biomass (Godoy et al., 2021; Molina-Santiago et al., 2016). The present study was conceived to provide insights into the tolerance of *Pseudomonas putida* DOT-T1E to *trans*-cinnamic acid and styrene. To achieve this, we used omics approaches to elucidate the response of wild-type and mutant strains to these chemicals in batch culture or after the sudden addition of the test compounds. By identifying the key molecular determinants of tolerance to these chemicals, this work sheds light on the response of this microorganism to aromatic chemicals of industrial interest.

1.2 Experimental procedures

1.2.1 Bacterial strains and growth conditions

Pseudomonas putida DOT-T1E was grown on M9 minimal medium with glucose 5 g L^{-1} (Abril et al., 1989) as the sole carbon source. When required, 10 mM *trans*-cinnamic acid and/or styrene (through the gas phase) were supplied. Cultures were incubated at 30°C and shaken on an orbital platform at 200 strokes per minute.

1.2.2 Growth parameters

To determine growth rate, overnight cultures of *P. putida* were harvested by centrifugation (13,000 $\times g$, 5 min) and washed once with M9 minimal medium (Abril et al., 1989). Cells were suspended to an OD_{660} of $\sim$0.1 in 25 mL of the test medium in 250 mL conical flasks. Doubling times were determined during exponential growth as a slope of the data points obtained by plotting CFU mL^{-1} against time.

To determine cell dry weight, samples of cultures were transferred into 2 mL pre-weighted Eppendorf tubes and pelleted at 13,000 $\times g$ for 10 min. The pellets were washed once with M9 medium and left to dry at 70°C for 48 h. Substrate consumption rates and specific carbon consumption rates were determined during the initial 24 h of culture as described by Dvorák and de Lorenzo (Dvořák & de Lorenzo, 2018). Cell growth was routinely monitored at 660 nm using a UV-1900i UV–vis spectrophotometer (Shimadzu, USA).

1.2.3 *Pseudomonas putida* DOT-T1E tolerance to *trans*-cinnamic acid and styrene over the long term

Overnight cultures were diluted to an OD_{660} of 0.1 and supplemented with different concentrations of *trans*-cinnamic acid (0, 15, 25, 50, 75, and 90 mM) or styrene (0.1 and 1% (v/v)) and grown and monitored under these conditions for 24 h. The number of viable cells was determined before aromatic compounds were added and after 4, 6 and 24 h.

1.2.4 Survival in response to *trans*-cinnamic acid or styrene sudden shock

Overnight cultures were diluted to an OD_{660} of 0.1 and grown under the same conditions until the cultures reached a turbidity of about 0.8 at 660 nm. Then the cultures were divided into three aliquots: to the first aliquot, 0.1% (v/v) styrene was added; to the second aliquot, 50 mM *trans*-cinnamic acid was added; and the last aliquot was kept as a control. The number of viable cells was determined before aromatic compounds were added and 10, 30 and 60 min later.

1.2.5 Analysis of phospholipids

Phospholipids were extracted by the method described by Bligh and Dyer (1959), then saponified and esterified as described by Junker and Ramos (1999). The fatty acids were identified by mass spectrometry after gas chromatographic separation.

1.2.6 Transcriptomics

To study the *P. putida* DOT-T1E transcriptome under different conditions, the strain was grown overnight in M9 minimal medium with glucose 5 g L^{-1} in the absence and in the presence of 10 mM *trans*-cinnamic acid and styrene supplied through the gas phase. On the following day, cultures were diluted to an OD_{660} of 0.1 and grown under the same conditions until the cultures reached the end of the exponential phase. Cells (20 mL) were harvested by centrifugation (5,000 $\times g$ for 10 min at 4°C) and stored at -80°C until processing. Three independent biological replicates were prepared.

RNA isolation was carried out according to TRIzol Reagent instructions (Invitrogen). Extracts were treated with RNase-free DNase. The integrity of total RNA and the presence of DNA contamination were assessed with a NanoDrop One. DNA removal was carried out via treatment with Nucleo-Spin RNA Plant (Macherey–Nagel). The integrity and quality of total RNA was assessed with an Agilent 2100 Bioanalyzer (Agilent Technologies). Removal of rRNA was performed using RiboZero rRNA removal (bacteria) kit from Illumina, and libraries of 100-bp single-end reads were prepared using a TruSeq Stranded Total RNA Kit (Illumina). Libraries were sequenced using a NextSeq550 sequencer (Illumina).

The raw reads were pre-processed with SeqTrimNext (Falgueras et al., 2010) using the specific NGS technology configuration parameters. This pre-processing keeps the longest and removes sequences below 25 bp. It also removes low-quality, ambiguous and low-complexity stretches, linkers, adapters, vector fragments, and contaminated sequences. Clean reads were aligned and annotated using the Pcl and Bamy reference genomes with Bowtie2 (Langmead & Salzberg, 2012) in BAM files, which were then sorted and indexed using SAMtools v1.484 (Li et al., 2009). Uniquely localized reads were used to calculate the read number value for each gene via Sam2counts (https://github.com/vsbuffalo/sam2counts). DEgenes Hunter was used to analyze differentially expressed genes (DEGs), which provides a combined

p-value calculated (based on Fisher's method) using the nominal *p*-values provided by edgeR (Robinson et al., 2010) and DEseq2 (Anders & Huber, 2010). This combined *p*-value was adjusted using the Benjamini-Hochberg (BH) procedure (false discovery rate approach) and used to rank all the obtained DEGs. For each gene, significance thresholds were established by combining p-value < 0.05 and $\log_2$ fold change > 2 or < -2. The annotated DEGs were used to identify the Gene Ontology functional categories and KEGG pathways. Gephi software (https://gephi.org) was used to generate the DEG networks (González-Gayte et al., 2017).

1.2.7 Proteomics

Proteomic analysis was carried out at the proteomic facility of CNB-CSIC (Madrid, Spain) using the iTRAQ procedure (Cuenca et al., 2016; Molina et al., 2019). To study the proteome of *P. putida* DOT-T1E, cells were cultured as above except that 30 mL of cultures with a turbidity of about 1 at 660 nm were harvested by centrifugation (5,000 $\times g$ for 10 min at 4°C), then washed twice with M9 medium. Cell pellets were then stored at -80°C. For the preparation of protein extracts, cell pellets were suspended in 600 µL of lysis buffer (Molina et al., 2019), and lysis was carried out at 4°C by sonication applying a 40 J dose with amplitude of vibration of 30% and pulses of 10 s followed by resting intervals of 5 s. To remove cellular debris, lysates were centrifuged for 20 min at 14,000 $\times g$ at 4°C. Protein (15 µg) was treated with 100 mM Tris (2-Carboxyethyl) phosphine hydrochloride (TCEP) to reduce disulfide bridges, alkylated with 200 mM chloroacetamide (CAA) and digested with trypsin. Upon peptide separation, samples were labelled with the TMT 8-plex or TMT 11-plex reagent (one label per sample). After 2 h labelling, samples were cleaned using a reverse C18 BoncElute Agilent column.

Protein identification and the analysis of differential expression were performed by Proteobiotics (Madrid, Spain). Peak lists were generated with the Mascot Daemon (version 2.5.1), OMSSA 2.1.9, X!TANDOM 23.02.01.1 and Myrimatch 2.2.140 softwares. The mgf files from each sample were merged and MS/MS spectra assigned using the non-redundant RefSeq protein entries for *P. putida* comprising 5313 protein sequences totaling 1,656,176 amino acids (National Center for Biotechnology Information download, 2021). We identified 1960 proteins, and the quantification revealed differential expression of 63 proteins in *trans*-cinnamic acid versus 163 proteins in styrene. In the presence of the two aromatic compounds, 305 proteins had differential

levels. The search was performed using the following criteria: tryptic peptides with a maximum of two missed cleavages, mass tolerances of 25 ppm on the parent ion and 0.02 Da on the MS/MS, fixed modification for carbamidomethylated cysteine, and variable modification for methionine oxidation. Peptides were identified with a q-value threshold below 0.05. Proteins were considered validated when at least two distinct peptides were detected. The false discovery rate for protein identification was estimated with a reversed decoy database to be less than 1%. Proteins showing an abundance change equal or higher than 1.5 ($\log_2$ fold change) and a q-value equal or lower than 0.05 were eventually considered as differentially abundant (Molina et al., 2019).

1.2.8 DNA techniques

DNA was manipulated using standard laboratory protocols (Martínez-García et al., 2014, 2015). Genomic DNA was isolated using the Wizard Genomic DNA purification kit (Promega, USA), while plasmid DNA was isolated with the QIAprep Spin Miniprep kit (Qiagen, USA). DNA concentration was measured with a NanoDrop One (Thermo Scientific, USA). PCR DNA amplification was performed with appropriate primers (Table S1.1), dNTPs and Phusion High-Fidelity DNA polymerase (Thermo Scientific, USA) or Taq DNA polymerase (Roche, Germany), as recommended by the manufacturers.

1.2.9 Electroporation

Electroporation of *Pseudomonas putida* DOT-T1E was performed as described elsewhere (Martínez-García et al., 2014, 2015), using a MicroPulser electroporator and Gene Pulser Cuvettes with 0.2 cm gap (Bio-Rad, USA). Transformants were selected on LB agar plates with kanamycin (25 μg mL^{-1}) and incubated at 30°C for 24 to 36 h.

1.2.10 Construction of stress response-deficient mutants

Inactivation of *sucC*, *pflU* and *arcA* was achieved as described by Godoy et al. (2021): a DNA fragment spanning the central part of these ORFs was amplified by PCR from *P. putida* DOT-T1E genomic DNA using appropriate primers (Table

S1.1). The resulting amplified DNA was cloned into pMBL-T (Santamaría-Hernando et al., 2022) to yield pMBL-T::sucC, pMBL-T::pflU and pMBL-T::arcA, respectively. These plasmids were digested with BamHI and then ligated to the BamHI kanamycin Ω-interposon fragment from plasmid pHP45ΩKm. The resulting chimeric plasmids were named pMBL-T::sucCΩKm, pMBL-T::pflUΩKm, and pMBL-T::arcAΩKm, respectively. These plasmids were individually electroporated into *P. putida* DOT-T1E and putative Km^R recombinant mutants were selected on kanamycin LB plates. A number of Km^R clones were retained, and Southern blotting was used to verify the insertional mutation in the respective gene (data not shown).

1.2.11 Glucose concentration in culture supernatants

For determination of glucose, cultures (1 mL) were centrifuged (13,000 $\times g$ for 10 min at 4°C), and supernatants were stored at -20°C until analyzed. For analysis of glucose, the D-glucose-HK Assay Kit was used according to the manufacturer's instructions. Measurements were performed using a TECAN Sunrise 200 microplate absorbance reader.

1.3 Results

1.3.1 Growth of DOT-T1E in the presence of different concentrations of *t*CA in liquid medium containing or not styrene in the gas phase

The genomic analysis of DOT-T1E indicated that this strain lacks the PAL enzyme for the conversion of phenylalanine into *trans*-cinnamic acid and the corresponding *trans*-cinnamic acid decarboxylase required to produce styrene (Udaondo et al., 2016). A number of *Pseudomonas* strains have been described that can use styrene as the sole C-source via the styrene monooxygenase pathway. In this pathway, the aromatic hydrocarbon is oxidized to produce styrene oxide, which is subsequently metabolized to phenylacetaldehyde and phenylacetic acid before it is directed to central metabolism (Hartmans et al., 1990). The metabolic analysis of the genome of this strain revealed that DOT-T1E lacks the styrene oxidation system (Udaondo et al., 2016). We found, as expected, that DOT-T1E does not grow with styrene when this compound was supplied as the sole C-source.

Although strains of *P. stutzeri* have been described that can use cinnamic acid as the sole C-source (Andreoni & Nestetti, 1986), no such findings have been published for *P. putida*. To confirm that *P. putida* DOT-T1E does not use *trans*-cinnamic acid as a C-source to produce biomass, we inoculated *P. putida* DOT-T1E in M9 minimal medium with 10 mM *trans*-cinnamic acid as the sole C-source at an initial turbidity of 0.05 at 660 nm, and monitored culture turbidity for 72 h. No growth was observed. To determine if these aromatic compounds affect growth, we set up cultures with glucose and 10 mM *trans*-cinnamic acid or styrene supplied through the gas phase and determined growth rates, cell density, and yields of the cultures (Table 1.1). We found that in the glucose medium the strain grew exponentially until reaching high cell density (Table 1.1) and a biomass yield of 0.4 ± 0.01 g/g glucose. Doubling time in this medium with glucose was around 90 min (Table 1.1). Growth with glucose as the carbon source was not halted in the presence of 10 mM *trans*-cinnamic acid or styrene in the gas phase although the growth rates and yields were slightly lower in the presence of the aromatics (Table 1.1), suggesting that the strain needed to expend energy in order to thrive in the presence of the chemicals. The growth yield in the presence of either aromatic compound was lower than without (i.e., 0.39 to 0.32 g/g glucose). This, therefore, confirms that DOT-T1E is a potential host for the biotransformation of phenylalanine into styrene via *trans*-cinnamic acid; however, production conditions will need to be optimized to decrease the intrinsic negative effects associated with the noxious nature of the chemicals.

Table 1.1: Growth characteristics of *P. putida* DOT-T1E with glucose in the absence and in the presence of *trans*-cinnamic acid and styrene in the gas phase.

Compounds in the culture medium	**tg**	**CFU $mL^{-1}{}_{max}$**	**Y**
Glucose	90.8 ± 0.0	6.67E+09 ± 1.18+08	0.40 ± 0.01
Glucose + styrene (g)	88.5 ± 20.7	2.28E+09 ± 1.53E+08	0.39 ± 0.02
Glucose + 10 mM *t*CA	96.5 ± 5.9	5.33E+09 ± 1.30E+09	0.33 ± 0.01
Glucose + 10 mM *t*CA + styrene (g)	96.8 ± 3.2	1.48E+09 ± 2.71E+08	0.32 ± 0.01

tg, generation time (min); CFU $mL^{-1}{}_{max}$, maximum colony forming units; Y, yield (g cells g^{-1} sugar consumed in 24 h). The data are the average of at least two independent assays done each in triplicate ± standard deviations.

We tested growth of DOT-T1E in the presence of increasing concentrations of *trans*-cinnamic acid to determine its inhibitory potential. To this end, we determined CFU mL^{-1} rather than conducting turbidity measurements, which would have given misleading results due to the ability of dead cells to affect turbidity. We found that

concentrations below 25 mM *trans*-cinnamic acid did not result in halted growth (Figure 1.1); however, concentrations above 50 mM not only prevented growth but also led to loss of cell viability after several hours of incubation. The number of CFU mL^{-1} decreased faster as the concentration of the acid increased in the medium (Figure 1.1).

It has been reported before that exposure of cells to subinhibitory concentrations of chemicals can induce defense mechanisms that lead to enhanced tolerance to the noxious chemicals (Heipieper et al., 2007; Ramos et al., 1998). For this reason, *P. putida* DOT-T1E cells were pre-grown on glucose plus 10 mM *trans*-cinnamic acid to see if pre-adaptation to this aromatic acid occurs and results in enhanced tolerance. To this end, cultures were transferred to the same medium but with 0, 15, 25, 50, 75 and 90 mM of the aromatic acid. Growth of the cells that were pre-exposed to *trans*-cinnamic acid was similar to the growth of cells that were not pre-exposed to the acid (Figure S1.1A).

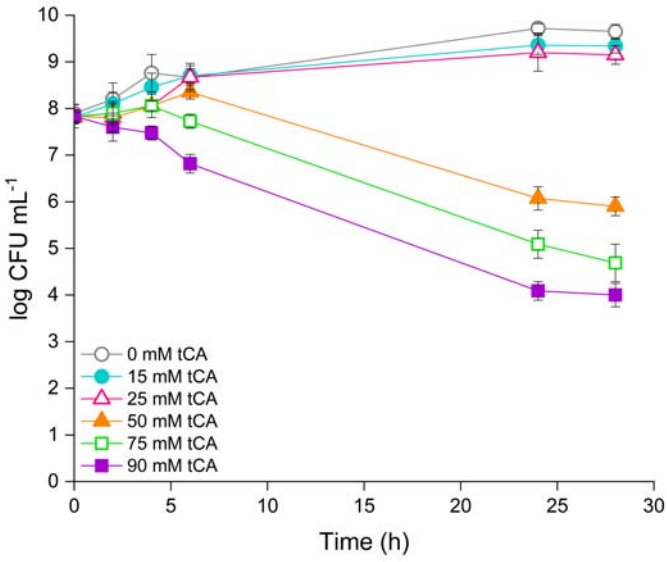

Figure 1.1: Tolerance of *P. putida* DOT-T1E to *trans*-cinnamic acid (0, 15, 25, 50, 75 and 90 mM) in M9 glucose. The results shown represent the averages and standard deviations of three independent assays. Control, grey open circles; with addition of *trans*-cinnamic acid at 15 mM (blue solid circle); 25 mM (pink open triangles); 50 mM (orange solid triangles); 75 mM (green open squares); and 90 mM (purple solid squares).

We also tested whether cells pre-exposed to styrene in the gas phase could enhance tolerance to *trans*-cinnamic acid. As above, styrene pre-exposed cells behaved

identically to cells that were not pre-exposed (Figure S1.1B). Similar results to those described above were obtained with *P. putida* DOT-T1E pre-grown with styrene and 10 mM *trans*-cinnamic acid in the liquid medium (Figure S1.1C).

Because styrene solubility in water is very low (310 mg L^{-1}), and *P. putida* DOT-T1E grows at saturating concentrations of styrene in water, the above series of assays cannot be performed for styrene. Instead, we analyzed the response of DOT-T1E growing in different culture media to sudden shocks of 0.1% (v/v) styrene or 50 mM of *trans*-cinnamic acid, as described below.

1.3.2 Survival of DOT-T1E in response to *trans*-cinnamic acid or styrene shock

In the following assays, we determined the survival in the short term of DOT-T1E grown on glucose, glucose plus 10 mM *t*CA, glucose plus styrene in the gas phase, and with the two test compounds simultaneously. In this series of assays, cells were grown until the mid of the exponential phase; at that point, we made a sudden addition of 50 mM *t*CA or 0.1% (v/v) styrene. We found that regardless of the growth conditions (i.e., glucose alone; glucose plus 10 mM *t*CA; glucose with styrene in gas phase; and glucose with the two aromatic compounds), DOT-T1E exposed to 50 mM *t*CA survived in the short term (i.e., 60 min) without a significant decrease in the number of viable cells (Figure 1.2).

In another series of assays, 0.1% (v/v) styrene was added to the liquid medium. For glucose-grown cells, upon styrene addition, only around 1 in 10^4 CFU mL^{-1} survived the solvent shock (Figure 1.2). This low number of viable cells remained constant for 60–180 min but began to recover after 4 h incubation, so that growth was restored (not shown). In contrast, when cells had been pre-adapted to styrene in the gas phase (in the absence or in the presence of *trans*-cinnamic acid), around 90% of cells survived. We also tested if pre-adaptation to 10 mM *trans*-cinnamic acid affected cell tolerance to a sudden styrene shock. We found an intermediate situation with 1 out 10^3 cells surviving a sudden styrene shock (Figure 1.2). These results suggest that this strain possesses a series of adaptive mechanisms for styrene, which are induced by either the aromatic hydrocarbon or the acidic aromatic compound.

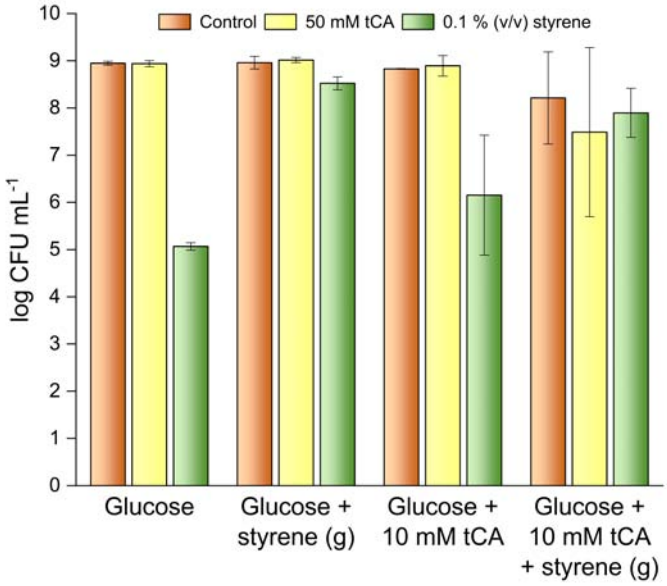

Figure 1.2: Survival of *P. putida* DOT-T1E to sudden shocks of *trans*-cinnamic acid (50 mM) and styrene (0.1% (v/v)) in cells grown on glucose, glucose plus styrene in the gas phase, glucose plus 10 mM *trans*-cinnamic acid or with the two test compounds simultaneously. The results shown are the averages and standard deviations of three independent assays of cells that survived a 60 min shock upon addition of 50 mM *trans*-cinnamic acid (yellow bars) or 0.1% (v/v) styrene (green bars). The control assay is represented in orange.

Segura et al. (2003) previously found that different *P. putida* strains exhibited differential sensitivity to toluene and xylenes. Of the tested strains, *P. putida* KT2440 was particularly sensitive to toluene regardless of the growth conditions. We have now grown KT2440 in M9 minimal medium with glucose in the absence and in the presence of styrene supplied through the gas phase and tested survival upon a sudden shock of 0.1% styrene. We found that the survival rate of KT2440 grown on glucose was below 1 in 10^8 CFU mL^{-1} (Figure S1.2A), and that the pre-growth in the presence of styrene had no effect on survival (Figure S1.2B). When the same assay was performed with *E. coli* ET8000, a potential chassis to produce styrene, survival to the sudden solvent shock was below 1 in 10^9 CFU mL^{-1} (Figure S1.2). This makes DOT-T1E a *sine qua non* chassis for production of this toxic chemical.

In previous studies, we reported that cells grown with toluene in the gas phase survived a sudden shock of 1% (v/v) toluene (Ramos et al., 1998). We grew DOT-T1E cells on M9 minimal medium with glucose and toluene supplied in the gas phase, and exposed these cells to sudden styrene shocks as above. We found that growth of

DOT-T1E in the presence of toluene enabled the strain to survive styrene shocks, as expected, which suggests that a series of common mechanisms are induced to protect cells against the presence of aromatic hydrocarbons (not shown).

In *Pseudomonas* it is well established that in response to a number of insults (toxic organic chemicals, metals, antibiotics, etc.) cells fortify their membranes by activation of a constitutively made *cis–trans* isomerase that catalyzes the isomerization of *cis* unsaturated fatty acids to their corresponding *trans*-isomers (Bernal et al., 2007a; Heipieper et al., 2007; Junker & Ramos, 1999; Weber et al., 1993, 1994; Wierckx et al., 2008, 2009). To confirm that styrene and *trans*-cinnamic acid provoked the general response to the chemicals under study, we determined *cis*/*trans* fatty acid ratios. The *cis*/*trans* ratio in glucose-grown cells was 4.03, with C16:1,9 *cis* being the most abundant unsaturated fatty acid (about 23% of total) (Table 1.2).

Table 1.2: Fatty acid composition of *P. putida* DOT-T1E cells grown on glucose in the absence or in the presence of *trans*-cinnamic acid (*t*CA), styrene supplied in the gas phase (g) or both aromatic compounds simultaneously (*t*CA + styrene (g)). Values are the average and standard derivations of three assays.

Fatty acid	**Growth medium**			
	Glucose	**Glucose + 10 mM *t*CA**	**Glucose + styrene (g)**	**Glucose + 10 mM *t*CA + styrene (g)**
C14:0	0.19 ± 0.01	0.20 ± 0.00	0.14 ± 0.02	0.15 ± 0.02
C15:0	0.04 ± 0.00	0.04 ± 0.01	0.11 ± 0.03	0.07 ± 0.00
C16:1,9 cis	23.14 ± 0.84	15.73 ± 1.10	19.51 ± 0.29	13.52 ± 2.89
C16:1,9 trans	10.49 ± 1.11	18.04 ± 0.97	12.56 ± 0.11	19.85 ± 0.88
C16:0	23.63 ± 0.44	23.77 ± 0.02	22.80 ± 1.11	23.45 ± 2.34
C17:cyclo	4.96 ± 0.14	5.68 ± 0.00	4.61 ± 0.66	4.63 ± 0.43
C17:0	0.06 ± 0.00	0.06 ± 0.00	0.42 ± 0.11	0.17 ± 0.05
C18:1,11 cis	32.40 ± 0.17	28.55 ± 0.82	32.68 ± 0.14	28.05 ± 0.08
C18:1,11 trans	3.28 ± 0.48	6.23 ± 0.95	4.98 ± 0.28	7.65 ± 3.54
C18:0	1.75 ± 0.00	1.64 ± 0.01	2.11 ± 0.27	1.82 ± 0.26
C19:cyclo	0.00 ± 0.00	0.00 ± 0.00	0.00 ± 0.00	0.00 ± 0.00
TOTAL (%)	100	100	100	100
cis/trans	4.03 ± 0.54	1.82 ± 0.22	2.97 ± 0.09	1.50 ± 0.34
sat/insat	0.37 ± 0.01	0.37 ± 0.00	0.37 ± 0.01	0.37 ± 0.04

When cells were grown in the presence of *trans*-cinnamic acid, styrene, or both compounds, the *cis*/*trans* ratio was lower, in the range of 2.9 to 1.5. Under these conditions, the level of C16:1,9 *cis* was almost as high as the corresponding *trans* isomers,

and the ratio of *trans* C18,1:11 was two-fold higher than in the absence of stressors (Table 1.2). These results support the notion that cells fortify their membranes via a fast *cis* to *trans* isomerization in response to toxic aromatic compounds.

1.3.3 Transcriptional and proteomic responses to *trans*-cinnamic acid and styrene

As a next step, we used omics approaches to analyze the specific responses of the strain to the stressors. Transcriptomic analyses were carried out in triplicate (see Volcano plots in Figure S1.3) and the values were considered statistically different if there was a change of $\log_2 \geq 2.0$ or $\log_2 \leq -2.0$ and a p-value < 0.05. Data were analyzed from different angles to extract as much information as possible. Tables 1.3 and 1.4 show that a limited number of genes were significantly up- or downregulated in response to the stressor. We found about 240 genes were overexpressed in response to styrene, 209 in response to *trans*-cinnamic acid and 337 in response to the simultaneous presence of both aromatic compounds (Table 1.3). Regarding downregulated genes, we found that 129, 132 and 141 genes were expressed at lower levels in the presence of styrene, *trans*-cinnamic acid, or both aromatic compounds, respectively (Table 1.4). It should be noted that a number of genes with unknown functions were also induced or repressed in response to either styrene or *trans*-cinnamic acid (Tables S1.2, S1.3 and S1.4). Proteomic and transcriptomic analyses revealed similar trends although, in general, the fold change of the induced and repressed proteins were lower. Below we analyze the transcriptomic data in detail and provide a summary of insights from the proteomic analysis.

Although the number of genes within a specific set of functions varied among the control (glucose) and the three tested conditions, a similar gene upregulation trend in the presence of aromatic chemicals was observed for transmembrane proteins and those involved in sugar uptake/metabolism, Krebs cycle, respiratory chains and ATP synthesis (Tables S1.3 and S1.4).

This common metabolic response to stressors may be related to the need to generate energy to overcome the negative effects of these molecules. In fact, we found that in cells growing with glucose as the sole carbon source, glucose was consumed at a higher rate in the presence of styrene regardless of the presence of *trans*-cinnamic acid (Figure 1.3). Also, because the growth yield was lower when these aromatics

were present, versus when glucose was the sole carbon source, we inferred that energy consumption is needed to cope with the toxicity.

Table 1.3: Number of genes upregulated of *P. putida* DOT-T1E in response to *trans*-cinnamic acid (*t*CA), styrene supplied in the gas phase or both aromatic compounds.

Gene category	***t*CA**	**Styrene (g)**	**Styrene (g) + *t*CA**
Amino acid and protein biosynthesis	40	24	59
Amino acid, peptide and protein metabolic process	0	6	6
Antiholins	2	2	1
Aromatic compound catabolic process	7	9	11
ATP synthesis	10	6	8
Cell division	0	6	0
Cell shape	4	1	2
DNA replication, recombination and repair	6	1	14
Efflux pump	10	10	11
Glyoxylate metabolic process	0	2	0
Krebs cycle	16	16	20
Lipid metabolic process	0	7	10
Membrane component	33	48	61
Oxidoreductase activity	4	1	0
Phosphate metabolism	0	1	1
Propionate metabolism	0	5	4
Respiration	24	24	23
Stress	17	21	41
Sugar uptake/metabolism	19	17	21
Sulfur metabolism	1	3	7
Transcription and translation	8	26	32
Urea cycle/nitrogen metabolism	8	4	5
TOTAL	209	240	337

Table 1.4: Number of genes downregulated of *P. putida* DOT-T1E in response to *trans*-cinnamic acid (*t*CA), styrene supplied in the gas phase or both aromatic compounds.

Gene category	***t*CA**	**Styrene (g)**	**Styrene (g) + *t*CA**
Amino acid and protein biosynthesis	5	2	3
Amino acid, peptide and protein metabolic process	24	19	17
Cell adhesion	0	1	1
Cell motility	3	3	2
Cell shape	5	4	4
Cell wall hydrolase	1	0	0
Efflux pump	2	3	3
Gluconeogenesis	1	1	1
Glyoxylate metabolic process	0	2	2
Krebs cycle	1	0	0
Lipid metabolic process	0	3	3
Membrane component	32	45	48
Nitrogen metabolism	1	0	1
Organic catabolic process	7	4	8
Polysaccharide biosynthetic process	0	1	2
Pyrroloquinoline quinone biosynthetic process	6	5	6
Respiration	2	2	5
Stress	9	8	5
Sugar uptake/metabolism	3	5	8
Transcription and translation	30	21	22
TOTAL	132	129	141

Glucose is metabolized in *P. putida* through three convergent pathways that convert glucose into 6-phosphogluconate (del Castillo et al., 2008). In response to the aromatic compounds, the porin OprB (involved in glucose uptake) and an ABC glucose transporter were induced by at least two-fold under all conditions (Table S1.3). This agrees with the genetic organization of the *oprB* gene being part of the operon containing the ABC transporter (Udaondo et al., 2018). We also found that the direct phosphorylation of glucose to glucose-6-phosphate catalyzed by glucose kinase (Glk) followed by glucose dehydrogenase (Zwf) was induced while the keto gluconate pathway was not. The final product of this branch for glucose metabolism is 6-phosphogluconate, which enters the Entner-Doudoroff pathway with EDD and EDA yielding glyceraldehyde-3-P and pyruvate. Our results show that the two steps of the Entner-Doudoroff pathway were induced. This is also consistent with the fact that *edd* belongs to an operon with the glucokinase gene (*glk*); as well as with the

fact that the *eda* gene is in an operon with *zwf* and *pgl* (Domínguez-Cuevas et al., 2006; Udaondo et al., 2018) (Table S1.3). Regarding repressed genes, we found that the genes for the biosynthesis of PQQ, the cofactor of gluconate dehydrogenase in the metabolism of glucose, were repressed as well as the gluconate transporter (Table S1.4). These findings support the hypothesis that under aromatic compound stress conditions, the glucose-6-phosphate pathway becomes predominant. Therefore, under aromatic stress conditions, it seems that glucose is preferentially assimilated through the glucose phosphorylative pathway.

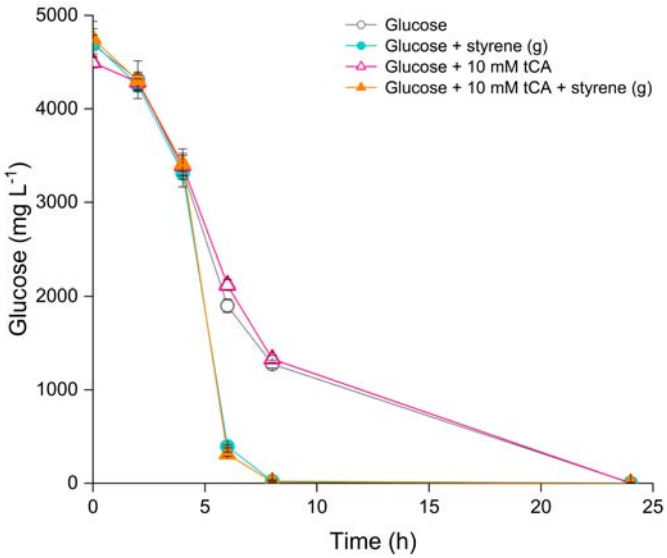

Figure 1.3: Glucose consumption by *P. putida* DOT-T1E in the absence and in the presence of non-metabolizable aromatic compounds. Control cells growing with glucose alone (grey open circles), glucose plus styrene in the gas phase (blue solid circles), glucose plus 10 mM *trans*-cinnamic acid (pink open triangles), or the two compounds simultaneously (orange solid triangles).

Genes encoding Krebs cycle enzymes were induced between 2.0 and 4.9-fold regardless of the aromatic in the culture medium. Some of the genes were organized in clusters such as *suc* (T1E_0425 to T1E_0429), *sdh* and *icd/idh* genes (T1E_0537 and T1E_0538). Two citrate synthase genes (*gltA* and *prpC*) (T1E_0434 and T1E_5347) were also induced, leading to an increased ability to channel acetyl-CoA quickly and efficiently into the respiratory chain. Phosphoenolpyruvate carboxylase, which is involved in replenishment of the Krebs cycle intermediate oxalacetic acid (OAA), was induced by about two-fold (Table S1.3). In response to stress created by styrene (with and without *trans*-cinnamic acid), an NADH oxido-reductase was induced, together

with a set of respiratory chain cytochromes (*nuoFIJKLM*) (T1E_4593, T1E_0717 to T1E_0720, T1E_0725, T1E_0824, T1E_0825, T1E_4136 to T1E_4145). The terminal CyoBCDE complex was also induced.

Along with the induction of an NADH-quinone oxidoreductase and a series of cytochromes, ATP synthase genes (*atpIBEFHAGDC*) were also induced by 2.2- to 5.2-fold (Table S1.3). Also related to energy use, genes in the urea cycle (*arc*) (T1E_1977 to T1E_1979) were induced 3- to 6-fold (Table S1.3). In accordance with these transcriptomic data, protein levels that increased in response to aromatic compounds were those involved in glucose metabolism, the Krebs cycle and respiratory chains (NADH oxidases and cytochromes) (Table S1.3).

Relevant to the induction of Krebs cycle genes was our observed repression of the glyoxylate shunt, along with repression of certain genes involved in the respiratory chain (i.e., *yce*, *ped*), which would be expected to accommodate changes to the cellular carbon flux (Table S1.4).

Other induced genes included a number of efflux pumps and stress response proteins, along with catabolic pathways for aromatics, which were highly induced (Table S1.3). We found that in response to *trans*-cinnamic acid, *ttgABC* genes (T1E_0243, T1E_0242 and T1E_0241) were induced between 2- and 3-fold, while *ttgDEF* (T1E_4281, T1E_4280 and T1E_4279) were induced between 2- and 4-fold in response to styrene. The greatest increase in protein levels corresponded to TtgGHI and TtgDEF efflux pumps, which were present at levels that were 2.5- and 3-fold higher than in the absence of aromatics (Table S1.5). In addition to the above efflux pumps known to be involved in aromatic extrusion, we found two undescribed efflux pumps—*mtrABC* and *yhiUVW*—that were induced between 2.3- and 5.7-fold, respectively (Table S1.3). The specific substrates of these efflux pumps are unknown.

Domínguez-Cuevas et al. (2006) reported that the stress response is needed to counteract the toxicity of aromatic compounds in *Pseudomonas*. Our observations confirm this by demonstrating that in the presence of only one aromatic compound (i.e., styrene or *trans*-cinnamic acid), there was an induction of UspA family members (T1E_0387, T1E_2745, T1E_5564, T1E_5566, T1E_5582 and T1E_5584), alkylperoxidases (T1E_4718), catalases (T1E_3479), DUF domain proteins (T1E_1888) and chaperones (i.e., ClpB (T1E_0798) and Hsp20 (T1E_5574)) (Table S1.3). When both aromatic compounds were present, they enhanced the stress imposed on the cells and

in addition to all of the above-mentioned defense systems, induced overexpression of a number of chaperones. This indicates that there is an additive effect when the two aromatic compounds are present. The chaperones that we found induced included the GroEL complex, SurA (T1E_2150), HtpG (T1E_2387) and GroSL (T1E_4380, T1E_4381), as well as enzymes related to general stress such as XenA/B (overexpressed by up to 7.7-fold) and, with oxygen stress such as glutathione transferases (T1E_0524, T1E_3573, T1E_4366) and a superoxide dismutase (T1E_1925) (Table S1.3). The activation of ROS proteins may be related to the accelerated electron flux through the respiratory chain and the production of reactive oxygen species (ROS). For stress response genes, proteomic analyses agreed with transcriptomic data. We found heightened levels of alkylhydroperoxidases, glutathione oxidase (involved in quenching ROS), and protein folding chaperones (Tables S1.3 and S1.5). The differences that we observed between the three conditions included changes in the induction of regulators: 26 were altered in the presence of styrene, 8 with *trans*-cinnamic acid and 32 in the presence of both.

Although neither styrene nor *trans*-cinnamic acid can be metabolized by the cells, they induced certain catabolic pathways. It is known that a number of regulators exhibit an effector specificity other than the catabolic pathway they regulate (Busch et al., 2007; Matilla et al., 2021). In the presence of styrene, the toluene dioxygenase pathway (*tod*) was induced, while in the presence of *trans*-cinnamic acid, the *p*-cumate pathway was induced (Table S1.3). In the presence of both compounds, pathways for the degradation of toluene and *p*-cumate were induced, although the level of induction was lower with both aromatic compounds—a result that may indicate that effector competition is occurring, as has been described for the TodS/TodT system (Busch et al., 2007; Lacal et al., 2006).

Among the set of membrane proteins that were induced, a number of them are known to be involved in maintaining cell membrane structure. The conserved Tol-Pal trans-envelope complex is important for outer membrane stability and cell division in Gram-negative bacteria (Gerding et al., 2007). It has been proposed that the Tol-Pal system mediates outer membrane constriction during cell division via cell wall tethering. For example, it has been shown that the TolB protein is involved in the maintenance of the *P. putida* cell membrane structure (Rodríguez-Herva et al., 2007). Related to this is the activation or overexpression of antiholins LrgA and LrgB, which were induced (3.7- to 5.0-fold) and which are thought to control peptidoglycan

hydrolysis. Our findings implicate them in the stress response as modulators of membrane integrity.

We observed signs of active protein synthesis in the three conditions with stressors (Table S1.3). This was likely an effort by the cell to replace damaged proteins, and the response was exacerbated when both aromatic compounds were simultaneously present (Table S1.3). In response to styrene, 18 genes involved in amino acid biosynthesis and 6 genes involved in protein synthesis were induced, suggesting a potential role for amino acid metabolism in styrene resistance. Also induced were *glnA* (glutamine synthetase) and *gltB* (glutamate synthase), which are needed for the incorporation of ammonium into organic carbon and its alternative channeling to amino acid biosynthesis. Regarding sulfur metabolism, we found that the cysteine biosynthesis cluster (T1E_0565, T1E_0566 and T1E_4456 to T1E_4460) was induced when styrene and *t*CA were present in the culture media (Table S1.3).

We also found that catabolism of histidine (His) and phenylalanine (Phe) was repressed in the presence of one or both of the aromatic compounds. Whether this results from the need for those amino acids for biosynthetic processes or repression due to their aromatic nature, is unknown.

Trans-cinnamic acid, styrene and their combination resulted in rather strong inhibition of a number of transporters. Some of these were found in operons related to the transport of amino acids (i.e., T1E_2666, T1E_2667, T1E_3208, T1E_0341, T1E_3315) and potassium (T1E_2369) (Table S1.4). While some transporters were downregulated in the presence of *trans*-cinnamic acid (i.e., T1E_1254, T1E_3944, T1E_0320, T1E_0710, etc.), this was not the case for styrene (Table S1.4). The additive toxicity of *trans*-cinnamic acid plus styrene was apparent by the fact that a large number of transporters were repressed only when the two aromatic compounds were present (i.e., T1E_2543, T1E_4501, T1E_4503, T1E_4502). No other common patterns were found, but the list of all genes repressed in each condition that we tested is provided in Table S1.4.

Proteomic analysis revealed a correlation between the upregulated genes and the proteins induced under the same conditions. In the presence of styrene or styrene plus *trans*-cinnamic acid, there were increased levels of proteins related to amino acid metabolism, aromatic compound catabolic pathways, efflux pumps, Krebs cycle, cell membrane, transcriptional regulators, and stress response proteins (Table S1.5).

1.3.4 Mutational analyses to identify genes functionally relevant to stress responses induced by *trans*-cinnamic acid or styrene

In order to test the importance of genes implicated in the stress response through transcriptional data, mutational analyses were carried out. For a number of the genes that we identified, mutants in *P. putida* DOT-T1E were already available (Rojas et al., 2001; Segura et al., 2001). We also constructed mutants related to the Krebs cycle (SucC, PflU) and urea cycle (ArcA) (see Experimental procedures section 1.2.10). Using this collection, the survival of each of the mutants to shocks of 50 mM *trans*-cinnamic acid or 0.1% (v/v) styrene was tested. We found that when the cells were grown on glucose or glucose plus styrene in the gas phase, the sudden shock of 50 mM *trans*-cinnamic acid was well tolerated by all mutants tested (Figure 1.4A, C).

Styrene is significantly more toxic than *trans*-cinnamic acid, and this was deduced because a number of mutants were extremely sensitive to a sudden styrene shock, although toxicity varied based on growth conditions. In wild-type DOT-T1E grown on glucose, the sudden addition of 0.1% (v/v) styrene led to loss of viability by 4 orders of magnitude. In the absence of pre-adaption to hydrocarbons, mutants deficient in TtgB or TtgH, or both, exhibited a loss of viability by around 7 orders of magnitude upon the sudden addition of the chemicals. In this regard, it is worth mentioning that this mutant in terms of efflux pumps is equivalent to KT2440, which exhibits the TtgABC efflux pump but not the other two efflux pumps identified here as relevant in tolerance to styrene, TtgDEF and TtgGHI. Under the same conditions, mutants deficient in PflU and SucC exhibited a 5 to 6 order of magnitude loss of cell viability (Figure 1.4A). Mutants for TtgD, TtgV, TtgR, FliA, FliP, FliL, Cti, CspA2, XenA, ET-Tu and ArcA suffered a drop in viability in response to a sudden styrene shock similar to the wild-type (Figure 1.4C). This suggests that TtgABC and, in particular, TtgGHI are relevant in the response to styrene as well as the Krebs cycle enzymes.

When cells were pre-induced with low concentrations of styrene (i.e., in the gas phase), the most sensitive single mutant was TtgH, which experienced a viability drop by 4 orders of magnitude (Figure 1.4B). Under the same conditions, the viability of the TtgB mutant decreased by around 2 orders of magnitude. It should be noted that the double mutant *ttgB/ttgH* was extremely sensitive to styrene shock, while this extreme sensitivity was not observed for a *ttgB/ttgD* double mutant (Figure 1.4B). No loss of viability was found with mutants in *sucC* or *pflU* when cells were pre-

induced with styrene (Figure 1.4B). Mutants for TtgD, TtgV, TtgR, FliA, FliP, FliL, Cti, CspA2, XenA, ET-Tu and ArcA pre-grown in the presence of styrene in the gas phase did not suffer a drop in viability in response to a sudden styrene shock similar to the wild-type (Figure 1.4D). This suggests that TtgGHI is the most relevant pump to styrene extrusion, while TtgABC and TtgDEF play accessory roles. Given that the *ttgGHI* efflux pump genes are on a self-transmissible plasmid, we predict that the transfer of this pump to other chassis would be useful for the bioproduction of aromatic compounds.

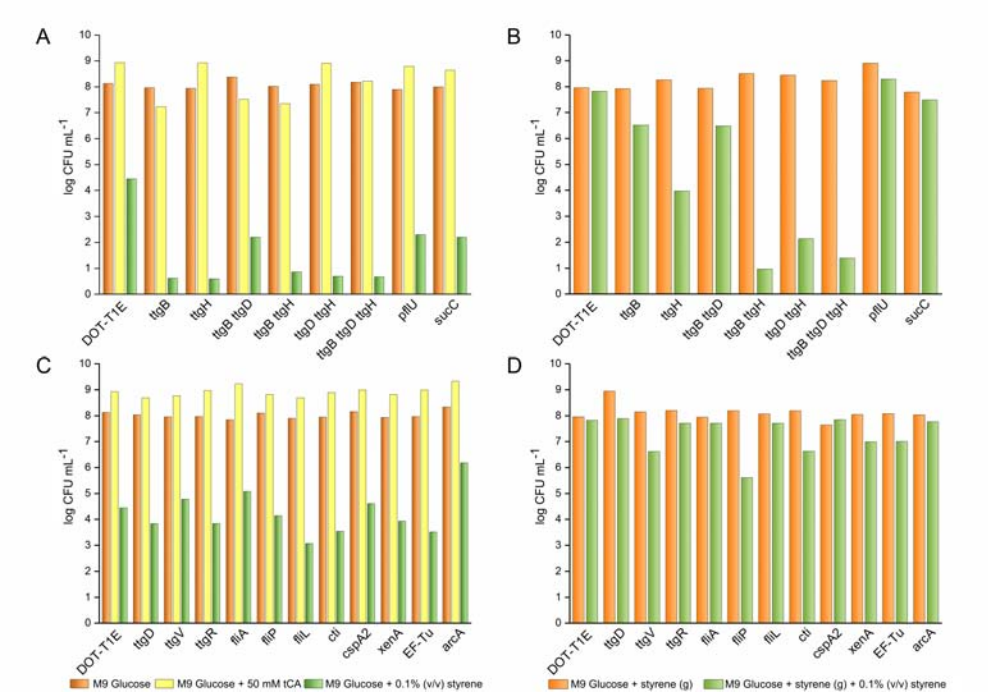

Figure 1.4: Survival of *P. putida* DOT-T1E mutants grown on glucose (A and C) or grown on glucose with styrene in the gas phase (B and D) after 60 min exposure to *trans*-cinnamic acid (50 mM) or styrene (0.1% (v/v)). Panel A and panel B show mutants highly sensitive to a sudden styrene shock when grown on glucose, while C and D show mutants as sensitive as the wild-type strain to styrene when grown on glucose. Control without addition, orange bars; plus 50 mM *trans*-cinnamic acid, yellow bars; plus 0.1% (v/v) styrene, green bars.

1.4 Discussion

Petrochemicals can be found all around us. They are components in the cars we drive, the fuels that power them, and are used to make packaging, textiles, paints, dyes, medical equipment, detergents and more. The manufacture of petrochemical compounds and their derivatives consume about 14% of the oil and gas used in the world (International Energy Agency, 2018). Petrochemicals provide us with an array of services, including sustenance, mobility and heating and cooling—services that encompass our universal needs as humans. Because we cannot replace goods produced from petrochemicals in the short term, the contribution of the petrochemical industry to climate change is often overlooked and receives less attention than the transport and energy sectors (Service, 2019).

Webb (2012) indicated that our dependency on dwindling fossil resources and our growing awareness of the dangers posed by climate change are major driving forces for the transition towards the production of sustainable compounds from renewable feedstocks, such as lignocellulosic residues (Bertacchi et al., 2022). Lignocellulose can be processed to separate cellulose and hemicellulose polysaccharides from lignin. The former can be broken into their constituent sugars using enzymatic cocktails (Álvarez et al., 2016; Bertacchi et al., 2022). Fermentation of the resulting monomeric sugars, which is known as a second-generation (2G) process (Valdivia et al., 2016), can be carried out at room temperature using recombinant microbial chassis. This process can be used to produce value-added chemicals and represents an approach that would have profound effects on the chemical industry by significantly reducing energy costs and CO_2 emissions (Bertacchi et al., 2022; Ramos & Duque, 2019).

We have concentrated our efforts on two aromatic compounds as potential bio-products from 2G sugars; namely, styrene and *trans*-cinnamic acid. Styrene is one of the most used chemicals because it is employed in the production of polymers. The total global production of styrene in 2010 was 25 million tons. Currently, about 90% of the world's production is based on the direct dehydrogenation of ethylbenzene under operating conditions that involve the use of temperatures above 600°C, iron oxide as a catalyst and a large amount of water vapor for heating purposes and reduction of coke formation (Gupta et al., 2022). Conventional styrene production processes consume 10 times as much energy as the production of similar chemicals (e.g., aromatic compounds such as benzene, toluene and xylene) and is, within the

petrochemical sector, a major contributor to greenhouse gas emissions, including methane and CO_2 (McKenna & Nielsen, 2011).

Although it may not be widely acknowledged, styrene is a biogenic product. Styrene is naturally synthesized by plants and microbes from L-phenylalanine, and it has been found as a trace metabolite in cheeses, where it can cause an aroma defect that leads to consumer rejection. It has also been reported to be released by plants of the family *Styracaceae* (Fernandez et al., 2005). McKenna and Nielsen (2011) revealed that co-expression of a phenylalanine ammonia lyase and a *trans*-cinnamic decarboxylase in *E. coli* leads to styrene production, although production required the supply of L-phenylalanine exogenously because the production level was low, and maximum productivity was inhibited by styrene's extreme toxicity. It has been recognized that the use of solvent-tolerant hosts may be a way to improve styrene biosynthesis (Machas et al., 2021; McKenna & Nielsen, 2011). *Trans*-cinnamic acid derivatives such as cinnamaldehyde, cinnamyl alcohol and hydro cinnamyl alcohol are widely used aroma compounds, with applications in the flavor, food, and cosmetic industry, as well as use as antimicrobials, a nematicide and anti-inflammatory agents. Therefore, this chemical is another interesting target for biological production.

Pseudomonas putida: a promising platform for aromatic chemical bioproduction

The effectiveness of various microbial hosts (e.g., *E. coli*, *Clostridium acetobutylicum*, *Corynebacteria* and yeasts) for the production of chemicals is often limited by the inherent sensitivity of the host to the chemical of interest. This is particularly true when synthetic pathways have been developed to produce aromatic hydrocarbons and medium chain alcohols such as butanol in *Clostridium* (Green, 2011; Re & Mazzoli, 2022); isobutanol in *E. coli* and yeasts (Atsumi et al., 2010; Yu et al., 2016a); and aromatic compounds (e.g., 2-phenylethanol and styrene) in *E. coli* (McKenna & Nielsen, 2011; Molina-Santiago et al., 2016).

Over the last 10 years, interest in using *P. putida* as a chassis for the production of industrially important chemicals (i.e., *p*-hydroxybenzoate or *p*-hydroxystyrene) (Verhoef et al., 2009, 2010) has significantly increased because of its advantages in robustness and metabolic versatility, and the fact that *Pseudomonas putida* is certified by NIH as safe to manipulate (Kampers et al., 2019). Furthermore, a number of

P. putida strains demonstrate resistance to aromatic compounds—in fact, some have been described to thrive in the presence of up to 90% toluene in double phase systems (Ramos et al., 2015).

Pseudomonas putida DOT-T1E strain was isolated by our group in Granada and it represents, together with the S12 strain (Weber et al., 1993), the most organic solvent-tolerant microorganism ever described. This makes it an ideal host for production of toxic chemicals such as aromatic hydrocarbons and aromatic amino acids. Previously, this strain was shown to be a suitable host for the production of *p*-hydroxybenzoate from sugars in a joint project that we developed with Dupont (Ramos-González et al., 2003). Later, we showed that it can be used to produce phenylalanine from sugars (Godoy et al., 2021).

In this study, we revealed the detailed physiological and biochemical responses of this strain to styrene and *trans*-cinnamic acid. Exposure to styrene or the aromatic acid activated a series of defensive tactics, some of which were 'common' in that they occurred after insult by a range of compounds (e.g., dyes, antibiotics and ROS generating compounds). These defensive tactics include the *cis–trans* isomerization of unsaturated fatty acids to strengthen the cell membrane (Heipieper et al., 2007; Junker & Ramos, 1999), and the synthesis of molecular chaperones that help to overcome the toxic effects of chemicals on unfolded proteins (Ramos et al., 2015; Segura et al., 2001). We found that the presence of *trans*-cinnamic acid and/or styrene led to changes in bacterial metabolism, with a shift to the glucose phosphorylative pathway, an increase in Krebs cycle enzymes, and the modification of the components of respiratory chains. As a consequence, higher respiration levels were observed, enabling extra energy to be generated in the presence of toxic compounds. The mechanism for extruding the toxic chemical(s) from the cell cytoplasm, periplasm and membrane was extremely important. Several RND family efflux pumps are key players in this process; specifically, TtgGHI (plasmid-encoded) and TtgABC (chromosomally encoded). In fact, mutants deficient in these efflux pumps were sensitive to the aromatic compounds, and this sensitivity was exacerbated when both styrene and *trans*-cinnamic acid were simultaneously present.

These results are in contrast with a recent study by Machas et al. (2021), which purports that the main response of *E. coli* at the transcriptional level involves: (i) general stress response (*rpoH* and *marA* genes); (ii) induction of membrane stability genes, such as those of phage shock protein response; and (iii) cell membrane mod-

ification, including those required for peptidoglycan cross-linking with lipoproteins. However, the study reported no induction of efflux pumps transporters. Thus, while the two Gram-negative *E. coli* and *P. putida* respond to solvents by strengthening cell membranes, *P. putida* uses an additional weapon, the induction of efflux pumps to keep intracellular solvent concentrations low.

Because *ttgGHI* genes are found on a self-transmissible plasmid that can be mobilized to other host platforms, such as the *E. coli* Gram-negative bacteria, our findings lay the foundation for new strategies to expand the range of toxic chemicals that other cell platforms can produce. Taken together, our findings provide deep insights that will help to advance the use of *P. putida* DOT-T1E and other microorganisms as aromatic chemical bioproduction chassis, and move us closer to achieving a more sustainable low-carbon green chemistry future. From a biosynthesis point of view, our results suggest that a synthetic pathway that enables the efficient conversion of phenylalanine to styrene without the accumulation of *trans*-cinnamic acid would produce high styrene yields.

Acknowledgements

This work was supported by grants from The Agencia Estatal de Investigación (AEI)—Ministry of Science and Technology RTI-2018-094370-B-100 and TED-2021-129632B-I00. The authors thank Rocío Palacios for technical support and Zulema Udaondo and Lázaro Molina for help with Volcano plots. We are thankful for experimental support from EEZ-CSIC Technical Services, CNB-CSIC proteomic services and the University of Málaga for genomic DNA sequencing services.

Author contributions

AGF: executed experiments, analyzed data, prepared art work. PG: executed experiments, analyzed data, prepared art work. ED: executed experiments, analyzed data, supervised work wrote the article. JLR: design the study, analyzed data, supervised work, wrote the article. All authors read and approved the final manuscript.

1.5 Supplementary Information

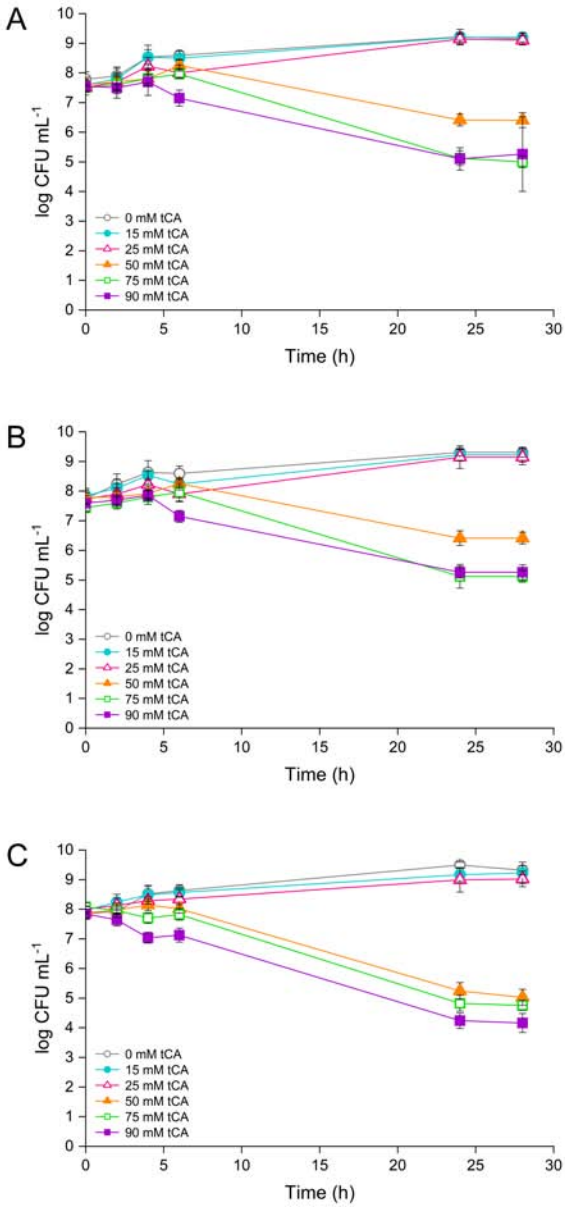

Figure S1.1: Tolerance of *P. putida* DOT-T1E to *trans*-cinnamic acid (0, 15, 25, 50, 75 and 90 mM) in A) M9 glucose plus 10 mM *trans*-cinnamic acid; B) M9 glucose plus styrene in the gas phase; and C) M9 glucose, 10 mM *trans*-cinnamic acid and styrene in the gas phase. The results represent the average and standard deviation of three independent assays. Control (grey open circles) or with the addition of *trans*-cinnamic acid at 15 mM (blue solid circles); 25 mM (pink open triangles); 50 mM (orange solid triangles); 75 mM (green open squares); and 90 mM (purple solid squares).

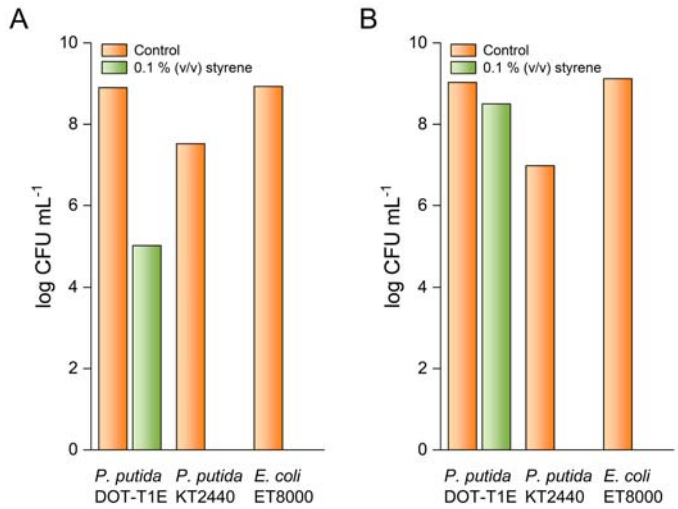

Figure S1.2: Survival of *P. putida* DOT-T1E, *P. putida* KT2440, and *E. coli* ET8000 grown on glucose (A) or grown on glucose with styrene in the gas phase (B) after 60 min exposure to styrene (0.1% (v/v)). Control without addition, orange bars; plus 0.1% (v/v) styrene, green bars.

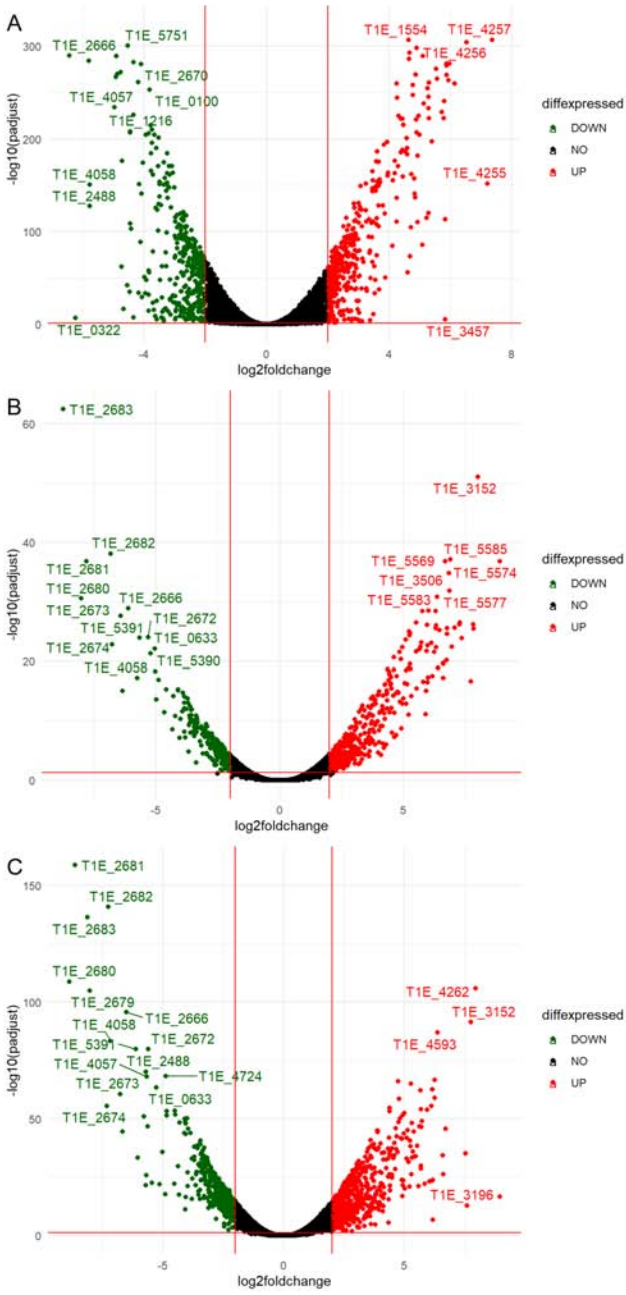

Figure S1.3: Volcano plot of *P. putida* DOT-T1E cells grown on M9 glucose plus 10 mM *trans*-cinnamic acid vs M9 glucose (A); M9 glucose with styrene in the gas phase vs M9 glucose (B); and M9 glucose plus 10 mM *trans*-cinnamic acid and styrene in the gas phase vs M9 glucose (C). Volcano plots showed that there were 973, 2200 and 2604 DEGs when cells were grown on styrene, *trans*-cinnamic acid or both compounds, respectively. The up-regulated genes were 548, 1137 and 1439, respectively, while 425, 1063 and 1165 were down-regulated genes.

Table S1.1: Primers used in this study.

Primer name	Sequence (5' → 3')
sucC3-F	CTGTAGTCGATCGTTCGAGCCG
sucC3-R	CAGGTTGACGATGTCCATGGT
pflU1-F	GTTCACGTAGGGGCCGCAGC
pflU1-R	CAGGTGCTCGGTTTCGGCAC
arcA1-F	GAACTGCTGTTCGACGATGTG
arcA1-R	GTGATGACCTCGATGCCGG

Table S1.2: Number of genes and proteins uncharacterized or without known function up- or downregulated in *P. putida* DOT-T1E in response to *trans*-cinnamic acid (*t*CA), styrene supplied in the gas phase or both compounds.

	Genes			**Proteins**		
	***t*CA**	**Styrene (g)**	**Styrene (g) + *t*CA**	***t*CA**	**Styrene (g)**	**Styrene (g) + *t*CA**
Up-regulated						
Uncharacterized	40	72	96	0	5	3
Unknown function	157	98	138	0	0	0
Down-regulated						
Uncharacterized	137	55	126	0	4	3
Unknown function	102	72	134	0	1	1

Table S1.3: Genes upregulated two-fold or more in response to *trans*-cinnamic acid (*t*CA), styrene supplied through the gas phase (Styrene (g)), or both compounds (*t*CA + Styrene (g)). Available on: https://microbialcellfactories.biomedcentral.com/articles/10.1186/s12934-023-02028-y.

Table S1.4: Genes downregulated two-fold or more in response to *trans*-cinnamic acid (*t*CA), styrene supplied through the gas phase (Styrene (g)), or both compounds (*t*CA + Styrene (g)). Available on: https://microbialcellfactories.biomedcentral.com/articles/10.1186/s12934-023-02028-y.

Table S1.5: Proteins induced 1.5-fold or more in response to styrene supplied through the gas phase (Styrene (g)), *trans*-cinnamic acid (*t*CA) or both compounds (Styrene(g) + *t*CA). Available on: https://microbialcellfactories.biomedcentral.com/articles/10.1186/s12934-023-02028-y.

Chapter 2

Engineering styrene biosynthesis: Designing a functional *trans*-cinnamic acid decarboxylase in *Pseudomonas*

Published as:

Ana García-Franco, Patricia Godoy, Estrella Duque and Juan L. Ramos. Engineering styrene biosynthesis: designing a functional *trans*-cinnamic acid decarboxylase in *Pseudomonas*. *Microbial Cell Factories*. **2024**, 23(69).

Abstract

We are interested in converting second generation feedstocks into styrene, a valuable chemical compound, using the solvent-tolerant *Pseudomonas putida* DOT-T1E as a chassis. Styrene biosynthesis takes place from L-phenylalanine (L-Phe) in two steps: firstly, L-Phe is converted into *trans*-cinnamic acid (*t*CA) by PAL enzymes and secondly, a decarboxylase yields styrene. This study focuses on designing and synthesizing a functional *trans*-cinnamic acid decarboxylase in *Pseudomonas putida*. To achieve this, we utilized the "wholesale" method, involving deriving two consensus sequences from multi-alignments of homologous yeast ferulate decarboxylase FDC1 sequences with >60% and >50% identity, respectively. These consensus sequences were used to design *Pseudomonas* codon-optimized genes named *psc1* and *psd1* and assays were conducted to test the activity in *P. putida*. Our results show that the PSC1 enzyme effectively decarboxylates *t*CA into styrene, whilst the PSD1 enzyme does not. The optimal conditions for the PSC1 enzyme, including pH and temperature, were determined. The DOT-T1E derivative *Pseudomonas putida* CM12-5 that overproduces L-Phe was used as the host for expression of *pal*/*psc1* genes to efficiently convert L-Phe into *t*CA, and the aromatic carboxylic acid into styrene. The highest styrene production was achieved when the *pal* and *psc1* genes were co-expressed as an operon in *P. putida* CM12-5. This construction yielded styrene production exceeding 220 mg L^{-1}. This study serves as a successful demonstration of our strategy to tailor functional enzymes for novel host organisms, thereby broadening their metabolic capabilities. This breakthrough opens the doors to the synthesis of aromatic hydrocarbons using *Pseudomonas putida* as a versatile biofactory.

Highlights

1. This study focuses on the conversion of sugars into styrene, a valuable chemical compound, using the solvent-tolerant *Pseudomonas putida* DOT-T1E as a chassis.
2. The biosynthesis of styrene involves a two-step process, starting with the conversion of L-phenylalanine into *trans*-cinnamic acid (*t*CA) through PAL enzymes, followed by decarboxylation to yield styrene.
3. A synthetic *trans*-cinnamic acid decarboxylase was designed using a novel "wholesale" approach that involved the derivation of consensus sequences from homologous yeast *FDC1* genes with >60% identity, leading to the design of a functional *Pseudomonas* codon-optimized protein named PSC1.
4. Assays demonstrated successful decarboxylation of *t*CA into styrene by the PSC1 enzyme.

5. Optimal conditions for PSC1 enzyme activity *in vivo* were determined, including pH and temperature. Highest styrene biosynthesis efficiency was achieved by co-expressing the *pal* and *psc1* genes as an operon in *P. putida* CM12-5, a *P. putida* DOT-T1E derivative that produces L-phenylalanine, showcasing the significance of coordinated expression for improved chemical production.

6. The utilization of the solvent-tolerant *Pseudomonas putida* chassis as a biofactory for styrene production highlights the potential of microbial engineering for sustainable and environmentally friendly chemical synthesis.

2.1 Introduction

Styrene is one of the most widely used starting materials for the production of plastics. It is used to make solid polystyrene, polystyrene copolymers, rubber, composites and many others (de Meester et al., 1977; IARC, 2019; McKenna & Nielsen, 2011). Current demand for styrene is estimated to be about 30 million metric tons per year (ChemAnalyst, 2023). It is mainly produced through chemo catalysis by the dehydrogenation of petroleum-derived ethylbenzene (Wu et al., 1981). This process requires about 3 metric tons of steam per metric ton of styrene, making styrene the most energy-intensive of all commodities derived from petrol (Worrell et al., 2000). Because of this, new more environmentally friendly approaches are needed for synthesis of this aromatic hydrocarbon.

An alternative approach to chemical synthesis relies on biorefineries that can produce styrene at room temperature and ambient pressure from sugars. Styrene can be biosynthesized from L-phenylalanine (L-Phe) through two enzymatic steps (Figure 2.1). First, a reaction catalyzed by phenylalanine ammonia lyase (PAL) converts L-Phe into *trans*-cinnamic acid (*t*CA) through its non-oxidative deamination (Gilbert & Tully, 1982; Moffitt et al., 2007; Qi et al., 2007; Vannelli et al., 2007; Xiang & Moore, 2005; Young & Neisht, 1966). Next, *t*CA is decarboxylated to styrene—a reaction that has been described in fungi and which is catalyzed by ferulic acid decarboxylases (Mukai et al., 2010).

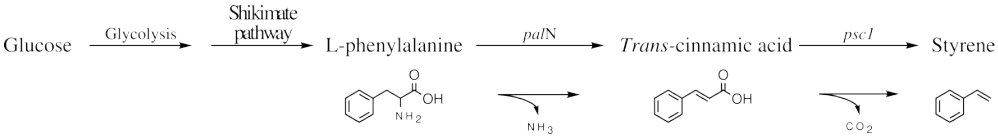

Figure 2.1: Enzymatic pathway to produce styrene from glucose, via the intermediates L-phenylalanine and *trans*-cinnamic acid. The two-step pathway from L-phenylalanine to styrene is achieved by co-expressing *palN*, encoding a phenylalanine ammonia lyase, and *psc1*, encoding a *trans*-cinnamic acid decarboxylase.

McKenna and Nielsen (2011) tested a wide range of PAL enzymes from eukaryotic and prokaryotic origins and showed that PAL enzymes from the cyanobacteria *Nostoc punctiforme* and *Anabaena variabilis* (Moffitt et al., 2007; Xiang & Moore, 2005) were highly specific for L-Phe deamination, and stoichiometrically converted L-Phe into *t*CA. McKenna and Nielsen (2011) also showed that the yeast ferulic acid decarboxylase FDC1 can convert *t*CA into styrene. Furthermore, it is known that a

PAL/FDC1 pathway operates in *Escherichia coli* and yeast, allowing production in the range of 29 to 260 mg L^{-1} (McKenna & Nielsen, 2011; McKenna et al., 2014). The limitations in styrene production seem to arise from the inherent toxicity of styrene, which results from its tendency to partition into cell membranes, where it disrupts membrane structure and proton gradients, leading to cell energy collapse and cell death (García-Franco et al., 2023; Horinouchi et al., 2010; Weber & de Bont, 1996).

Pseudomonas putida DOT-T1E is extremely tolerant to styrene, as the strain is able to grow in a second phase of this aromatic hydrocarbon as well as other toxic compounds such as toluene (García-Franco et al., 2023; Segura et al., 2005). Tolerance of DOT-T1E to these chemicals is the result of a number of adaptations, which include: (1) the presence of a series of efflux pumps that remove solvents from cell membranes and the periplasmic space (Ramos et al., 1998; Rojas et al., 2003); (2) the ability to strengthen membranes via phospholipid adjustments, such as the *cis* to *trans* isomerization of fatty acid chains and the biosynthesis of cardiolipin as a head group (Bernal et al., 2007b; García-Franco et al., 2023; Junker & Ramos, 1999); (3) the presence of a series of chaperones that help to fold newly synthesized proteins (Segura et al., 2005); (4) the expression of a number of oxidative stress proteins that can quench the reactive oxygen species that result from the uncoupling of respiratory chains (Bernal et al., 2007b; García-Franco et al., 2023; Ramos et al., 2015; Rojas et al., 2003; Segura et al., 2005); and (5) an enhanced ability to generate energy through robust carbon metabolism fluxes. In addition, previous assays had shown that DOT-T1E does not use *t*CA or styrene as a C-source (García-Franco et al., 2023; Udaondo et al., 2016).

Given these characteristics, along with the fact that the metabolic map of the strain is known (Udaondo et al., 2016) and the ease with which *P. putida* DOT-T1E can be genetically manipulated, this strain has gained interest as a platform for the biosynthesis of highly toxic aromatic compounds. Godoy et al. (2021) and Molina-Santiago et al. (2016) described strain CM12-5, a *P. putida* DOT-T1E derivative which can be used as a chassis for production of aromatic compounds from L-Phe. This mutant produces excess L-Phe and was generated through chemical mutagenesis and inactivation of a series of phenylalanine metabolism genes. The genes that were mutated in CM12-5 were: T1E_0122 and T1E_3356 (4-hydroxyphenylpyruvate dioxygenases involved in the transformation of phenylpyruvate to 2-hydroxyphenylpyruvate), T1E_4057 (a phenylalanine 4-monooxygenase involved in transforming phenylalanine to ty-

rosine), T1E_1753 (an enzyme that converts phenylalanine to 2-phenylacetamide) and T1E_1616 (an aldehyde dehydrogenase that transforms phenylacetaldehyde to phenylacetate). This *P. putida* CM12-5 mutant was found to be able to produce excess L-Phe that was excreted to the medium (Molina-Santiago et al., 2016).

Based on findings from McKenna and Nielsen (2011) that cyanobacterial PAL enzymes can stoichiometrically transform L-Phe into *t*CA, these genes were incorporated into the *P. putida* CM12-5 chassis. When a PAL enzyme is incorporated in the genetic background of the *P. putida* CM12-5 strain, it effectively converted L-Phe into *t*CA (Molina-Santiago et al., 2016). The modified strain was able to synthesize *t*CA at 190 mg per liter in 48 hours of growth (Molina-Santiago et al., 2016). While these findings are promising, the key remaining challenge for the efficient biosynthesis of styrene is the need for a functional *trans*-cinnamic acid decarboxylase in this chassis. The only known enzymes able to convert *t*CA into styrene are fungal ferulate decarboxylases, but expressing eukaryotic genes in prokaryotes, and in *Pseudomonas* in particular, presents consistent challenges, due to (i) the inherent disorganization of eukaryotic proteins compared to their prokaryotic counterparts; (ii) eukaryotic proteins often require chemical modifications for activation or to achieve optimal activity, processes not typically carried out by prokaryotes; and (iii) the inappropriate expression of eukaryotic genes may lead to the formation of aggregates, such as inclusion bodies of the recombinant protein (Sahdev et al., 2008). Recent progress in overcoming these challenges has been achieved through the development of optimized genes. This includes leveraging host codon preferences, designing vectors with modulable promoters, and refining culture conditions (Khow & Suntrarachun, 2012). While significant strides have been made in this field, specific obstacles still persist.

A notable recent advancement in protein design involves the expression of "consensus" sequences, as detailed by Sternke et al. (2019, 2020). These researchers proposed that consensus-derived proteins, utilizing a "wholesale" approach, encapsulate the evolutive trajectory of a group of proteins with conserved domains or regions. The consensus design involves creating a sequence based on the most frequent residues in a multiple sequence alignment of proteins from the same family. Despite differences in overall residue composition from naturally occurring sequences, consensus proteins have been described as active and thermodynamically stable. The conservation of residues in active sites and binding interaction interfaces in consensus sequences is key in designing active proteins derived from consensus (Sternke et al., 2020). In fact,

these authors explored across several protein families and found that their consensus proteins folded well and some displayed increased thermodynamic stability compared to natural homologs.

Here, we address the challenge of designing *in silico* and synthesizing *in vitro* a gene that gives rise to a functional *trans*-cinnamic acid decarboxylase (PSC1) that converts the aromatic carboxylic acid into styrene when expressed in *P. putida*. Furthermore, when the *psc1* gene was co-expressed with a *pal* gene in the solvent-tolerant L-phenylalanine overproducer *P. putida* CM12-5 strain, styrene from glucose was produced in minimal medium, paving the way for the sustainable production of this valuable aromatic hydrocarbon.

2.2 Materials and methods

2.2.1 Chemicals

Chemicals used in this study were purchased from Sigma-Aldrich and include L-Phe, *t*CA, styrene, acetonitrile and phosphoric acid.

2.2.2 Bacterial strains, plasmids and growth conditions

Strains and plasmids used in this study are listed in Table 2.1. *P. putida* strains were grown on M9 minimal medium with glucose 5 g L^{-1} (Abril et al., 1989) as the sole carbon source. When required, different concentrations of L-Phe or *t*CA were supplied. Cultures were incubated at 30°C and shaken on an orbital platform at 200 strokes per minute (unless otherwise indicated). *E. coli* DH5α was used for cloning experiments and cells were grown on LB at 37°C. Growth of liquid cultures was determined by following the turbidity of (OD_{660}) of the cultures. Antibiotics were added, when needed, to reach the following final concentrations: 100 µg mL^{-1} ampicillin (Ap), 25 µg mL^{-1} kanamycin (Km), 10 µg mL^{-1} gentamycin (Gm) and 10 µg mL^{-1} rifampicin (Rif). When indicated, 1 mM 2-methylbenzoate (2-MB) was added to the medium.

Table 2.1: Bacterial strains and plasmids used in this study.

Strain or plasmid	Characteristics	Reference
Strains		
Pseudomonas putida		
DOT-T1E	Rif^R, Tol^R	Ramos et al. (1995)
CM12-5	Rif^R, Tol^R, overproduces L-Phe	Molina-Santiago et al. (2016)
Escherichia coli		
DH5α	Cloning host for pSEVA plasmids	Grant et al. (1990)
Plasmids		
pSEVA238	Expression vector; *ori*pBBR1, *xylS*-Pm, Km^R	Silva-Rocha et al. (2013)
pPALN	pSEVA238 derivative carrying pal genes from *Nostoc punctiforme* and *Streptomyces maritimus*	Molina-Santiago et al. (2016)
pPALN_C1	pSEVA238 derivative carrying pal genes from *Nostoc punctiforme* and *Streptomyces maritimus* and *psc1* gene	This work
pSEVA632	Expression vector; oripBBR1, Gm^R	Silva-Rocha et al. (2013)
pPSC1	pSEVA632 derivative carrying *psc1* gene	This work
pPSD1	pSEVA632 derivative carrying *psd1* gene	This work

Rif^R, rifampicin-resistant; Gm^R, gentamycin-resistant; Km^R, kanamycin-resistant; Tol^R, toluene tolerant; L-Phe, L-phenylalanine; *ori*pBBR1, origin of replication pBBR1; *xylS*-Pm, XylS-Pm regulator/promoter system.

2.2.3 DNA techniques

DNA was manipulated using standard laboratory protocols (Martínez-García et al., 2014, 2015). Genomic DNA was isolated using the Wizard Genomic DNA purification kit (Promega USA), while plasmid DNA was isolated with the QIAprep Spin Miniprep kit (Qiagen, USA). DNA concentration was measured with a NanoDrop One (Thermo Scientific, USA). PCR DNA amplification was performed with universal primers, dNTPs and Phusion High-Fidelity DNA polymerase (Thermo Scientific, USA) or Taq DNA polymerase (Roche, Germany), as recommended by the manufacturers.

2.2.4 Electroporation

Electroporation of *P. putida* strains was performed as described elsewhere (Martínez-García et al., 2014, 2015), using a MicroPulser electroporator and Gene Pulser Cuvettes with 0.2 cm gap (Bio-Rad, USA). Transformants were selected on LB agar plates with kanamycin or gentamycin and incubated at 30°C for 24 h.

2.2.5 *In silico* identification of sequences with high similarity to the *Saccharomyces cerevisiae* enzyme *trans*-cinnamic acid decarboxylase 1 (FDC1). Design and *in vitro* synthesis of FDC1-like enzymes

The *S. cerevisiae* FDC1 sequence was used as a query to identify in UniProtKB homologous sequences using BLAST (Altschul et al., 1997). UniProtKB was used because it is a large resource of protein sequences with detailed annotations and cross-references to external data collections such as DDBJ/EMBL/GenBank (Boutet et al., 2007). Multiple alignments of different homologous sequences were performed using the MultAlin program (http://multalin.toulouse.inra.fr/multalin/). A consensus sequence from each multiple alignment was derived.

Once the protein consensus sequences were obtained, the synthesis of the corresponding *Pseudomonas* codon-optimized genes was carried out by GenScript®. The synthetic genes (*psc1* and *psd1*) were cloned into the Gm^R, broad-host range pSEVA632 plasmid (Silva-Rocha et al., 2013), flanked by enzyme restriction sites (BamHI and EcoRI) and transformed into *E. coli* DH5α cells. Next, the resulting plasmids pPSC1 and pPSD1 were transformed into *P. putida* DOT-T1E, *P. putida* CM12-5 and *P. putida* CM12-5 (pPALN) strains. The correct cloning of the synthetic variants was confirmed by DNA sequencing. To construct pPALN_C1, the *psc1* gene was sub-cloned from pPSC1 (BamHI and EcoRI fragment) into pPALN downstream of the *pal* genes.

2.2.6 PAL activity assay in *P. putida* whole cells

The activity of PAL was tested at different pH and temperatures. To this end, *P. putida* CM12-5 (pPALN) cells were grown in M9 minimal medium with glucose as the carbon source. At OD_{660} 0.4 to 0.6, 1 mM 2-MB was added to the cultures to induce expression of the *pal* genes from the XylS regulated Pm promoter (Ramos et al., 1987). At OD_{660} 1, the cultures were concentrated to an OD_{660} of 10 in 4 mL of M9 medium without glucose, supplemented with 100 mg L^{-1} of L-Phe. The cultures were incubated in test tubes for 24 h at 200 rpm, within a temperature range of 18 to 37°C and a pH range of 5.8 to 7.6. Supernatant aliquots were taken at different time points between 0 and 24 h for metabolite analysis. Samples were prepared by removing 1 mL of culture from test tubes and pelleting the cells at 11,000 $\times g$ for 4 min. The supernatant (0.75 mL) was then transferred to a glass vial for HPLC analysis

of L-Phe utilization and *t*CA production. Initial consumption rates (mg L^{-1} h^{-1}) were determined by calculating the slope of a trendline in the first two hours of the assay.

2.2.7 *Trans*-cinnamic acid decarboxylase activity assay in *P. putida* whole cells

The procedure was carried out as described above except that the strain used bore the pPSC1 or pPSD1 plasmid and the substrate used was 100 mg L^{-1} of *t*CA. Previously, we tested the functionality of the synthetic genes (*psc1* and *psd1*). To this end, *P. putida* CM12-5 transformants bearing a plasmid encoding the PSC1 or PSD1 protein were grown in M9 minimal medium with glucose as the sole C-source in the presence of 0.25, 0.5 or 1 mM *t*CA.

2.2.8 Styrene production from glucose by *P. putida*

The strains *P. putida* CM12-5 (pPALN, pPSC1) and *P. putida* CM12-5 (pPALN_C1) were tested for styrene production. The procedure was as follows: cells were grown in M9 minimal medium with glucose as the carbon source. At OD_{660} 0.4–0.6, 1 mM 2-MB was added to the cultures and at OD_{660} 1, the cultures were concentrated to an OD_{660} of 10 in 4 mL of the same medium (pH 7). The cultures were incubated for 62 h in 20 mL gas-tight HS vials, sealed to prevent styrene losses, at 30°C and 200 rpm. Then, total styrene content was analyzed as described below. Simultaneously, additional replicates were set up to collect supernatant aliquots and determine the concentrations of glucose, L-Phe and *t*CA.

2.2.8.1 Metabolite analysis

L-Phe and *t*CA levels were determined in culture supernatants using an Agilent/HP 1050 HPLC System (Agilent/HP, USA), equipped with a Nova-Pak C18 column (4 µm, 3.9 mm×150 mm, Waters) and coupled to a DAD detector. Milli-Q H_2O acidulated with 0.1% (v/v) H_3PO_4 (A), and acetonitrile:H_2O (90:10, v/v) supplemented with 0.1% H_3PO_4 (B) were used as eluents. Samples (20 µL) were injected for analysis at a constant flow rate of 1 mL min^{-1} for isocratic separation using a mixture of 40% (v/v) A and 60% (v/v) B. When an elution gradient was required, the same

eluents were used with the following ramp of solvents and times: the method started with 2 min at 95% A; then, mobile phase changed to 20% B within 8 min. Finally, the mobile phase was returned to the initial conditions with a 3 min hold time. Column temperature was 20°C. Under these conditions, the eluent was monitored at 215 nm for L-Phe and at 280 nm for *t*CA.

Glucose determination in supernatants was carried out using the D-glucose-HK Assay Kit (Megazyme, Ireland) according to manufacturer's instructions. Absorbance measurements were carried out using a TECAN Sunrise 200 microplate absorbance reader (Tecan GmbH, Austria).

2.2.8.2 Styrene analysis

Styrene measurements were performed by HS-SPME coupled to GC–MS. The chromatographic separation was carried out using an Agilent 7890A gas chromatograph (Agilent, USA) with a Zebron™ ZB-5MS column (30 m, 0.23 mm ID, 0.23 µm film) (Phenomenex, USA). Helium gas was used as the carrier gas at a 1.2 mL min^{-1} flow rate. The samples were injected in split mode (100:1) and the injector temperature was held at 240°C. The column temperature program started at 40°C for 2 min and then ramped up to 240°C at 10°C per min, and held there for 2 min. A mass spectrometer detector was used (model Quattro micro GC; Waters, USA) with an electron impact ionization source of 70 eV. The temperatures of the MS source and MS transfer line were set at 240°C.

SPME fiber assembly Divinylbenzene/Carboxen/Polydimethylsiloxane (DVB/-CAR/PDMS, 50/30 µm, 23 ga) was used for the HS-SPME procedure. The pre-incubation time was 3 min. The incubation was carried out at 40°C and 500 rpm for 15 min. The desorption temperature was 240°C and the desorption time was 2 min.

Styrene and other biotransformation products present in the samples were unequivocally identified by matching the corresponding mass spectra with a standard NIST17 spectral database.

2.2.9 Phylogenetic tree

We constructed a phylogenetic tree to understand the relationships between the sequences with >50% identity with FDC1 from *S. cerevisiae* (see Figure S2.1). Sequences were aligned with Muscle software and served as input to construct the phylogenetic tree with IQ-TREE software version 1.6.12 (parameters -nt AUTO, -bb 1000 -m TESTMERGE -safe) (Hoang et al., 2018; Nguyen et al., 2015). The maximum likelihood tree was constructed following the LG + I + G4 evolution model, which was the best fit according to ModelFinder (Kalyaanamoorthy et al., 2017), with 1000 bootstrap replicates. Finally, the phylogenetic tree was plotted using iTOL v6 software.

2.2.10 Statistical analysis

Two-tailed Student's *t*-tests were performed to determine the statistical significance for two-group comparisons. For three-group comparisons, ANOVA analysis was conducted. If statistical significance was found, the Tukey test was performed between paired groups. Differences were considered to be significant if a *p*-value < 0.05 was obtained.

2.3 Results

2.3.1 Design and synthesis of a functional *trans*-cinnamic acid decarboxylase in *P. putida*

The expression of eukaryotic genes in *P. putida* is a challenge, and when expression is achieved, the resulting proteins may not be functional or exhibit low activity, as was the case when a *Pseudomonas* codon-optimized yeast FDC enzyme was expressed in *P. putida* (not shown). We then searched in NCBI and other databases for prokaryotic enzymes similar to *S. cerevisiae* FDC1; however, no results were returned. We also carried out BLAST searches using the FDC1 enzyme sequence in the UniProtKB database (Boutet et al., 2007). This returned a limited number of eukaryotic proteins with identities ranging from 88.9 to 50% (see Table S2.1), and their phylogenetic relationship is shown in Figure S2.1. To avoid synthesizing and testing a number of

codon-optimized eukaryotic genes in *P. putida*, we carried out *de novo* design of a protein using the "wholesale" method. Sternke et al. (2019) revealed that this strategy results in proteins with high stability because the consensus sequence consolidates the evolutionary history of the protein to yield enhanced stability and functionality. We used two series of homologous FDC1 sequences, which were stratified according to percentage of identity. The alignment of the proteins with >60% identity (8 sequences) and >50% identity (74 sequences) to FDC1 from *S. cerevisiae* is shown in Figure S2.2 and Figure S2.3, respectively. A consensus sequence for each of the two series was derived. At each position in these sequences, the chosen amino acid was the most probable one based on frequency of appearance. When the program did not derive a residue, the language system shown in Table S2.2 was used.

When designing polypeptide sequences, the amino acid that was present in the highest proportion was chosen. When proportions were the same for two amino acids, either of the two possible amino acids was selected indiscriminately. When no amino acid was present in higher proportion, we attempted to maintain the protein's charge as neutral as possible by choosing either a polar, uncharged amino acid (i.e., asparagine (N) or glutamine (Q)). For gaps in aligned sequences—when the alignment resulted in the absence of an amino acid—that residue was eliminated. However, if the gap was due to non-matching amino acids, the one present in the highest proportion was selected. If there was no consensus amino acid, to fill in gaps rather than predicting the most probable residue based on language models (Michaud et al., 2022), we opted to incorporate alanine as it is a neutral amino acid whose small volume is known to minimally affect protein folding (Fernandez-Escamilla et al., 2004; Yang & Zhang, 2015). The amino acid consensus sequences (Figure S2.2 and Figure S2.3) were converted into *Pseudomonas* codon-optimized genes that we named *psc1* (for proteins with >60% identity; Table S2.3) and *psd1* (for proteins exhibiting >50% identity; Table S2.4). The genes were synthesized by GenScript®, cloned into the broad-host range pSEVA632 (Gm^R) plasmid, and transformed into *E. coli* DH5α and *P. putida* CM12-5.

2.3.2 *In vivo* assay of a synthetic *trans*-cinnamic acid decarboxylase in *P. putida*

P. putida CM12-5 transformants bearing a plasmid encoding the PSC1 or PSD1 protein were grown in M9 minimal medium with glucose as the sole C-source in

the presence of 0.25, 0.5 or 1 mM *t*CA. We found that *t*CA levels did not decrease when *P. putida* CM12-5 strain expressed the PSD1 enzyme, as was the case for the control without an *fdc* gene; however, when the strain carried the PSC1 enzyme, *t*CA disappeared from the medium after a 24 h incubation with 0.25 or 0.5 mM *t*CA. When 1 mM *t*CA was added, its concentration dropped by half within the same timeframe (Figure 2.2). At all *t*CA concentrations tested, the differences in *t*CA concentration at 24 h were statistically significant between PSC1 and PSD1 ($p < 0.05$).

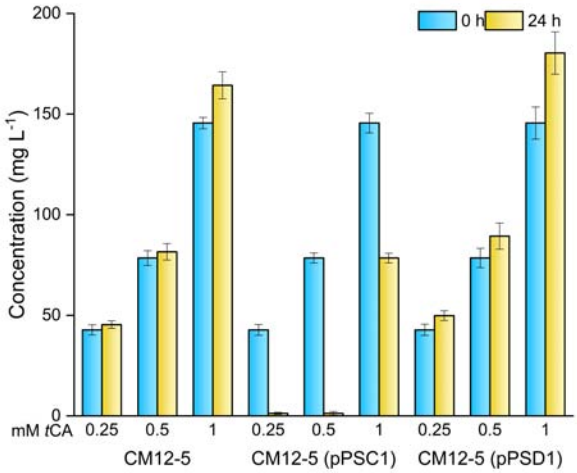

Figure 2.2: *Trans*-cinnamic acid consumption by *P. putida* CM12-5 expressing different *trans*-cinnamic acid decarboxylases. *P. putida* CM12-5 without plasmid or bearing the plasmid pPSC1 or pPSD1 were grown on M9 minimal medium with glucose supplemented with 0.25, 0.5 or 1 mM *trans*-cinnamic acid. *t*CA concentrations were determined at the beginning of the assay (blue bars) and after 24 h cultivation (yellow bars). ANOVA analysis was performed for three-group comparisons and the Tukey test was carried out between paired groups to determine the statistical significance (p-value < 0.05). The results shown are the averages and standard deviations of three independent assays.

This revealed that PSC1 is a novel functional enzyme capable of metabolizing *t*CA. As expected, at any concentration of *t*CA and with both constructions, L-Phe accumulated in culture medium as its metabolism is blocked in the CM12-5 mutant strain (data not shown), which supports the hypothesis that the metabolism of *t*CA does not interfere with the general physiology of the strain.

Next, we tested the conversion of *t*CA into styrene under different growth conditions. As expected, the control—*P. putida* CM12-5 (pPSC1) in the absence of *t*CA—did not produce styrene in medium with glucose; however, when 0.25 mM *t*CA was added, a single conversion peak was recorded at 24 and 48 h. The mass spectra of this peak was compared to the NIST17 spectral database, which unequivocally

identified it as styrene (Figure S2.4), confirming that styrene is biosynthesized by the strain from *t*CA. We determined the conversion rate of *t*CA under different temperatures and pH, using resting cell assays with cells suspended at an OD_{660} of 10 in M9 minimal medium without glucose but containing 100 mg L^{-1} *t*CA. The chosen pH range covered values between 5.8 and 7.6, which align with the pH range for the growth of *P. putida* (Moore et al., 2006). We found significantly higher conversion rates at pH 5.8 and 6.6 (26.2–32.2 mg L^{-1} h^{-1}) than at pH values that exceeded 6.6 (Figure 2.3A). *P. putida* thrives at temperatures from 18 to 37°C, and the optimal temperature for conversion was 37°C with lower rates of transformation at 18°C (Figure 2.3B).

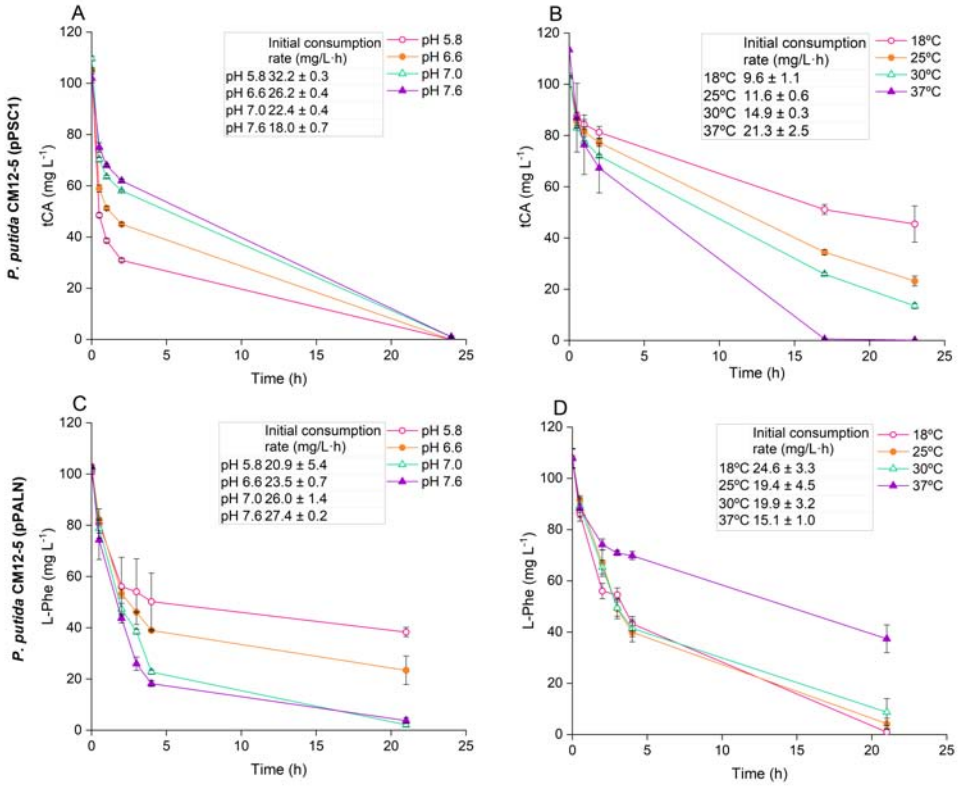

Figure 2.3: *Trans*-cinnamic acid and L-phenylalanine consumption by *P. putida* CM12-5 (pPSC1) (A and B) and *P. putida* CM12-5 (pPALN) (C and D), respectively, at different pH and temperatures. For pH assays (A and C), cultures were grown at pH 5.8, pink open circles; pH 6.6, orange solid circles; pH 7.0, green open triangles; and pH 7.6, purple solid triangles. For temperature assays (B and D), cultures were grown in M9 minimal medium at pH 7.0 at 18°C, pink open circles; 25°C, orange solid circles; 30°C, green open triangles; and 37°C, purple solid triangles. Initial consumption rates correspond to the slope of a trendline during the first two hours of cultivation. The results shown are the averages and standard deviations of three independent assays.

2.3.3 Conversion of L-phenylalanine into *trans*-cinnamic acid

Because production of styrene will require coupling of the whole set of reactions from glucose to L-Phe, we transformed CM12-5 with the construct made by Molina-Santiago et al. (2016), which expresses the *pal* genes from the Pm promoter. We cultured *P. putida* CM12-5 (pPALN) on glucose as the sole C-source in the absence and in the presence of 1 mM L-Phe. As expected, we found that *P. putida* CM12-5 without the *pal* genes accumulated L-Phe in the culture medium over time, reaching 217.2 ± 41.8 mg L^{-1} in the absence of the amino acid. Spiking L-Phe to a level of 170 mg L^{-1} at t = 0 h did not prevent accumulation of this amino acid, reaching a final concentration of 356.9 ± 5.5 mg L^{-1} of L-Phe (Table 2.2). This indicated that intracellular accumulation of L-Phe from glucose was not subject to feedback inhibition by this aromatic amino acid. When *pal* genes were expressed in the *P. putida* CM12-5 strain, L-Phe transiently accumulated and *t*CA was detected in the culture medium, reaching a concentration of 91.0 ± 19.2 to 199.7 ± 19.3 mg L^{-1} (Table 2.2). As above, the presence of excess L-Phe did not result in inhibition of the synthesis of *t*CA or L-Phe.

Table 2.2: Biosynthesis of L-phenylalanine and *trans*-cinnamic acid by *P. putida* CM12-5 and *P. putida* CM12-5 (pPALN).

	[L-Phe] $T_{0\,h}$ (mg L^{-1})	**[L-Phe] $T_{24\,h}$ (mg L^{-1})**	**[*t*CA] $T_{24\,h}$ (mg L^{-1})**
CM12-5	0	217.2 ± 41.8	0
	173.2 ± 0.9	356.9 ± 5.5	0
CM12-5 (pPALN)	0	141.8 ± 33.8	91.0 ± 11.2
	173.6 ± 0.1	263.9 ± 41.0	119.7 ± 19.3

Assays were done in M9 minimal medium with glucose as the sole C-source with and without the addition of 1 mM L-Phe (173 ± 1 mg L^{-1}). The concentration of L-phenylalanine and *trans*-cinnamic acid was determined after 24 h of cultivation. The data in the table are the average and standard deviation of three independent assays.

PAL activity was analyzed using resting cell assays with cells suspended at an OD_{660} of 10 in M9 minimal medium without glucose but containing 100 mg L^{-1} L-Phe. The rates of L-Phe consumption during the first two hours of cultivation at pH 6.6 and 7.6 were 23.5 ± 0.7 to 27.4 ± 0.2 mg L^{-1} h^{-1} and the production of *t*CA was 22.5 ± 0.6 to 26.6 ± 0.7 mg L^{-1} h^{-1} with >97% of L-Phe converted into *t*CA. At pH of 5.8 we also found stoichiometric conversion of L-Phe into *t*CA, but the rate of accumulation was half of that at neutral pH (Figure 2.3C). At pH 7, the effect

of temperature between 18 and 37°C was tested (Figure 2.3D). Maximal rates were observed in the range between 18 and 30°C, with lower activity at 37°C and eventual cessation of *t*CA production, in agreement with the limited viability of *P. putida* at the highest temperature tested.

At pH 7.0 and 30°C, all L-Phe was converted into *t*CA. These results are in line with earlier studies, which show that the first step in the pathway is highly specific for the intended L-Phe substrate—a fact that will be advantageous for controlling the synthesis of aromatic hydrocarbons (i.e., styrene) from sugars.

2.3.4 Styrene biosynthesis from glucose

Next, we investigated the bioconversion of glucose into styrene using *P. putida* CM12-5 (pPALN, pPSC1). These assays were conducted in M9 minimal medium with 0.5% (w/v) glucose at pH 7.0 and 30°C. We selected these conditions because at this pH and temperature, the *in vivo* performance of both enzymes, although not reaching their highest activity levels, approached their optimal activity range (see Figure 2.3). After culturing for 24 h, we measured the production of 158 ± 6 mg L^{-1} of styrene. It should be noted that only a small proportion of L-Phe and *t*CA remained in the supernatants (Figure 2.4). As expected, the control strain *P. putida* CM12-5 did not produce styrene and only accumulated L-Phe in supernatants.

In an effort to enhance styrene production, the broad-host range plasmid pPALN_C1 (Table 2.1) bearing both *pal* genes and *psc1* gene in tandem was constructed. The genes were expressed under the XylS-dependent Pm promoter in the presence of 1 mM 2-MB to maximize expression levels as described before by Ramos et al. (1987). The recombinant *P. putida* CM12-5 (pPALN_C1) was grown in M9 minimal medium with 0.5% (v/v) glucose as described above. Under these conditions, the strain produced 221 ± 6 mg L^{-1} styrene (Figure 2.4), showing significantly superior efficiency ($p < 0.05$) compared to the *P. putida* CM12-5 (pPALN, pPSC1) strain. The estimated yield was 44 ± 1 mg styrene per g glucose.

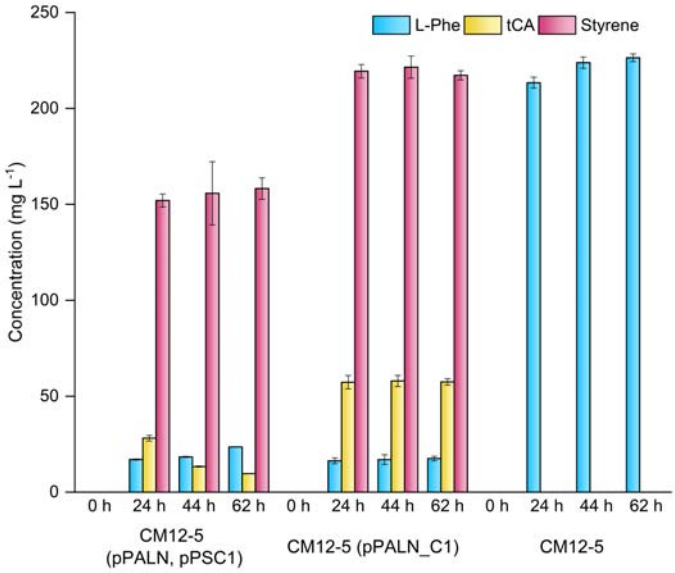

Figure 2.4: Biosynthesis of styrene by *P. putida* derivatives from glucose. The strains used were *P. putida* CM12-5 (pPALN, pPSC1), *P. putida* CM12-5 (pPALN_C1) and *P. putida* CM12-5 as control. Cells were grown on M9 minimal medium with 0.5% (w/v) glucose as the sole C-source. Production of L-phenylalanine (blue bars), *trans*-cinnamic acid (yellow bars) and styrene (pink bars) was determined. Two-tailed Student's *t*-tests were performed to determine the statistical significance for two-group comparisons ($p < 0.05$). The results shown are the averages and standard deviations of three independent assays.

2.4 Discussion

P. putida DOT-T1E and its derivative CM12-5 are highly solvent-tolerant strains that can thrive in the presence of aromatic hydrocarbons such as toluene, xylene, ethylbenzene and styrene, and they are considered useful chassis for the biosynthesis of aromatic compounds (Ramos et al., 1995). These strains acquired tolerance to these compounds through adjustments in the phospholipid composition of cell membranes, increased robustness of the protein folding machinery, and a set of efflux pumps that extrude solvents to the external environment from the cytoplasm, periplasm, and cell membranes (Ramos et al., 2015). In addition to solvent tolerance, a crucial characteristic of microbial chassis for chemical production (Bird et al., 2023; Danchin, 2022) is the ability to maintain the integrity of the desired product(s). In the case of the *P. putida* CM12-5 strain, a phenylalanine-producing strain, catabolism of the aromatic amino acid is blocked. Additionally, the strain does not metabolize *t*CA and styrene,

compounds that can be made from L-Phe (García-Franco et al., 2023). This makes this strain a promising candidate for the synthesis of these aromatic compounds.

In the current solvent-tolerant platform, we used a two-step conversion of L-Phe into styrene (Figure 2.1). In the initial step, we utilized PAL enzymes, which have been demonstrated by McKenna and Nielsen (2011) to efficiently catalyze this reaction (Figure 2.1). The second step in the proposed styrene biosynthesis pathway involves the decarboxylation of *t*CA by a ferulic decarboxylase (FDC), which exhibits *trans*-cinnamate decarboxylase activity and results in the production of styrene (Figure 2.1). Our approach to design a functional *trans*-cinnamic decarboxylase was based on Sternke et al. (2019), who proposed that consensus sequences derived from multi-alignment of protein families, in the so-called "wholesale" approach, yield functional and thermodynamically stable proteins. Following several multi-alignments of FDC proteins, consensus sequences were derived, and the protein was translated to DNA with *Pseudomonas* codon-optimized sequences. From the alignment of 8 FDC sequences with >60% identity to the *S. cerevisiae* enzyme, we derived PSC1, which was shown to be functional in *P. putida*. The PSC1 enzyme consists of 502 amino acids and differs by 114 residues from the FDC1 of *S. cerevisiae*. Another variant, named PSD1, differs by 230 residues from PSC1 and 223 residues from FDC1 of *S. cerevisiae*, and it was found to be non-functional. Studies by Bailey et al. (2018) and Duță et al. (2022) demonstrated that specific residues (I189, Q192, I330, F397, I398) in the *S. cerevisiae* FDC1 enzyme are crucial for substrate binding/catalysis, and these residues are conserved in the PSC1 enzyme. However, in the PSD1 protein sequence, F397 was replaced by Y, and I398 by T. Whether these residues are responsible for the lack of activity of the PSD1 enzyme remains unknown. Our current results suggest that PSC1 is a dimeric enzyme that utilizes the atypical prenylated flavin mononucleotide as a cofactor (García-Franco *et al*., unpublished).

In the pursuit of establishing a platform for the bioproduction of styrene as a sustainable alternative to petroleum-derived styrene, a high production titer is needed. Previous studies by Lee et al. (2019) and Grubbe et al. (2020) underscored this necessity. In our assays, *P. putida* CM12-5 derivatives carrying the *palN/psc1* operon exhibited production titers of 221 ± 6 mg L^{-1}, and our results support that almost 100% of L-Phe produced by CM12-5 (pPALN_C1) was eventually converted into styrene, with a minor fraction transiently accumulating as *t*CA when the process initiated from glucose. This also indicates that the majority of the synthesized *t*CA is

rapidly converted to styrene. Furthermore, additional assays supplementing *P. putida* CM12-5 (pPALN_C1) suspensions with exogenous L-Phe (i.e. 1 mM) confirmed its complete conversion to styrene. Consequently, our findings pinpoint that the limiting step in the production of styrene is the intracellular production of L-Phe, emphasizing the need to increase L-Phe yields in this platform.

Our assays revealed that co-expressing the *pal* and *psc1* genes as an operon led to a 25% increase in styrene production compared to the levels achieved when the genes were expressed individually in two different plasmids. This enhanced production likely relates to (i) reduced basal maintenance energy for cells with a single plasmid versus strains with two plasmids that require two antibiotics for selection, and (ii) a more efficient conversion of L-Phe into *t*CA and styrene, preventing the accumulation of the amino acid. It is known that excess L-Phe inhibits prephenate dehydrogenase (PheA), an enzyme crucial in L-Phe biosynthesis (Molina-Santiago et al., 2016; Zhan et al., 2022). Therefore, the controlled expression of genes involved in the biotransformation process of styrene biosynthesis is critical.

Molina-Santiago et al. (2016) described that a *P. putida* CM12-5 derivative produced a maximum titer of approximately 600 mg L^{-1} L-Phe after 24 to 48 h of culture in M9 with 1.5% (w/v) glucose. Since stoichiometric conversion of L-Phe into styrene takes place, we assumed that in conditions where 600 mg L^{-1} of L-Phe are reached, its complete conversion to styrene would lead to a production of 378 mg L^{-1} of styrene, surpassing the solubility of styrene in water. Our earlier study (García-Franco et al., 2023) indicated that the growth rate and viability of *P. putida* DOT-T1E are only marginally lower in the presence of styrene compared to growth without solvent. Hence, we hypothesize that the balance of host fitness would probably remain unaffected by the potentially achievable titer of 378 mg L^{-1}. Nonetheless, implementing strategies to recover styrene concurrently during production could prove valuable in mitigating any metabolic burden of solvent tolerance, thus allowing for resource redirection to maximize styrene yields. Since our system attains maximum titer after 24 h cultivation, adopting a fed-batch system with advanced recovery and gas stripping techniques could potentially yield styrene productivity comparable to that achieved in studies carried out by Nielsen's group, i.e., 836 mg L^{-1} (Grubbe et al., 2020; Lee et al., 2019; Liang et al., 2020; Liu et al., 2018; McKenna & Nielsen, 2011; McKenna et al., 2015). Similarly to our earlier research (Godoy et al., 2021), approximately 12% of available sugars in lignocellulose wastes

are converted into L-Phe. Given that we have verified the stoichiometry of L-Phe conversion into styrene, we estimate the production of 8.5 tons of styrene in a 2G biorefinery capable of processing 1,000 tons of feedstock daily, equivalent to 3,100 tons of styrene annually. Therefore, for a more efficient biofactory, efforts to increase the intracellular production of L-Phe, the starting chemical for styrene biosynthesis, are needed.

To sum up, our results demonstrate the success of the "wholesale" approach for designing enzymes capable of converting *trans*-cinnamic acid into styrene and functioning actively in novel hosts. These findings open up new avenues for the design of new-to-nature pathways for the synthesis of high-value added chemicals, marking a significant stride towards the sustainable bioproduction of chemicals.

Acknowledgements

The work in our laboratory was funded by grants from the Ministry of Science and Innovation of Spain (Plan Nacional PDI-2018-094370BI00 and Transición Ecológica y Resilencia TED2021-129632BI00). We thank Ben Pakuts for critically reading the manuscript, Tamara Gómez for assisting with the phylogenetic tree, Jesús de la Torre for helping with protein expression assays, and José Miguel Ramos (CIC-UGR) and Rafael Núñez (SIC-EEZ) for conducting the GC-MS analyses.

Author contributions

AGF: executed experiments, analyzed data, methodology, art work, reviewed and edited the manuscript. PG: executed experiments, analyzed data, methodology, reviewed and edited the manuscript. ED: executed experiments, funding acquisition, project administration, reviewed and edited the manuscript. JLR: conceptualization, funding acquisition, validation, supervision, wrote the original draft.

2.5 Supplementary Information

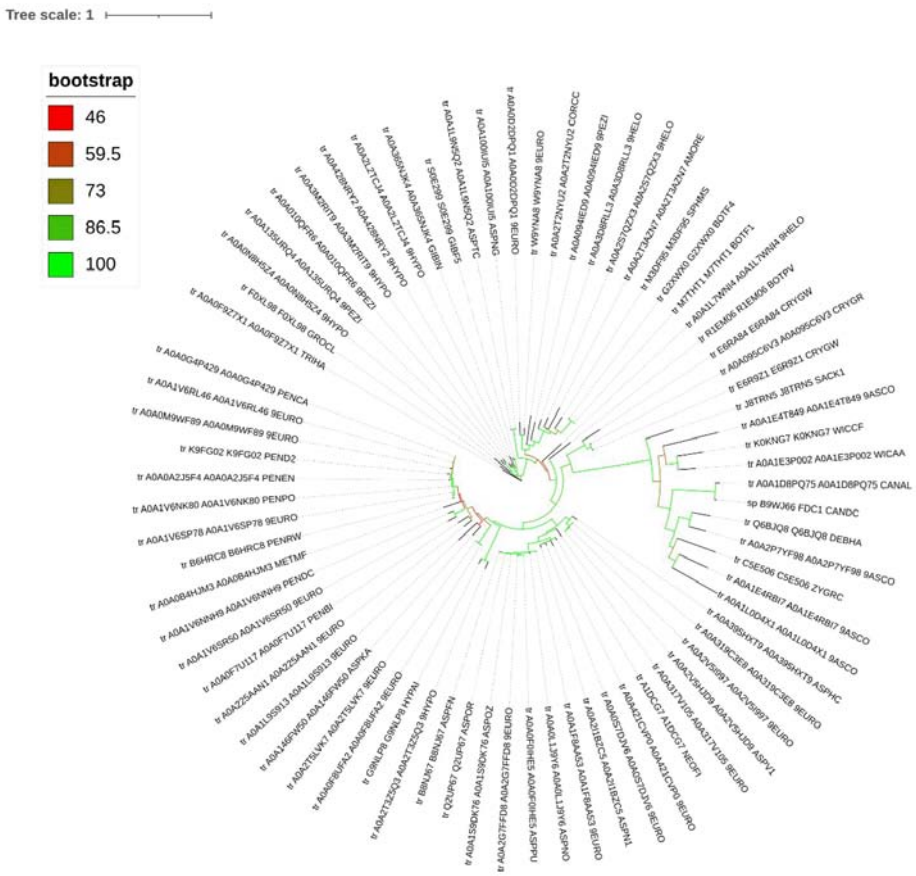

Figure S2.1: Phylogenetic relationships of FDC1 from *Saccharomyces cerevisiae* with homologous sequences from different organisms exhibiting > 50% identity. Colors of the branches represent levels of significance obtained in the bootstrapping analysis (1000 replicates).

Figure S2.2: Multialignment of FDC1 from *Saccharomyces cerevisiae* and FDC from different organisms exhibiting >60% identity. The consensus sequence derived from the multialignment was used to design the PSC1 protein. Red and blue residues show conservation in the sequences.

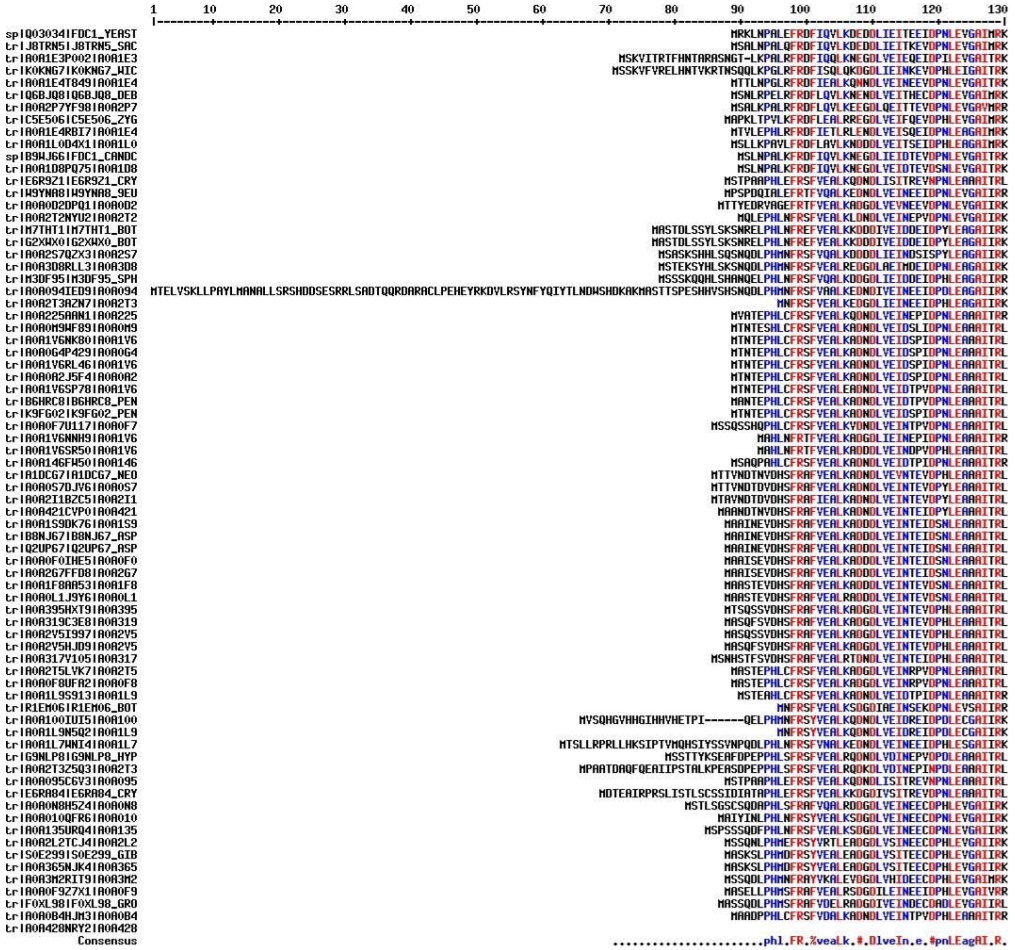

Figure S2.3: Multialignment of FDC1 from *Saccharomyces cerevisiae* and FDC from different organisms exhibiting >50% identity. The consensus sequence derived from the multialignment was used to design the PSD1 protein. Red and blue residues show conservation in the sequences.

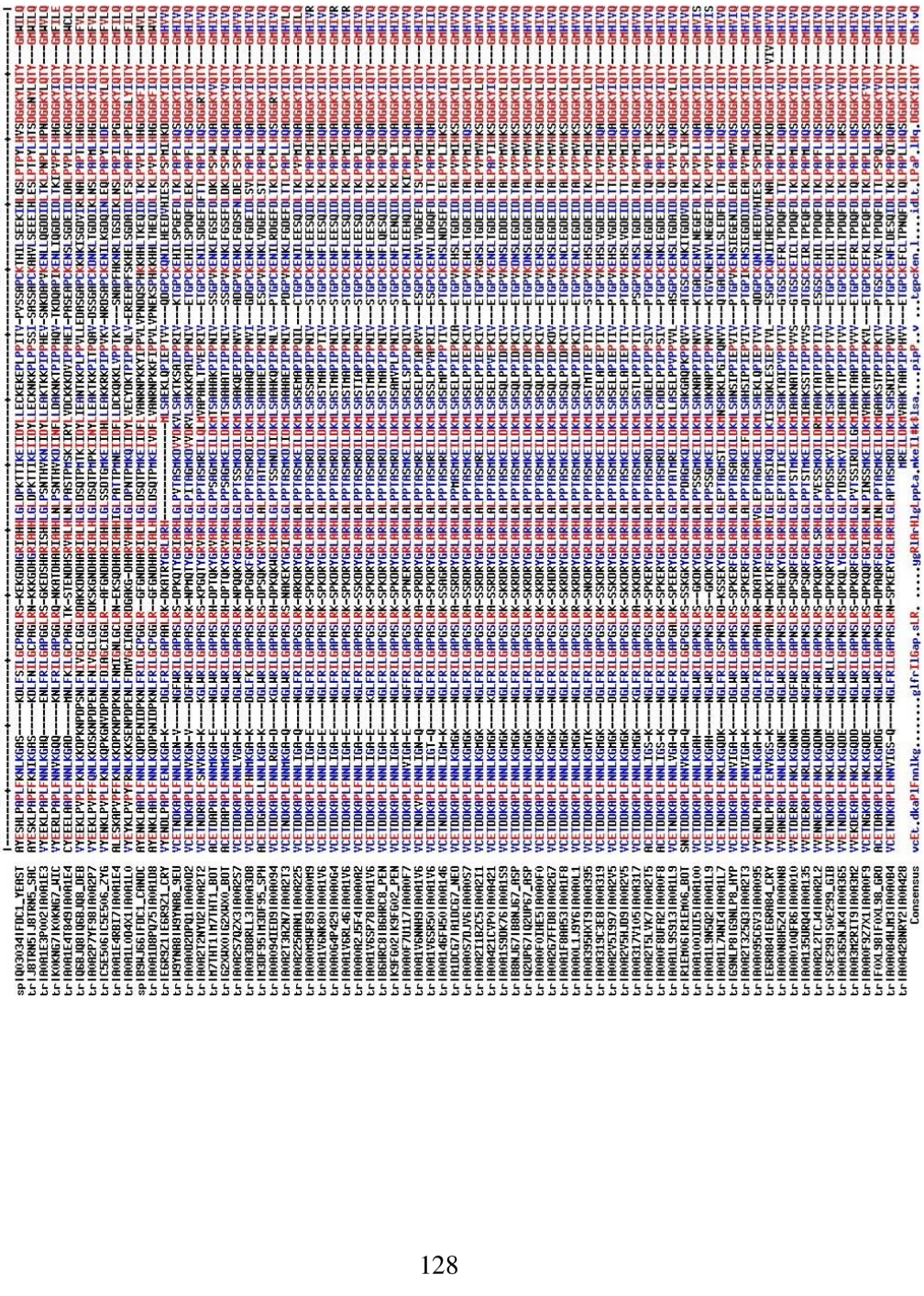

Figure S2.3 (continued)

Figure S2.3 (continued)

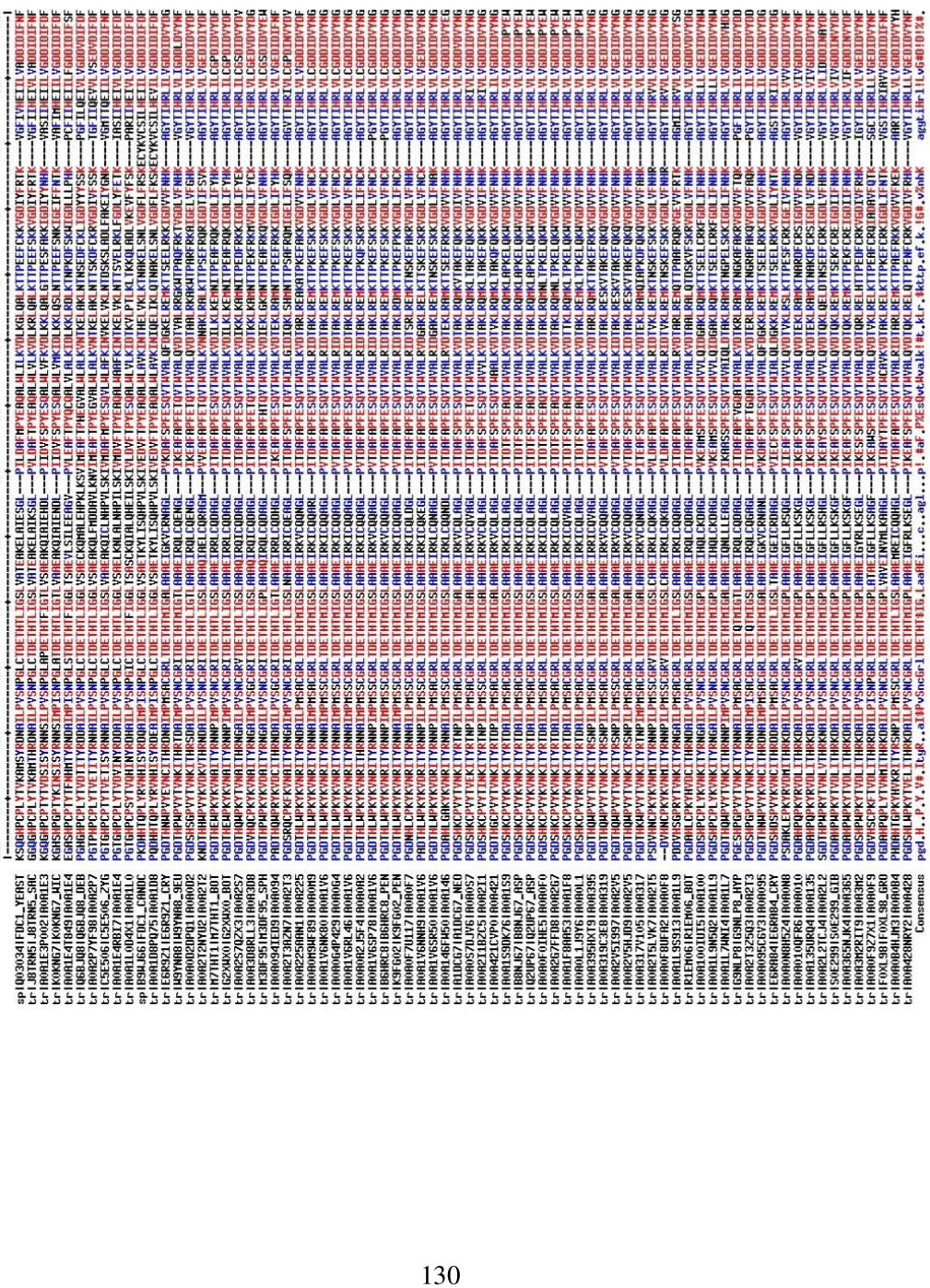

Figure S2.3 (continued)

Figure S2.3 (continued)

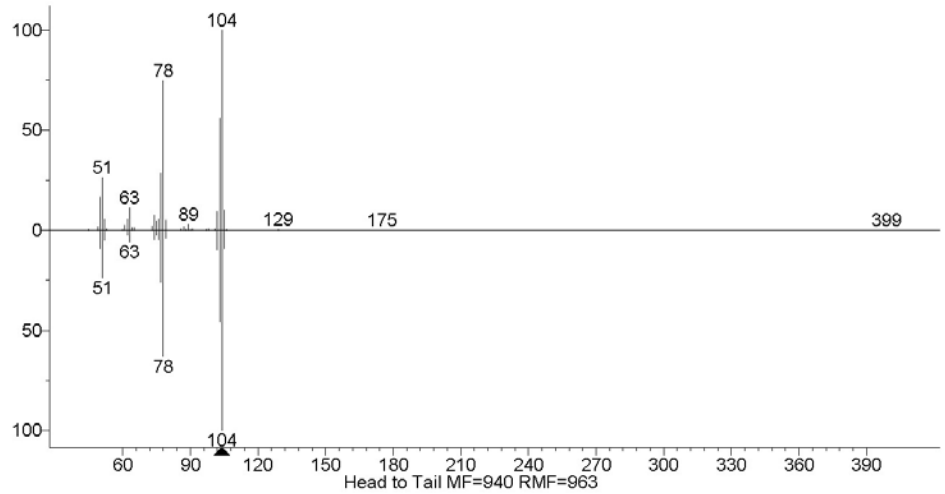

Figure S2.4: Identification of styrene produced by *P. putida* bearing the *PSC1* gene. Head-to-tail comparison of the standard mass spectra showing the relative abundance of the mass-to-charge ratio of styrene from the NIST17 library (lower) with that of the dominant metabolite peak obtained in *P. putida* CM12-5 pPSC1 culture from glucose and 0.25 mM *trans*-cinnamic acid added to the medium (upper).

Table S2.1: Similar proteins (> 50% identity) to FDC1 from *Saccharomyces cerevisiae* obtained using BLAST.

Protein and species	**Length**[a]	**Identity percentage (%)**[b]	**UniProtKB accession number**
FDC1 *Saccharomyces kudriavzevii*	503	88.9	J8TRN5
FDC1 *Wickerhamomyces anomalus*	518	68.2	A0A1E3P002
FDC1 *Wickerhamomyces ciferrii*	523	63.7	K0KNG7
FDC1 *[Candida] pseudohaemulonis*	512	61.2	A0A2P7YF98
FDC1 *Debaryomyces hansenii*	513	61.1	Q6BJQ8
FDC1 *Candida dubliniensis*	513	60.6	B9WJ66
FDC1 *[Candida] arabinofermentans*	501	60.0	A0A1E4T849
FDC1 *Candida albicans*	513	59.8	A0A1D8PQ75
FDC1 *Zygosaccharomyces rouxii*	511	59.6	C5E506
FDC1 *Hyphopichia burtonii*	510	58.6	A0A1E4RBI7
FDC1 *[Candida] intermedia*	511	56.7	A0A1L0D4X1
FDC1 *Cryptococcus gattii serotype B (strain WM276 / ATCC MYA-4071) (Filobasidiella gattii) (Cryptococcus bacillisporus)*	435	54.1	E6R9Z1
FDC1 *Capronia coronata*	498	53.8	W9YNA8
3-octaprenyl-4-hydroxybenzoate carboxy-lyase *Metarhizium majus (strain ARSEF 297)*	411	53.1	A0A0B4HJM3
FDC1 *Cryptococcus gattii serotype B (strain R265) (Filobasidiella gattii) (Cryptococcus bacillisporus)*	501	52.5	A0A095C6V3
FDC1 *Neonectria ditissima*	507	52.2	A0A0N8H5Z4
Multifunctional fusion protein *Talaromyces atroroseus*	1348	52.2	A0A225AAN1
FDC1 *Corynespora cassiicola Philippines*	497	51.8	A0A2T2NYU2
FDC1 *Phialophora americana*	499	51.8	A0A0D2DPQ1
FDC1 *Botryotinia fuckeliana (strain BcDW1)*	513	51.8	M7THT1
FDC1 *Botryotinia fuckeliana (strain T4)*	513	51.6	G2XWX0

FDC1 *Neosartorya fischeri*	505	51.4	A1DCG7
FDC1 *Fusarium sp. AF-8*	406	51.4	A0A428NRY2
FDC1 *Cryptococcus gattii serotype B (strain WM276 / ATCC MYA-4071) (Filobasidiella gattii) (Cryptococcus bacillisporus)*	523	51.4	E6RA84
FDC1 *Rutstroemia sp. NJR-2017a WRK4*	511	51.2	A0A2S7QZX3
FDC1 *Aspergillus turcosus*	504	51.1	A0A421CVP0
FDC1 *Pseudogymnoascus sp. VKM F-4520 (FW-2644)*	589	51.0	A0A094IED9
FDC1 *Colletotrichum fioriniae PJ7*	503	51.0	A0A010QFR6
FDC1 *Penicillium nordicum*	500	51.0	A0A0M9WF89
FDC1 *Penicillium polonicum*	500	50.9	A0A1V6NK80
FDC1 *Penicillium digitatum (strain PHI26 / CECT 20796) (Green mold)*	499	50.9	K9FG02
FDC1 *Aspergillus lentulus*	505	50.9	A0A0S7DJV6
FDC1 *Aspergillus oryzae*	503	50.9	A0A1S9DK76
FDC1 *Aspergillus flavus*	503	50.9	B8NJ67
FDC1 *Aspergillus oryzae*	503	50.9	Q2UP67
FDC1 *Aspergillus parasiticus*	503	50.9	A0A0F0IHE5
FDC1 *Aspergillus arachidicola*	503	50.9	A0A2G7FFD8
FDC1 *Hypocrea atroviridis*	512	50.8	G9NLP8
FDC1 *Grosmannia clavigera*	500	50.8	F0XL98
FDC1 *Trichoderma asperellum CBS 433.97*	525	50.8	A0A2T3Z5Q3
FDC1 *Aspergillus homomorphus*	503	50.8	A0A395HXT9
FDC1 *Penicillium camemberti FM 013*	500	50.7	A0A0G4P429
FDC1 *Aspergillus novofumigatus IBT 16806*	505	50.7	A0A2I1BZC5
FDC1 *Aspergillus bombycis*	503	50.7	A0A1F8AA53
FDC1 *Aspergillus ochraceoroseus IBT 24754*	502	50.7	A0A2T5LVK7
FDC1 *Fusarium venenatum*	503	50.6	A0A2L2TCJ4

FDC1 *Aspergillus uvarum CBS 121591*	503	50.6	A0A319C3E8
FDC1 *Penicillium expansum*	500	50.5	A0A0A2J5F4
FDC1 *Penicillium brasilianum*	503	50.5	A0A0F7U117
FDC1 *Aspergillus sclerotioniger CBS 115572*	505	50.5	A0A317V105
FDC1 *Sphaerulina musiva*	508	50.5	M3DF95
FDC1 *Coleophoma cylindrospora*	513	50.4	A0A3D8RLL3
FDC1 *Penicillium decumbens*	497	50.4	A0A1V6NNH9
FDC1 *Penicillium solitum*	500	50.3	A0A1V6RL46
FDC1 *Aspergillus nomius NRRL 131317*	503	50.3	A0A0L1J9Y6
FDC1 *Gibberella fujikuroi*	503	50.2	S0E299
FDC1 *Gibberella intermedia (Bulb rot disease fungus) (Fusarium proliferatum)*	503	50.2	A0A365NJK4
FDC1 *Fusarium kuroshium*	503	50.2	A0A3M2RIT9
FDC1 *Aspergillus violaceofuscus*	503	50.2	A0A2V5HJD9
FDC1 *Amorphotheca resinae ATCC 22711*	496	50.2	A0A2T3AZN7
FDC1 *Aspergillus indologenus CBS 114.80*	503	50.2	A0A2V5I997
FDC1 *Penicillium flavigenum*	500	50.1	A0A1V6SP78
FDC1 *Penicillium rubens*	500	50.1	B6HRC8
FDC1 *Trichoderma harzianum*	499	50.1	A0A0F9Z7X1
FDC1 *Aspergillus rambellii*	497	50.1	A0A0F8UFA2
FDC1 *Aspergillus luchuensis*	500	50.1	A0A146FW50
FDC1 *Aspergillus niger*	517	50.0	A0A100IUI5
FDC1 *Aspergillus tubingensis*	493	50.0	A0A1L9N5Q2
FDC1 *Penicillium steckii*	495	50.0	A0A1V6SR50
FDC1 *Botryosphaeria parva*	495	50.0	R1EM06
FDC1 *Colletotrichum salicis*	505	50.0	A0A135URQ4
FDC1 *Penicilliopsis zonata CBS 506.65*	498	50.0	A0A1L9S913
FDC1 *Phialocephala subalpina*	528	50.0	A0A1L7WNI4

[a]Protein length (number of amino acids).

[b]Percentage of residues identical to those of the enzyme *trans*-cinnamic acid decarboxylase from *Saccharomyces cerevisiae* (Ferulic acid decarboxylase, FDC1).

Table S2.2: Symbols present in the consensus sequences derived from multi-alignment of FDC homologous proteins and amino acids to replace them at the indicated position.

Symbol	Amino acids
!	Isoleucine (I) o Valine (V)
$	Leucine (L) o Methionine (M)
%	Phenylalanine (F) o Tyrosine (Y)
#	Asparagine (N), Aspartic Acid (D), Glutamine (Q), Glutamic Acid (E)

Table S2.3: DNA and protein sequences of PSC1.

DNA sequence of *psc1*

ATGAGCGCCCTGAACCCGGCCCTGCGTTTCCGTGATTTCATCCAGGTGCTGAAGAACGAAGGCGATCTGATCGAAATCA
CCACCGAGGTGGACCCGAACCTGGAAGTGGGTGCCATCACCCGCAAAGTGTACGAAGAGAAGCTGCCGGCCCCGCTGTT
CAACAACCTGAAAGGCGCCAGCAAGAACCTGTTCAACATCCTGGGTTGCCCGGGTGGCCTGCGTAGCAAGAAAGGCAAC
GACCATGCCCGTATCGCCCTGCATCTGGGCCTGGATAGCCAGACCCCGATGAAGAAAATCATCGACTATCTGCTGGAAG
CCAAAACCAAGAAACCGATCCCGCCGCACGAGGTGCCGGCCAGCGGTGCCCCGTGCAAGGAAAACCTGCTGAGCGGCGA
TGAGATCGACCTGACCAGCCTGCCGGTGCCGCTGCTGCACCATGGTGATGGTGGCAAATACATCCAGACCTATGGCATG
TGGGTGCTGCAGACCCCGGACAAGAGCTGGACCAACTGGAGCATCGCCCGCGGCATGGTGGTGGATGACAAGCACATCA
CCGGCCTGGTGATCAACCCGCAGCATATCCGTCAGGTGGCCGATGCCTGGGCCGCCATCGGCAAGGGCGACAAAATCCC
GTTCGCCCTGTGCTTCGGTGTGCCGCCGGCCGCCATCCTGGTTAGCAGCATGCCGATCCCGGAAGGTGCCACCGAGAGC
GATTACATCGGTGCCCTGCTGGGTGAAAGCCTGCCGGTGGTGAAATGCGAGACCAACGACCTGATGGTGCCGGCCACCA
GCGAAATCGTGTTCGAGGGCACCCTGGATCTGAACGACCTGGTGCCGGAAGGTCCGTTCGGCGAGATGCACGGCTATGT
GTTCCCGGGTCAGGGTCATCCGTGCCCGCTGTACACCGTGAACGCCATCACCTATCGCAACAACGCCATCCTGCCCGTG
AGCAACCCGGGTCTGTGCACCGATGAAACCCATACCCTGATCGGCGGCCTGGTTAGCGCCGAAGCCAAGCAGCTGGCCA
TCGAGCATGGCGTGCCGATCCTGGATGCCTTCACCCCGTATGAAGCCCAGGCCCTGTGGCTGGCCCTGAAAGTGGACCT
GAAGAAACTGCAGGCCCTGAAAACCAACCCGAAGGAGTTCAGCAAGAAAGTGGGCGACATCTACTTCCGCAGCAAAGTG
GGCTTCATCATCCACGAGATCATCCTGGTGGGCGATGACATCGATATCTTCGACTTCCGCAAGGTGATCTGGGCCTATA
CCACCCGCCATACCCCGGTGGATGACCAGTACTATTTCGATGACGTGAAAGCCTTCGCCCTGGCCCCGTTCGTGAGCCA
GAGCCCGCGCATCAAGACCCTGAAAGGCGGCAAGTGCGTGACCAACTGCATCTTCCCGCAGCAGTACGAACGCGATGTG
GACTTCGTGACCTGCAACTTCGATGGCTATCCGGAAGAGATCAAGGACAAAGTGCTGCAGAACTGGAGCGCCTACGGCT
ATAAGTAA

Protein sequence of PSC1

MSALNPALRFRDFIQVLKNEGDLIEITTEVDPNLEVGAITRKVYEEKLPAPLFNNLKGASKNLFNILGCPGGLRSKKGN
DHARIALHLGLDSQTPMKKIIDYLLEAKTKKPIPPHEVPASGAPCKENLLSGDEIDLTSLPVPLLHHGDGGKYIQTYGM
WVLQTPDKSWTNWSIARGMVVDDKHITGLVINPQHIRQVADAWAAIGKGDKIPFALCFGVPPAAILVSSMPIPEGATES
DYIGALLGESLPVVKCETNDLMVPATSEIVFEGTLDLNDLVPEGPFGEMHGYVFPGQGHPCPLYTVNAITYRNNAILPV
SNPGLCTDETHTLIGGLVSAEAKQLAIEHGVPILDAFTPYEAQALWLALKVDLKKLQALKTNPKEFSKKVGDIYFRSKV
GFIIHEIILVGDDIDIFDFRKVIWAYTTRHTPVDDQYYFDDVKAFALAPFVSQSPRIKTLKGGKCVTNCIFPQQYERDV
DFVTCNFDGYPEEIKDKVLQNWSAYGYK

Table S2.4: DNA and protein sequences of PSD1.

DNA sequence of *psd1*

```
ATGCCGCACCTGTTCCGCTTCGTGGAAGCCCTGAAAGATGACCTGGTGGAAATCAACGAAGATCCGAACCTGGAAGCCG
GTGCCATCCGTGTGTGCGAGACCGACAAAGCCCCGCTGTTCAACAACCTGAAGGGCGGCCTGTTCCGCATCCTGGGTGC
CCCGAGCCTGCGTTATGGTCGCCTGGCCCGCCATCTGGGCCTGCCGCCGACCGCCATGAAGGAAATCCTGGATAAAATG
CTGAGCGCGGCCGCCGCCGCCCCGATCCCGCCGGCCGCCGTGGCCACCGGCCCGTGCAAGGAGAACGCCCTGGCGGCGG
CCGCCATCGATCTGACCGCCCTGCCGGCCCCGGCCCTGCACCAGGCCGACGGTGGCAAATACATCCAGACCTATGGCAT
GCATATCGTGCAGAGCCCGGATGGCAAGTGGACCAACTGGAGCATCGCCCGTGCCATGGTGGCCGACGCCAACCACCTG
GCCGGCCTGGTGATCGAACCGCAGCACATCTGGCAGATCCATCAGATGTGGAAGAAAGAGGGCAAAGATGTGCCGTGGG
CCCTGGCCTTCGGTGTGCCGCCGGCGGCCATCGCCAGCAGCATGCCGATCCCGGATGGTGTGAGCGAAGCCGCCTATGT
GGGTGCCGCCGCCGGTGCCGCCCTGGCCGTGGTGAAGTGCGATACCAACGACCTGGCCGTGCCGGCCGCCAGCGAAATC
GTGTTCGAGGGCACCCTGAGCATCACCGAAACCGCCCCGGAGGGTCCGTTCGGTGAAATGCACGGCTATGTGTTCCCGG
GTGATGCCCATGCCGCCCCGGCCTACGCCGTGAACGCCATCACCTATCGTGCCGCCGCCATCCTGCCCGTGAGCAACTG
CGGTCGTCTGACCGACGAAACCCACACCATGATCGGCGCCCTGGCCGCCGCCGAGATCGCCGCCGCCTGCGCGGCCGCC
GGTCTGCCGATCGCCGATGCCTTCGCCCCGTTCGAAAGCCAGGTGACCTGGGTGGCCCTGAAGGTGGACACCGCCAAAC
TGCGTGCCATGAAGACCACCCCGGCCGAGTTCGCCAAAGCCGTGGGTGACGCCGTGTTCAACCACAAGGCCGGCTACAC
CATCCATCGCCTGGTGCTGGTGGGCGATGACATCGATGTGTATAACGCCAAAGATGTGTGGGCCTTCACCCGTTGCCGT
CCGGATGAGTTCTTCGAGGACGTGGGCTTCCCGCTGATCCCGTATATGAGCCATGGTGGCCCGGGTGGCAAGGTTGTGA
GCGATGCCCTGCCGGAATACACCGGTTGGGCCGACTTCAGCTATCCGGAGAAGAAAGTGTGGGGCTTCTAA
```

Protein sequence of PSD1

```
MPHLFRFVEALKDDLVEINEDPNLEAGAIRVCETDKAPLFNNLKGGLFRILGAPSLRYGRLARHLGLPPTAMKEILDKM
LSAAAAAPIPPAAVATGPCKENALAAAAIDLTALPAPALHQADGGKYIQTYGMHIVQSPDGKWTNWSIARAMVADANHL
AGLVIEPQHIWQIHQMWKKEGKDVPWALAFGVPPAAIASSMPIPDGVSEAAYVGAAAGAALAVVKCDTNDLAVPAASEI
VFEGTLSITETAPEGPFGEMHGYVFPGDAHAAPAYAVNAITYRAAAILPVSNCGRLTDETHTMIGALAAAEIAAACAAA
GLPIADAFAPFESQVTWVALKVDTAKLRAMKTTPAEFAKAVGDAVFNHKAGYTIHRLVLVGDDIDVYNAKDVWAFTRCR
PDEFFEDVGFPLIPYMSHGGPGGKVVSDALPEYTGWADFSYPEKKVWGF
```

Chapter 3

Sustainable biosynthesis of styrene: Exploiting a consensus-designed decarboxylase, its purification and crystal structure

Ana García-Franco, Jesús de la Torre, Patricia Godoy, Estrella Duque, Carmen López, José A. Gavira and Juan L. Ramos.

Manuscript in preparation for submission.

Abstract

Microbial biosynthesis of aromatic compounds offers significant advantages over petrochemical methods, which rely on fossil fuels and high energy inputs. Microbial fermentations occur at room temperature and ambient pressure, reducing carbon emissions and energy consumption by up to 90%. Genetic engineering of microbial chassis is key to optimizing biosynthetic processes, enabling efficient production of aromatic compounds from sugars. However, the intrinsic toxicity of these compounds presents challenges. *Pseudomonas putida* DOT-T1E, known for its tolerance to solvents, is ideal for producing toxic compounds. Styrene biosynthesis involves converting phenylalanine into *trans*-cinnamate via PAL enzymes, followed by decarboxylation to styrene. This second step is challenging, as *trans*-cinnamic acid decarboxylases have only been described in fungi. PSC1, a consensus protein designed from multiple fungal ferulate decarboxylases, enables styrene production in *Pseudomonas*. PSC1 is a globular dimer with a molecular mass of 104.7 kDa, high thermal stability (T_m 63°C), and activity at temperatures up to 50°C. The crystal structure of PSC1, determined at 2.1 Å, reveals a homodimer with three domains per monomer. A hydrophobic pocket in domain 2, essential for cofactor and substrate binding, was identified. Mutagenesis shows that Arg175, Glu280 and Glu285 are critical for catalysis, as replacing them with alanine abolished the decarboxylation.

3.1 Introduction

The microbial biosynthesis of aromatic compounds, including styrene, styrene oxide, hydroxystyrene, *trans*-cinnamic acid (*t*CA), and others, stands out for its unparalleled efficiency and environmental friendliness (Kang et al., 2015; Lee et al., 2019; Liang et al., 2020; Liu et al., 2018; Machas et al., 2017; McKenna & Nielsen, 2011; McKenna et al., 2013; Nijkamp et al., 2007; Otto et al., 2020). Unlike chemical processes that heavily rely on fossil fuels and require high pressure, high temperature and toxic catalyzers; microbial fermentations operate at room temperature and ambient pressure. This not only reduces the carbon footprint but also minimizes energy consumption. Recent studies have highlighted the potential of microbial cell factories in synthesizing valuable chemicals with up to 90% lower CO_2 emissions compared to their chemical counterparts (Fackler et al., 2021; Godar et al., 2021; Rabinovitch-Deere et al., 2013; Ramos & Duque, 2019).

Genetic engineering plays a crucial role in enabling microbes to efficiently produce aromatic compounds from aromatic amino acids. Bird et al. (2023), in their review on the definition of host platforms for biosynthesis of value-added chemicals, discussed that choosing the right host platform is the key to optimizing biosynthetic processes, and suggested that factors such as the tolerance of the host to substrates and products, understanding the host's metabolism, availability of catabolic pathways and tools for stable heterologous gene expression, are all essential considerations when designing a successful biosynthetic pathway.

The biosynthesis of aromatic hydrocarbons is challenging because of their intrinsic toxicity to living organisms (Heipieper & Martínez, 2018; Sikkema et al., 1995). These compounds disrupt the phospholipid bilayer and interfere with the generation of the proton motive force, collapsing ATP synthesis and eventually leading to cell death (Bitzenhofer et al., 2024; Ramos et al., 2015; Udaondo et al., 2013). However, certain strains of the species *Pseudomonas putida* have demonstrated remarkable tolerance to organic solvents, offering a promising solution for the biosynthesis of these toxic compounds. Tolerance to solvents in *P. putida* is achieved through multifactorial defense mechanisms such as efflux pumps that reduce intracellular toxin levels, membrane strengthening via *cis* to *trans* isomerization of unsaturated fatty acids, enhanced synthesis of saturated fatty acids, and activation of a general stress response involving chaperones that fold/refold proteins and enzymes that remove

reactive oxygen species (ROS) (García-Franco et al., 2023, 2024). The extent of these responses varies with the strain and the toxic compound.

Regarding the genetic manipulation of strains of *P. putida*, significant advances have been made in developing a robust toolkit for their genetic manipulation, including the implementation of mini-transposons, expression vectors, regulatable promoters and "mecano" SEVA plasmids (Arce-Rodríguez et al., 2021; Martínez-García et al., 2014, 2017). These tools have paved the way for enhanced control and efficiency in the genetic modifications of microorganisms from these species.

The metabolic pathways of *P. putida*, particularly strains related to *P. putida* KT2440, have been extensively studied revealing intricate networks for balanced growth using different C, N, S and P sources (Nogales et al., 2020; Udaondo et al., 2013). The chemical synthesis of styrene, known as one of the most polluting petrochemical processes, is being targeted for replacement by eco-friendly biological processes (García-Franco et al., 2024; McKenna & Nielsen, 2011). To this end, the highly solvent tolerant *P. putida* DOT-T1E and S12 are potential chassis for the production of styrene (García-Franco et al., 2024; Webb et al., 2022). Based on the analysis of Udaondo et al. (2016), we found that *P. putida* DOT-T1E requires two additional enzymes to convert the aromatic amino acid phenylalanine (L-Phe) into styrene, namely: a phenylalanine ammonia lyase (PAL) to convert L-Phe into *t*CA and a *trans*-cinnamic acid decarboxylase to convert the latter into styrene. The conversion of L-Phe into styrene is equimolar, and the concentration of the aromatic amino acid determines the yield of styrene. Under laboratory growth conditions, *P. putida* produces limited amounts of L-Phe due to dedicated genetic regulation of the biosynthetic genes and appropriate feedback inhibition of the chorismate mutase/prephenate dehydratase (PheA) protein. This protein is involved in the biosynthesis of phenylpyruvate, a precursor of L-Phe in the biosynthesis of this aromatic amino acid (Loeschcke & Thies, 2020; Molina-Henares et al., 2009). Molina-Santiago et al. (2016) engineered DOT-T1E to optimize L-Phe production, which required inactivating five pathways for L-Phe degradation and a mutation in the *pheA* gene to remove feedback inhibition by the amino acid. The mutant strain, named CM12-5, produced 340 mg L^{-1} of the amino acid. Furthermore, the strain synthesized *t*CA from L-Phe using PAL enzymes from cyanobacteria, showing the efficiency of the enzymatic conversion in *P. putida* CM12-5 (García-Franco et al., 2024; Molina-Santiago et al., 2016).

Nielsen's group demonstrated that fungal ferulic acid decarboxylase (FDC EC:4.1.1.102) from *Saccharomyces cerevisiae* can convert *t*CA into styrene when the gene was cloned and expressed in *Escherichia coli* (McKenna & Nielsen, 2011). This reaction is similarly catalyzed by various other fungal ferulic (*trans*-cinnamic) acid decarboxylases (Bailey et al., 2018; Bhuiya et al., 2015; Duță et al., 2022; Nagy et al., 2019; Richard et al., 2015). However, due to the inefficiency of the *Saccharomyces* FDC in *Pseudomonas* (attributed to low gene expression and/or protein instability), a more functional *trans*-cinnamic acid decarboxylase was needed.

In pursuit of efficient styrene production in the solvent-tolerant *P. putida* DOT-T1E, García-Franco et al. (2024) employed innovative strategies, including the development of a consensus PSC1 enzyme based on multiple sequence alignment (MSA) as described by Sternke et al. (2019). The PSC1 consensus sequence was derived from the MSA of eight fungal FDCs, each exhibiting over 60% identity to the enzyme from *S. cerevisiae*. Whilst typical average identities between consensus sequences and MSAs range from 40% to 60% (Sternke et al., 2019, 2020), PSC1, designed with a criterion of >60% identity to *S. cerevisiae* FDC1, shows an identity that ranges from 72% to 80% with the enzymes used for the MSA (see Table S3.1).

Fungal ferulic acid decarboxylases, such as those transforming *t*CA, belong to the UbiD family of decarboxylases. Their biochemical characterization has revealed valuable insights into the role of prenylated FMN (prFMN) as a cofactor (Bailey et al., 2018; Nagy et al., 2019). Studies by Leys' lab and others on UbiD decarboxylases from *Aspergillus niger* and *S. cerevisiae*, uncovered that the prFMN cofactor exists in two distinct forms: $\text{prFMN}_{\text{iminium}}$ (active in catalysis) and $\text{prFMN}_{\text{ketimine}}$ (the inactive form) (Figure S3.1) (Bailey et al., 2018; Bloor et al., 2023; Ferguson et al., 2016; Nagy et al., 2019; Payne et al., 2015; Roberts & Leys, 2022).

The biosynthesis of prFMN appears to be a universal process (Batyrova et al., 2020; Wang et al., 2018b) and in *P. putida* is likely to take place as depicted in Figure 3.1. Initially, FMN is reduced by NADPH through the action of flavin oxidoreductases (Fre). In *P. putida* DOT-T1E, this reaction involves the gene products of T1E_5625 and/or T1E_1776. Subsequently, prFMN is made from reduced FMN (FMN_{red}) in a reaction catalyzed by the UbiX enzyme (T1E_1538), which attaches a non-aromatic ring to the flavin via dimethylallyl monophosphate (DMAP). DMAP itself is made from mevalonate via dimethylallyl pyrophosphate (DMAPP) and its subsequent dephosphorylation by NudF/NudC (T1E_1192, T1E_3285) (Udaondo et al., 2013).

In vivo evidence suggests that in *P. putida*, prFMN can be incorporated into different apoenzymes, such as PSC1, although binding of the cofactor is labile.

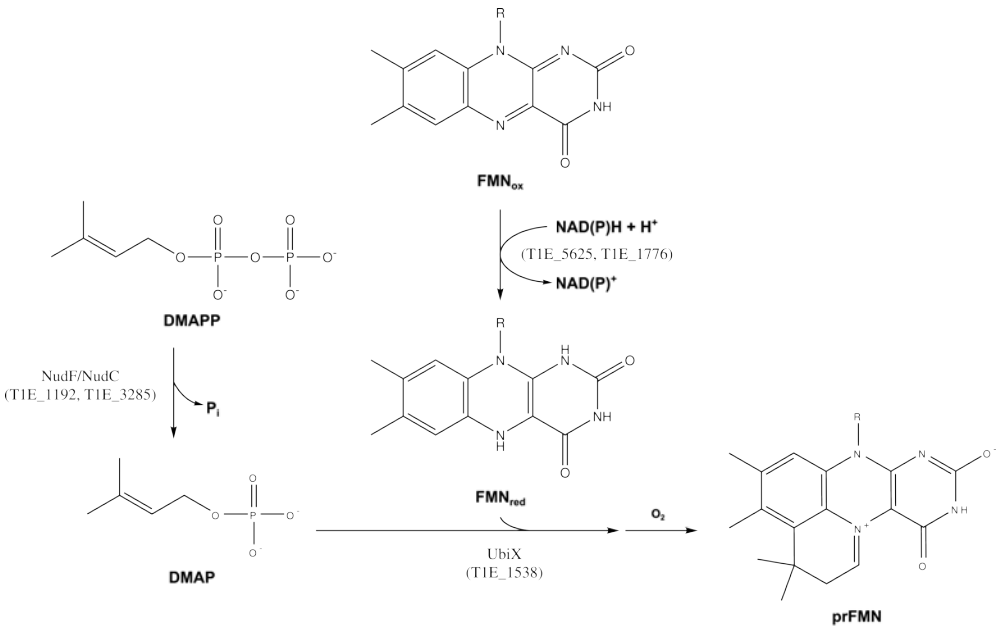

Figure 3.1: Schematic overview of the biosynthesis of prFMN in *Pseudomonas putida*. The T1E numbers represent the locus tag in the *P. putida* DOT-T1E genome. Abbreviations: DMAPP, dimethylallyl pyrophosphate; DMAP, dimethylallyl monophosphate; FMN_{ox}, oxidized flavin mononucleotide; FMN_{red}, reduced flavin mononucleotide; prFMN, prenylated FMN.

To advance the industrial development of styrene biosynthesis in *P. putida* CM12-5, efforts have been directed toward purifying and characterizing the PSC1 enzyme, determining its physico-chemical properties, substrate specificity and structural characteristics. The high thermostability and substrate specificity of PSC1 make it a promising candidate for enhancing styrene production in microbial systems.

3.2 Materials and methods

3.2.1 Bacterial strains, plasmids and culture media

The *E. coli* BL21 (DE3) strain (Studier & Moffatt, 1986) was used for protein overexpression, and *E. coli* DH5α (Grant et al., 1990) was used for gene cloning. *E. coli* cells were grown in LB medium at temperatures ranging from 18°C to 37°C.

P. putida strains were grown on M9 minimal medium with glucose as the sole carbon source (Abril et al., 1989) at 30°C. Plasmids used or constructed in this study are listed in Table S3.2. Rifampicin (Rif) and gentamycin (Gm) were added, when required, to reach a final concentration of 10 μg mL^{-1}, and kanamycin (Km) to 25 μg mL^{-1}.

3.2.2 Protein purification

To purify the PSC1 protein, a *Pseudomonas* codon-optimized *psc1* gene was designed and cloned in pET28(b) for expression, with the coding region located downstream of a His-tag sequence. Induction assays at different temperatures and various IPTG concentrations revealed that the highest protein yields were obtained when bacteria were grown at 30°C with 1 mM IPTG. For the protein purification, induced cells (1–2 g) were resuspended in 25 mL of lysis buffer (50 mM Tris-HCl, 500 mM NaCl, 1 mM DTT, 10 mM imidazole and 10% (v/v) glycerol) supplemented with an EDTA-free protease inhibitor mixture. Cell lysis was achieved by passing the sample through a French press three times at a pressure of 1,000 psi. The lysate was centrifuged at 6,000 $\times g$ for 30 minutes, and the supernatant was filtered using sterile 0.22 μm filters before loading onto a 5 mL His-Trap chelating column (GE Healthcare, St. Gibes, UK). The proteins were eluted using a gradient of 10 to 500 mM imidazole in the above buffer. The purity of the eluted protein fractions was evaluated using 12% (w/v) SDS-PAGE gels. Homogeneous protein fractions were dialyzed overnight against a buffer made of 50 mM HEPES (pH 7.0), 150 mM NaCl and 10% (v/v) glycerol. For the sedimentation rate analysis and dynamic light scattering assays, the concentration of glycerol was reduced to 2% (v/v) in the dialysis buffer, whilst for crystallization trials the NaCl and glycerol in the dialysis buffer were 50 mM and 2% (v/v), respectively.

3.2.3 Analytical ultracentrifugation

An Optima XL-I analytical ultracentrifuge (Beckman-Coulter, Palo Alto, CA) equipped with a UV-visible absorbance detection system was used. Experiments were carried out at 20°C using an AnTi50 rotor, and absorbance measurements were taken at 280 nm. Sedimentation velocity experiments were performed using standard double sector Epon-Charcoal centerpieces (12-mm optical path) at a rotation speed of 48,000 rpm. Sedimentation coefficient distributions were derived by performing

direct linear least-squares boundary fitting of the sedimentation velocity profiles using the SEDFIT software (Brown & Schuck, 2008; Zhao et al., 2010). SEDNTERP software (Philo, 2023) was used to adjust S values to standard conditions (20°C and water). Apparent weight-average buoyant molecular weights were obtained by fitting a single species model to the experimental data using a MATLAB programme based on the conservation of signal algorithm. Protein molecular weights were calculated using a partial specific protein volume of 0.725 cm^3/g.

3.2.4 Dynamic light scattering (DLS)

The protein mass was determined using the Svedberg equation, with the sedimentation coefficient (S) obtained by sedimentation rate analysis, and the diffusion coefficient (D) obtained by DLS.

$$M = \frac{RTs}{(1-\bar{v}\rho)D}$$

Svedberg equation. T, R, $\bar{v}$ and ρ are the absolute temperature in Kelvin, the universal gas constant, the partial specific volume of the protein (obtained from its sequence) and the density of the buffer, respectively.

3.2.5 Differential scanning fluorimetry (DSF)

Thermal denaturation assays were performed using a MyIQ2 Real-Time PCR instrument (Fernández et al., 2019). A 25 µL solution of PSC1 at concentrations of 2, 5 and 10 µM supplemented with 5x SYPRO orange in 50 mM Hepes (pH 7.0) and 150 mM NaCl, was heated from 23°C to 85°C at a rate of 1°C per minute. Fluorescence emission was continuously monitored, and melting temperatures (T_m) were determined using Bio-Rad iQ5 software.

3.2.6 Plasmid DNA extraction and generation of the mutant proteins of PSC1

Highly pure plasmid DNA was obtained using the NZYMiniprep commercial kit (NZYTech) according to the manufacturer's instructions. Cells (2 mL) from a 24-

hour culture in LB medium with gentamycin were centrifuged at 13,000 rpm for 1 minute. Point mutations at positions 175, 189, 192, 285 and 330 were generated by replacing these residues with alanine using the method described by Li and Wilkinson (1997). Arginine 175 was also replaced by Lysine and Glutamate 285 by Aspartate. Point mutations at positions F397 and I398, and a double mutant at these positions, were also generated, replacing them with tyrosine and threonine, respectively, or both residues were replaced by tyrosine and threonine. The replacements in these two latter positions correspond to the amino acids located in the alignment of PSC1 with *A. niger* FDC1. To generate the mutants, the plasmid pSEVA632_C1, carrying the 1509 nucleotide sequence encoding the PSC1 protein, was used as a template. Mutations were generated by PCR with the specific primers listed in Table S3.3. In a first step, the PCR reaction (final volume 24 µL) contained a mixture of 100 ng of template plasmid DNA; 150 mM of each dNTP; 200 ng of the specific forward primers; 1U Pfu turbo DNA polymerase (StrataGene); 1U Taq polymerase (Roche) and 1x buffer supplied with Pfu turbo enzyme. A parallel amplification reaction was also set up but with 200 ng of the specific reverse primers. The thermocycler program for each set of reactions was 3 cycles at 95°C for 30 seconds, 55°C for 60 seconds and 68°C for 6 minutes, cooling to 14°C for 10 minutes. DNA was denatured at 95°C for 2 minutes before the first cycle. Once the reactions were tempered, both amplification products were pooled in a single 0.2 mL eppendorf tube. A thermocycler program of 22 cycles of 95°C for 30 seconds, 55°C for 60 seconds and 68°C for 6 minutes, cooling to 14°C for 10 minutes, was set up. Then, 15 µL of the product of this reaction was cleaved with 10U of DpnI (New England Biolabs) for 14 hours at 37°C. Subsequently, the entire reaction was transformed into competent *E. coli* DH5α cells by heat shock and spread on solid Luria-Bertani (LB) medium supplemented with 10 µg mL^{-1} gentamycin. The mutants were identified by Sanger sequencing using the M13Fw and M13Rv primers (Table S3.3).

3.2.7 Substrate profile of PSC1

Since we found that the PSC1 protein lost the prFMN cofactor during purification, the substrate profile was assayed *in vivo* according to Nagy et al. (2019), except that we used *P. putida* CM12-5 bearing pPSC1, or mutant variants, and the cell suspension was prepared as follows: cultures were allowed to reach a turbidity of $\sim$1 at 660 nm, then the cells were harvested by centrifugation at 6,000 $\times g$ for 3 min and suspended

to reach a cell density of ∼10. Cells were incubated at temperatures between 18°C and 50°C, then the substrates were added to reach a final concentration of 0.25 mM. The substrates used included *t*CA, chlorogenic acid, *p*-coumaric acid, *trans*-ferulic acid, *trans*-sinapic acid and 3,4-dimethoxycinnamic acid. Their concentration in the culture medium were measured over time by HPLC, as described by García-Franco et al. (2024).

3.2.8 Crystallization of PSC1

PSC1 was freshly purified as described above, concentrated to 10-12 mg mL^{-1} and then dialyzed against a buffer made of 50 mM HEPES (pH 7.0), 50 mM NaCl and 2% (v/v) glycerol. Initial crystallization screenings were carried out at 20°C with a dispenser in sitting-drop vapor diffusion plates using commercially available crystallization screens (HR I and II from Hampton Research and Morpheus I and II from Molecular Dimensions). Several conditions produced crystalline material but the most promising one was grown in condition #6 of HR I containing 200 mM $MgCl_2$, 100 mM Tris-HCl pH 8.5 and 30% (w/v) PEG 4K. For data collection, some crystals were soaked with a cryoprotectant solution prepared by adding 15% (v/v) of glycerol to the crystallization condition. Crystals, with and without cryoprotectant, were flash-cooled in liquid nitrogen. Diffraction data were collected at the beamline XALOC of the Spanish Synchrotron radiation source, Alba (Barcelona, Spain). Diffraction data were indexed and integrated with XDS (Kabsch, 2010) and scaled and reduced with AIMLESS (Evans & Murshudov, 2013) of the CCP4 program suite (Collaborative Computational Project, 1994). Molecular replacement was done using the best-scored AlphaFold2 (Jumper et al., 2021) model as the search model in Molrep (Vagin & Teplyakov, 2010). Refinement was continued with Refmac (Murshudov et al., 2011) and *phenix.refine* (Afonine et al., 2010) of the CCP4 (Collaborative Computational Project, 1994) and *PHENIX* (Adams et al., 2010) suites, respectively. Visual inspection, manual building, water positioning, and ligands identification were done in Coot (Emsley et al., 2010). Final refinement was done, including Translation-Libration-Screw (TLS) parameterization (Painter & Merritt, 2006), and the quality of the models was regularly verified with MolProbity (Chen et al., 2010) and the PDB validation server before being deposited in the PDBe (Velankar et al., 2010). The coordinates and the experimental structure factors have been deposited in the Protein Data Bank (PDB) under the accession code 9GQR.

The PDBsum server was used to identify the secondary structural elements and to define each domain composition (Laskowski et al., 2018). The PISA server was used to calculate the most probable quaternary structures assemblies (Krissinel & Henrick, 2007). Graphical representation of structural models was prepared with PyMol (DeLano, 2002).

3.3 Results

3.3.1 Purification of PSC1 protein, molecular mass and oligomeric state

The *psc1* gene encodes a 502-amino-acid protein with an estimated molecular mass of 55.4 kDa, which falls within the typical mass range for UbiD family enzymes (55-59 kDa) (Jacewicz et al., 2013). The PSC1 protein was purified as described in Materials and methods section 3.2.2, and it exhibited high solubility. SDS-PAGE revealed a series of fractions with a homogenous protein of approximately 55 kDa (Figure S3.2) which were pooled for further assays.

To further investigate the size and shape of PSC1, analytical ultracentrifugation sedimentation studies were undertaken. The ratio of the frictional coefficient of PSC1 to that of an ideal globular protein (f/f_0 ratio) was found to be 1.258 (Table 3.1), indicating that PSC1 is predominantly globular with some elliptical characteristics. Sedimentation gradient analysis revealed that over 94% of the protein corresponded to a single species with a sedimentation coefficient of 5.19 S (Figure 3.2). When corrected to standard conditions (the density and viscosity of water at 20°C), the sedimentation coefficient ($S_{20,w}$) was calculated to be 5.994 S (Table 3.1). These analyses suggest a molecular mass of 104,691 Da for PSC1, indicating that this enzyme exists as a dimer in solution, consistent with the crystal structure of the *A. niger* and *S. cerevisiae* FDC enzyme.

Table 3.1: Parameters of the ultracentrifugation sedimentation analysis.

Parameter	**PSC1**
Peak	94.6%
sw (S)	5.190
Sw (20,w) (S)	5.994
C (mg/mL)	0.3988
% of total	93.487
Coefficient of friction (f/f_0)	1.258
Mw (Da)	104,691
vbar (cm^3/g)	0.744
vbar20 (cm^3/g)	0.744
Hydration (g/g)	0.000
Buffer density (g/cm^3)	1.0141
Relative viscosity (cP)	1.1018
Minimum Mw for compact sphere (Da)	74,202
Stokes Radius (20°C) (nm)	3.95
a/b (oblate)	5.53
a/b (prolate)	5.12

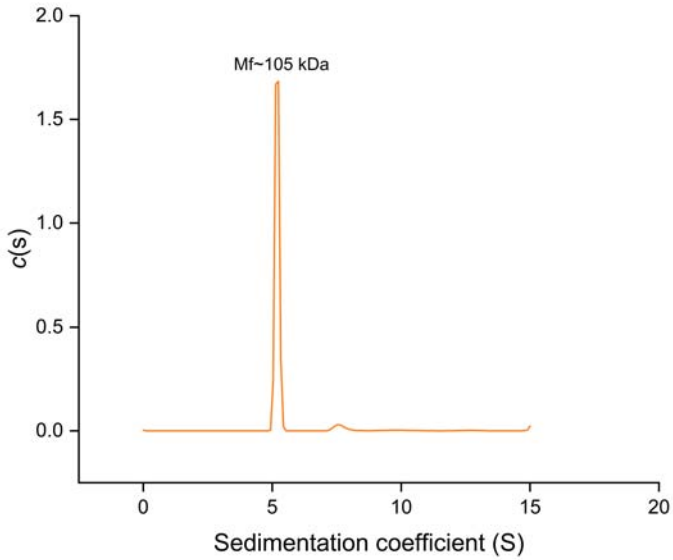

Figure 3.2: Sedimentation velocity analytical ultracentrifugation of PSC1. The assays were conducted at 20°C, using an AnTi50 rotor, under the specific conditions described in Materials and methods section 3.2.3.

3.3.2 Thermal stability

Following the protocol described in Materials and methods section 3.2.5, the midpoint temperature of unfolding transition (T_m) for PSC1 was found to be 63°C (Figure 3.3). After storing the purified protein for four weeks at 4°C, the T_m was determined again, also yielding an unfolding temperature of 63°C. This consistency suggests that the consensus PSC1 protein is highly stable, with melting temperature typical of extremophilic proteins. Certain decarboxylases are known to be stabilized by metal ions (e.g., Mn^{2+}, Zn^{2+}, Ca^{2+}) (Anand et al., 2002; Li et al., 2012; Moomaw et al., 2009; Vladimirova et al., 2016). To explore this possibility, we also conducted differential scanning fluorimetry (DSF) assays in the presence of 1 mM of different metals (Mg^{2+}, Mn^{2+} and Ca^{2+}). The assay results indicated a T_m of 63°C, suggesting that these metals do not contribute to the stabilization of the protein.

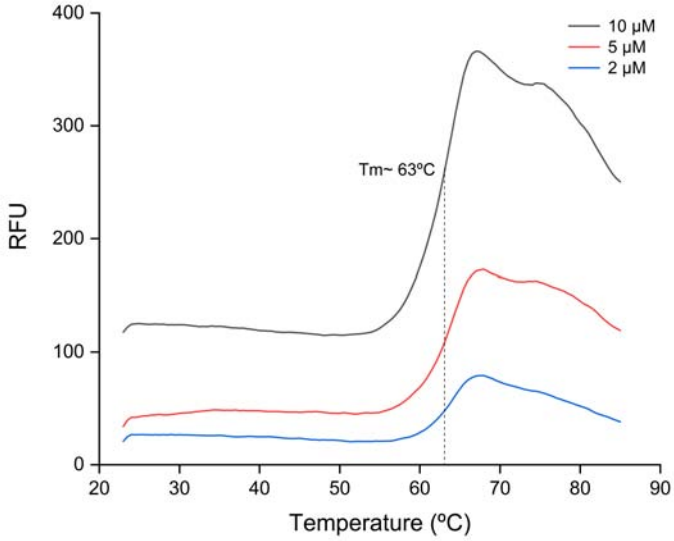

Figure 3.3: Thermal unfolding behavior of PSC1. The effect of the incubation temperature on the thermal stability of PSC1 at 2, 5 and 10 µM in HAM buffer at pH 7 is recorded. The unfolding temperature (T_m) was determined using the Bio-Rad iQ5 software.

Nagy et al. (2019) reported that the optimal *in vivo* temperature for FDC1 of *S. cerevisiae* is 35°C, but the T_m of FDC1 remains unknown. Given the apparent thermoresistance characteristics of PSC1, we tested *in vivo* conversion of *t*CA to styrene over a broad range of temperatures, up to 50°C (higher temperatures could not be tested due to fast death of cells). We observed a rapid conversion of *t*CA into styrene at all tested temperatures, with the initial consumption rate being higher at

50°C and 45°C (Table 3.2), i.e. 12.8 ± 0.3 μmol L^{-1} min^{-1} at 50°C versus 4.0 ± 0.3 μmol L^{-1} min^{-1} at 25°C.

Table 3.2: Initial consumption rates of *trans*-cinnamic acid at different temperatures. Resting cells of *Pseudomonas putida* CM12-5 (pPSC1) were prepared as described in Materials and methods section 3.2.7. The concentration of *trans*-cinnamic acid was monitored for 30 min, during which a linear decrease in substrate levels was observed. Data are the mean values and standard deviations from three independent assays.

Temperature (°C)	**Initial consumption rate (μmol L^{-1} min^{-1})**
18	3.4 ± 0.4
25	4.0 ± 0.3
30	4.6 ± 0.1
37	6.0 ± 0.3
45	10.6 ± 0.7
50	12.8 ± 0.3

3.3.3 The PSC1 enzyme exhibits narrow substrate specificity

Fungal FDC enzymes typically exhibit broad substrate specificity (Nagy et al., 2019), so we tested if analogues of *t*CA (Figure S3.3) could serve as potential substrates for PSC1. Our studies with *P. putida* CM12-5 expressing PSC1 revealed that PSC1 effectively transformed *t*CA and at lower rates *p*-coumaric acid, but failed to decarboxylate other derivatives such as chlorogenic acid, *trans*-ferulic acid, 3,4-dimethoxycinnamic acid and *trans*-sinapic acid (Table 3.3).

Table 3.3: Initial consumption rates of *trans*-cinnamic acid and analogues. Resting cells of *Pseudomonas putida* CM12-5 (pPSC1) were prepared as described in Materials and methods section 3.2.7. Substrate concentrations were monitored for 30 min, during which a linear decrease in substrate levels was observed. Data are the mean values and standard deviations from three independent assays.

Substrate	**Initial consumption rate (μmol L^{-1} min^{-1})**
Trans-cinnamic acid	4.8 ± 0.3
p-coumaric acid	2.0 ± 0.8
Chlorogenic acid	0.3 ± 0.2
Trans-ferulic acid	0.9 ± 0.7
3,4-Dimethoxycinnamic acid	0.2 ± 0.1
Trans-sinapic acid	0.6 ± 0.4

3.3.4 PSC1 crystal structure determination and identification of critical catalytic residues

We aimed to determine the crystal structure of the consensus PSC1 protein. The crystal structure of PSC1 was solved at a resolution of 2.1 Å, belonging to space group P1. Data collection and statistical details are summarized in Table 3.4. The PSC1 structure is a homodimer, with a Matthews coefficient of 2.15 and 43% solvent content. The dimeric quaternary structure was also confirmed with PISA (Krissinel & Henrick, 2007), with an interface buried area of 3500 $Å^2$ and a solvation free energy gain of -58 kcal/mol. The interface is also stabilized by the formation of three salt bridges and 29 potential hydrogen bonds.

The organization of the secondary structural elements (β-sheets and α-helices) in each monomer resembled that of other deposited 3D structural models of proteins of the UbiD family. Each PSC1 monomer is composed of three domains. Domains 1 and 2 from the N-terminal end of the monomer are connected to the third domain by a long alpha-helix (helix 14) (Figure 3.4A and Figure S3.4). The first domain presents a central four-stranded β-sheet surrounded by six α-helices. Helix 4 connects this domain to domain 2, which contains a core β-sheet capped by multiple α-helices (Figure S3.4). The third domain has a similar structure to that of the second domain, with a core β-sheet that is capped by multiple α-helices, although it is smaller in size. A long, flexible loop connects to the C-terminal helix (α24) and the terminus. PSC1 dimerization takes place through the third domain of each monomer, resulting in a U-shaped dimer (Figure 3.4B), as previously described (Bhuiya et al., 2015).

Table 3.4: Data collection and refinement statistics. Statistics for the highest-resolution shell are shown in parentheses.

	PSC1
Data collection	
Synchrotron / beamline	ESRF / ID30B
Space group	P1
Cell dimensions	
a, b, c (Å)	56.63, 66.28, 72.67
α, β, γ (°)	71.67, 73.08, 69.88
Resolution range	52.04 - 2.10 (2.14 - 2.10)
Completeness (%)	93.30 (61.90)
Multiplicity	2.2 (1.9)
Mean I/sigma(I)	5.1 (1.0)
Wilson B-factor (Å^2)	40.07
R-merge	0.124 (1.48)
CC1/2	0.993 (0.619)
Refinement	
No. reflections	50145 (1784)
R_{work} / R_{free}	21.43 / 24.73
No. atoms	8330
Protein	8010
Ligand/ion	42
Water	278
R.m.s. deviations	
Bond lengths (Å)	0.003
Bond angles (°)	0.58
Ramachandran	
Allowed (%)	97.06
Outliers (%)	0.00
Average B-factor (Å^2)	53.22
Macromolecules	53.39
Ligands	66.55
Solvent	46.50
PDB ID	9GQR

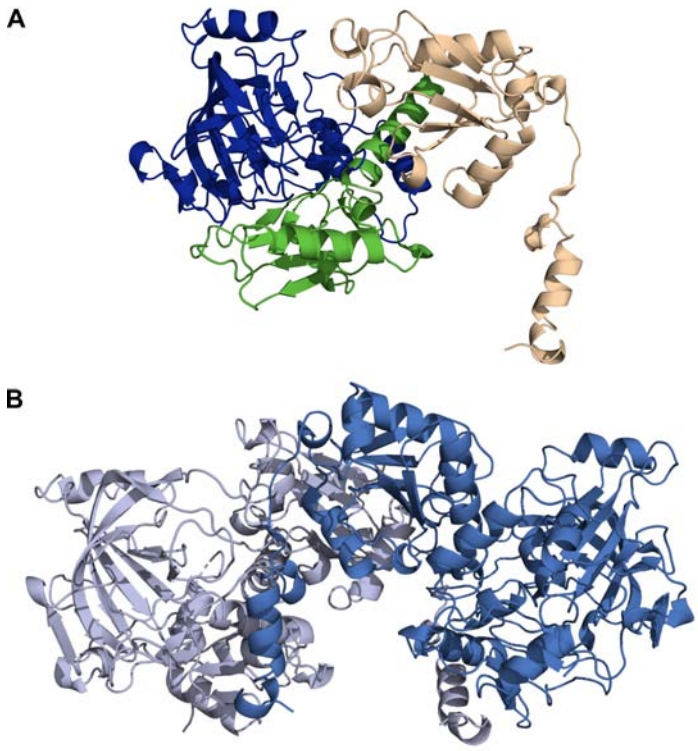

Figure 3.4: Monomeric and dimeric structure of PSC1. A) Ribbon diagram of the PSC1 monomer. The three domains are colour-coded: domain 1 (green), domain 2 (blue) and domain 3 (yellow). B) Ribbon diagram of the PSC1 dimer, highlighting the interaction between domain 3 of both monomers (shown in light blue and dark blue, respectively).

Structural comparison of PSC1 with entries in the Protein Data Bank (PDB) using PDBeFold (Krissinel & Henrick, 2004) revealed a high structural similarity with other crystallized UbiD-family decarboxylases, as expected. The highest similarity was found with the FDC1 from *S. cerevisiae* (79% amino-acid sequence identity, Z-score = 25.2; 0.79 Å root mean square deviation [RMSD]; PDB entry 4S13) (Figure 3.5A). PSC1 also showed similarity to *Candida dubliniensis* FDC (71% amino-acid sequence identity; Z-score of 24.2; and RMSD of 1.21 Å; PDB entry 4ZAD) (Figure 3.5B) and the FDC1 from *A. niger* (53% amino-acid sequence identity, Z = 22.5; 1.39 Å RMSD; PDB entry 7NF3) (Figure 3.5C).

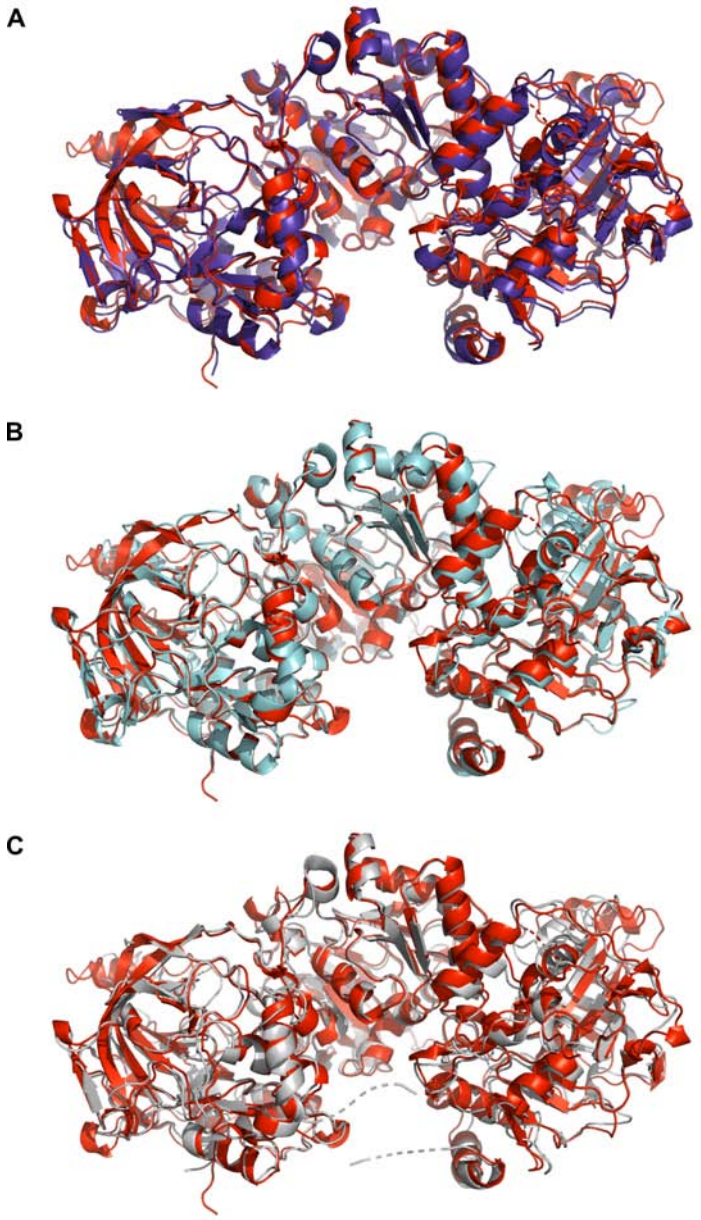

Figure 3.5: Superimposition of the dimeric form of PSC1 (red) with A) FDC1 from *Saccharomyces cerevisiae* (PDB ID 4S13) (purple), B) FDC1 from *Candida dubliniensis* (PDB ID 4ZAD) (cyan), and C) FDC1 from *Aspergillus niger* (PDB ID 7NF3) (gray), with RMSD of 0.79, 1.21 and 1.39 Å, respectively.

Co-crystallization assays and biochemical studies of FDC from *A. niger* and *S. cerevisiae* revealed that a large hydrophobic pocket, located within domain 2, is involved in interactions with the prFMN cofactor and influences substrate specificity. Alignment of these fungal FDC proteins and PSC1 allowed us to identify that the hydrophobic pocket includes residues I189, Q192, I330, F397 and I398 in PSC1. Using the approach described in Materials and methods section 3.2.6, we generated single amino-acid replacements using site-directed mutagenesis (Table 3.5). The mutants I189A, Q192A, I330A, F397Y, I398T, and the double mutant F397Y + I398T, failed to decarboxylate *t*CA, suggesting that these mutations disrupted the capacity of the enzyme to bind to its cofactor.

In the *A. niger* FDC1 protein, the catalytic residues correspond to Glu277, Arg173 and Glu282. Sequence comparison showed that these corresponding residues are invariantly conserved across UbiD family enzymes, with the corresponding residues in PSC1 identified as Arg175, Glu280 and Glu285. This set of residues forms an ionic network within the active site, which is consistent with the decarboxylation mechanisms of UbiD enzymes, involving proton transfer during the reaction (Bailey et al., 2018). As expected, and consistent with previous findings in FDCs, replacement of Glu285 with alanine resulted in a mutant devoid of activity (Table 3.5). Similarly, replacement of Arg175 with alanine also abolished enzymatic activity. However, when Arg175 was replaced by lysine and Glu285 with aspartate, the resulting mutants retained nearly 60% of the original activity (Table 3.5).

Table 3.5: Enzymatic activity of PSC1 mutants compared to the wild type. Data are presented as the mean percentage of activity relative to the wild-type PSC1 (set at 100%, equivalent to 4.7 µmol min^{-1}) ± standard deviation of three independent assays.

PSC1 mutant	**Percentage of activity (%)**
PSC1 (control)	100 ± 1.0
I189A	13.8 ± 2.1
Q192A	1.4 ± 0.6
I330A	3.5 ± 1.9
F397Y	4.1 ± 0.8
I398T	0.4 ± 1.2
F397Y + I398T	1.4 ± 2.5
R175A	3.3 ± 0.2
R175K	59.1 ± 1.4
E285A	1.9 ± 5.4
E285D	59.7 ± 0.8

3.4 Discussion

Decarboxylation is a pivotal biochemical process that involves enzymes utilizing a variety of cofactors, such as pyridoxal phosphate, metal ions and flavin derivatives such as FMN and FAD. According to Batyrova et al. (2020), over 110 families of decarboxylases exist, each with diverse mechanisms and functions, underscoring their involvement in a broad range of physiological roles.

The UbiD family of decarboxylases, particularly the FDC enzymes, has raised significant interest due to their ability to convert a number of substrates into value-added chemicals. For example, Nielsen's group demonstrated the conversion of *t*CA into styrene using *E. coli* expressing the *S. cerevisiae* FDC1 gene (McKenna & Nielsen, 2011). These enzymes are also noteworthy because they use the rare prFMN cofactor (Marshall et al., 2017). UbiD family enzymes can either retain the cofactor, displaying a pale yellow color when purified, or lose it during purification. The solvent-tolerant *P. putida* DOT-T1E can synthesize prFMN (P. Godoy, A. García-Franco and J. L. Ramos, unpublished), and our studies suggest that a functional *trans*-cinnamic acid decarboxylase assembles *in vivo*, as confirmed in the *P. putida* expressing the *psc1* gene, which converted *t*CA into styrene (García-Franco et al., 2024). However, the purified PSC1 enzyme was colorless, and its absorbance scans suggest that the purified protein corresponded to the apoenzyme (our unpublished results). We hypothesize that prFMN binds to the apoenzyme with low affinity or that its binding is unstable.

Several studies have shown that FDC enzymes exhibit broad substrate specificity, decarboxylating ortho-, meta-, or para-substituted cinnamic acid derivatives. However, despite a good sequence alignment of PSC1 with FDC1 from *A. niger* and *S. cerevisiae* (Bailey et al., 2018; Bhuiya et al., 2015; Mukai et al., 2010; Nagy et al., 2019; Payne et al., 2015), which revealed the conservation of an apolar binding pocket for prFMN cofactor and substrates, PSC1 enzyme exhibited a narrower substrate range, decarboxylating only *t*CA and *p*-coumaric acid. This contrasts with the broader substrate specificity described for the *S. cerevisiae* FDC1 (Nagy et al., 2019). Docking simulations of PSC1 with prFMN and substrates, compared to the co-crystal of FDC1 from *A. niger*, do not explain this discrepancy, indicating the need for further biochemical analyses.

PSC1 is a consensus-derived protein, and Sternke et al. (2019) highlighted that consensus sequences derived from MSA (wholesale approach) represent the evolutionary trajectory of a protein family, enhancing stability and functionality. For PSC1, this approach proved valuable in designing a protein that works in a prokaryotic microorganism despite its eukaryotic origin (García-Franco et al., 2024). Although the wholesale approach does not directly select for activity, conserved sequences often correlate with functional conservation, particularly in active sites and monomer interaction surfaces. This was evident when the structure of the monomer of PSC1 was aligned with the *A. niger* FDC1 monomer; despite only 52% of the overall sequence being conserved, both models superpose with just 1.39 Å RMSD (Figure S3.5). Notably, the FDC1 of *A. niger* was not included in the MSA used to derive the PSC1 consensus sequence due to its <60% identity with the *S. cerevisiae* FDC1 enzyme. Consensus proteins derived from both limited and extensive sequence sets have demonstrated enhanced thermotolerance. The PSC1 protein exhibits a T_m of 63°C, consistent with high thermostability, although comparison with the T_m of extant proteins is not possible due to the lack of data. It should be mentioned that a consensus phytase designed from 13 sequences showed an increased T_m of 15-26°C (Lehmann et al., 2002) with respect to extant proteins. The high thermostability of PSC1 is further supported by our observation that the rate of conversion of *t*CA increased with temperature, peaking at 45-50°C in *P. putida*, compared to the optimal 37°C for the FDC1 of *S. cerevisiae* expressed in *E. coli*.

Our crystallographic analysis of PSC1 revealed a high structural resemblance to previously crystallized UbiD family members. The close similarity between PSC1 and FDC1 from *C. dubliniensis*, *A. niger* and *S. cerevisiae* suggested that stability features are probably imprinted in the consensus sequence, making the wholesale approach effective for stabilizing proteins. Sequence comparison and alignment of PSC1 with crystallized proteins identified critical residues in the cofactor/substrate binding region and catalysis. Mutations in the cofactor binding residues generally resulted in loss of activity, consistent with our observation of a low affinity for prFMN or labile interaction between prFMN and the apoenzyme.

Previous analysis revealed that residues such as Arg173 and Glu282 in *A. niger* FDC1 are crucial for decarboxylation via proton transfer. Mutants such as R173A and E282Q in *A. niger* were found to be catalytically inactive (Bailey et al., 2018; Payne et al., 2015) and exhibited altered UV-visible spectra, which was interpreted as

a potential ionic network involved in cofactor maturation and catalysis. Our results show that the corresponding residues in PSC1, Arg175 and Glu285, are essential for decarboxylation. Notably, lysine can substitute Arg at position 175, and aspartate can replace Glu at position 285, consistent with the decarboxylation mechanisms. This aligns with García-Franco et al. (2024), who demonstrated that PSC1 activity is pH-dependent, with an optimal pH of 7, underscoring the importance of acidic residues in the decarboxylation process.

This study highlights the potential of consensus sequence design to enhance enzyme stability and function, providing a viable approach for expressing eukaryotic enzymes in prokaryotic systems. Further research into optimizing these designs could advance synthetic biology and industrial biotechnology. However, we acknowledge that the conversion rates of *t*CA to styrene are relatively low, probably due to the weak binding affinity of prFMN to PSC1. We are currently designing mutants with a higher affinity to test whether this improves the biosynthesis rates of styrene.

Acknowledgements

The work in our laboratory was funded by grants from the Spanish Ministry of Science and Innovation (Plan Nacional PDI-2018-094370BI00 and Transición Ecológica y Resilencia TED2021-129632BI00). We thank Angela Tate for improving the language of the manuscript. We thank Tino Krell for critical reading of the manuscript and suggestions.

Author Contributions

AGF: methodology, validation, investigation, writing draft. JDT: investigation, methodology. PG: investigation, methodology, writing draft. ED: investigation, supervision, writing draft. CL: methodology. JAG: investigation, data curation, visualization, supervision, writing draft. JLR: conceptualization, writing-original draft, supervision, project administration, funding acquisition, writing-final version.

3.5 Supplementary Information

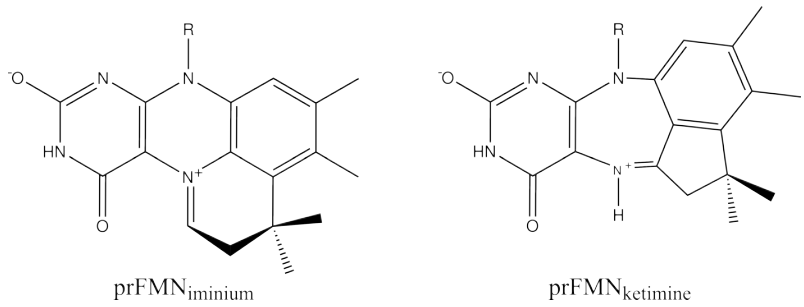

Figure S3.1: Chemical structures of the prFMN$_{iminium}$ and prFMN$_{ketimine}$ models. Modified from Payne et al. (2015).

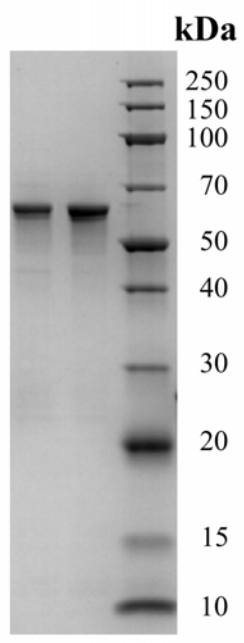

Figure S3.2: Electrophoretic separation of purified PSC1. After the SDS-PAGE separation in 12% (w/v) polyacrylamide gel, a band of ~55 kDa was identified.

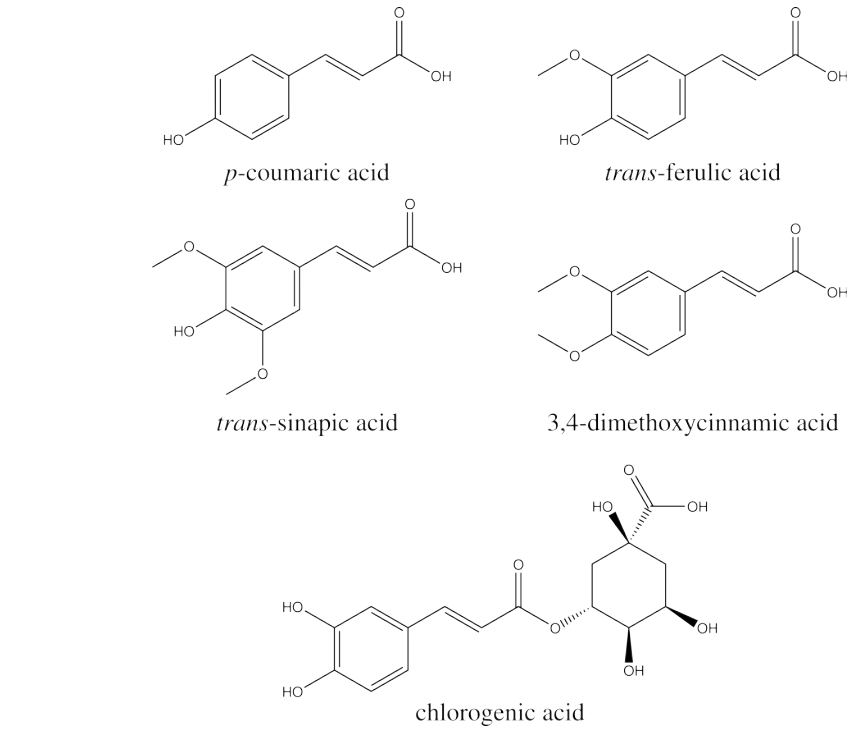

Figure S3.3: Chemical structures of *trans*-cinnamic acid analogues tested as PSC1 substrates.

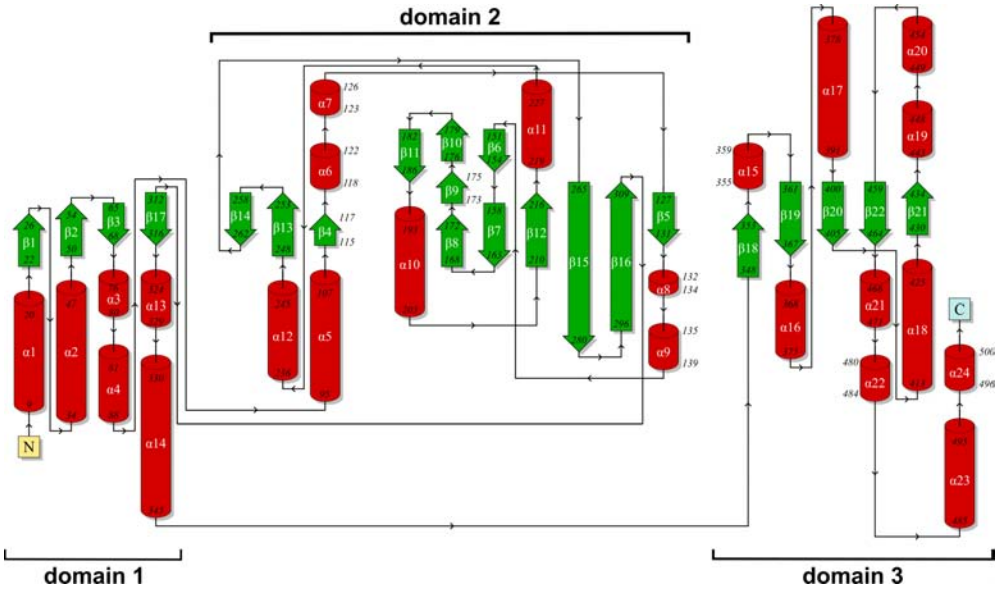

Figure S3.4: Schematic representation showing the topology of PSC1, with the three domains of the monomer indicated. α-helices are represented in red while β-strands are represented in green.

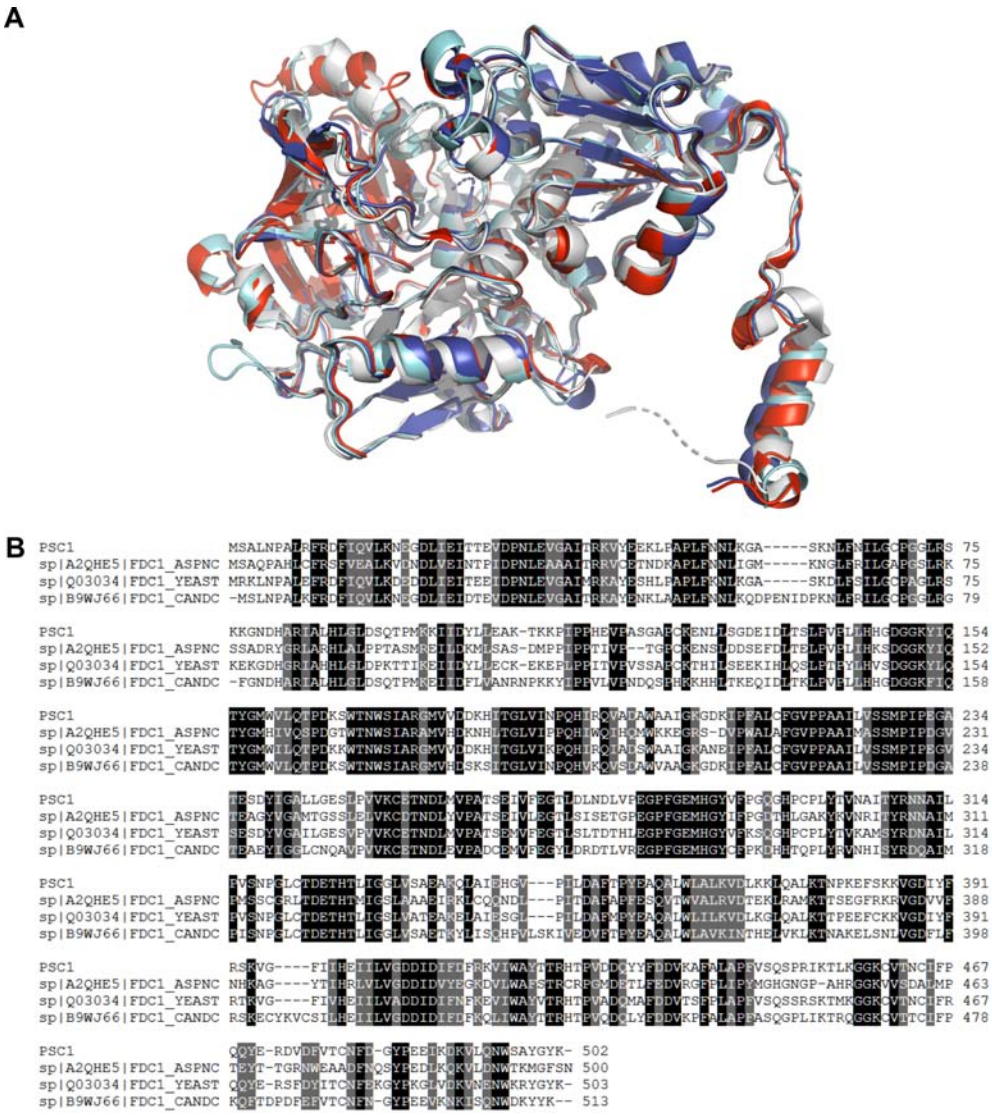

Figure S3.5: A) Superimposition of one of the two monomers of PSC1 (PDB ID 9GQR) (red) with one monomer of FDC1 from *Saccharomyces cerevisiae* (PDB ID 4S13) (blue), *Candida dubliniensis* (PDB ID 4ZAD) (cyan) and *Aspergillus niger* (PDB ID 7NF3) (gray). B) Sequence alignment between PSC1 and FDC1 from *Aspergillus niger* (UniProtKB ID: A2QHE5), *Saccharomyces cerevisiae* (UniProtKB ID: Q03034) and *Candida dubliniensis* (UniProtKB ID: B9WJ66). The overall identity is 52, 77 and 61%, respectively. Identical residues are highlighted in dark gray, while conserved residues are highlighted in light gray.

Table S3.1: Percent identity matrix for eight ferulic acid decarboxylases used in the multiple sequence alignment for designing PSC1. The values represent the percentage of sequence identity between each pair of enzymes, including PSC1.

Yeast species	*Saccharomyces cerevisiae*	*Saccharomyces kudriavzevii*	*Wickerhamomyces anomalus*	*Wickerhamomyces ciferrii*	*Debaryomyces hansenii*	*[Candida] pseudohaemulonis*	*[Candida] arabinofermentans*	*Candida dubliniensis*	PSC1
Saccharomyces cerevisiae	100	89	68	64	61	61	60	61	77
Saccharomyces kudriavzevii	89	100	67	63	62	63	60	61	78
Wickerhamomyces anomalus	68	67	100	75	64	64	63	61	80
Wickerhamomyces ciferrii	64	63	75	100	59	61	63	61	75
Debaryomyces hansenii	61	62	64	59	100	80	59	63	74
[Candida] pseudohaemulonis	61	63	64	61	80	100	58	62	76
[Candida] arabinofermentans	60	60	63	63	59	58	100	59	73
Candida dubliniensis	61	61	61	61	63	62	59	100	72
PSC1	77	78	80	75	74	76	73	72	100

Table S3.2: Strains and plasmids used in this study.

Strain or plasmid	Characteristics	Reference
Strains		
Pseudomonas putida		
CM12-5	DOT-T1E derivative that overproduces L-Phe. Rif^R, Tol^R	Molina-Santiago et al. (2016)
Escherichia coli		
DH5α	Cloning host. F^- *endAI hsdRJ7* ($r_K^- m_K^+$) *supE44 thi-1* λ*-recAl gyrA96 relAI deoR* Δ(*lacZYA-argF*)-U169 Φ80dlacZΔM15	Grant et al. (1990)
BL21 (DE3)	F^-, *ompT*, *hsdS* ($r_B^- m_B^-$), *gal*, *dcm*, *lon*	Studier and Moffatt (1986)
Plasmids		
pET28(b)	Expression vector, 6xHIS. Km^R	Novagen
pET28(b)::PSC1	pET28(b) bearing the ORF PSC1. Km^R	This work
pPSC1	pSEVA632 derivative carrying psc1 gene. Gm^R	García-Franco et al. (2024)
pPSC1(I189A)	PSC1 bearing the ORF PSC1 with isoleucine at position 189 replaced by alanine. Gm^R	This work
pPSC1(Q192A)	PSC1 bearing the ORF PSC1 with glutamine at position 192 replaced by alanine. Gm^R	This work
pPSC1(I330A)	PSC1 bearing the ORF PSC1 with isoleucine at position 330 replaced by alanine. Gm^R	This work
pPSC1(F397Y)	PSC1 bearing the ORF PSC1 with phenylalanine at position 397 replaced by tyrosine. Gm^R	This work
pPSC1(I398T)	PSC1 bearing the ORF PSC1 with isoleucine at position 398 replaced by threonine. Gm^R	This work
pPSC1(F397Y, I398T)	PSC1 bearing the ORF PSC1 with phenylalanine at position 397 replaced by tyrosine and isoleucine at position 398 replaced by threonine. Gm^R	This work
pPSC1(R175A)	PSC1 bearing the ORF PSC1 with arginine at position 175 replaced by alanine. Gm^R	This work
pPSC1(R175K)	PSC1 bearing the ORF PSC1 with arginine at position 175 replaced by lysine. Gm^R	This work
pPSC1(E285A)	PSC1 bearing the ORF PSC1 with glutamic acid at position 285 replaced by alanine. Gm^R	This work
pPSC1(E285D)	PSC1 bearing the ORF PSC1 with glutamic acid at position 285 replaced by aspartic acid. Gm^R	This work

Abbreviations: Rif^R, Gm^R, Km^R and Tol^R stand for resistance to rifampicin, gentamycin, kanamycin and toluene, respectively. L-Phe, L-phenylalanine; Tol, toluene.

Table S3.3: Primers used in this study.

Name	**Sequence (5' → 3')**	**Description or purpose**
C1 Fw(NdeI)	CGCATATGAGCGCCCTGAACCCGG	Construction of pET28(b)::PSC1
C1 Rv(XhoI)	CTCGAGTTACTTATAGCCGTAGGCGCTCC	Construction of pET28(b)::PSC1
C1 Rv1	CTGCGGGTTGGCCACCAG	Construction of PSC1 (I189A) mutants
C1 Fw1	CTGGTGGCCAACCCGCAG	Construction of PSC1 (I189A) mutants
C1 Rv2	GGATATGCGCCGGGTTGATCA	Construction of PSC1 (Q192A) mutants
C1 Fw2	TGATCAACCCGGCGCATATCC	Construction of PSC1 (Q192A) mutants
C1 Rv4	CCGCCGGCCAGGGTATG	Construction of PSC1 (I330A) mutants
C1 Fw4	CCTGGCCGGCGGCCTGGTTA	Construction of PSC1 (I330A) mutants
C1 Rv5	TGATCTCGTGGATGATGTAGCCCAC	Construction of PSC1 (F397Y) mutants
C1 Fw5	GTGGGCTACATCATCCACGAGATCA	Construction of PSC1 (F397Y) mutants
C1 Rv6	TGATCTCGTGGATGGTGAAGCCCAC	Construction of PSC1 (I398T) mutants
C1 Fw6	GTGGGCTTCACCATCCACGA	Construction of PSC1 (I398T) mutants
C1 Rv7	TGATCTCGTGGATGGTGTAGCCCAC	Construction of PSC1 (F397Y, I398T) mutants
C1 Fw7	GTGGGCTACACCATCCACGAG	Construction of PSC1 (F397Y, I398T) mutants
M13Rv	CAGGAAACAGCTATGAC	Sequencing of cloned fragments in pSEVA632
M13Fw	GTAAAACGACGGCCAGT	Sequencing of cloned fragments in pSEVA632

Nucleotide triplets modified to generate PSC1 mutants are underlined.

IV

Discussion

Styrene is one of the most important monomers in the production of synthetic materials such as polystyrene, styrene-butadiene rubber and acrylonitrile butadiene styrene, with an annual global demand of over 37 million metric tons (ChemAnalyst, 2023). Traditionally, styrene is synthesized from petroleum-derived ethylbenzene through an energy-intensive catalytic dehydrogenation at around 600°C (Tossavainen, 1978). This petrochemical route contributes significantly to global energy consumption and carbon dioxide emissions, raising concerns about its long-term sustainability. As the world shifts towards greener technologies, finding sustainable alternatives for styrene production has become a critical objective for the chemical industry. In this context, this PhD thesis has focused on the biosynthesis of styrene from sugars present in renewable feedstocks, such as lignocellulosic biomass, using the *Pseudomonas putida* DOT-T1E strain as the chassis.

Microbial tolerance to aromatic hydrocarbons: a key factor in industrial bioproduction

One of the main challenges in microbial production of aromatic compounds is their inherent toxicity to the producing organisms. Aromatic hydrocarbons such as toluene, styrene and *trans*-cinnamic acid (*t*CA) are highly lipophilic, which allows them to disrupt microbial cell membranes, causing a loss of membrane integrity, energy collapse and eventually cell death (Sikkema et al., 1994; Weber & de Bont, 1996). These compounds typically have log P_{OW} (partition coefficient in an octanol-water biphasic system) in the range of 1.5 to 4. In contrast, solvents with log P_{OW} values below 1.5 or above 4 are generally less toxic and better tolerated by microorganisms (de Smet et al., 1978; Inoue & Horikoshi, 1991; Vermuë et al., 1993). However, the toxicity of a solvent is also influenced by the intrinsic tolerance of specific bacterial strains (Ramos et al., 2002). For instance, certain strains of *Pseudomonas putida*, including *P. putida* IH-2000 (Inoue & Horikoshi, 1989), S12 (Hartmans et al., 1990) and DOT-T1E (Ramos et al., 1995), exhibit high tolerance to toluene and similar solvents, making them promising candidates for producing aromatic compounds. Since the styrene log P_{OW} is similar to that of toluene, we hypothesized that *P. putida* DOT-T1E could serve as an effective host for the production of other toxic compounds, due to its inherent solvent tolerance.

Chapter 1 explores the physiological and genetic responses of *P. putida* DOT-T1E to the toxic effects of *t*CA and styrene, identifying several tolerance mechanisms that make this strain an ideal chassis for industrial bioproduction. Our results show that *P. putida* DOT-T1E mounts a multifaceted defense response against *t*CA and styrene, which includes the activation of efflux pumps, *cis-trans* isomerization of unsaturated fatty acids and the upregulation of stress response proteins such as chaperones and reactive oxygen species (ROS)-scavenging enzymes (García-Franco et al., 2023). Through mutant analysis, we identified efflux pumps as being the most critical element of solvent resistance, with the TtgGHI pump being the most efficient for removing toxic compounds (Molina et al., 2011; Rodríguez-Herva et al., 2007; Rojas et al., 2001). This efflux pump is regulated by the transcriptional repressor TtgV (Rojas et al., 2003), which binds to DNA at the promoter region of *ttgV/ttgG*. TtgV physically obstructs RNA polymerase access and induces a structural distortion in DNA preventing transcription (Lu et al., 2010). Different compounds, such as aromatic hydrocarbons or aliphatic alcohols, bind to TtgV, triggering a conformational change that releases it from the operator site. This release allows RNA polymerase to access the *ttgG-ttgV* promoter region, initiating the transcription of *ttgG* and *ttgV*. This leads to an induced expression of the *ttgGHI* operon by 2.3- to 3-fold (Fillet et al., 2012; Guazzaroni et al., 2004, 2007). This efflux system plays a crucial role in preventing the accumulation of styrene and *t*CA inside the cell, thereby maintaining cellular homeostasis.

Another relevant factor in solvent tolerance is the strengthening of the cellular membranes. This is an immediate response and involves the activation of a *cis-trans* isomerase that converts *cis* unsaturated fatty acids into their *trans* isomers, making the membrane less permeable to hydrophobic compounds (Junker & Ramos, 1999; Weber et al., 1994). Our findings show a significant reduction in the *cis/trans* fatty acid ratio in *P. putida* cells exposed to styrene and *t*CA, confirming that this isomerization mechanism plays a relevant role in the tolerance of the organism to these toxic compounds.

The integration of omics approaches allowed us to identify key regulatory networks and stress response pathways that contribute to the robust performance of *P. putida* DOT-T1E in the presence of toxic aromatic hydrocarbons (García-Franco et al., 2023). Transcriptomic analyses revealed the upregulation of several metabolic pathways, including those involved in glucose uptake and the Entner-Doudoroff pathway,

suggesting an increased energy demand when cells are exposed to styrene and *t*CA. This metabolic shift is essential to support the biosynthesis of protective molecules and the active extrusion of toxic compounds. Additionally, bacterial cells initiate a stress response programme, characterized by the synthesis of various chaperones and ROS-scavenging enzymes, such as peroxidases, catalases, glutathione transferases, and superoxide dismutase. The activation of these ROS-removing proteins may be linked to membrane destabilization, which accelerates electron flow through the respiratory chain, leading to increased production of ROS.

These findings highlight the potential of *P. putida* as a platform for the industrial production of styrene and other aromatic compounds, and give the strain a significant advantage over other microbial chassis that are more sensitive to these stressors, such as *Escherichia coli* and *Saccharomyces cerevisiae* (McKenna & Nielsen, 2011; McKenna et al., 2014).

Designing a functional *trans*-cinnamic acid decarboxylase in *Pseudomonas*

Following the metabolic process described by McKenna and Nielsen (2011), *P. putida* DOT-T1E requires two key enzymes to convert L-Phe into styrene: 1) a phenylalanine ammonia lyase (PAL), which converts L-Phe into *t*CA, and 2) a *trans*-cinnamic acid decarboxylase to convert the *t*CA into styrene. Molina-Santiago et al. (2016) successfully engineered *P. putida* DOT-T1E to efficiently overproduce L-Phe and further enable *t*CA biosynthesis by expressing PAL enzymes from *Nostoc punctiforme* and *Streptomyces maritimus*. To successfully synthesize styrene from renewable feedstocks such as glucose, it was necessary to implement the enzymatic step that converts *t*CA into styrene in *P. putida* DOT-T1E.

A major challenge in engineering this biosynthetic pathway is that *trans*-cinnamic acid decarboxylases have been primarily characterized in fungi, and their functionality in bacterial systems such as *P. putida* is limited. **Chapter 2** describes the "wholesale" protein design approach we adopted (Sternke et al., 2019, 2020) to develop a synthetic *trans*-cinnamic acid decarboxylase that functions effectively in *Pseudomonas*. This involved deriving consensus sequences from the multiple sequence alignments (MSA) of fungal ferulic acid decarboxylases (FDCs) that share high identity to FDC1 from *S.*

cerevisiae. Using this data, we designed two synthetic decarboxylase variants, PSC1 and PSD1, and tested their functionality in *P. putida*. Whilst the PSC1 enzyme showed robust activity in converting *t*CA to styrene, PSD1 did not exhibit any activity.

The biochemical characterization of fungal ferulic acid decarboxylases has provided valuable insights into the role of prenylated FMN (prFMN) as a cofactor, which exists in two forms: the active $prFMN_{iminium}$ and the inactive $prFMN_{ketimine}$. The biosynthesis of prFMN appears to be a conserved process across species (Batyrova et al., 2020; Wang et al., 2018b). In *P. putida*, prFMN is probably synthesized in the following steps: first, FMN is reduced by NADPH via flavin oxidoreductases and then, the UbiX enzyme catalyses the conversion of reduced FMN to prFMN via dimethylallyl monophosphate (DMAP), which originates from dimethylallyl pyrophosphate (DMAPP) after its dephosphorylation by NudF/NudC. *In vivo* evidence suggests that prFMN can be incorporated into various apoenzymes in *P. putida*, such as PSC1, although the stability of prFMN binding to PSC1 remains relatively weak.

The PSC1 enzyme was found to be highly specific for *t*CA and operated *in vivo* under optimal conditions at moderate temperatures and neutral pH, producing up to 220 mg L^{-1} of styrene in *P. putida* cultures. Whilst this production level is promising, it remains below the threshold required for industrial-scale applications. However, the successful expression and functionality of *Pseudomonas* codon-optimized PSC1 in *P. putida* demonstrates that consensus-designed proteins can be both stable and functional in non-native hosts. This highlights the potential of the "wholesale" approach for enzyme design, which could be further applied to other biosynthetic pathways for the production of valuable chemicals from renewable resources.

Purification and crystal structure of PSC1

In industrial settings, enzymes must be robust and thermally stable to withstand the demanding conditions of large-scale fermentation. To better understand the structure-function relationship of the PSC1 enzyme, **Chapter 3** focuses on its purification and structural characterization. This analysis aims to provide valuable insights on the potential catalytic capabilities of the enzyme.

The PSC1 enzyme was purified as a homodimer with a molecular mass of approximately 104.7 kDa. The enzyme exhibited notable thermal stability, with a

denaturation midpoint (T_m) of 63°C, and retained activity after prolonged storage at 4°C. This resilience is important for industrial applications, where enzymes must remain functional over extended periods and at elevated temperatures. Such enhanced thermotolerance highlights the potential of consensus design for generating enzymes, in line with previous findings reported for other enzymes (Lehmann et al., 2002).

Fungal FDCs, in general, exhibit a broad substrate specificity, as they are able to decarboxylate not only *t*CA, but also a wide range of substituted derivatives (Nagy et al., 2019). Kinetic analysis of FDC1 from *S. cerevisiae* (Bhuiya et al., 2015) showed that the enzyme has similar V_{max} values for ferulic acid and *p*-coumaric acid, with slightly higher affinity for ferulic acid (K_m = 0.79 mM) than for *p*-coumaric acid (K_m = 0.92 mM). In other studies, Payne et al. (2015) reported that FDC1 has the highest catalytic efficiency with cinnamic acid (k_{cat} = 7.6 s^{-1}, K_m = 22 mM), but lower efficiency with other substrates such as α-fluorocinnamic acid (k_{cat} = 2.1 s^{-1}, K_m = 18 mM) and 2,3,4,5,6-pentafluorocinnamic acid (k_{cat} = 0.5 s^{-1}, K_m = 42 mM). These data highlight the broad substrate specificity of *S. cerevisiae* FDC1 for natural compounds such as ferulic and cinnamic acid, but reduced activity with fluorinated substrates. Similarly, Nagy et al. (2019) reported that in *in vivo* assays, *S. cerevisiae* FDC1 catalysed the complete conversion of cinnamic acid and various brominated and methoxylated phenylacrylic acids in short (<24 h) or moderate (<72 h) time frames.

In contrast, **Chapter 3** reveals that PSC1 has a narrower substrate specificity compared to fungal FDCs, primarily converting *t*CA to styrene, with only limited activity toward other cinnamic acid derivatives, such as *p*-coumaric acid. This restricted substrate range limits the versatility of the enzyme, suggesting that further engineering of the consensus enzyme might be required to broaden the functionality of PSC1 toward a wider array of aromatic compounds, depending on industrial needs. Regardless of this difference in substrate specificity, the high thermal stability of PSC1 highlights its potential for industrial applications.

The determination of the crystal structure of PSC1 at a resolution of 2.1 Å provided detailed insights into its catalytic mechanism. The active site of the enzyme contains a hydrophobic pocket that is essential for substrate binding, with key residues —Arg175, Glu280 and Glu285— playing a central role in catalysis. These residues align with those found in FDC1 from *S. cerevisiae* and *Aspergillus niger* (Bailey et al., 2018). Site-directed mutagenesis confirmed their importance, as substituting them with alanine abolished the decarboxylation activity.

Additionally, the structural insights gained from the crystal structure open up ways for further optimization, either by enhancing substrate affinity or by engineering the enzyme to perform under various industrial conditions. The success of consensus design in creating enzymes that are both stable and highly specific for their substrates shows its potential for the development of biocatalysts tailored to specific industrial needs, such as the production of other aromatic compounds or the degradation of environmental pollutants in bioremediation processes.

The challenge of xylose metabolism to efficiently use second-generation feedstocks

As discussed above, there is an increasing interest in developing biotechnological solutions that use renewable feedstocks as an alternative to petrochemical processes. Glucose, a first-generation (1G) sugar, has been successfully converted into styrene (McKenna & Nielsen, 2011; McKenna et al., 2014), and as discussed in **Chapter 2**, our strain *P. putida* CM12-5 (pPALN_C1) is capable of producing styrene from glucose. However, second-generation (2G) substrates, such as lignocellulosic biomass, present additional challenges due to the diverse range of compounds they contain. Lignocellulosic biomass, composed of cellulose, hemicellulose and lignin, is a highly abundant resource that offers the advantage of not competing with food production, unlike 1G biofuels, which compete with food crops for arable land. This makes lignocellulosic biomass an ideal feedstock for the production of 2G biofuels and bioproducts. Despite its potential, the use of lignocellulosic biomass requires intense pretreatment and enzyme cocktails to release fermentable sugars, which increases the cost of producing value-added products from these substrates.

Techno-economic analyses have emphasized the importance of fully utilizing the diverse range of sugars present in lignocellulosic biomass to achieve cost-competitive production of biofuels and bioproducts (Valdivia et al., 2016). A major limitation of many microbial platforms, including *P. putida*, is their inability to efficiently metabolize C5 sugars such as xylose, which is abundant in lignocellulosic biomass. In our group we engineered *P. putida* CM12-5 to efficiently use xylose as a carbon source by disrupting the *gcd* gene, which encodes glucose/xylose dehydrogenase, and introducing the xylose isomerase (*xylA*), xylulokinase (*xylB*) and the xylose-proton symporter (*xylE*) genes, which enable the conversion of xylose into xylulose-

5-phosphate, an intermediate of the pentose phosphate pathway (Godoy et al., 2021). Subsequently, to enable styrene biosynthesis, *palN* and *psc1* genes were transferred into the strain, yielding *P. putida* CM12-5 Δ*gcd* (p*xylABE*) (pPALN_C1).

Our results (manuscript in preparation) show that the engineered strain was able to efficiently grow on both glucose and xylose, as well as on a mixture of the two sugars. When cultivated on 2G hydrolysates derived from pre-treated corn stover and sugarcane straw, the strain exhibited limited growth rates and relatively low production of styrene titres, likely due to the inherent toxicity of 2G hydrolysates, which requires further studies. In any case, by engineering *P. putida* to metabolize xylose, we have significantly expanded the substrate range of this platform, enhancing its versatility for industrial applications. We expect that this development not only enhances the overall productivity of the system but also reduces the cost of production by maximizing the use of available carbon sources in lignocellulose hydrolysates.

Future Remarks

The findings of this PhD thesis have significant implications for both the chemical industry and environmental sustainability. Microbial production of styrene using *P. putida* offers a promising alternative to traditional petrochemical methods, which are energy-intensive and environmentally harmful. By shifting to bio-based styrene production, we would be able to reduce dependence on fossil fuels and support the circular economy by leveraging renewable feedstocks such as lignocellulosic biomass. Abundant agricultural residues, such as corn stover and sugarcane straw, provide sustainable and readily available raw materials, further contributing to the bioeconomy. This research demonstrates the potential of *P. putida* as a robust microbial platform for the sustainable production of styrene from lignocellulosic biomass, offering a viable alternative to conventional petrochemical processes.

Despite these advances, several challenges remain. Current styrene titres, although promising, are still below the levels needed for industrial-scale production. Future research should focus on optimizing the metabolic pathways involved in styrene biosynthesis. For instance, increasing intracellular L-Phe availability, optimizing the co-expression of PAL and PSC1, minimizing metabolic burden, and optimizing the PSC1 enzyme to improve both its activity and stability. Additionally, scaling up the

production process and developing *in situ* styrene extraction techniques are crucial to mitigate toxicity during production. Further research is also needed to increase the tolerance of *P. putida* to inhibitory by-products from lignocellulosic biomass hydrolysis, such as furfural and acetic acid, which can negatively impact cell growth and styrene production.

For a successful scale-up to larger bioreactors, improving styrene yield during fermentation is a top priority. As described by McKenna et al. (2015), one effective approach for boosting styrene production is *in situ* extraction of styrene as it is being synthesized, either through solvent extraction or gas stripping. This strategy reduces product toxicity —a major challenge in microbial styrene production— by continuously removing styrene from the culture medium before it reaches inhibitory concentrations. Solvent extraction using biocompatible solvents such as bis(2-ethylhexyl) phthalate has been shown to increase styrene yields by 320%, whilst gas stripping allows efficient capture of styrene vapors, which can be collected by condensation. Adapting these *in situ* extraction techniques to *P. putida* bioprocesses could significantly enhance productivity, making the process more viable at an industrial scale.

Additionally, the conversion of lignocellulosic biomass into styrene presents additional issues due to the complexity and heterogeneity of the biomass and the presence of inhibitory chemicals. Whilst the engineered strain performed well with 1G sugars such as glucose, 2G substrates derived from lignocellulosic biomass are more challenging to process. The presence of toxic by-products such as furfural and acetic acid are obstacles to efficient fermentation. Enhancing the resistance of DOT-T1E to these inhibitors is essential for improving styrene production yields from 2G feedstocks.

Addressing these issues is critical for maximizing microbial performance and product yields. With continued optimization, this platform has the potential to revolutionize the production of styrene and other aromatic compounds, paving the way for a greener and more sustainable chemical industry. The advancements demonstrated in this PhD thesis also open up avenues for producing other added-value compounds, further expanding the impact of this technology on reducing our reliance on fossil fuels.

V

Conclusions

Conclusions

1. *Pseudomonas putida* DOT-T1E exhibits high tolerance to toxic aromatic compounds, making it a robust chassis for the production of styrene and *trans*-cinnamic acid (*t*CA). This tolerance is facilitated by an interplay of cellular responses that include efflux pumps, modification of cell membrane phospholipids, induction of stress chaperones and detoxification of oxygen radicals. This makes *P. putida* DOT-T1E a viable microbial platform for the sustainable production of aromatic compounds, opening up new possibilities for bio-based chemical manufacturing.

2. In glucose-growing cells, the addition of styrene and *t*CA induces key metabolic pathways, such as the Entner-Doudoroff pathway and the Krebs cycle. This suggests an efficient management of cellular energy to meet the energy demands for extrusion and defence against toxic compounds. Such metabolic adaptability is critical for the large-scale production of value-added chemicals, further supporting the potential of *P. putida* in green chemistry applications.

3. Metabolic mapping suggests that DOT-T1E may be able to synthesize styrene from L-phenylalanine (L-Phe) via a two-step process: deamination of the amino acid to *t*CA followed by decarboxylation to produce styrene. The conversion of *t*CA into styrene posed challenges, as available eukaryotic *trans*-cinnamic acid decarboxylases were not stably expressed in *Pseudomonas*. To overcome this, we used the "wholesale" protein design approach, synthesizing a consensus-based *trans*-cinnamic acid decarboxylase (PSC1). A codon-optimized gene for *P. putida* was constructed *in vitro*, and its expression *in vivo* yielded a functional *trans*-cinnamic acid decarboxylase. The successful expression of PSC1 in *P. putida* demonstrates the potential of the "wholesale" approach for enzyme design.

4. The co-expression of PSC1 with PAL in *P. putida* CM12-5, a DOT-T1E derivative that overproduces and accumulates L-Phe in the outer medium, enabled styrene synthesis from sugars. These sugars could be either pure compounds or derived from second-generation (2G) hydrolysates, such as those obtained from corn stover or sugarcane straw.

5. The consensus-designed PSC1 decarboxylase is a dimer in solution, exhibiting high thermal stability and restricted substrate specificity (limited to *t*CA and *p*-coumaric acid). These properties make PSC1 a suitable candidate for industrial applications, where the stability of the enzymes is critical.

6. The crystal structure of PSC1, resolved at 2.1 Å, revealed that the protein folds in three domains. Domain 1, located at the N-terminal end, is followed by domain 2, which contains a hydrophobic pocket crucial for cofactor binding and substrate recognition. Domain 3, positioned at the C-terminal end, is involved in dimerization. Additionally, three key residues —Arg175, Glu280 and Glu285— were identified as essential for catalysis. Mutation of these residues to alanine abolished decarboxylase activity, confirming the importance of these residues for the enzyme function.

Conclusiones

1. *Pseudomonas putida* DOT-T1E exhibe una alta tolerancia a compuestos aromáticos tóxicos, lo que la convierte en un chasis robusto para la producción de estireno y ácido *trans*-cinámico (*t*CA, *trans-cinnamic acid*). Esta tolerancia es facilitada mediante una interacción de respuestas celulares que incluye bombas de eflujo, modificación de los fosfolípidos de la membrana celular, inducción de chaperonas de estrés y detoxificación de radicales de oxígeno. Esto hace que *P. putida* DOT-T1E sea una plataforma microbiana viable para la producción sostenible de compuestos aromáticos, abriendo nuevas posibilidades para la producción de compuestos químicos de base biológica.

2. En células que crecen con glucosa, la adición de estireno y *t*CA induce rutas metabólicas claves, como la ruta de Entner-Doudoroff y el ciclo de Krebs. Esto sugiere una gestión eficiente de la energía celular para satisfacer las demandas energéticas de la extrusión y defensa contra compuestos tóxicos. Tal adaptabilidad metabólica es fundamental para la producción a gran escala de productos químicos de alto valor añadido, lo que refuerza el potencial de *P. putida* en aplicaciones de química verde.

3. El mapeo metabólico sugiere que DOT-T1E podría sintetizar estireno a partir de L-fenilalanina (L-Phe, *L-phenylalanine*) mediante un proceso de dos pasos: la desaminación del aminoácido hacia *t*CA, seguida de su descarboxilación para producir estireno. La conversión de *t*CA en estireno presentó desafíos, ya que las descarboxilasas de ácido *trans*-cinámico disponibles de origen eucariota no se expresaban de manera estable en *Pseudomonas*. Para superar este inconveniente, utilizamos el enfoque de diseño de proteínas "wholesale", sintetizando una ácido *trans*-cinámico descarboxilasa basada en secuencias consenso (PSC1). Se construyó *in vitro* un gen optimizado para *P. putida*, y su expresión *in vivo* dio lugar a una ácido *trans*-cinámico descarboxilasa funcional. La expresión exitosa de PSC1 en *P. putida* demuestra el potencial

del enfoque “wholesale” para el diseño de enzimas.

4. La coexpresión de PSC1 con PAL en *P. putida* CM12-5, una cepa derivada de DOT-T1E que sobreproduce y acumula L-Phe en el medio externo, permitió la síntesis de estireno a partir de azúcares. Estos azúcares podían ser tanto puros como provenientes de hidrolizados de segunda generación (2G) obtenidos de residuos agrícolas como el rastrojo de maíz o el bagazo de caña de azúcar.

5. La descarboxilasa diseñada por consenso PSC1 es un dímero en solución, exhibe una alta estabilidad térmica y especificidad de sustrato (limitada a *t*CA y ácido *p*-cumárico). Estas propiedades hacen que PSC1 sea un candidato adecuado para aplicaciones industriales, donde la estabilidad de las enzimas es crítica.

6. La estructura cristalina de PSC1, resuelta a 2.1 Å, reveló que la proteína se pliega en tres dominios. El dominio 1, ubicado en el extremo N-terminal, es seguido por el dominio 2, que contiene un bolsillo hidrofóbico crucial para la unión de cofactores y el reconocimiento de sustratos. El dominio 3, ubicado en el extremo C-terminal, está involucrado en la dimerización. Además, se identificaron tres residuos clave —Arg175, Glu280 y Glu285— como esenciales para la catálisis. La mutación de estos residuos a alanina eliminó la actividad descarboxilasa, lo que confirma la importancia de estos residuos para la función de la enzima.

VI

References

References

Abavisani, M., Goudarzi, M., Ghalavand, Z., Hajikhani, B., Rad, Z. R., Rad, Z. R., & Hashemi, A. (2021). Evaluation of efflux pumps overexpression and β-lactamase genes among colistin resistant *Pseudomonas aeruginosa*. *Gene Reports*, *24*(101301). https://doi.org/10.1016/j.genrep.2021.101301

Abram, K. Z., & Udaondo, Z. (2020). Towards a better metabolic engineering reference: the microbial chassis. *Microbial Biotechnology*, *13*(1), 17–18. https://doi.org/10.1111/1751-7915.13363

Abril, M. A., Michan, C., Timmis, K. N., & Ramos, J. L. (1989). Regulator and enzyme specificities of the TOL plasmid-encoded upper pathway for degradation of aromatic hydrocarbons and expansion of the substrate range of the pathway. *Journal of Bacteriology*, *171*(12), 6782–6790. https://doi.org/10.1128/jb.171.12.6782-6790.1989

Adams, B. L. (2016). The next generation of synthetic biology chassis: moving synthetic biology from the laboratory to the field. *ACS synthetic biology*, *5*(12), 1328–1330. https://doi.org/10.1021/ACSSYNBIO.6B00256

Adams, P. D., Afonine, P. V., Bunkó, G., Chen, V. B., Davis, I. W., Echols, N., Headd, J. J., Hung, L.-W., Kapral, G. J., Grosse-Kunstleve, R. W., Mccoy, A. J., Moriarty, N. W., Oeffner, R., Read, R. J., Richardson, D. C., Richardson, J. S., Terwilliger, T. C., & Zwart, P. H. (2010). PHENIX: a comprehensive Python-based system for macromolecular structure solution. *Acta Crystallographica. Section D, Biological Crystallography*, *66*(Pt 2), 213–221. https://doi.org/10.1107/S0907444909052925

Adkins, J., Pugh, S., McKenna, R., & Nielsen, D. R. (2012). Engineering microbial chemical factories to produce renewable "biomonomers". *Frontiers in Microbiology*, *3*(AUG), 30963. https://doi.org/10.3389/fmicb.2012.00313

Aeschlimann, J. R. (2003). The role of multidrug efflux pumps in the antibiotic resistance of *Pseudomonas aeruginosa* and other gram-negative bacteria. Insights from the society of infectious diseases pharmacists. *Pharmacotherapy*, *23*(7), 916–924. https://doi.org/10.1592/PHCO.23.7.916.32722

Afonine, P. V., Mustyakimov, M., Grosse-Kunstleve, R. W., Moriarty, N. W., Langan, P., & Adams, P. D. (2010). Joint X-ray and neutron refinement with *phenix.refine*. *Acta Crystallographica. Section D, Biological Crystallography*, *66*(Pt 11), 1153–1163. https://doi.org/10.1107/S0907444910026582

Aguado, R., Olazar, M., San José, M. J., Gaisán, B., & Bilbao, J. (2002). Wax formation in the pyrolysis of polyolefins in a conical spouted bed reactor. *Energy and Fuels*, *16*(6), 1429–1437. https://doi.org/10.1021/EF020043W

Akhtar, J., Idris, A., & Abd. Aziz, R. (2014). Recent advances in production of succinic acid from lignocellulosic biomass. *Applied Microbiology and Biotechnology*, *98*(3), 987–1000. https://doi.org/10.1007/s00253-013-5319-6

Alguel, Y., Meng, C., Terán, W., Krell, T., Ramos, J. L., Gallegos, M. T., & Zhang, X. (2007). Crystal structures of multidrug binding protein TtgR in complex with antibiotics and plant antimicrobials. *Journal of Molecular Biology*, *369*(3), 829–840. https://doi.org/10.1016/J.JMB.2007.03.062

Alonso, A., Morales, G., Escalante, R., Campanario, E., Sastre, L., & Martinez, J. L. (2004). Overexpression of the multidrug efflux pump SmeDEF impairs *Stenotrophomonas maltophilia* physiology. *Journal of Antimicrobial Chemotherapy*, *53*(3), 432–434. https://doi.org/10.1093/jac/dkh074

Altschul, S. F., Madden, T. L., Schäffer, A. A., Zhang, J., Zhang, Z., Miller, W., & Lipman, D. J. (1997). Gapped BLAST and PSI-BLAST: a new generation of protein database search programs. *Nucleic Acid Research*, *25*(17), 3389–3402. https://doi.org/10.1093/nar/25.17.3389

Álvarez, C., Reyes-Sosa, F. M., & Díez, B. (2016). Enzymatic hydrolysis of biomass from wood. *Microbial Biotechnology*, *9*(2), 149–156. https://doi.org/10.1111/1751-7915.12346

Amore, R., Wilhelm, M., & Hollenberg, C. P. (1989). The fermentation of xylose-an analysis of the expression of *Bacillus* and *Actinoplanes* xylose isomerase genes in yeast. *Applied Microbiology and Biotechnology*, *30*, 351–357.

Anand, R., Dorrestein, P. C., Kinsland, C., Begley, T. P., & Ealick, S. E. (2002). Structure of oxalate decarboxylase from *Bacillus subtilis* at 1.75 Å resolution. *Biochemistry*, *41*(24), 7659–7669. https://doi.org/10.1021/bi0200965

Anders, S., & Huber, W. (2010). Differential expression analysis for sequence count data. *Genome Biology*, *11*, R106. https://doi.org/10.1186/gb-2010-11-10-r106

Andreoni, V., & Nestetti, G. (1986). Comparative analysis of different *Pseudomonas* strains that degrade cinnamic acid. *Applied and Environmental Microbiology*, *52*(4), 930–934. https://doi.org/10.1128/aem.52.4.930-934.1986

Aono, R., Aibe, K., Inoue, A., & Horikoshi, K. (1991). Preparation of organic solvent-tolerant mutants from *Escherichia coli* K-12. *Agricultural and Biological Chemistry*, *55*(7), 1935–1938. https://doi.org/10.1080/00021369.1991.10870883

Arce-Rodríguez, A., Benedetti, I., Borrero-de Acuña, J. M., Silva-Rocha, R., & de Lorenzo, V. (2021). Standardization of inducer-activated broad host range expression modules: debugging and refactoring an alkane-responsive AlkS/PalkB device. *Synthetic Biology*, *6*(1), 1–11. https://doi.org/10.1093/SYNBIO/YSAB030

Atsumi, S., Wu, T.-Y., Machado, I. M., Huang, W.-C., Chen, P.-Y., Pellegrini, M., & Liao, J. C. (2010). Evolution, genomic analysis, and reconstruction of isobutanol tolerance in *Escherichia coli*. *Molecular Systems Biology*, *6*, 449. https://doi.org/10.1038/msb.2010.98

Averesch, N. J., & Rothschild, L. J. (2019). Metabolic engineering of *Bacillus subtilis* for production of *para*-aminobenzoic acid – unexpected importance of carbon source is an advantage for space application. *Microbial Biotechnology*, *12*(4), 703–714. https://doi.org/10.1111/1751-7915.13403

Bailey, S. S., Payne, K. A., Fisher, K., Marshall, S. A., Cliff, M. J., Spiess, R., Parker, D. A., Rigby, S. E., & Leys, D. (2018). The role of conserved residues in Fdc decarboxylase in prenylated flavin mononucleotide oxidative maturation, cofactor isomerization, and catalysis. *Journal of Biological Chemistry*, *293*(7), 2272–2287. https://doi.org/10.1074/jbc.RA117.000881

Bañares, A. B., Nisola, G. M., Valdehuesa, K. N. G., Lee, W.-K., & Chung, W.-J. (2021). Understanding D-xylonic acid accumulation: a cornerstone for better metabolic engineering approaches. *Applied Microbiology and Biotechnology*, *105*(13), 5309–5324. https://doi.org/10.1007/s00253-021-11410-y

Baral, N. R., Sundstrom, E. R., Das, L., Gladden, J., Eudes, A., Mortimer, J. C., Singer, S. W., Mukhopadhyay, A., & Scown, C. D. (2019). Approaches for more efficient biological conversion of lignocellulosic feedstocks to biofuels

and bioproducts. *ACS Sustainable Chemistry and Engineering*, *7*(10), 9062–9079. https://doi.org/10.1021/acssuschemeng.9b01229

Batianis, C., Kozaeva, E., Damalas, S. G., Martín-Pascual, M., Volke, D. C., Nikel, P. I., & Martins dos Santos, V. A. (2020). An expanded CRISPRi toolbox for tunable control of gene expression in *Pseudomonas putida*. *Microbial Biotechnology*, *13*(2), 368–385. https://doi.org/10.1111/1751-7915.13533

Bator, I., Wittgens, A., Rosenau, F., Tiso, T., & Blank, L. M. (2020). Comparison of three xylose pathways in *Pseudomonas putida* KT2440 for the synthesis of valuable products. *Frontiers in Bioengineering and Biotechnology*, *7*(480), 1–18. https://doi.org/10.3389/FBIOE.2019.00480

Batyrova, K. A., Khusnutdinova, A. N., Wang, P. H., Di Leo, R., Flick, R., Edwards, E. A., Savchenko, A., & Yakunin, A. F. (2020). Biocatalytic *in vitro* and *in vivo* FMN prenylation and (de)carboxylase activation. *ACS Chemical Biology*, *15*(7), 1874–1882. https://doi.org/10.1021/acschembio.0c00136

Becker, J., & Wittmann, C. (2015). Advanced biotechnology: Metabolically engineered cells for the bio-based production of chemicals and fuels, materials, and health-care products. *Angewandte Chemie - International Edition*, *54*(11), 3328–3350. https://doi.org/10.1002/ANIE.201409033

Becker, J., & Wittmann, C. (2019). A field of dreams: Lignin valorization into chemicals, materials, fuels, and health-care products. *Biotechnology Advances*, *37*(6), 107360. https://doi.org/10.1016/J.BIOTECHADV.2019.02.016

Bernal, P., Muñoz-Rojas, J., Hurtado, A., Ramos, J. L., & Segura, A. (2007a). A *Pseudomonas putida* cardiolipin synthesis mutant exhibits increased sensitivity to drugs related to transport functionality. *Environmental Microbiology*, *9*(5), 1135–1145. https://doi.org/10.1111/j.1462-2920.2006.01236.x

Bernal, P., Segura, A., & Ramos, J. L. (2007b). Compensatory role of the *cis-trans*-isomerase and cardiolipin synthase in the membrane fluidity of *Pseudomonas putida* DOT-T1E. *Environmental Microbiology*, *9*(7), 1658–1664. https://doi.org/10.1111/J.1462-2920.2007.01283.X

Berner, M., Krug, D., Bihlmaier, C., Vente, A., Müller, R., & Bechthold, A. (2006). Genes and enzymes involved in caffeic acid biosynthesis in the Actinomycete *Saccharothrix espanaensis*. *Journal of Bacteriology*, *188*(7), 2666–2673. https://doi.org/10.1128/JB.188.7.2666-2673.2006

Bertacchi, S., Jayaprakash, P., Morrissey, J. P., & Branduardi, P. (2022). Interdependence between lignocellulosic biomasses, enzymatic hydrolysis and yeast cell

factories in biorefineries. *Microbial Biotechnology*, *15*(3), 985–995. https://doi.org/10.1111/1751-7915.13886

Beuttler, H., Hoffmann, J., Jeske, M., Hauer, B., Schmid, R. D., Altenbuchner, J., & Urlacher, V. B. (2011). Biosynthesis of zeaxanthin in recombinant *Pseudomonas putida*. *Applied Microbiology and Biotechnology*, *89*(4), 1137–1147. https://doi.org/10.1007/S00253-010-2961-0

Bhuiya, M. W., Lee, S. G., Jez, J. M., & Yu, O. (2015). Structure and mechanism of ferulic acid decarboxylase (FDC1) from *Saccharomyces cerevisiae*. *Applied and Environmental Microbiology*, *81*(12), 4216–4223. https://doi.org/10.1128/AEM.00762-15

Bird, L. J., Kundu, B. B., Tschirhart, T., Corts, A. D., Su, L., Gralnick, J. A., Ajo-Franklin, C. M., & Glaven, S. M. (2021). Engineering wired life: synthetic biology for electroactive bacteria. *ACS Synthetic Biology*, *10*(11), 2808–2823. https://doi.org/10.1021/ACSSYNBIO.1C00335

Bird, L. J., Mickol, R. L., Eddie, B. J., Thakur, M., Yates, M. D., & Glaven, S. M. (2023). Marinobacter: A case study in bioelectrochemical chassis evaluation. *Microbial Biotechnology*, *16*(3), 494–506. https://doi.org/10.1111/1751-7915.14170

Bitzenhofer, N. L., Höfel, C., Thies, S., Weiler, A. J., Eberlein, C., Heipieper, H. J., Batra-Safferling, R., Sundermeyer, P., Heidler, T., Sachse, C., Busche, T., Kalinowski, J., Belthle, T., Drepper, T., Jaeger, K.-E., & Loeschcke, A. (2024). Exploring engineered vesiculation by *Pseudomonas putida* KT2440 for natural product biosynthesis. *Microbial Biotechnology*, *17*(1), e14312. https://doi.org/10.1111/1751-7915.14312

Bitzenhofer, N. L., Kruse, L., Thies, S., Wynands, B., Lechtenberg, T., Rönitz, J., Kozaeva, E., Wirth, N. T., Eberlein, C., Jaeger, K. E., Nikel, P. I., Heipieper, H. J., Wierckx, N., & Loeschcke, A. (2021). Towards robust *Pseudomonas* cell factories to harbour novel biosynthetic pathways. *Essays in Biochemistry*, *65*(2), 319–336. https://doi.org/10.1042/EBC20200173

Blair, J. M., Webber, M. A., Baylay, A. J., Ogbolu, D. O., & Piddock, L. J. (2015). Molecular mechanisms of antibiotic resistance. *Nature Reviews. Microbiology*, *13*(1), 42–51. https://doi.org/10.1038/NRMICRO3380

Blatt, L. M., Davis, J. M., Klein, S. B., & Taylor, M. W. (1996). The biologic activity and molecular characterization of a novel synthetic interferon-alpha species,

consensus interferon. *Journal of Interferon and Cytokine Research*, *16*(7), 489–499. https://doi.org/10.1089/JIR.1996.16.489

Bligh, E. G., & Dyer, W. J. (1959). A rapid method of total lipid extraction and purification. *Canadian Journal of Biochemistry and Physiology*, *37*, 911–917. https://doi.org/10.1139/o59-099

Bloor, S., Michurin, I., Titchiner, G. R., & Leys, D. (2023). Prenylated flavins: structures and mechanisms. *FEBS Journal*, *290*(9), 2232–2245. https://doi.org/10.1111/FEBS.16371

Bond, J. (1989). Review of the toxicology of styrene. *Critical Reviews in Toxicology*, *19*(3), 227–249. https://doi.org/10.3109/10408448909037472

Boutet, E., Lieberherr, D., Tognolli, M., Schneider, M., & Bairoch, A. (2007). UniProtKB/Swiss-Prot. *Methods in Molecular Biology*, *406*, 89–112. https://doi.org/10.1007/978-1-59745-535-0_4

Branduardi, P. (2021). Closing the loop: the power of microbial biotransformations from traditional bioprocesses to biorefineries, and beyond. *Microbial Biotechnology*, *14*(1), 68–73. https://doi.org/10.1111/1751-7915.13713

Brown, P. H., & Schuck, P. (2008). A new adaptive grid-size algorithm for the simulation of sedimentation velocity profiles in analytical ultracentrifugation. *Computer Physics Communications*, *178*(2), 105–120. https://doi.org/10.1016/j.cpc.2007.08.012

Bugg, T., Foght, J. M., Pickard, M. A., & Gray, M. R. (2000). Uptake and active efflux of polycyclic aromatic hydrocarbons by *Pseudomonas fluorescens* LP6a. *Applied and Enviornmental Microbiology*, *66*(12), 5387–5392. https://doi.org/10.1128/AEM.66.12.5387-5392.2000

Buijs, N. A., Siewers, V., & Nielsen, J. (2013). Advanced biofuel production by the yeast *Saccharomyces cerevisiae*. *Current Opinion in Chemical Biology*, *17*(3), 480–488. https://doi.org/10.1016/J.CBPA.2013.03.036

Busch, A., Lacal, J., Martos, A., Ramos, J. L., & Krell, T. (2007). Bacterial sensor kinase TodS interacts with agonistic and antagonistic signals. *Proceedings of the National Academy of Sciences of the United States of America*, *104*(34), 13774–13779. https://doi.org/10.1073/PNAS.0701547104

Calero, P., Jensen, S. I., & Nielsen, A. T. (2016). Broad-host-range ProUSER vectors enable fast characterization of inducible promoters and optimization of p-coumaric acid production in *Pseudomonas putida* KT2440. *ACS Synthetic Biology*, *5*(7), 741–753. https://doi.org/10.1021/ACSSYNBIO.6B00081

Calero, P., & Nikel, P. I. (2019). Chasing bacterial chassis for metabolic engineering: a perspective review from classical to non-traditional microorganisms. *Microbial Biotechnology*, *12*(1), 98–124. https://doi.org/10.1111/1751-7915.13292

Cao, M., Gao, M., Suástegui, M., Mei, Y., & Shao, Z. (2020). Building microbial factories for the production of aromatic amino acid pathway derivatives: From commodity chemicals to plant-sourced natural products. *Metabolic Engineering*, *58*, 94–132. https://doi.org/10.1016/j.ymben.2019.08.008

ChemAnalyst. (2023). Styrene market size, share, industry analysis and forecast, 2030. https://www.chemanalyst.com/industry-report/styrene-market-650

Chen, C. Y., Georgiev, I., Anderson, A. C., & Donald, B. R. (2009). Computational structure-based redesign of enzyme activity. *Proceedings of the National Academy of Sciences of the United States of America*, *106*(10), 3764–3469. https://doi.org/10.1073/PNAS.0900266106

Chen, S., Chu, J., Zhuang, Y., & Zhang, S. (2005). Enhancement of inosine production by *Bacillus subtilis* through suppression of carbon overflow by sodium citrate. *Biotechnology Letters*, *27*(10), 689–692. https://doi.org/10.1007/s10529-005-4686-1

Chen, V. B., Arendall III, W. B., Headd, J. J., Keedy, D. A., Immormino, R. M., Kapral, G. J., Murray, L. W., Richardson, J. S., & Richardson, D. C. (2010). MolProbity: all-atom structure validation for macromolecular crystallography. *Acta Crystallographica. Section D, Biological Crystallography*, *66*(Pt 1), 12–21. https://doi.org/10.1107/S0907444909042073

Clarke, C. F. (2000). New advances in coenzyme Q biosynthesis. *Protoplasma*, *213*, 134–147. https://doi.org/10.1007/BF01282151

Clausen, M., Lamb, C. J., Megnet, R., & Doerner, P. W. (1994). PAD1 encodes phenylacrylic acid decarboxylase which confers resistance to cinnamic acid in *Saccharomyces cerevisiae*. *Gene*, *142*(1), 107–112. https://doi.org/10.1016/0378-1119(94)90363-8

Collaborative Computational Project, N. 4. (1994). The CCP4 suite: programs for protein crystallography. *Acta Crystallographica. Section D, Biological Crystallography*, *50*(Pt 5), 760–763. https://doi.org/10.1107/S0907444994003112

Conti, B., Maltoni, C., Perino, G., & Ciliberti, A. (1988). Long-Term carcinogenicity bioassays on styrene administered by inhalation, ingestion and injection and styrene oxide administered by ingestion in Sprague-Dawley rats, and para-methylstyrene administered by ingestion in Sprague-Dawley rats and Swiss

Mice. *Annals of the New York Academy of Sciences*, *534*(1), 203–234. https://doi.org/10.1111/J.1749-6632.1988.TB30112.X

Costa-Gutierrez, S. B., Adler, C., Espinosa-Urgel, M., & de Cristóbal, R. E. (2022). *Pseudomonas putida* and its close relatives: mixing and mastering the perfect tune for plants. *Applied Microbiology and Biotechnology*, *106*(9-10), 3351–3367. https://doi.org/10.1007/S00253-022-11881-7

Cronan, J. E. J., & Rock, C. O. (2008). Biosynthesis of membrane lipids. *EcoSal Plus*, *3*(1), 1–44. https://doi.org/10.1128/ecosalplus.3.6.4

Cuenca, M. d. S., Roca, A., Molina-Santiago, C., Duque, E., Armengaud, J., Gómez-Garcia, M. R., & Ramos, J. L. (2016). Understanding butanol tolerance and assimilation in *Pseudomonas putida* BIRD-1: An integrated omics approach. *Microbial Biotechnology*, *9*(1), 100–115. https://doi.org/10.1111/1751-7915.12328

Cywar, R. M., Rorrer, N. A., Hoyt, C. B., Beckham, G. T., & Chen, E. Y. X. (2022). Bio-based polymers with performance-advantaged properties. *Nature Reviews Materials*, *7*(2), 83–103. https://doi.org/10.1038/s41578-021-00363-3

Daddaoua, A., Krell, T., & Ramos, J.-L. (2009). Regulation of glucose metabolism in *Pseudomonas*: the phosphorylative branch and Entner-Doudoroff enzymes are regulated by a repressor containing a sugar isomerase domain. *The Journal of Biological Chemistry*, *284*(32), 21360–21368. https://doi.org/10.1074/jbc.M109.014555

Dai, M., Fisher, H. E., Temirov, J., Kiss, C., Phipps, M. E., Pavlik, P., Werner, J. H., & Bradbury, A. R. (2007). The creation of a novel fluorescent protein by guided consensus engineering. *Protein Engineering, Design & Selection*, *20*(2), 69–79. https://doi.org/10.1093/PROTEIN/GZL056

Danchin, A. (2022). *In vivo*, *in vitro* and *in silico*: an open space for the development of microbe-based applications of synthetic biology. *Microbial biotechnology*, *15*(1), 42–64. https://doi.org/10.1111/1751-7915.13937

Daniels, C., Godoy, P., Duque, E., Molina-Henares, M. A., De La Torre, J., Del Arco, J. M., Herrera, C., Segura, A., Guazzaroni, M. E., Ferrer, M., & Ramos, J. L. (2010). Global regulation of food supply by *Pseudomonas putida* DOT-T1E. *Journal of Bacteriology*, *192*(8), 2169–2181. https://doi.org/10.1128/JB.01129-09

de Meester, C., Poncelet, F., Roberfroid, M., Rondelet, J., & Mercier, M. (1977). Mutagenicity of styrene and styrene oxide. *Mutation Research/Fundamental and Molecular Mechanisms of Mutagenesis*, *56*(2), 147–152. https://doi.org/10.1016/0027-5107(77)90202-0

de Smet, M. J., Kingma, J., & Witholt, B. (1978). The effect of toluene on the structure and permeability of the outer and cytoplasmic membranes of *Escherichia coli*. *Biochimica et Biophysica Acta*, *506*(1), 64–80. https://doi.org/10.1016/0005-2736(78)90435-2

de Vries, R. P., & Visser, J. (2001). *Aspergillus* enzymes involved in degradation of plant cell wall polysaccharides. *Microbiology and Molecular Biology Reviews*, *65*(4), 497–522. https://doi.org/10.1128/MMBR.65.4.497-522.2001

del Castillo, T., Duque, E., & Ramos, J. L. (2008). A set of activators and repressors control peripheral glucose pathways in *Pseudomonas putida* to yield a common central intermediate. *Journal of Bacteriology*, *190*(7), 2331–2339. https://doi.org/10.1128/JB.01726-07

del Castillo, T., Ramos, J. L., Rodríguez-Herva, J. J., Fuhrer, T., Sauer, U., & Duque, E. (2007). Convergent peripheral pathways catalyze initial glucose catabolism in *Pseudomonas putida*: genomic and flux analysis. *Journal of Bacteriology*, *189*(14), 5142–5152. https://doi.org/10.1128/JB.00203-07

DeLano, W. L. (2002). Pymol: an open-source molecular graphics tool. *CCP4 Newsletter on Protein Crystallography*.

Domínguez-Cuevas, P., González-Pastor, J. E., Marqués, S., Ramos, J. L., & De Lorenzo, V. (2006). Transcriptional tradeoff between metabolic and stress-response programs in *Pseudomonas putida* KT2440 cells exposed to toluene. *Journal of Biological Chemistry*, *281*(17), 11981–11991. https://doi.org/10.1074/JBC.M509848200

Duque, E., Segura, A., Mosqueda, G., & Ramos, J. L. (2001). Global and cognate regulators control the expression of the organic solvent efflux pumps TtgABC and TtgDEF of *Pseudomonas putida*. *Molecular Microbiology*, *39*(4), 1100–1106. https://doi.org/10.1046/j.1365-2958.2001.02310.x

Duque, E., Udaondo, Z., Molina, L., de la Torre, J., Godoy, P., & Ramos, J. L. (2022). Providing octane degradation capability to *Pseudomonas putida* KT2440 through the horizontal acquisition of *oct* genes located on an integrative and conjugative element. *Environmental Microbiology Reports*, *14*(6), 934–946. https://doi.org/10.1111/1758-2229.13097

Duță, H., Filip, A., Nagy, L. C., Nagy, E. Z. A., Tőtős, R., & Bencze, L. C. (2022). Toolbox for the structure-guided evolution of ferulic acid decarboxylase (FDC). *Scientific Reports*, *12*(1), 1–11. https://doi.org/10.1038/s41598-022-07110-w

Dvořák, P., & de Lorenzo, V. (2018). Refactoring the upper sugar metabolism of *Pseudomonas putida* for co-utilization of cellobiose, xylose, and glucose. *Metabolic Engineering*, *48*, 94–108. https://doi.org/10.1016/J.YMBEN.2018.05.019

Eda, S., Maseda, H., & Nakae, T. (2003). An elegant means of self-protection in Gram-negative bacteria by recognizing and extruding xenobiotics from the periplasmic space. *The Journal of Biological Chemistry*, *278*(4), 2085–2088. https://doi.org/10.1074/jbc.C200661200

Ellis, G. A., Tschirhart, T., Spangler, J., Walper, S. A., Medintz, I. L., & Vora, G. J. (2019). Exploiting the feedstock flexibility of the emergent synthetic biology chassis *Vibrio natriegens* for engineered natural product production. *Marine Drugs*, *17*(12), 679. https://doi.org/10.3390/MD17120679

Elmore, J. R., Dexter, G. N., Salvachúa, D., O'Brien, M., Klingeman, D. M., Gorday, K., Michener, J. K., Peterson, D. J., Beckham, G. T., & Guss, A. M. (2020). Engineered *Pseudomonas putida* simultaneously catabolizes five major components of corn stover lignocellulose: Glucose, xylose, arabinose, *p*-coumaric acid, and acetic acid. *Metabolic Engineering*, *62*, 62–71. https://doi.org/10.1016/J.YMBEN.2020.08.001

Emsley, P., Lohkamp, B., Scott, W. G., & Cowtan, K. (2010). Features and development of Coot. *Acta Crystallographica. Section D, Biological Crystallography*, *66*(Pt 4), 486–501. https://doi.org/10.1107/S0907444910007493

Evans, K., Adewoye, L., & Poole, K. (2001). MexR repressor of the mexAB-oprM multidrug efflux operon of *Pseudomonas aeruginosa*: identification of MexR binding sites in the mexA-mexR intergenic region. *Journal of Bacteriology*, *183*(3), 807–812. https://doi.org/10.1128/JB.183.3.807-812.2001

Evans, P. R., & Murshudov, G. N. (2013). How good are my data and what is the resolution? *Acta Crystallographica. Section D, Biological Crystallography*, *69*(Pt 7), 1204–1214. https://doi.org/10.1107/S0907444913000061

Fackler, N., Heijstra, B. D., Rasor, B. J., Brown, H., Martin, J., Ni, Z., Shebek, K. M., Rosin, R. R., Simpson, S. D., Tyo, K. E., Giannone, R. J., Hettich, R. L., Tschaplinski, T. J., Leang, C., Brown, S. D., Jewett, M. C., & Köpke, M.

(2021). Stepping on the gas to a circular economy: accelerating development of carbon-negative chemical production from gas fermentation. *Annual Review of Chemical and Biomolecular Engineering*, *12*, 439–470. https://doi.org/10.1146/ANNUREV-CHEMBIOENG-120120-021122

Faizal, I., Dozen, K., Hong, C. S., Kuroda, A., Takiguchi, N., Ohtake, H., Takeda, K., Tsunekawa, H., & Kato, J. (2005). Isolation and characterization of solvent-tolerant *Pseudomonas putida* strain T-57, and its application to biotransformation of toluene to cresol in a two-phase (organic-aqueous) system. *Journal of Industrial Microbiology and Biotechnology*, *32*(11-12), 542–547. https://doi.org/10.1007/S10295-005-0253-Y

Falgueras, J., Lara, A. J., Fernández-Pozo, N., Cantón, F. R., Pérez-Trabado, G., & Claros, M. G. (2010). SeqTrim: A high-throughput pipeline for preprocessing any type of sequence read. *BMC Bioinformatics*, *11*(38). https://doi.org/10.1186/1471-2105-11-38

Fargione, J., Hill, J., Tilman, D., Polasky, S., & Hawthorne, P. (2008). Land clearing and the biofuel carbon debt. *Science*, *319*(5867), 1235–1238. https://doi.org/10.1126/SCIENCE.1152747

Ferguson, K. L., Arunrattanamook, N., & Marsh, E. N. (2016). Mechanism of the novel prenylated flavin-containing enzyme ferulic acid decarboxylase probed by isotope effects and linear free-energy relationships. *Biochemistry*, *55*(20), 2857–2863. https://doi.org/10.1021/acs.biochem.6b00170

Fernandez, X., Lizzani-Cuvelier, L., Loiseau, A. M., Perichet, C., Delbecque, C., & Arnaudo, J. F. (2005). Chemical composition of the essential oils from Turkish and Honduras Styrax. *Flavour and Fragrance Journal*, *20*(1), 70–73. https://doi.org/10.1002/ffj.1370

Fernández, M., Rico-Jiménez, M., Ortega, Á., Daddaoua, A., García, A. I. G., Martín-Mora, D., Torres, N. M., Tajuelo, A., Matilla, M. A., & Krell, T. (2019). Determination of ligand profiles for *Pseudomonas aeruginosa* solute binding proteins. *International Journal of Molecular Sciences*, *20*(20), 5156. https://doi.org/10.3390/IJMS20205156

Fernandez-Escamilla, A. M., Rousseau, F., Schymkowitz, J., & Serrano, L. (2004). Prediction of sequence-dependent and mutational effects on the aggregation of peptides and proteins. *Nature Biotechnology*, *22*(10), 1302–1306. https://doi.org/10.1038/nbt1012

Fernando, D. M., & Kumar, A. (2013). Resistance-Nodulation-Division multidrug efflux pumps in Gram-negative bacteria: role in virulence. *Antibiotics*, *2*(1), 163–181. https://doi.org/10.3390/antibiotics2010163

Fillet, S., Daniels, C., Pini, C., Krell, T., Duque, E., Bernal, P., Segura, A., Lu, D., Zhang, X., & Ramos, J. L. (2012). Transcriptional control of the main aromatic hydrocarbon efflux pump in *Pseudomonas*. *Environmental Microbiology Reports*, *4*(2), 158–167. https://doi.org/10.1111/J.1758-2229.2011.00255.X

Garcia, J. M., & Robertson, M. L. (2017). The future of plastics recycling. *Science*, *358*(6365), 870–872. https://doi.org/10.1126/science.aaq0324

García-Franco, A., Godoy, P., Duque, E., & Ramos, J. L. (2024). Engineering styrene biosynthesis: designing a functional *trans*-cinnamic acid decarboxylase in *Pseudomonas*. *Microbial Cell Factories*, *23*(69). https://doi.org/10.1186/s12934-024-02341-0

García-Franco, A., Godoy, P., Duque, E., & Ramos, J. L. (2023). Insights into the susceptibility of *Pseudomonas putida* to industrially relevant aromatic hydrocarbons that it can synthesize from sugars. *Microbial Cell Factories*, *22*(22). https://doi.org/10.1186/s12934-023-02028-y

Gerding, M. A., Ogata, Y., Pecora, N. D., Niki, H., & de Boer, P. A. J. (2007). The *trans*-envelope Tol-Pal complex is part of the cell division machinery and required for proper outer-membrane invagination during cell constriction in *E. coli*. *Molecular Microbiology*, *63*(4), 1008–1025. https://doi.org/10.1111/j.1365-2958.2006.05571.x

Gibbs, B., & Mulligan, C. (1997). Styrene toxicity: an ecotoxicological assessment. *Ecotoxicology and Environmental Safety*, *38*(3), 181–194. https://doi.org/10.1006/eesa.1997.1526

Gibson, D. T., Hensley, M., Yoshioka, H., & Mabry, T. J. (1970). Formation of (+)-*cis*-2,3-dihydroxy-1-methylcyclohexa-4,6-diene from toluene by *Pseudomonas putida*. *Biochemistry*, *9*(7), 1626–1630. https://doi.org/10.1021/BI00809A023

Gilbert, H. J., & Tully, M. (1982). Synthesis and degradation of phenylalanine ammonia-lyase of *Rhodosporidium toruloides*. *Journal of Bacteriology*, *150*(2), 498–505. https://doi.org/10.1128/jb.150.2.498-505.1982

Giver, L., Gershenson, A., Freskgard, P.-O., & Arnold, F. H. (1998). Directed evolution of a thermostable esterase. *Proceedings of the National Academy of*

Sciences of the United States of America, *95*(22), 12809–12813. https://doi.org/10.1073/pnas.95.22.12809

Godar, A., Kamoku, C., Nielsen, D., & Wang, X. (2021). Synthetic biology strategies to address waste CO_2 loss during biofuel production. *Current Opinion in Environmental Science & Health*, *24*(100305). https://doi.org/10.1016/j.coesh.2021.100305

Godoy, P., García-Franco, A., Recio, M. I., Ramos, J. L., & Duque, E. (2021). Synthesis of aromatic amino acids from 2G lignocellulosic substrates. *Microbial Biotechnology*, *14*(5), 1931–1943. https://doi.org/10.1111/1751-7915.13844

Godoy, P., Udaondo, Z., Duque, E., & Ramos, J. L. (2024). Biosynthesis of fragrance 2-phenylethanol from sugars by *Pseudomonas putida*. *Biotechnology for Biofuels and Bioproducts*, *17*(51), 1–12. https://doi.org/10.1186/S13068-024-02498-1

González-Gayte, I., Bautista-Moreno, R., Seoane-Zonjic, P., & Claros, M. G. (2017). DEgenes Hunter - A flexible R pipeline for automated RNA-seq studies in organisms without reference genome. *Genomics and Computational Biology*, *3*(3), 31. https://doi.org/10.18547/GCB.2017.VOL3.ISS3.E31

Graf, N., & Altenbuchner, J. (2014). Genetic engineering of *Pseudomonas putida* KT2440 for rapid and high-yield production of vanillin from ferulic acid. *Applied Microbiology and Biotechnology*, *98*(1), 137–149. https://doi.org/10.1007/S00253-013-5303-1

Grant, S. G., Jessee, J., Bloom, F. R., & Hanahan, D. (1990). Differential plasmid rescue from transgenic mouse DNAs into *Escherichia coli* methylation-restriction mutants. *Proceedings of the National Academy of Sciences of the United States of America*, *87*(12), 4645–4649. https://doi.org/10.1073/PNAS.87.12.4645

Green, E. M. (2011). Fermentative production of butanol — the industrial perspective. *Current Opinion in Biotechnology*, *22*(3), 337–343. https://doi.org/10.1016/j.copbio.2011.02.004

Grkovic, S., Brown, M. H., & Skurray, R. A. (2002). Regulation of bacterial drug export systems. *Microbiology and Molecular Biology Reviews*, *66*(4), 671–701. https://doi.org/10.1128/mmbr.66.4.671-701.2002

Grogan, D. W., & Cronan, J. E. (1997). Cyclopropane ring formation in membrane lipids of bacteria. *Microbiology and Molecular Biology Reviews*, *61*(4), 429–441. https://doi.org/10.1128/mmbr.61.4.429-441.1997

Grubbe, W. S., Rasor, B. J., Krüger, A., Jewett, M. C., & Karim, A. S. (2020). Cell-free styrene biosynthesis at high titers. *Metabolic Engineering*, *61*, 89–95. https://doi.org/10.1016/j.ymben.2020.05.009

Gu, W., Yang, J., Lou, Z., Liang, L., Sun, Y., Huang, J., Li, X., Cao, Y., Meng, Z., & Zhang, K.-Q. (2011). Structural basis of enzymatic activity for the ferulic acid decarboxylase (FADase) from *Enterobacter* sp. Px6-4. *PLoS One*, *6*(1), e16262. https://doi.org/10.1371/JOURNAL.PONE.0016262

Guazzaroni, M. E., Krell, T., Gutiérrez del Arroyo, P., Vélez, M., Jiménez, M., Rivas, G., & Ramos, J. L. (2007). The transcriptional repressor TtgV recognizes a complex operator as a tetramer and induces convex DNA bending. *Journal of Molecular Biology*, *369*(4), 927–939. https://doi.org/10.1016/J.JMB.2007.04.022

Guazzaroni, M. E., Terán, W., Zhang, X., Gallegos, M.-T., & Ramos, J. L. (2004). TtgV bound to a complex operator site represses transcription of the promoter for the multidrug and solvent extrusion TtgGHI pump. *Journal of Bacteriology*, *186*(10), 2921–2927. https://doi.org/10.1128/JB.186.10.2921-2927.2004

Gulmezian, M., Hyman, K. R., Marbois, B. N., Clarke, C. F., & Javor, G. T. (2007). The role of UbiX in *Escherichia coli* coenzyme Q biosynthesis. *Archives of Biochemistry and Biophysics*, *467*(2), 144–153. https://doi.org/10.1016/J.ABB.2007.08.009

Gupta, R., Uslu, H., & Majumder, S. (2022). Production of styrene from dehydrogenation of ethylbenzene. *Chemical Engineering and Technology*, *45*(5), 817–823. https://doi.org/10.1002/CEAT.202100577

Hancock, R. E. W. (1997). The bacterial outer membrane as a drug barrier. *Trends in Microbiology*, *5*(1), 37–42. https://doi.org/10.1016/S0966-842X(97)81773-8

Hannon, M., Gimpel, J., Tran, M., Rasala, B., & Mayfield, S. (2010). Biofuels from algae: challenges and potential. *Biofuels*, *1*(5), 763–784. https://doi.org/10.4155/BFS.10.44

Hartmans, S., van der Werf, M. J., & de Bont, J. A. M. (1990). Bacterial degradation of styrene involving a novel flavin adenine dinucleotide-dependent styrene monooxygenase. *Applied and Environmental Microbiology*, *56*(5), 1347–1351. https://doi.org/10.1128/aem.56.5.1347-1351.1990

Hatti-Kaul, R., Törnvall, U., Gustafsson, L., & Börjesson, P. (2007). Industrial biotechnology for the production of bio-based chemicals–a cradle-to-grave

perspective. *Trends in Biotechnology*, *25*(3), 119–124. https://doi.org/10.1016/J.TIBTECH.2007.01.001

Hearn, E. M., Dennis, J. J., Gray, M. R., & Foght, J. M. (2003). Identification and characterization of the *emhABC* efflux system for polycyclic aromatic hydrocarbons in *Pseudomonas fluorescens* cLP6a. *Journal of Bacteriology*, *185*(21), 6233–6240. https://doi.org/10.1128/JB.185.21.6233-6240.2003

Heer, D., & Sauer, U. (2008). Identification of furfural as a key toxin in lignocellulosic hydrolysates and evolution of a tolerant yeast strain. *Microbial Biotechnology*, *1*(6), 497–506. https://doi.org/10.1111/j.1751-7915.2008.00050.x

Heipieper, H. J., & Martínez, P. M. (2018). Toxicity of hydrocarbons to microorganisms. In *Cellular ecophysiology of microbe: Hydrocarbon and lipid interactions* (pp. 335–344). Springer, Cham. https://doi.org/10.1007/978-3-319-50542-8{_}45

Heipieper, H. J., Neumann, G., Cornelissen, S., & Meinhardt, F. (2007). Solvent-tolerant bacteria for biotransformations in two-phase fermentation systems. *Applied Microbiology and Biotechnology*, *74*(5), 961–973. https://doi.org/10.1007/S00253-006-0833-4

Hendriks, A., & Zeeman, G. (2009). Pretreatments to enhance the digestibility of lignocellulosic biomass. *Bioresource Technology*, *100*(1), 10–18. https://doi.org/10.1016/j.biortech.2008.05.027

Hill, J., Nelson, E., Tilman, D., Polasky, S., & Tiffany, D. (2006). Environmental, economic, and energetic costsand benefits of biodiesel and ethanol biofuels. *PNAS*, *103*(30), 11206–11210. https://doi.org/nvironmental,economic,andenergeticcostsandbenefitsofbiodieselandethanolbio-fuels.PNAS,103(30),11206âĂŞ11210.

Hoang, D. T., Chernomor, O., von Haeseler, A., Minh, B. Q., & Vinh, L. S. (2018). UFBoot2: Improving the ultrafast bootstrap approximation. *Mol. Biol. Evol*, *35*(2), 518–522. https://doi.org/10.1093/molbev/msx281

Horcajada, J. P., Montero, M., Oliver, A., Sorlí, L., Luque, S., Gómez-Zorrilla, S., Benito, N., & Grau, S. (2019). Epidemiology and treatment of multidrug-resistant and extensively drug-resistant *Pseudomonas aeruginosa* infections. *Clinical Microbiology Reviews*, *32*(4), 00031–19. https://doi.org/10.1128/CMR.00031-19

Horinouchi, T., Tamaoka, K., Furusawa, C., Ono, N., Suzuki, S., Hirasawa, T., Yomo, T., & Shimizu, H. (2010). Transcriptome analysis of parallel-evolved

Escherichia coli strains under ethanol stress. *BMC genomics*, *11*(579). https://doi.org/10.1186/1471-2164-11-579

Huccetogullari, D., Luo, Z. W., & Lee, S. Y. (2019). Metabolic engineering of microorganisms for production of aromatic compounds. *Microbial Cell Factories*, *18*(1), 41. https://doi.org/10.1186/s12934-019-1090-4

Huertas, M.-J., Duque, E., Marqués, S., & Ramos, J. L. (1998). Survival in soil of different toluene-degrading *Pseudomonas* strains after solvent shock. *Applied and Environmental Microbiology*, *64*(1), 38–42. https://doi.org/10.1128/AEM.64.1.38-42.1998

Hüsken, L. E., Dalm, M. C., Tramper, J., Wery, J., de Bont, J. A., & Beeftink, R. (2001). Integrated bioproduction and extraction of 3-methylcatechol. *Journal of Biotechnology*, *88*(1), 11–19. https://doi.org/10.1016/S0168-1656(01)00252-8

IARC. (2019). Styrene, styrene-7,8-oxide, and quinoline. In *International agency for research on cancer* (pp. 37–266, Vol. 121).

Inoue, A., & Horikoshi, K. (1989). A *Pseudomonas* thrives in high concentrations of toluene. *Nature*, *338*, 264–266. https://doi.org/10.1038/338264a0

Inoue, A., & Horikoshi, K. (1991). Estimation of solvent-tolerance of bacteria by the solvent parameter log P. *Journal of Fermentation and Bioengineering*, *71*(3), 194–196. https://doi.org/10.1016/0922-338X(91)90109-T

International Energy Agency. (2018). *The Future of Petrochemicals* (tech. rep.). https://www.iea.org/reports/the-future-of-petrochemicals

Isikgor, F. H., & Becer, C. R. (2015). Lignocellulosic biomass: a sustainable platform for the production of bio-based chemicals and polymers. *Polymer Chemistry*, *6*(25), 4497–4559. https://doi.org/10.1039/C5PY00263J

Isken, S., & de Bont, J. A. M. (1996). Active efflux of toluene in a solvent-resistant bacterium. *Journal of Bacteriology*, *178*(20), 6056–6058. https://doi.org/10.1128/jb.178.20.6056-6058.1996

Jacewicz, A., Brunner, K., Schnell, R., & Schneider, G. (2013). Structural insights into the UbiD protein family from the crystal structure of PA0254 from *Pseudomonas aeruginosa*. *PLoS One*, *8*(5), e63161. https://doi.org/10.1371/journal.pone.0063161

Jäckel, C., Kast, P., & Hilvert, D. (2008). Protein design by directed evolution. *Annual Review of Biophysics*, *37*, 153–173. https://doi.org/10.1146/annurev.biophys.37.032807.125832

Jain, A., Sarsaiya, S., Kumar Awasthi, M., Singh, R., Rajput, R., Mishra, U. C., Chen, J., & Shi, J. (2022). Bioenergy and bio-products from bio-waste and its associated modern circular economy: Current research trends, challenges, and future outlooks. *Fuel*, *307*, 121859–121871. https://doi.org/10.1016/J.FUEL.2021.121859

Jang, Y.-S., Lee, J. Y., Lee, J., Park, J. H., Im, J. A., Eom, M.-H., Lee, J., Lee, S.-H., Song, H., Cho, J.-H., Seung, D. Y., & Lee, S. Y. (2012). Enhanced butanol production obtained by reinforcing the direct butanol-forming route in *Clostridium acetobutylicum*. *mBio*, *3*(5), 00314–12. https://doi.org/10.1128/mBio.00314-12

Jeong, H., Barbe, V., Lee, C. H., Vallenet, D., Yu, D. S., Choi, S. H., Couloux, A., Lee, S. W., Yoon, S. H., Cattolico, L., Hur, C. G., Park, H. S., Ségurens, B., Kim, S. C., Oh, T. K., Lenski, R. E., Studier, F. W., Daegelen, P., & Kim, J. F. (2009). Genome sequences of *Escherichia coli* B strains REL606 and BL21(DE3). *Journal of Molecular Biology*, *394*(4), 644–652. https://doi.org/10.1016/J.JMB.2009.09.052

Jiménez-Arroyo, C., Tamargo, A., Molinero, N., & Moreno-Arribas, M. V. (2022). The gut microbiota, a key to understanding the health implications of micro(nano)plastics and their biodegradation. *Microbial Biotechnology*, *16*(1), 34–53. https://doi.org/10.1111/1751-7915.14182

Jiménez-Bonilla, P., & Wang, Y. (2018). *In situ* biobutanol recovery from clostridial fermentations: a critical review. *Critical Reviews in Biotechnology*, *38*(3), 469–482. https://doi.org/10.1080/07388551.2017.1376308

Jumper, J., Evans, R., Pritzel, A., Green, T., Figurnov, M., Ronneberger, O., Tunyasuvunakool, K., Bates, R., Žídek, A., Potapenko, A., Bridgland, A., Meyer, C., Kohl, S. A., Ballard, A. J., Cowie, A., Romera-Paredes, B., Nikolov, S., Jain, R., Adler, J., … Hassabis, D. (2021). Highly accurate protein structure prediction with AlphaFold. *Nature*, *596*(7873), 583–589. https://doi.org/10.1038/S41586-021-03819-2

Junker, F., & Ramos, J. L. (1999). Involvement of the *cis/trans* isomerase Cti in solvent resistance of *Pseudomonas putida* DOT-T1E. *Journal of Bacteriology*, *181*(18), 5693–5700. https://doi.org/10.1128/jb.181.18.5693-5700.1999

Kabsch, W. (2010). XDS. *Acta Crystallographica. Section D, Biological Crystallography*, *66*(Pt 2), 125–132. https://doi.org/10.1107/S0907444909047337

Kalyaanamoorthy, S., Minh, B. Q., Wong, T. K., von Haeseler, A., & Jermiin, L. S. (2017). ModelFinder: fast model selection for accurate phylogenetic estimates. *Nature Methods*, *14*(6), 587–589. https://doi.org/10.1038/nmeth.4285

Kampers, L. F. C., Volkers, R. J. M., & Martins dos Santos, V. A. P. (2019). *Pseudomonas putida* kt2440 is HV1 certified, not GRAS. *Microbial Biotechnology*, *12*(5), 845–848. https://doi.org/10.1111/1751-7915.13443

Kang, S.-Y., Choi, O., Lee, J. K., Ahn, J.-O., Ahn, J. S., Hwang, B. Y., & Hong, Y.-S. (2015). Artificial *de novo* biosynthesis of hydroxystyrene derivatives in a tyrosine overproducing *Escherichia coli* strain. *Microbial Cell Factories*, *14*(78). https://doi.org/10.1186/S12934-015-0268-7

Keasling, J. D. (2010). Manufacturing molecules through metabolic engineering. *Science*, *330*(6009), 1355–1358. https://doi.org/10.1126/science.1193990

Keshavarz-Tohid, V., Vacheron, J., Dubost, A., Prigent-Combaret, C., Taheri, P., Tarighi, S., Taghavi, S. M., Moënne-Loccoz, Y., & Muller, D. (2019). Genomic, phylogenetic and catabolic re-assessment of the *Pseudomonas putida* clade supports the delineation of *Pseudomonas alloputida* sp. nov., *Pseudomonas inefficax* sp. nov., *Pseudomonas persica* sp. nov., and *Pseudomonas shirazica* sp. nov. *Systematic and Applied Microbiology*, *42*(4), 468–480. https://doi.org/10.1016/J.SYAPM.2019.04.004

Keweloh, H., & Heipieper, H. I. (1996). *Trans* unsaturated fatty acids in bacteria. *Lipids*, *31*(2), 129–137. https://doi.org/10.1007/BF02522611

Keweloh, H., Weyrauch, G., & Rehm, H. J. (1990). Phenol-induced membrane changes in free and immobilized *Escherichia coli*. *Applied Microbiology and Biotechnology*, *33*(1), 66–71. https://doi.org/10.1007/BF00170572

Khow, O., & Suntrarachun, S. (2012). Strategies for production of active eukaryotic proteins in bacterial expression system. *Asian Pacific Journal of Tropical Biomedicine*, *2*(2), 159–162. https://doi.org/10.1016/S2221-1691(11)60213-X

Kim, K. H., Kabir, E., & Kabir, S. (2015). A review on the human health impact of airborne particulate matter. *Environment International*, *74*, 136–143. https://doi.org/10.1016/J.ENVINT.2014.10.005

Kim, N.-K., Lee, S.-H., & Park, H.-D. (2022). Current biotechnologies on depolymerization of polyethylene terephthalate (PET) and repolymerization of reclaimed monomers from PET for bio-upcycling: A critical review. *Biore-*

source Technology, *363*(127931). https://doi.org/10.1016/J.BIORTECH.2022.127931

Kim, P. I., Ryu, J., Kim, Y. H., & Chi, Y.-T. (2010). Production of biosurfactant lipopeptides iturin A, fengycin, and surfactin A from *Bacillus subtilis* CMB32 for control of *Colletotrichum gloeosporioides*. *Journal of Microbiology and Biotechnology*, *20*(1), 138–145. https://doi.org/10.4014/jmb.0905.05007

Klinke, H. B., Thomsen, A. B., & Ahring, B. K. (2004). Inhibition of ethanol-producing yeast and bacteria by degradation products produced during pre-treatment of biomass. *Applied Microbiology and Biotechnology*, *66*, 10–26. https://doi.org/10.1007/s00253-004-1642-2

Kopec, J., Schnell, R., & Schneider, G. (2011). Structure of PA4019, a putative aromatic acid decarboxylase from *Pseudomonas aeruginosa*. *Acta Crystalographica. Section F, Structural Biology and Crystallization Communications*, *67*(Pt 10), 1184–1188. https://doi.org/10.1107/S174430911102923X

Krell, T., Lacal, J., Guazzaroni, M. E., Busch, A., Silva-Jiménez, H., Fillet, S., Reyes-Darías, J. A., Muñoz-Martínez, F., Rico-Jiménez, M., García-Fontana, C., Duque, E., Segura, A., & Ramos, J. L. (2012). Responses of *Pseudomonas putida* to toxic aromatic carbon sources. *Journal of Biotechnology*, *160*(1-2), 25–32. https://doi.org/10.1016/J.JBIOTEC.2012.01.026

Krell, T., Terán, W., Mayorga, O. L., Rivas, G., Jiménez, M., Daniels, C., Molina-Henares, A. J., Martínez-Bueno, M., Gallegos, M. T., & Ramos, J. L. (2007). Optimization of the palindromic order of the TtgR operator enhances binding cooperativity. *Journal of Molecular Biology*, *369*(5), 1188–1199. https://doi.org/10.1016/J.JMB.2007.04.025

Kries, H., Blomberg, R., & Hilvert, D. (2013). *De novo* enzymes by computational design. *Current Opinion in Chemical Biology*, *17*(2), 221–228. https://doi.org/10.1016/J.CBPA.2013.02.012

Krissinel, E., & Henrick, K. (2004). Secondary-structure matching (SSM), a new tool for fast protein structure alignment in three dimensions. *Acta Crystallographica. Section D, Biological Crystallography*, *60*(Pt 12 Pt 1), 2256–2268. https://doi.org/10.1107/S0907444904026460

Krissinel, E., & Henrick, K. (2007). Inference of macromolecular assemblies from crystalline state. *Journal of Molecular Biology*, *372*(3), 774–797. https://doi.org/10.1016/j.jmb.2007.05.022

Krivoruchko, A., & Nielsen, J. (2015). Production of natural products through metabolic engineering of *Saccharomyces cerevisiae*. *Current Opinion in Biotechnology*, *35*, 7–15. https://doi.org/10.1016/J.COPBIO.2014.12.004

Kusumawardhani, H., Hosseini, R., & de Winde, J. H. (2018). Solvent tolerance in bacteria: fulfilling the promise of the biotech era? *Trends in Biotechnology*, *36*(10), 1025–1039. https://doi.org/10.1016/J.TIBTECH.2018.04.007

Lacal, J., Busch, A., Guazzaroni, M.-E., Krell, T., & Ramos, J. L. (2006). The TodS-TodT two-component regulatory system recognizes a wide range of effectors and works with DNA-bending proteins. *The Proceedings of the National Academy of Sciences*, *103*(21), 8191–8196. https://doi.org/10.1073/pnas.0602902103

Lacal, J., Guazzaroni, E., Busch, A., Krell, T., & Ramos, J. L. (2008). Hierarchical binding of the TodT response regulator to its multiple recognition sites at the *tod* pathway operon promoter. *Journal of Molecular Biology*, *376*(2), 325–337. https://doi.org/10.1016/j.jmb.2007.12.004

Lan, C. L., & Chen, S. L. (2016). The decarboxylation of α,β-unsaturated acid catalyzed by prenylated FMN-dependent ferulic acid decarboxylase and the enzyme inhibition. *The Journal of Organic Chemistry*, *81*(19), 9289–9295. https://doi.org/10.1021/ACS.JOC.6B01872

Lane, M. D., & Seelig, B. (2014). Advances in the directed evolution of proteins. *Current Opinion in Chemical Biology*, *22*, 129–136. https://doi.org/10.1016/j.cbpa.2014.09.013

Langmead, B., & Salzberg, S. L. (2012). Fast gapped-read alignment with Bowtie 2. *Nature Methods*, *9*(4), 357–359. https://doi.org/10.1038/nmeth.1923

Laskowski, R. A., Jabłońska, J., Pravda, L., Vařeková, R. S., & Thornton, J. M. (2018). PDBsum: Structural summaries of PDB entries. *Protein Science*, *27*(1), 129–134. https://doi.org/10.1002/pro.3289

Le Meur, S., Zinn, M., Egli, T., Thöny-Meyer, L., & Ren, Q. (2012). Production of medium-chain-length polyhydroxyalkanoates by sequential feeding of xylose and octanoic acid in engineered *Pseudomonas putida* KT2440. *BMC Biotechnology*, *12*(53), 1–12. https://doi.org/10.1186/1472-6750-12-53

Leavell, M. D., McPhee, D. J., & Paddon, C. J. (2016). Developing fermentative terpenoid production for commercial usage. *Current Opinion in Biotechnology*, *37*, 114–119. https://doi.org/10.1016/J.COPBIO.2015.10.007

Lee, J. H., & Wendisch, V. F. (2017). Biotechnological production of aromatic compounds of the extended shikimate pathway from renewable biomass. *Journal of Biotechnology*, *257*, 211–221. https://doi.org/10.1016/J.JBIOTEC.2016.11.016

Lee, K., Bang, H. B., Lee, Y. H., & Jeong, K. J. (2019). Enhanced production of styrene by engineered *Escherichia coli* and *in situ* product recovery (ISPR) with an organic solvent. *Microbial Cell Factories*, *18*(79). https://doi.org/10.1186/s12934-019-1129-6

Lehmann, M., Loch, C., Middendorf, A., Studer, D., Lassen, S. F., Pasamontes, L., van Loon, A. P., & Wyss, M. (2002). The consensus concept for thermostability engineering of proteins: further proof of concept. *Protein engineering*, *15*(5), 403–411. https://doi.org/10.1093/PROTEIN/15.5.403

Leibman, K. (1975). Metabolism and toxicity of styrene. *Environmental Health Perspectives*, *11*, 115–119. https://doi.org/10.1289/ehp.7511115

Li, H., Handsaker, B., Wysoker, A., Fennell, T., Ruan, J., Homer, N., Marth, G., Abecasis, G., Durbin, R., & 1000 Genome Project Data Processing Subgroup. (2009). The Sequence Alignment/Map format and SAMtools. *Bioinformatics*, *25*(16), 2078–2079. https://doi.org/10.1093/BIOINFORMATICS/BTP352

Li, S., & Wilkinson, M. F. (1997). Site-directed mutagenesis: a two-step method using PCR and Dpn I. *Biotechniques*, *23*(4), 588–590. https://doi.org/10.2144/97234BM05

Li, T., Huo, L., Pulley, C., & Liu, A. (2012). Decarboxylation mechanisms in biological system. *Bioorganic Chemistry*, *43*, 2–14. https://doi.org/10.1016/j.bioorg.2012.03.001

Li, X. Z., Zhang, L., & Poole, K. (1998). Role of the multidrug efflux systems of *Pseudomonas aeruginosa* in organic solvent tolerance. *Journal of Bacteriology*, *180*(11), 2987–2991. https://doi.org/10.1128/JB.180.11.2987-2991.1998

Liang, L., Liu, R., Foster, K. E., Choudhury, A., Cook, S., Cameron, J. C., Srubar, W. V., & Gill, R. T. (2020). Genome engineering of *E. coli* for improved styrene production. *Metabolic Engineering*, *57*, 74–84. https://doi.org/10.1016/j.ymben.2019.09.007

Lijinsky, W. (1986). Rat and mouse forestomach tumors induced by chronic oral administration of styrene oxide. *Journal of the National Cancer Institute*, *77*(2), 471–476. https://doi.org/10.1093/JNCI/77.2.471

Lin, F., Ferguson, K. L., Boyer, D. R., Lin, X. N., & Marsh, E. N. G. (2015). Isofunctional enzymes PAD1 and UbiX catalyze formation of a novel cofactor required by ferulic acid decarboxylase and 4-hydroxy-3-polyprenylbenzoic acid decarboxylase. *ACS Chemical Biology*, *10*(4), 1137–1144. https://doi.org/10.1021/cb5008103

Linger, J. G., Vardon, D. R., Guarnieri, M. T., Karp, E. M., Hunsinger, G. B., Franden, M. A., Johnson, C. W., Chupka, G., Strathmann, T. J., Pienkos, P. T., & Beckham, G. T. (2014). Lignin valorization through integrated biological funneling and chemical catalysis. *The Proceedings of the National Academy of Sciences (PNAS)*, *111*(33), 12013–12018. https://doi.org/10.1073/pnas.1410657111

Liu, C., Men, X., Chen, H., Li, M., Ding, Z., Chen, G., Wang, F., Liu, H., Wang, Q., Zhu, Y., Zhang, H., & Xian, M. (2018). A systematic optimization of styrene biosynthesis in *Escherichia coli* BL21(DE3). *Biotechnology for Biofuels*, *11*(14). https://doi.org/10.1186/s13068-018-1017-z

Liu, H., Sun, Y., Ramos, K. R. M., Nisola, G. M., Valdehuesa, K. N. G., Lee, W. K., Park, S. J., & Chung, W. J. (2013). Combination of Entner-Doudoroff pathway with MEP increases isoprene production in engineered *Escherichia coli*. *PLoS ONE*, *8*(12), 1–7. https://doi.org/10.1371/journal.pone.0083290

Loeschcke, A., & Thies, S. (2015). *Pseudomonas putida*-a versatile host for the production of natural products. *Applied Microbiology and Biotechnology*, *99*(15), 6197–6214. https://doi.org/10.1007/S00253-015-6745-4

Loeschcke, A., & Thies, S. (2020). Engineering of natural product biosynthesis in *Pseudomonas putida*. *Current Opinion in Biotechnology*, *65*, 213–224. https://doi.org/10.1016/J.COPBIO.2020.03.007

Lohner, K. (1991). Effects of small organic molecules on phospholidpid phase transitions. *Chemistry and Physics of Lipids*, *57*(2-3), 341–362. https://doi.org/10.1016/0009-3084(91)90085-P

Lomovskaya, O., Lee, A., Hoshino, K., Ishida, H., Mistry, A., Warren, M. S., Boyer, E., Chamberland, S., & Lee, V. J. (1999). Use of a genetic approach to evaluate the consequences of inhibition of efflux pumps in *Pseudomonas aeruginosa*. *Antimicrobial Agents and Chemotherapy*, *43*(6), 1340–1346. https://doi.org/10.1128/AAC.43.6.1340

Lomovskaya, O., Warren, M. S., Lee, A., Galazzo, J., Fronko, R., Lee, M., Blais, J., Cho, D., Chamberland, S., Renau, T., Leger, R., Hecker, S., Watkins, W.,

Hoshino, K., Ishida, H., & Lee, V. J. (2001). Identification and characterization of inhibitors of multidrug resistance efflux pumps in *Pseudomonas aeruginosa*: novel agents for combination therapy. *Antimicrobial Agents and Chemotheraphy*, *45*(1), 105–116. https://doi.org/10.1128/AAC.45.1.105-116.2001

Lu, D., Fillet, S., Meng, C., Alguel, Y., Kloppsteck, P., Bergeron, J., Krell, T., Gallegos, M.-T., Ramos, J., & Zhang, X. (2010). Crystal structure of TtgV in complex with its DNA operator reveals a general model for cooperative DNA binding of tetrameric gene regulators. *Genes & Development*, *24*(22), 2556–2565. https://doi.org/10.1101/gad.603510

Machas, M., Kurgan, G., Abed, O. A., Shapiro, A., Wang, X., & Nielsen, D. (2021). Characterizing *Escherichia coli*'s transcriptional response to different styrene exposure modes reveals novel toxicity and tolerance insights. *Journal of Industrial Microbiology and Biotechnology*, *48*(kuab019), 19. https://doi.org/10.1093/jimb/kuab019

Machas, M. S., McKenna, R., & Nielsen, D. R. (2017). Expanding upon styrene biosynthesis to engineer a novel route to 2-phenylethanol. *Biotechnology Journal*, *12*(10). https://doi.org/10.1002/BIOT.201700310

Marshall, S. A., Payne, K. A., Fisher, K., White, M. D., Ní Cheallaigh, A., Balaikaite, A., Rigby, S. E., & Leys, D. (2019). The UbiX flavin prenyltransferase reaction mechanism resembles class I terpene cyclase chemistry. *Nature Communications*, *10*(2357), 1–10. https://doi.org/10.1038/s41467-019-10220-1

Marshall, S. A., Payne, K. A., & Leys, D. (2017). The UbiX-UbiD system: The biosynthesis and use of prenylated flavin (prFMN). *Archives of Biochemistry and Biophysics*, *632*, 209–221. https://doi.org/10.1016/J.ABB.2017.07.014

Martínez-García, E., Aparicio, T., Goñi-Moreno, A., Fraile, S., & de Lorenzo, V. (2015). SEVA 2.0: an update of the Standard European Vector Architecture for de-/re-construction of bacterial functionalities. *Nucleic Acids Research*, *43*(D1), D1183–D1189. https://doi.org/10.1093/NAR/GKU1114

Martínez-García, E., De Lorenzo, V., Benenson, Y., & Lutolf, M. (2017). Molecular tools and emerging strategies for deep genetic/genomic refactoring of *Pseudomonas*. *Current Opinion in Biotechnology*, *47*, 120–132. https://doi.org/10.1016/j.copbio.2017.06.013

Martínez-García, E., Nikel, P. I., Aparicio, T., & de Lorenzo, V. (2014). *Pseudomonas* 2.0: genetic upgrading of *P. putida* KT2440 as an enhanced host for heterologous gene expression. *Microbial Cell Factories*, *13*(159), 1–15. https://doi.org/10.1186/s12934-014-0159-3

Mathuriya, A. S., & Yakhmi, J. V. (2016). Microbial fuel cells - Applications for generation of electrical power and beyond. *Critical Reviews in Microbiology*, *42*(1), 127–143. https://doi.org/10.3109/1040841X.2014.905513

Matilla, M. A., Martín-Mora, D., Gavira, J. A., & Krell, T. (2021). *Pseudomonas aeruginosa* as a model to study chemosensory pathway signaling. *Microbiology and Molecular Biology Reviews*, *85*(1), e00151. https://doi.org/10.1128/MMBR.00151-20

Matte, A., Grosse, S., Bergeron, H., Abokitse, K., & Lau, P. C. (2010). Structural analysis of *Bacillus pumilus* phenolic acid decarboxylase, a lipocalin-fold enzyme. *Acta Crystallographica. Section F, Structural Biology and Crystallization Communications*, *66*(Pt 11), 1407–1414. https://doi.org/10.1107/S174430911003246X

Mavrodi, D. V., Paulsen, I. T., Ren, Q., & Loper, J. E. (2007). Genomics of *Pseudomonas fluorescens* Pf-5. In *Pseudomonas: A model system in biology* (pp. 3–30). Springer Netherlands.

McKenna, R., Moya, L., McDaniel, M., & Nielsen, D. R. (2015). Comparing *in situ* removal strategies for improving styrene bioproduction. *Bioprocess and Biosystems Engineering*, *38*(1), 165–174. https://doi.org/10.1007/s00449-014-1255-9

McKenna, R., & Nielsen, D. R. (2011). Styrene biosynthesis from glucose by engineered *E. coli*. *Metabolic Engineering*, *13*(5), 544–554. https://doi.org/10.1016/j.ymben.2011.06.005

McKenna, R., Thompson, B., Pugh, S., & Nielsen, D. R. (2014). Rational and combinatorial approaches to engineering styrene production by *Saccharomyces cerevisiae*. *Microbial Cell Factories*, *13*, 123. https://doi.org/10.1186/s12934-014-0123-2

McKenna, R., Pugh, S., Thompson, B., & Nielsen, D. R. (2013). Microbial production of the aromatic building-blocks (*S*)-styrene oxide and (*R*)-1,2-phenylethanediol from renewable resources. *Biotechnology Journal*, *8*(12), 1465–1475. https://doi.org/10.1002/BIOT.201300035

Meijnen, J.-P., de Winde, J. H., & Ruijssenaars, H. J. (2008). Engineering *Pseudomonas putida* S12 for efficient utilization of D-xylose and L-arabinose. *Applied and Environmental Microbiology*, *74*(16), 5031–5037. https://doi.org/10.1128/AEM.00924-08

Mi, J., Becher, D., Lubuta, P., Dany, S., Tusch, K., Schewe, H., Buchhaupt, M., & Schrader, J. (2014). *De novo* production of the monoterpenoid geranic acid by metabolically engineered *Pseudomonas putida*. *Microbial Cell Factories*, *13*(170). https://doi.org/10.1186/S12934-014-0170-8

Miao, C., Xinshu, Z., Yang, L., Li, H., Lv, P., & Luo, W. (2023). Study on extraction of lignin and synthesis of lignin-based epoxy resins using ionic liquid. *Biomass Conversion and Biorefinery*, *13*, 1115–1126. https://doi.org/10.1007/s13399-021-01295-2

Michaud, J. M., Madani, A., & Fraser, J. S. (2022). A language model beats alphafold2 on orphans. *Nature Biotechnology*, *40*(11), 1576–1577. https://doi.org/10.1038/s41587-022-01466-0

Miller, R. R., Newhook, R., & Poole, A. (1994). Styrene production, use, and human exposure. *Critical reviews in toxicology*, *24 Suppl*(s1). https://doi.org/10.3109/10408449409020137

Mine, T., Morita, Y., Kataoka, A., Mizushima, T., & Tsuchiya, T. (1999). Expression in *Escherichia coli* of a new multidrug efflux pump, MexXY, from *Pseudomonas aeruginosa*. *Antimicrobial Agents and Chemotherapy*, *43*(2), 415–417. https://doi.org/10.1128/AAC.43.2.415

Moffitt, M. C., Louie, G. V., Bowman, M. E., Pence, J., Noel, J. P., & Moore, B. S. (2007). Discovery of two cyanobacterial phenylalanine ammonia lyases: kinetic and structural characterization. *Biochemistry*, *46*(4), 1004–1012. https://doi.org/10.1021/bi061774g

Mohr, A., & Raman, S. (2013). Lessons from first generation biofuels and implications for the sustainability appraisal of second generation biofuels. *Energy Policy*, *63*(100), 114–122. https://doi.org/10.1016/J.ENPOL.2013.08.033

Molina, L., Duque, E., Gómez, M. J., Krell, T., Lacal, J., García-Puente, A., García, V., Matilla, M. A., Ramos, J. L., & Segura, A. (2011). The pGRT1 plasmid of *Pseudomonas putida* DOT-T1E encodes functions relevant for survival under harsh conditions in the environment. *Environmental Microbiology*, *13*(8), 2315–2327. https://doi.org/10.1111/j.1462-2920.2011.02492.x

Molina, L., Geoffroy, V. A., Segura, A., Udaondo, Z., & Ramos, J. L. (2016). Iron uptake analysis in a set of clinical isolates of *Pseudomonas putida*. *Frontiers in Microbiology*, *7*(2100), 1–14. https://doi.org/10.3389/fmicb.2016.02100

Molina, L., La Rosa, R., Nogales, J., & Rojo, F. (2019). Influence of the Crc global regulator on substrate uptake rates and the distribution of metabolic fluxes in *Pseudomonas putida* KT2440 growing in a complete medium. *Environmental microbiology*, *21*(11), 4446–4459. https://doi.org/10.1111/1462-2920.14812

Molina-Henares, M. A., García-Salamanca, A., Molina-Henares, A. J., de la Torre, J., Herrera, M. C., Ramos, J. L., & Duque, E. (2009). Functional analysis of aromatic biosynthetic pathways in *Pseudomonas putida* KT2440. *Microbial Biotechnology*, *2*(1), 91–100. https://doi.org/10.1111/J.1751-7915.2008.00062.X

Molina-Santiago, C., Cordero, B. F., Daddaoua, A., Udaondo, Z., Manzano, J., Valdivia, M., Segura, A., Ramos, J. L., & Duque, E. (2016). *Pseudomonas putida* as a platform for the synthesis of aromatic compounds. *Microbiology*, *162*(9), 1535–1543. https://doi.org/10.1099/mic.0.000333

Moomaw, E. W., Angerhofer, A., Moussatche, P., Ozarowski, A., García-Rubio, I., & Richards, N. G. (2009). Metal dependence of oxalate decarboxylase activity. *Biochemistry*, *48*(26), 6116–6125. https://doi.org/10.1021/BI801856K

Moore, E. R. B., Tindall, B. J., Martins Dos Santos, V. A. P., Pieper, D. H., Ramos, J. L., & Palleroni, N. J. (2006). Nonmedical: *Pseudomonas putida*. *Prokaryotes*, *6*, 646–703. https://doi.org/10.1007/0-387-30746-X_21

Moreno, R., Fonseca, P., & Rojo, F. (2012). Two small RNAs, CrcY and CrcZ, act in concert to sequester the Crc global regulator in *Pseudomonas putida*, modulating catabolite repression. *Molecular Microbiology*, *83*(1), 24–40. https://doi.org/10.1111/J.1365-2958.2011.07912.X

Mosqueda, G., & Ramos, J. L. (2000). A set of genes encoding a second toluene efflux system in *Pseudomonas putida* DOT-T1E is linked to the *tod* genes for toluene metabolism. *Journal of Bacteriology*, *182*(4), 937–943. https://doi.org/10.1128/JB.182.4.937-943.2000

Mosqueda, G., Ramos-González, M. I., & Ramos, J. L. (1999). Toluene metabolism by the solvent-tolerant *Pseudomonas putida* DOT-T1 strain, and its role in solvent impermeabilization. *Gene*, *232*(1), 69–76. https://doi.org/10.1016/s0378-1119(99)00113-4

Mukai, N., Masaki, K., Fujii, T., Kawamukai, M., & Iefuji, H. (2010). PAD1 and FDC1 are essential for the decarboxylation of phenylacrylic acids in *Saccharomyces cerevisiae*. *Journal of Bioscience and Bioengineering*, *109*(6), 564–569. https://doi.org/10.1016/j.jbiosc.2009.11.011

Muñoz-Rojas, J., Bernal, P., Duque, E., Godoy, P., Segura, A., & Ramos, J.-L. (2006). Involvement of cyclopropane fatty acids in the response of *Pseudomonas putida* KT2440 to freeze-drying. *Applied and Enviornmental Microbiology*, *72*(1), 472–477. https://doi.org/10.1128/AEM.72.1.472-477.2006

Murshudov, G. N., Skubák, P., Lebedev, A. A., Pannu, N. S., Steiner, R. A., Nicholls, R. A., Winn, M. D., Long, F., & Vagin, A. A. (2011). REFMAC5 for the refinement of macromolecular crystal structures. *Acta Crystallographica. Section D, Biological Crystallography*, *67*(Pt 4), 355–367. https://doi.org/10.1107/S0907444911001314

Mycroft, Z., Gomis, M., Mines, P., Law, P., & Bugg, T. D. H. (2015). Biocatalytic conversion of lignin to aromatic dicarboxylic acids in *Rhodococcus jostii* RHA1 by re-routing aromatic degradation pathways. *Green Chemistry*, *17*, 4974–4979. https://doi.org/10.1039/C5GC01347J

Nagy, E. Z. A., Nagy, C. L., Filip, A., Nagy, K., Gál, E., Tőtős, R., Poppe, L., Paizs, C., & Bencze, L. C. (2019). Exploring the substrate scope of ferulic acid decarboxylase (FDC1) from *Saccharomyces cerevisiae*. *Scientific Reports*, *9*(647). https://doi.org/10.1038/s41598-018-36977-x

Nakae, T., Nakajima, A., Ono, T., Saito, K., & Yoneyama, H. (1999). Resistance to β-lactam antibiotics in *Pseudomonas aeruginosa* due to interplay between the MexAB-OprM efflux pump and β-lactamase. *Antimicrobial Agents and Chemotherapy*, *43*(5), 1301–1303. https://doi.org/10.1128/AAC.43.5.1301

Nelson, K. E., Weinel, C., Paulsen, I. T., Dodson, R. J., Hilbert, H., Martins dos Santos, V. A., Fouts, D. E., Gill, S. R., Pop, M., Holmes, M., Brinkac, L., Beanan, M., DeBoy, R. T., Daugherty, S., Kolonay, J., Madupu, R., Nelson, W., White, O., Peterson, J., … Fraser, C. M. (2002). Complete genome sequence and comparative analysis of the metabolically versatile *Pseudomonas putida* KT2440. *Environmental Microbiology*, *4*(12), 799–808. https://doi.org/10.1046/J.1462-2920.2002.00366.X

Nguyen, L.-T., Schmidt, H. A., von Haeseler, A., & Minh, B. Q. (2015). IQ-TREE: A fast and effective stochastic algorithm for estimating maximum-likelihood

phylogenies. *Molecular Biology and Evolution*, *32*(1), 268–174. https://doi.org/10.1093/MOLBEV/MSU300

Ni, Y., & Sun, Z. (2009). Recent progress on industrial fermentative production of acetone-butanol-ethanol by *Clostridium acetobutylicum* in China. *Applied Microbiology and Biotechnology*, *83*(3), 415–423. https://doi.org/10.1007/s00253-009-2003-y

Nicolaou, S. A., Gaida, S. M., & Papoutsakis, E. T. (2010). A comparative view of metabolite and substrate stress and tolerance in microbial bioprocessing: From biofuels and chemicals, to biocatalysis and bioremediation. *Metabolic Engineering*, *12*(4), 307–331. https://doi.org/10.1016/J.YMBEN.2010.03.004

Nijkamp, K., van Luijk, N., de Bont, J. A., & Wery, J. (2005). The solvent-tolerant *Pseudomonas putida* S12 as host for the production of cinnamic acid from glucose. *Applied Microbiology and Biotechnology*, *69*(2), 170–177. https://doi.org/10.1007/S00253-005-1973-7

Nijkamp, K., Westerhof, R. G. M., Ballerstedt, H., de Bont, J. A., & Wery, J. (2007). Optimization of the solvent-tolerant *Pseudomonas putida* S12 as host for the production of *p*-coumarate from glucose. *Applied Microbiology and Biotechnology*, *74*(3), 617–624. https://doi.org/10.1007/s00253-006-0703-0

Nikaido, H. (1996). Multidrug efflux pumps of Gram-negative bacteria. *Journal of Bacteriology*, *178*(20), 5853–5859. https://doi.org/10.1128/jb.178.20.5853-5859.1996

Nikaido, H. (1998). Antibiotic resistance caused by Gram-negative multidrug efflux pumps. *Clinical Infectious Diseases*, *27*, S32–S41. https://academic.oup.com/cid/article/27/Supplement_1/S32/459233

Nikaido, H., & Pagès, J. M. (2012). Broad-specificity efflux pumps and their role in multidrug resistance of Gram-negative bacteria. *FEMS microbiology reviews*, *36*(2), 340–363. https://doi.org/10.1111/J.1574-6976.2011.00290.X

Nikaido, H., & Takatsuka, Y. (2009). Mechanisms of RND multidrug efflux pumps. *Biochimica et Biophysica Acta*, *1794*(5), 769–781. https://doi.org/10.1016/j.bbapap.2008.10.004

Nikel, P. I., & de Lorenzo, V. (2018). *Pseudomonas putida* as a functional chassis for industrial biocatalysis: from native biochemistry to *trans*-metabolism. *Metabolic Engineering*, *50*, 142–155. https://doi.org/10.1016/J.YMBEN.2018.05.005

Nikel, P. I., Martínez-García, E., & De Lorenzo, V. (2014). Biotechnological domestication of pseudomonads using synthetic biology. *Nature Reviews Microbiology 2014 12:5*, *12*(5), 368–379. https://doi.org/10.1038/nrmicro3253

Noda, S., Miyazaki, T., Miyoshi, T., Miyake, M., Okai, N., Tanaka, T., Ogino, C., & Kondo, A. (2011). Cinnamic acid production using *Streptomyces lividans* expressing phenylalanine ammonia lyase. *Journal of Industrial Microbiology and Biotechnology*, *38*(5), 643–648. https://doi.org/10.1007/s10295-011-0955-2

Nogales, J., Mueller, J., Gudmundsson, S., Canalejo, F. J., Duque, E., Monk, J., Feist, A. M., Ramos, J. L., Niu, W., & Palsson, B. O. (2020). High-quality genome-scale metabolic modelling of *Pseudomonas putida* highlights its broad metabolic capabilities. *Environmental Microbiology*, *22*(1), 255–269. https://doi.org/10.1111/1462-2920.14843

O'Brien, H. E., Thakur, S., & Guttman, D. S. (2011). Evolution of plant pathogenesis in *Pseudomonas syringae*: a genomics perspective. *Annual Review of Microbiology*, *49*, 269–289. https://doi.org/10.1146/annurev-phyto-072910-095242

Ohji, S., Yamazoe, A., Hosoyama, A., Tsuchikane, K., Ezaki, T., & Fujita, N. (2014). The complete genome sequence of *Pseudomonas putida* NBRC 14164T confirms high intraspecies variation. *Genome Announcements*, *2*(1), 00029–14. https://doi.org/10.1128/GENOMEA.00029-14

Okusu, H., Ma, D., & Nikaido, H. (1996). AcrAB efflux pump plays a major role in the antibiotic resistance phenotype of *Escherichia coli* multiple-antibiotic-resistance (Mar) mutants. *Journal of Bacteriology*, *178*(1), 306–308. https://doi.org/10.1128/jb.178.1.306-308.1996

Opgenorth, P., Costello, Z., Okada, T., Goyal, G., Chen, Y., Gin, J., Benites, V., De Raad, M., Northen, T. R., Deng, K., Deutsch, S., Baidoo, E. E., Petzold, C. J., Hillson, N. J., Garcia Martin, H., & Beller, H. R. (2019). Lessons from two Design-Build-Test-Learn cycles of dodecanol production in *Escherichia coli* aided by machine learning. *ACS synthetic biology*, *8*(6), 1337–1351. https://doi.org/10.1021/ACSSYNBIO.9B00020

Otero, J. M., Cimini, D., Patil, K. R., Poulsen, S. G., Olsson, L., & Nielsen, J. (2013). Industrial systems biology of *Saccharomyces cerevisiae* enables novel succinic acid cell factory. *PLoS ONE*, *8*(1), e54144. https://doi.org/10.1371/journal.pone.0054144

Otto, M., Wynands, B., Lenzen, C., Filbig, M., Blank, L. M., & Wierckx, N. (2019). Rational engineering of phenylalanine accumulation in *Pseudomonas taiwanensis* to enable high-yield production of *trans*-cinnamate. *Frontiers in Bioengineering and Biotechnology*, *7*, 312. https://doi.org/10.3389/fbioe.2019.00312

Otto, M., Wynands, B., Marienhagen, J., Blank, L. M., & Wierckx, N. (2020). Benzoate synthesis from glucose or glycerol using engineered *Pseudomonas taiwanensis*. *Biotechnology Journal*, *15*(11), e2000211. https://doi.org/10.1002/BIOT.202000211

Paatero, A., Rosti, K., Shkumatov, A. V., Sele, C., Brunello, C., Kysenius, K., Singha, P., Jokinen, V., Huttunen, H., & Kajander, T. (2016). Crystal structure of an engineered LRRTM2 synaptic adhesion molecule and a model for neurexin binding. *Biochemistry*, *55*(6), 914–926. https://doi.org/10.1021/acs.biochem.5b00971

Pagot, Y., Belin, J. M., Husson, F., & Spinnler, H. (2007). Metabolism of phenylalanine and biosynthesis of styrene in *Penicillium camemberti*. *Journal of Diary Research*, *74*(2), 180–185. https://doi.org/10.1017/S0022029906002251

Painter, J., & Merritt, E. A. (2006). TLSMD web server for the generation of multi-group TLS models. *Journal of Applied Crystallography*, *39*, 109–111. https://doi.org/10.1107/S0021889805038987

Palleroni, N. J. (2015). *Pseudomonas*. In *Bergey's manual of sistematic of archaea and bacteria* (pp. 1–105, Vol. 4). https://doi.org/10.1002/9781118960608.gbm01210

Parales, R. E., Parales, J. V., Pelletier, D. A., & Ditty, J. L. (2008). Diversity of microbial toluene degradation pathways. *Advances in Applied Microbiology*, *64*, 1–73. https://doi.org/10.1016/S0065-2164(08)00401-2

Payne, K. A., White, M. D., Fisher, K., Khara, B., Bailey, S. S., Parker, D., Rattray, N. J., Trivedi, D. K., Goodacre, R., Beveridge, R., Barran, P., Rigby, S. E., Scrutton, N. S., Hay, S., & Leys, D. (2015). New cofactor supports α,β-unsaturated acid decarboxylation via 1,3-dipolar cycloaddition. *Nature*, *522*(7557), 497–501. https://doi.org/10.1038/nature14560

Pereyra-Camacho, M. A., & Pardo, I. (2024). Plastics and the sustainable development goals: from waste to wealth with microbial recycling and upcycling. *Microbial Biotechnology*, *17*(4), e14459. https://doi.org/10.1111/1751-7915.14459

Philo, J. S. (2023). SEDNTERP: a calculation and database utility to aid interpretation of analytical ultracentrifugation and light scattering data. *European Biophysics Journal*, *52*(4-5), 233–266. https://doi.org/10.1007/s00249-023-01629-0

Philp, J. C., Ritchie, R. J., & Allan, J. E. M. (2013). Biobased chemicals: The convergence of green chemistry with industrial biotechnology. *Trends in Biotechnology*, *31*(4), 219–222. https://doi.org/10.1016/j.tibtech.2012.12.007

Phoenix, P., Keane, A., Patel, A., Bergeron, H., Ghoshal, S., & Lau, P. C. (2003). Characterization of a new solvent-responsive gene locus in *Pseudomonas putida* F1 and its functionalization as a versatile biosensor. *Environmental Microbiology*, *5*(12), 1309–1327. https://doi.org/10.1111/J.1462-2920.2003.00426.X

Piddock, L. J. V. (2006). Multidrug-resistance efflux pumps-not just for resistance. *Nature Reviews. Microbiology*, *4*(8), 629–636. https://doi.org/10.1038/nrmicro1464

Pini, C. V., Bernal, P., Godoy, P., Ramos, J. L., & Segura, A. (2009). Cyclopropane fatty acids are involved in organic solvent tolerance but not in acid stress resistance in *Pseudomonas putida* DOT-T1E. *Microbial Biotechnology*, *2*(2), 253–261. https://doi.org/10.1111/J.1751-7915.2009.00084.X

Pinkart, H. C., & White, D. C. (1997). Phospholipid biosynthesis and solvent tolerance in *Pseudomonas putida* strains. *Journal of Bacteriology*, *179*(13), 4219–4226. https://doi.org/10.1128/jb.179.13.4219-4226.1997

Poblete-Castro, I., Borrero-De Acuña, J. M., Nikel, P. I., Kohlstedt, M., & Wittmann, C. (2017). Host organism: *Pseudomonas putida*. In *Industrial biotechnology: Microorganisms* (pp. 299–326). https://doi.org/10.1002/9783527807796.ch8

Polizzi, K. M., Chaparro-Riggers, J. F., Vazquez-Figueroa, E., & Bommarius, A. S. (2006). Structure-guided consensus approach to create a more thermostable penicillin G acylase. *Biotechnology Journal*, *1*(5), 531–536. https://doi.org/10.1002/BIOT.200600029

Ponomarkov, V., Cabral, J. R., Wahrendorf, J., & Galendo, D. (1984). A carcinogenicity study of styrene-7,8-oxide in rats. *Cancer Letters*, *24*(1), 95–101. https://doi.org/10.1016/0304-3835(84)90085-5

Poole, K. (2008). Bacterial multidrug efflux pumps serve other functions. *Microbe*, *3*(4), 179–185. https://doi.org/10.1128/microbe.3.179.1

Poole, K., & Srikumar, R. (2001). Multidrug efflux in *Pseudomonas aeruginosa*: components, mechanisms and clinical significance. *Current Topics in Medicinal Chemistry*, *1*(1), 59–71. https://doi.org/10.2174/1568026013395605

Pope, J. M., & Dubro, D. W. (1986). The interaction of *n*-alkanes and *n*-alcohols with lipid bilayer membranes: a ^{2}H-NMR study. *Biochimica et Biophysica Acta*, *858*(2), 243–253. https://doi.org/10.1016/0005-2736(86)90329-9

Porebski, B. T., & Buckle, A. M. (2016). Consensus protein design. *Protein Engineering, Design and Selection*, *29*(7), 245–251. https://doi.org/10.1093/PROTEIN/GZW015

Prieto, A., Escapa, I. F., Martínez, V., Dinjaski, N., Herencias, C., de la Peña, F., Tarazona, N., & Revelles, O. (2016). A holistic view of polyhydroxyalkanoate metabolism in *Pseudomonas putida*. *Environmental Microbiology*, *18*(2), 341–357. https://doi.org/10.1111/1462-2920.12760

Pringle, M. J., & Miller, K. W. (1979). Differential effects on phospholipid phase transitions produced by structurally related long-chain alcohols. *Biochemistry*, *18*(15), 3314–3320. https://doi.org/10.1021/bi00582a018

Qi, W. W., Vannelli, T., Breinig, S., Ben-Bassat, A., Gatenby, A. A., Haynie, S. L., & Sariaslani, F. S. (2007). Functional expression of prokaryotic and eukaryotic genes in *Escherichia coli* for conversion of glucose to *p*-hydroxystyrene. *Metabolic Engineering*, *9*(3), 268–276. https://doi.org/10.1016/j.ymben.2007.01.002

Qureshi, N., Ezeji, T. C., Ebener, J., Dien, B. S., Cotta, M. A., & Blaschek, H. P. (2007). Butanol production by *Clostridium beijerinckii*. Part I: Use of acid and enzyme hydrolyzed corn fiber. *Bioresource Technology*, *99*(13), 5915–5922. https://doi.org/10.1016/j.biortech.2007.09.087

Rabinovitch-Deere, C. A., Oliver, J. W., Rodriguez, G. M., & Atsumi, S. (2013). Synthetic biology and metabolic engineering approaches to produce biofuels. *Chemical Reviews*, *113*(7), 4611–4632. https://doi.org/10.1021/CR300361T

Ragauskas, A. J., Beckham, G. T., Biddy, M. J., Chandra, R., Chen, F., Davis, M. F., Davison, B. H., Dixon, R. A., Gilna, P., Keller, M., Langan, P., Naskar, A. K., Saddler, J. N., Tschaplinski, T. J., Tuskan, G. A., & Wyman, C. E. (2014). Lignin valorization: Improving lignin processing in the biorefinery. *Science*, *344*(6185), 1246843. https://doi.org/10.1126/science.1246843

Rahimi, A., & García, J. M. (2017). Chemical recycling of waste plastics for new materials production. *Nature Reviews Chemistry*, *1*(0046). https://doi.org/10.1038/S41570-017-0046

Ramos, J. L., Cuenca, M. S., Molina-Santiago, C., Segura, A., Duque, E., Gómez-García, M. R., Udaondo, Z., & Roca, A. (2015). Mechanisms of solvent resistance mediated by interplay of cellular factors in *Pseudomonas putida*. *FEMS Microbiology Reviews*, *39*(4), 555–566. https://doi.org/10.1093/femsre/fuv006

Ramos, J. L., Duque, E., Gallegos, M. T., Godoy, P., Ramos-González, M. I., Rojas, A., Terán, W., & Segura, A. (2002). Mechanisms of solvent tolerance in Gram-negative bacteria. *Annual Review of Microbiology*, *56*(1), 743–768. https://doi.org/10.1146/annurev.micro.56.012302.161038

Ramos, J. L., Duque, E., Godoy, P., & Segura, A. (1998). Efflux pumps involved in toluene tolerance in *Pseudomonas putida* DOT- T1E. *Journal of Bacteriology*, *180*(13), 3323–3329. https://doi.org/10.1128/jb.180.13.3323-3329.1998

Ramos, J. L., Duque, E., Huertas, M. J., & Haïdour, A. (1995). Isolation and expansion of the catabolic potential of a *Pseudomonas putida* strain able to grow in the presence of high concentrations of aromatic hydrocarbons. *Journal of Bacteriology*, *177*(14), 3911–3916. https://doi.org/10.1128/jb.177.14.3911-3916.1995

Ramos, J. L., Duque, E., Rodríguez-Herva, J. J., Godoy, P., Haïdour, A., Reyes, F., & Fernández-Barrero, A. (1997). Mechanisms for solvent tolerance in bacteria. *Journal of Biological Chemistry*, *272*(7), 3887–3890. https://doi.org/10.1074/jbc.272.7.3887

Ramos, J. L., Valdivia, M., García-Lorente, F., & Segura, A. (2016). Benefits and perspectives on the use of biofuels. *Microbial Biotechnology*, *9*(4), 436–440. https://doi.org/10.1111/1751-7915.12356

Ramos, J. L., Wasserfallen, A., Rose, K., & Timmis, K. N. (1987). Redesigning metabolic routes: manipulation of TOL plasmid pathway for catabolism of alkylbenzoates. *Science*, *235*(4788), 593–596. https://doi.org/10.1126/science.3468623

Ramos, J. L., & Duque, E. (2019). Twenty-first-century chemical odyssey: fuels versus commodities and cell factories versus chemical plants. *Microbial Biotechnology*, *12*(2), 200–209. https://doi.org/10.1111/1751-7915.13379

Ramos, J. L., Martínez-Bueno, M., Molina-Henares, A. J., Terán, W., Watanabe, K., Zhang, X., Gallegos, M. T., Brennan, R., & Tobes, R. (2005). The TetR family of transcriptional repressors. *Microbiology and Molecular Biology Reviews*, *69*(2), 326–356. https://doi.org/10.1128/MMBR.69.2.326-356.2005

Ramos, J. L., Pakuts, B., Godoy, P., García-Franco, A., & Duque, E. (2022). Addressing the energy crisis: using microbes to make biofuels. *Microbial Biotechnology*, *15*(4), 1026–1030. https://doi.org/10.1111/1751-7915.14050

Ramos-González, M.-I., Ben-Bassat, A., Campos, M.-J., & Ramos, J. L. (2003). Genetic engineering of a highly solvent-tolerant *Pseudomonas putida* strain for biotransformation of toluene to *p*-hydroxybenzoate. *Applied and Environmental Microbiology*, *69*(9), 5120–5127. https://doi.org/10.1128/AEM.69.9.5120-5127.2003

Rangarajan, E. S., Li, Y., Iannuzzi, P., Tocilj, A., Hung, L.-W., Matte, A., & Cygler, M. (2004). Crystal structure of a dodecameric FMN-dependent UbiX-like decarboxylase (Pad1) from *Escherichia coli* O157: H7. *Protein Science*, *13*(11), 3006–3016. https://doi.org/10.1110/PS.04953004

Re, A., & Mazzoli, R. (2022). Current progress on engineering microbial strains and consortia for production of cellulosic butanol through consolidated bioprocessing. *Microbial Biotechnology*, *16*(2), 238–261. https://doi.org/10.1111/1751-7915.14148

Renewable Fuels Association. (2024). *2024 Ethanol Industry Outlook* (tech. rep.). Renewable Fuels Association.

Richard, P., Viljanen, K., & Penttilä, M. (2015). Overexpression of PAD1 and FDC1 results in significant cinnamic acid decarboxylase activity in *Saccharomyces cerevisiae*. *AMB Express*, *5*(12). https://doi.org/10.1186/S13568-015-0103-X

Roberts, G. W., & Leys, D. (2022). Structural insights into UbiD reversible decarboxylation. *Current Opinion in Structural Biology*, *75*(102432). https://doi.org/10.1016/j.sbi.2022.102432

Robinson, M. D., Mccarthy, D. J., & Smyth, G. K. (2010). edgeR: a bioconductor package for differential expression analysis of digital gene expression data. *Bioinformatics*, *26*(1), 139–140. https://doi.org/10.1093/bioinformatics/btp616

Roca, A., Pizarro-Tobías, P., Udaondo, Z., Fernández, M., Matilla, M. A., Molina-Henares, M. A., Molina, L., Segura, A., Duque, E., & Ramos, J. L. (2013). Analysis of the plant growth-promoting properties encoded by the genome of

the rhizobacterium *Pseudomonas putida* BIRD-1. *Environmental Microbiology*, *15*(3), 780–794. https://doi.org/10.1111/1462-2920.12037

Rodríguez, H., Angulo, I., de las Rivas, B., Campillo, N., Páez, J. A., Muñoz, R., & Mancheño, J. M. (2010). *p*-Coumaric acid decarboxylase from *lactobacillus plantarum*: structural insights into the active site and decarboxylation catalytic mechanism. *Proteins: Structure, Function, and Bioinformatics*, *78*(7), 1662–1676. https://doi.org/10.1002/PROT.22684

Rodríguez-Herva, J. J., García, V., Hurtado, A., Segura, A., & Ramos, J. L. (2007). The ttgGHI solvent efflux pump operon of *Pseudomonas putida* DOT-T1E is located on a large self-transmissible plasmid. *Environmental Microbiology*, *9*(6), 1550–1561. https://doi.org/10.1111/J.1462-2920.2007.01276.X

Rojas, A., Duque, E., Mosqueda, G., Golden, G., Hurtado, A., Ramos, J. L., & Segura, A. (2001). Three efflux pumps are required to provide efficient tolerance to toluene in *Pseudomonas putida* DOT-T1E. *Journal of Bacteriology*, *183*(13), 3967–3973. https://doi.org/10.1128/JB.183.13.3967-3973.2001

Rojas, A., Segura, A., Guazzaroni, E., Terán, W., Hurtado, A., Gallegos, T., & Ramos, J. L. (2003). *In vivo* and *in vitro* evidence that TtgV is the specific regulator of the TtgGHI multidrug and solvent efflux pump of *pseudomonas putida*. *Journal of Bacteriology*, *185*(16), 4755–4763. https://doi.org/10.1128/JB.185.16.4755-4763.2003

Sahdev, S., Khattar, S. K., & Saini, K. S. (2008). Production of active eukaryotic proteins through bacterial expression systems: a review of the existing biotechnology strategies. *Molecular and cellular biochemistry*, *307*(1-2), 249–264. https://doi.org/10.1007/S11010-007-9603-6

Sainsbury, P. D., Hardiman, E. M., Ahmad, M., Otani, H., Seghezzi, N., Eltis, L. D., & Bugg, T. D. (2013). Breaking down lignin to high-value chemicals: The conversion of lignocellulose to vanillin in a gene deletion mutant of *Rhodococcus jostii* RHA1. *ACS Chemical Biology*, *8*(10), 2151–2156. https://doi.org/10.1021/CB400505A

Santamaría-Hernando, S., De Bruyne, L., Höfte, M., & Ramos-González, M. I. (2022). Improvement of fitness and biocontrol properties of *Pseudomonas putida* via an extracellular heme peroxidase. *Microbial Biotechnology*, *15*(10), 2652–2666. https://doi.org/10.1111/1751-7915.14123

Sarria, S., Kruyer, N. S., & Peralta-Yahya, P. (2017). Microbial synthesis of medium-chain chemicals from renewables. *Nature Biotechnology*, *35*(12), 1158–1166. https://doi.org/10.1038/nbt.4022

Schwanemann, T., Otto, M., Wierckx, N., & Wynands, B. (2020). *Pseudomonas* as versatile aromatics cell factory. *Biotechnology Journal*, *15*(11), e1900569. https://doi.org/10.1002/BIOT.201900569

Segura, A., Duque, E., Hurtado, A., & Ramos, J. L. (2001). Mutations in genes involved in the flagellar export apparatus of the solvent-tolerant *Pseudomonas putida* DOT-T1E strain impair motility and lead to hypersensitivity to toluene shocks. *Journal of Bacteriology*, *183*(14), 4127–4133. https://doi.org/10.1128/JB.183.14.4127-4133.2001

Segura, A., Rojas, A., Hurtado, A., Huertas, M. J., & Ramos, J. L. (2003). Comparative genomic analysis of solvent extrusion pumps in *Pseudomonas* strains exhibiting different degrees of solvent tolerance. *Extremophiles*, *7*(5), 371–376. https://doi.org/10.1007/s00792-003-0331-x

Segura, A., Duque, E., Mosqueda, G., Ramos, J. L., & Junker, F. (1999). Multiple responses of Gram-negative bacteria to organic solvents. *Environmental Microbiology*, *1*(3), 191–198. https://doi.org/10.1046/J.1462-2920.1999.00033.X

Segura, A., Godoy, P., van Dillewijn, P., Hurtado, A., Arroyo, N., Santacruz, S., & Ramos, J.-L. (2005). Proteomic analysis reveals the participation of energy- and stress-related proteins in the response of *Pseudomonas putida* DOT-T1E to toluene. *Journal of Bacteriology*, *187*(17), 5937–5945. https://doi.org/10.1128/JB.187.17.5937-5945.2005

Segura, A., Molina, L., Fillet, S., Krell, T., Bernal, P., Muñoz-Rojas, J., & Ramos, J. L. (2012). Solvent tolerance in Gram-negative bacteria. *Current Opinion in Biotechnology*, *23*(3), 415–421. https://doi.org/10.1016/j.copbio.2011.11.015

Service, R. F. (2019). Can the world make the chemicals it needs without oil? *Science*. https://doi.org/10.1126/SCIENCE.AAZ5517

Shen, C. R., Lan, E. I., Dekishima, Y., Baez, A., Cho, K. M., & Liao, J. C. (2011). Driving forces enable high-titer anaerobic 1-butanol synthesis in *Escherichia coli*. *Applied and Enviornmental Microbiology*, *77*(9), 2905–2915. https://doi.org/10.1128/AEM.03034-10

Sikkema, J., de Bont, J. A. M., & Poolman, B. (1994). Interactions of cyclic hydrocarbons with biological membranes. *Journal of Biological Chemistry*, *269*(11), 8022–8028.

Sikkema, J., de Bont, J. A. M., & Poolman, B. (1995). Mechanisms of membrane toxicity of hydrocarbons. *Microbiology Reviews*, *59*(2), 201–222.

Silhavy, T. J., Kahne, D., & Walker, S. (2010). The bacterial cell envelope. *Cold Spring Harbor Perspectives in Biology*, *2*(5), a000414. https://doi.org/10.1101/cshperspect.a000414

Silva-Rocha, R., Martínez-García, E., Calles, B., Chavarría, M., Arce-Rodríguez, A., de las Heras, A., Páez-Espino, D., Durante-Rodríguez, G., Kim, J., Nikel, P. I., & de Lorenzo, V. (2013). The Standard European Vector Architecture (SEVA): a coherent platform for the analysis and deployment of complex prokaryotic phenotypes. *Nucleic Acids Research*, *41*(Database issue), D666–D675. https://doi.org/10.1093/nar/gks1119

Singh, R., Kumar, M., Mittal, A., & Mehta, P. K. (2016). Microbial enzymes: industrial progress in 21st century. *3 Biotech*, *6*(174), 1–15. https://doi.org/10.1007/s13205-016-0485-8

Sonnleitner, E., Abdou, L., & Haas, D. (2009). Small RNA as global regulator of carbon catabolite repression in *Pseudomonas aeruginosa*. *Proceedings of the National Academy of Sciences of the United States of America*, *106*(51), 21866–21871. https://doi.org/10.1073/pnas.0910308106

Spence, E. M., Calvo-Bado, L., Mines, P., & Bugg, T. D. (2021). Metabolic engineering of *Rhodococcus jostii* RHA1 for production of pyridine-dicarboxylic acids from lignin. *Microbial Cell Factories*, *20*(15). https://doi.org/10.1186/s12934-020-01504-z

Sravan, J. S., & Mohan, S. V. (2022). Hybrid electrosynthesis as non-genetic approach for regulating microbial metabolism towards waste valorization in circular framework. *Microbial Biotechnology*. https://doi.org/10.1111/1751-7915.14143

Stein, T. (2005). *Bacillus subtilis* antibiotics: structures, syntheses and specific functions. *Molecular Microbiology*, *56*(4), 845–857. https://doi.org/10.1111/j.1365-2958.2005.04587.x

Steipe, B., Schiller, B., Pluäckthun, A., & Steinbacher, S. (1994). Sequence statistics reliably predict stabilizing mutations in a protein domain. *Journal of Molecular Biology*, *240*(3), 188–192. https://doi.org/10.1006/JMBI.1994.1434

Sternke, M., Tripp, K. W., & Barrick, D. (2019). Consensus sequence design as a general strategy to create hyperstable, biologically active proteins. *Proceedings of the National Academy of Sciences of the United States of America*, *116*(23), 11275–11284. https://doi.org/10.1073/pnas.1816707116

Sternke, M., Tripp, K. W., & Barrick, D. (2020). The use of consensus sequence information to engineer stability and activity in proteins. *Methods in enzymology*, *643*, 149–179. https://doi.org/10.1016/BS.MIE.2020.06.001

Straathof, A. J., Wahl, S. A., Benjamin, K. R., Takors, R., Wierckx, N., & Noorman, H. J. (2019). Grand research challenges for sustainable industrial biotechnology. *Trends in Biotechnology*, *37*(10), 1042–1050. https://doi.org/10.1016/J.TIBTECH.2019.04.002

Studier, F. W., & Moffatt, B. A. (1986). Use of bacteriophage T7 RNA polymerase to direct selective high-level expression of cloned genes. *Journal of Molecular Biology*, *189*(1), 113–130. https://doi.org/10.1016/0022-2836(86)90385-2

Sullivan, B. J., Durani, V., & Magliery, T. J. (2011). Triosephosphate isomerase by consensus design: dramatic differences in physical properties and activity of related variants. *Journal of Molecular Biology*, *413*(1), 195–208. https://doi.org/10.1016/J.JMB.2011.08.001

Sullivan, K. P., Werner, A. Z., Ramirez, K. J., Ellis, L. D., Bussard, J. R., Black, B. A., Brandner, D. G., Bratti, F., Buss, B. L., Dong, X., Haugen, S. J., Ingraham, M. A., Konev, M. O., Michener, W. E., Miscall, J., Pardo, I., Woodworth, S. P., Guss, A. M., Román-Leshkov, Y., … Beckham, G. T. (2022). Mixed plastics waste valorization through tandem chemical oxidation and biological funneling. *Science*, *378*(6616), 207–211. https://doi.org/10.1126/science.abo4626

Sumi, C. D., Yang, B. W., Yeo, I.-C., & Hahm, Y. T. (2015). Antimicrobial peptides of the genus *Bacillus*: a new era for antibiotics. *Canadian Journal of Microbiology*, *61*(2), 93–103. https://doi.org/10.1139/cjm-2014-0613

Terán, W., Felipe, A., Fillet, S., Guazzaroni, M.-E., Krell, T., Ruiz, R., Ramos, J. L., & Gallegos, M.-T. (2007). Complexity in efflux pump control: cross-regulation by the paralogues TtgV and TtgT. *Molecular Microbiology*, *66*(6), 1416–1428. https://doi.org/10.1111/j.1365-2958.2007.06004.x

Terán, W., Felipe, A., Segura, A., Rojas, A., Ramos, J.-L., & Gallegos, M.-T. (2003). Antibiotic-dependent induction of *Pseudomonas putida* DOT-T1E TtgABC efflux pump is mediated by the drug binding repressor TtgR. *Antimicrobial*

Agents and Chemotherapy, *47*(10), 3067–3072. https://doi.org/10.1128/AAC.47.10.3067-3072.2003

Terán, W., Krell, T., Ramos, J. L., & Gallegos, M. T. (2006). Effector-repressor interactions, binding of a single effector molecule to the operator-bound TtgR homodimer mediates derepression. *The Journal of Biological Chemistry*, *281*(11), 7102–7109. https://doi.org/10.1074/JBC.M511095200

Tomás-Pejó, E., & Olsson, L. (2015). Influence of the propagation strategy for obtaining robust *Saccharomyces cerevisiae* cells that efficiently co-ferment xylose and glucose in lignocellulosic hydrolysates. *Microbial Biotechnology*, *8*(6), 999–1005. https://doi.org/10.1111/1751-7915.12280

Tossavainen, A. (1978). Styrene use and occupational exposure in the plastics industry. *Scandinavian Journal of Work, Environment and Health*, *4*(Suppl. 2), 7–13. https://doi.org/10.5271/sjweh.2732

Tripp, K. W., Sternke, M., Majumdar, A., & Barrick, D. (2017). Creating a homeodomain with high stability and DNA binding affinity by sequence averaging. *Journal of the American Chemical Society*, *139*(14), 5051–5060. https://doi.org/10.1021/jacs.6b11323

Tropel, D., & Van Der Meer, J. R. (2004). Bacterial transcriptional regulators for degradation pathways of aromatic compounds. *Microbiology and Molecular Biology Reviews*, *68*(3), 474–500. https://doi.org/10.1128/MMBR.68.3.474-500.2004

Udaondo, Z., Duque, E., Fernández, M., Molina, L., de la Torre, J., Bernal, P., Niqui, J. L., Pini, C., Roca, A., Matilla, M. A., Molina-Henares, M. A., Silva-Jiménez, H., Navarro-Avilés, G., Busch, A., Lacal, J., Krell, T., Segura, A., & Ramos, J. L. (2012). Analysis of solvent tolerance in *Pseudomonas putida* DOT-T1E based on its genome sequence and a collection of mutants. *FEBS Letters*, *586*(18), 2932–2938. https://doi.org/10.1016/j.febslet.2012.07.031

Udaondo, Z., Molina, L., Daniels, C., Gómez, M. J., Molina-Henares, M. A., Matilla, M. A., Roca, A., Fernández, M., Duque, E., Segura, A., & Ramos, J. L. (2013). Metabolic potential of the organic-solvent tolerant *Pseudomonas putida* DOT-T1E deduced from its annotated genome. *Microbial Biotechnology*, *6*(5), 598–611. https://doi.org/10.1111/1751-7915.12061

Udaondo, Z., Molina, L., Segura, A., Duque, E., & Ramos, J. L. (2016). Analysis of the core genome and pangenome of *Pseudomonas putida*. *Environmental Microbiology*, *18*(10), 3268–3283. https://doi.org/10.1111/1462-2920.13015

Udaondo, Z., Ramos, J. L., Segura, A., Krell, T., & Daddaoua, A. (2018). Regulation of carbohydrate degradation pathways in *Pseudomonas* involves a versatile set of transcriptional regulators. *Microbial Biotechnology*, *11*(3), 442–454. https://doi.org/10.1111/1751-7915.13263

Uekert, T., Singh, A., DesVeaux, J. S., Ghosh, T., Bhatt, A., Yadav, G., Afzal, S., Walzberg, J., Knauer, K. M., Nicholson, S. R., Beckham, G. T., & Carpenter, A. C. (2023). Technical, economic, and environmental comparison of closed-loop recycling technologies for common plastics. *ACS Sustainable Chemistry and Engineering*, *11*(3), 965–978. https://doi.org/10.1021/acssuschemeng.2c05497

Ursino, E., Albertini, A. M., Fiorentino, G., Gabrieli, P., Scoffone, V. C., Pellegrini, A., Gasperi, G., Di Cosimo, A., & Barbieri, G. (2020). *Bacillus subtilis* as a host for mosquitocidal toxins production. *Microbial Biotechnology*, *13*(6), 1972–1982. https://doi.org/10.1111/1751-7915.13648

Vagin, A., & Teplyakov, A. (2010). Molecular replacement with MOLREP. *Acta Crystallographica. Section D, Biological Crystallography*, *66*(Pt 1), 22–25. https://doi.org/10.1107/S0907444909042589

Valdivia, M., Galan, J. L., Laffarga, J., & Ramos, J. L. (2016). Biofuels 2020: Biorefineries based on lignocellulosic materials. *Microbial Biotechnology*, *9*(5), 585–594. https://doi.org/10.1111/1751-7915.12387

Valdivia, M., Galan, J. L., Laffarga, J., & Ramos, J. L. (2020). A research and technology valuation model for decision analysis in the environmental and renewable energy sectors. *Renewable and Sustainable Energy Reviews*, *122*(109726). https://doi.org/10.1016/J.RSER.2020.109726

van Dijl, J. M., & Hecker, M. (2013). *Bacillus subtilis*: from soil bacterium to super-secreting cell factory. *Microbial Cell Factories*, *12*(3), 1–6. https://doi.org/10.1186/1475-2859-12-3

van den Berg, H., & van der Ham, L. (2010). Dehydrogenation of ethylbenzene sing CO_2 – A process design study. *Chemical Engineering Transactions*, *21*, 337–342. https://doi.org/10.3303/CET102100157

Vannelli, T., Xue, Z., Breinig, S., Qi, W. W., & Sariaslani, F. S. (2007). Functional expression in *Escherichia coli* of the tyrosine-inducible tyrosine ammonia-lyase enzyme from yeast *Trichosporon cutaneum* for production of *p*-hydroxycinnamic acid. *Enzyme and Microbial Technology*, *41*(4), 413–422. https://doi.org/10.1016/J.ENZMICTEC.2007.03.013

Vargiu, A. V., & Nikaido, H. (2012). Multidrug binding properties of the AcrB efflux pump characterized by molecular dynamics simulations. *PNAS*, *109*(50), 20637–20642. https://doi.org/10.1073/pnas.1218348109

Velankar, S., Best, C., Beuth, B., Boutselakis, C. H., Cobley, N., Sousa Da Silva, A. W., Dimitropoulos, D., Golovin, A., Hirshberg, M., John, M., Krissinel, E. B., Newman, R., Oldfield, T., Pajon, A., Penkett, C. J., Pineda-Castillo, J., Sahni, G., Sen, S., Slowley, R., … Kleywegt, G. J. (2010). PDBe: Protein Data Bank in Europe. *Nucleic Acids Research*, *38*(Database issue), D308–D317. https://doi.org/10.1093/nar/gkp916

Verhoef, S., Ballerstedt, S., Volkers, H. J. M., Winde, R. J. M., De, J. H., & Ruijssenaars, H. J. (2010). Comparative transcriptomics and proteomics of *p*-hydroxybenzoate producing *Pseudomonas putida* S12: novel responses and implications for strain improvement. *Applied Microbiology And Biotechnology*, *87*(2), 679–690. https://doi.org/10.1007/s00253-010-2626-z

Verhoef, S., Wierckx, N., Westerhof, R. G. M., de Winde, J. H., & Ruijssenaars, H. J. (2009). Bioproduction of *p*-hydroxystyrene from glucose by the solvent-tolerant bacterium *Pseudomonas putida* S12 in a two-phase water-decanol fermentation. *Applied and Environmental Microbiology*, *75*(4), 931–936. https://doi.org/10.1128/AEM.02186-08

Vermuë, M., Sikkema, J., Verheul, A., Bakker, R., & Tramper, J. (1993). Toxicity of homologous series of organic solvents for the gram-positive bacteria *Arthrobacter* and *Nocardia* Sp. and the gram-negative bacteria *Acinetobacter* and *Pseudomonas* Sp. *Biotechnology and Bioengineering*, *42*(6), 747–758. https://doi.org/10.1002/bit.260420610

Vladimirova, A., Patskovsky, Y., Fedorov, A. A., Bonanno, J. B., Fedorov, E. V., Toro, R., Hillerich, B., Seidel, R. D., Richards, N. G., Almo, S. C., & Raushel, F. M. (2016). Substrate distortion and the catalytic reaction mechanism of 5-carboxyvanillate decarboxylase. *Journal of the American Chemical Society*, *138*(3), 826–836. https://doi.org/10.1021/jacs.5b08251

Wang, C., Thygesen, A., Liu, Y., Li, Q., Yang, M., Dang, D., Wang, Z., Wan, Y., Lin, W., & Xing, J. (2013). Bio-oil based biorefinery strategy for the production of succinic acid. *Biotechnology for Biofuels*, *6*(74). https://doi.org/10.1186/1754-6834-6-74

Wang, J., Shen, X., Rey, J., Yuan, Q., & Yan, Y. (2018a). Recent advances in microbial production of aromatic natural products and their derivatives. *Applied Micro-*

biology and Biotechnology, *102*(1), 47–61. https://doi.org/10.1007/s00253-017-8599-4

Wang, P.-H., Khusnutdinova, A. N., Mahadevan, R., Edwards, E. A., & Yakunin, A. F. (2018b). Biosynthesis and activity of prenylated FMN cofactors. *Cell Chemical Biology*, *25*(5), 560–570. https://doi.org/10.1016/j.chembiol.2018.02.007

Webb, J. (2012). Climate change and society: The chimera of behaviour change technologies. *British Sociological Association*, *46*(1), 109–125. https://doi.org/10.1177/0038038511419196

Webb, J. P., Paiva, A. C., Rossoni, L., Alstrom-Moore, A., Springthorpe, V., Vaud, S., Yeh, V., Minde, D.-P., Langer, S., Walker, H., Hounslow, A., Nielsen, D. R., Larson, T., Lilley, K., Stephens, G., Thomas, G. H., Bonev, B. B., Kelly, D. J., Conradie, A., & Green, J. (2022). Multi-omic based production strain improvement (MOBpsi) for bio-manufacturing of toxic chemicals. *Metabolic Engineering*, *72*, 133–149. https://doi.org/10.1016/J.YMBEN.2022.03.004

Webber, M. A., & Piddock, L. J. V. (2003). The importance of efflux pumps in bacterial antibiotic resistance. *Journal of Antimicrobial Chemotherapy*, *51*(1), 9–11. https://doi.org/10.1093/jac/dkg050

Weber, F. J., & de Bont, J. A. M. (1996). Adaptation mechanisms of microorganisms to the toxic effects of organic solvents on membranes. *Biochimica et Biophysica Acta*, *1286*(3), 225–245. https://doi.org/10.1016/S0304-4157(96)00010-X

Weber, F. J., Isken, S., & De Bont, J. A. M. (1994). *Cis/trans* isomerization of fatty acids as a defence mechanism of *Pseudomonas putida* strains to toxic concentrations of toluene. *Microbiology*, *140*(8), 2013–2017. https://doi.org/10.1099/13500872-140-8-2013

Weber, F. J., Ooijkaas, L. P., Schemen, R. M., Hartmans, S., & De Bont, J. A. (1993). Adaptation of *Pseudomonas putida* S12 to high concentrations of styrene and other organic solvents. *Applied and environmental microbiology*, *59*(10), 3502–3504. https://doi.org/10.1128/AEM.59.10.3502-3504.1993

Weiland, F., Kohlstedt, M., & Wittmann, C. (2022). Guiding stars to the field of dreams: Metabolically engineered pathways and microbial platforms for a sustainable lignin-based industry. *Metabolic Engineering*, *71*, 13–41. https://doi.org/10.1016/j.ymben.2021.11.011

Weimer, A., Kohlstedt, M., Volke, D. C., Nikel, P. I., & Wittmann, C. (2020). Industrial biotechnology of *Pseudomonas putida*: advances and prospects. *Applied Microbiology and Biotechnology*, *104*(18), 7745–7766. https://doi.org/10.1007/S00253-020-10811-9

White, D. G., Goldman, J. D., Demple, B., & Levy, S. B. (1997). Role of the *acrAB* locus in organic solvent tolerance mediated by expression of *marA*, *soxS*, or *robA* in *Escherichia coli*. *Journal of Bacteriology*, *179*(19), 6122–6126. https://doi.org/10.1128/jb.179.19.6122-6126.1997

White, M. D., Payne, K. A. P., Fisher, K., Marshall, S. A., Parker, D., Rattray, N. J. W., Trivedi, D. K., Goodacre, R., Rigby, S. E. J., Scrutton, N. S., Hay, S., & Leys, D. (2015). UbiX is a flavin prenyltransferase required for bacterial ubiquinone biosynthesis. *Nature*, *522*(7557), 502–506. https://doi.org/10.1038/nature14559

Wierckx, N., Ballerstedt, H., de Bont, J. A. M., & Wery, J. (2005). Engineering of solvent-tolerant *Pseudomonas putida* S12 for bioproduction of phenol from glucose. *Applied and Enviornmental Microbiology*, *71*(12), 8221–8227. https://doi.org/10.1128/AEM.71.12.8221-8227.2005

Wierckx, N., Ballerstedt, H., De Bont, J. A., De Winde, J. H., Ruijssenaars, H. J., & Wery, J. (2008). Transcriptome analysis of a phenol-producing *Pseudomonas putida* S12 construct: Genetic and physiological basis for improved production. *Journal of Bacteriology*, *190*(8), 2822–2830. https://doi.org/10.1128/JB.01379-07

Wierckx, N., Ruijssenaars, H. J., de Winde, J. H., Schmid, A., & Blank, L. M. (2009). Metabolic flux analysis of a phenol producing mutant of *Pseudomonas putida* S12: verification and complementation of hypotheses derived from transcriptomics. *Journal of biotechnology*, *143*(2), 124–129. https://doi.org/10.1016/J.JBIOTEC.2009.06.023

Wilhelm, M., & Hollenberg, C. P. (1985). Nucleotide sequence of the *Bacillus subtilis* xylose isomerase gene: extensive homology between the *Bacillus* and *Escherichia coli* enzyme. *Nucleic Acids Research*, *13*(15), 5717–5722. https://doi.org/10.1093/nar/13.15.5717

Wirtz, P., & Steipe, B. (1999). Intrabody construction and expression III: engineering hyperstable V_H domains. *Protein Science*, *8*(11), 2245–2250. https://doi.org/10.1110/PS.8.11.2245

Worrell, E., Phylipsen, D., Einstein, D., & Martin, N. (2000). *Energy Use and Energy Intensity of the U.S. Chemical Industry* (tech. rep.). Lawrence Berkeley National Laboratory. Berkeley, California. https://escholarship.org/uc/item/2925w8g6

Wu, C.-Y., Kobylinski, T. P., & Bozik, J. E. (1981). Preparation of styrene from ethylbenzene.

Wu, W., Huang, J., & Xu, Z. (2024). Antibiotic influx and efflux in *Pseudomonas aeruginosa*: Regulation and therapeutic implications. *Microbial Biotechnology*, *17*(5), e14487. https://doi.org/10.1111/1751-7915.14487

Wynands, B., Lenzen, C., Otto, M., Koch, F., Blank, L. M., & Wierckx, N. (2018). Metabolic engineering of *Pseudomonas taiwanensis* VLB120 with minimal genomic modifications for high-yield phenol production. *Metabolic Engineering*, *47*, 121–133. https://doi.org/10.1016/J.YMBEN.2018.03.011

Xiang, L., & Moore, B. S. (2005). Biochemical characterization of a prokaryotic phenylalanine ammonia lyase. *Journal of Bacteriology*, *187*(12), 4286–4289. https://doi.org/10.1128/JB.187.12.4286-4289.2005

Yamane, K., Wachino, J.-I., Suzuki, S., Kimura, K., Shibata, N., Kato, H., Shibayama, K., Konda, T., & Arakawa, Y. (2007). New plasmid-mediated fluoroquinolone efflux pump, QepA, found in an *Escherichia coli* clinical isolate. *Antimicrobial Agents and Chemotherapy*, *51*(9), 3354–3360. https://doi.org/10.1128/AAC.00339-07

Yang, B., & Wyman, C. E. (2008). Pretreatment: The key to unlocking low-cost cellulosic ethanol. *Biofuels, Bioproducts and Biorefining*, *2*(1), 26–40. https://doi.org/10.1002/BBB.49

Yang, J., Zhao, G., Sun, Y., Zheng, Y., Jiang, X., Liu, W., & Xian, M. (2012). Bio-isoprene production using exogenous MVA pathway and isoprene synthase in *Escherichia coli*. *Bioresource Technology*, *104*, 642–647. https://doi.org/10.1016/j.biortech.2011.10.042

Yang, J., & Zhang, Y. (2015). I-TASSER server: new development for protein structure and function predictions. *Nucleic Acids Research*, *43*(W1), W174–W181. https://doi.org/10.1093/nar/gkv342

Young, M. R., & Neisht, A. C. (1966). Properties of the ammonia-lyases deaminating phenylalanine and related compounds in *Triticum aestivum* and *Pteridium aquilinum*. *Phytochemistry*, *5*, 1121–1132.

Yu, C., Simmons, B. A., Singer, S. W., Thelen, M. P., & VanderGheynst, J. S. (2016a). Ionic liquid-tolerant microorganisms and microbial communities for lignocellulose conversion to bioproducts. *Applied microbiology and biotechnology*, *100*(24), 10237–10249. https://doi.org/10.1007/S00253-016-7955-0

Yu, S., Plan, M. R., Winter, G., & Krömer, J. O. (2016b). Metabolic engineering of *Pseudomonas putida* KT2440 for the production of *para*-hydroxy benzoic acid. *Frontiers in Bioengineering and Biotechnology*, *4*(90). https://doi.org/10.3389/FBIOE.2016.00090

Yuzbashev, T. V., Yuzbasheva, E. Y., Sobolevskaya, T. I., Laptev, I. A., Vybornaya, T. V., Larina, A. S., Matsui, K., Fukui, K., & Sineoky, S. P. (2010). Production of succinic acid at low pH by a recombinant strain of the aerobic yeast *Yarrowia lipolytica*. *Biotechnology and Bioengineering*, *107*(4), 673–682. https://doi.org/10.1002/bit.22859

Zakzeski, J., Bruijnincx, P. C., Jongerius, A. L., & Weckhuysen, B. M. (2010). The catalytic valorization of lignin for the production of renewable chemicals. *Chemical Reviews*, *110*(6), 3552–3599. https://doi.org/10.1021/CR900354U

Zhan, Y., Shi, J., Xiao, Y., Zhou, F., Wang, H., Xu, H., Li, Z., Yang, S., Cai, D., & Chen, S. (2022). Multilevel metabolic engineering of *Bacillus licheniformis* for *de novo* biosynthesis of 2-phenylethanol. *Metabolic Engineering*, *70*, 43–54. https://doi.org/10.1016/j.ymben.2022.01.007

Zhang, Y., Stepanova, S., Van Aelst, K., & Sels, B. F. (2023). Consider lignin's hydroxyl groups content and type, its molecular weight and content when converting it into epoxy resin. *Current Opinion in Green and Sustainable Chemistry*, *40*(100750). https://doi.org/10.1016/j.cogsc.2022.100750

Zhao, H., Brown, P. H., Balbo, A., Fernández-Alonso, M. D. C., Polishchuck, N., Chaudhry, C., Mayer, M. L., Ghirlando, R., & Schuck, P. (2010). Accounting for solvent signal offsets in the analysis of interferometric sedimentation velocity data. *Macromolecular Bioscience*, *10*(7), 736–745. https://doi.org/10.1002/MABI.200900456

Zhao, H., & Arnold, F. H. (1999). Directed evolution converts subtilisin E into a functional equivalent of thermitase. *Protein Engineering*, *12*(1), 47–53. https://doi.org/10.1093/protein/12.1.47

Zylstra, G. J., Mccombie, W. R., Gibson, D. T., & Finette, B. A. (1988). Toluene degradation by *Pseudomonas putida* Fl: genetic organization of the *tod*

operon. *Applied and Enviornmental Microbiology*, *54*(6), 1498–1503. https://doi.org/10.1128/aem.54.6.1498-1503.1988